Amplitude modulation and energy conservation of pulsation modes in delta Scuti stars

Dominic M. Bowman

Jeremiah Horrocks Institute for Mathematics, Physics and Astronomy

University of Central Lancashire

October 2016

Declaration

The work presented in this thesis was carried out at the Jeremiah Horrocks Institute for Mathematics, Physics and Astronomy, University of Central Lancashire.

I declare that while registered as a candidate for the research degree, I have not been a registered candidate or enrolled student for another award of the University or other academic or professional institution.

I declare that no material contained in the thesis has been used in any other submission for an academic award. Data, figures and models used in this thesis that are not my own are clearly cited in the text.

Signature: **Date:** 28th October 2016

Type of Award: PhD in Astronomy

School: Physical Sciences and Computing

Abstract

The pulsations in δ Sct stars are excited by a heat engine driving mechanism caused by increased opacity in their surface layers, and have pulsation periods of order a few hours. Space based observations in the last decade have revealed a diverse range of pulsational behaviour in these stars, which is investigated using an ensemble of 983 δ Sct stars observed continuously for 4 yr by the *Kepler* Space Telescope. A statistical search for amplitude modulation of pulsation modes is carried out and it is shown that 61.3 per cent of the 983 δ Sct stars exhibit significant amplitude modulation in at least a single pulsation mode, and that this is uncorrelated with effective temperature and surface gravity. Hence, the majority of δ Sct stars exhibit amplitude modulation, with time-scales of years and longer demonstrated to be significant in these stars both observationally and theoretically.

An archetypal example of amplitude modulation in a δ Sct star is KIC 7106205, which contains only a single pulsation mode that varies significantly in amplitude whilst all other pulsation modes stay constant in amplitude and phase throughout the 4-yr *Kepler* data set. Therefore, the visible pulsational energy budget in this star, and many others, is not conserved over 4 yr.

Models of beating of close-frequency pulsation modes are used to identify δ Sct stars with frequencies that lie closer than $0.001 \, \mathrm{d}^{-1}$, which are barely resolved using 4 yr of *Kepler* observations, and maintain their independent identities over 4 yr. Mode coupling models are used to quantify the strength of coupling and distinguish between non-linearity in the form of combination frequencies and non-linearity in

the form of resonant mode coupling for families of pulsation modes in several stars.

The changes in stellar structure caused by stellar evolution are investigated for two high amplitude δ Sct (HADS) stars in the *Kepler* data set, revealing a positive quadratic change in phase for the fundamental and first overtone radial modes in KIC 5950759. The observed phase modulation of the radial modes in this star is two orders of magnitude larger than predicted by stellar evolutionary models, yet is consistent with the prediction of increasing periods of radial modes for stars on the main sequence.

The statistical analysis of 983 δ Sct stars, including the results from the search for amplitude modulation, is a valuable resource for ongoing and future space missions such as K2, TESS and PLATO, because the high quality 4-yr *Kepler* data set will not be surpassed for some time. The observational studies of individual stars in this thesis provide strong evidence that non-linear processes are clearly at work in the majority of δ Sct stars, and provide valuable constraints for future asteroseismic modelling.

Contents

List of Tables

List of Figures

Acknowledgements

First and foremost, I wish to thank my PhD supervisor Professor Don Kurtz, who has provided me with a wealth of knowledge and experience over the last three years. He is an expert in astronomy, the English language and many other fascinating subjects. I have been fortunate to have Don as a mentor and I am extremely grateful for all his support.

I would also like to thank Dr. Daniel Holdsworth and Dr. Simon Murphy who have been valued collaborators and have been instrumental in many different aspects of my PhD. I am grateful to all my collaborators and those who have contributed to the research in my thesis over the last three years. I look forward to continued collaborations in the future with all of you.

I would also like to gratefully acknowledge the support from the Jeremiah Horrocks Institute at UCLan, its director and my second supervisor Professor Derek Ward-Thompson, the UK Science and Technology Facilities Council (STFC) and the Royal Astronomical Society (RAS) for financial support during my studies. I am grateful to my thesis examiners, Professor Douglas Gough and Dr. Stewart Eyres, who agreed to read my thesis and provide feedback on its content.

This thesis has made use of public *Kepler* data via the MAST archive, with funding for the *Kepler* mission provided by the NASA Science Mission directorate. I appreciate all those who helped make the *Kepler* mission successful and provided the community with exquisite data. I would like to thank Randy Thompson, who provided me with a lot of help in the early days of my PhD when I was learning

to use the MAST interface, which resulted in a promise to acknowledge him in my thesis.

Finally, I would like to thank my parents, to whom I owe a great deal, and all my family, friends and fellow postgraduate students who have supported me over the last three years. There are too many to name but you know who you are.

Preface

Context

Astronomy covers numerous aspects of physics and mathematics across many orders of magnitude in size, from the quantum mechanical laws that determine nuclear fusion reactions in the centre of a star, to the dynamics of galaxy clusters over cosmological distances. Astronomy studies the smallest and largest known structures in the universe and the physical laws that govern them. Over the last century, a general description of stellar structure and evolution has been developed. However, the inclusion of physics such as rotation, binarity, pulsation and magnetic fields causes stellar structure and evolution to become more complicated.

Using traditional observational techniques such as photometry and spectroscopy, one barely scratches beneath the visible surface of a star, because these methods are only sensitive to the stellar atmosphere. Until the advent of asteroseismology, astronomy lacked the techniques to validate or invalidate theoretical predictions of the interior conditions of a star through observation and experimentation. This is famously encapsulated by the famous text *The Internal Constitution of the Stars* published in 1926 by Sir Arthur Stanley Eddington, who asked the following questions:

> *"At first sight it would seem that the deep interior of the Sun and stars*
> *is less accessible to scientific investigation than any other region in the*

universe. Our telescopes may probe farther and farther into the depths of space; but how can we ever obtain certain knowledge of that which is hidden behind substantial barriers? What appliance can pierce through the outer layers of a star and test the conditions within?"

Asteroseismology is the tool that Eddington sought, which provides direct insight of the interior of a star by studying its oscillations. The pulsations within an oscillating star are governed by the physics of stellar structure, so from observations and analysis of these pulsations the interior properties of a star can be measured. Many different types of pulsator have been discovered, including our nearest stellar neighbour — the Sun. Its proximity has allowed the Sun to be extensively studied since the discovery of its oscillations in the 1960s. Asteroseismology has rapidly expanded in recent years because of improvements in instrumentation, and has been applied to many types of stars across a wide range in stellar mass and for different stages of stellar evolution.

Motivation

This thesis is centred on a group of variable stars called δ Sct stars, which are the most common type of pulsator among the intermediate-mass A and F stars, and have been studied since their discovery in the early twentieth century. Historically, using several hours of ground-based observations, these variable stars were straightforward to classify because they have similar effective temperatures and pulsate with periods of order hours and minutes.

Prior to the twenty-first century, only a handful of δ Sct stars had been extensively studied using ground based campaigns, which provided intermittent observations with duty cycles typically less than 50 per cent. These investigations were limited by the data coverage and precision of the instrumentation used, but revealed

that we lack a complete physical description of these pulsators, primarily because of the diversity of observed pulsations in these stars. A few δ Sct stars were found to exhibit a phenomenon called amplitude modulation — in the time domain this appears as a change in the maxima and minima of the light excursions over time, and in the Fourier domain this appears as variable pulsation mode amplitudes. Naturally, this causes problems for intermittent observations over a few days if the pulsation mode amplitudes of a variable star change on time-scales of order years to decades. From only a few in-depth studies it was not clear what determines this effect in δ Sct stars, as not all stars exhibited such behaviour. This provides strong motivation to study amplitude modulation in δ Sct stars further.

The space-based telescopes CoRoT and *Kepler*, which were launched in 2006 and 2009, respectively, have led to a photometry revolution. The *Kepler* Space Telescope provided a large increase in high quality observations of hundreds of thousands of stars, including many δ Sct stars. This thesis addresses Eddington's questions by using asteroseismology to expand our understanding of δ Sct stars and studies the incidence of amplitude modulation in approximately 1000 δ Sct stars. The general theme of this thesis is the journey through the discoveries that were made throughout the work.

Chapter 1

Introduction

1.1 Asteroseismology

Almost a century ago, Sir Arthur Stanley Eddington proposed that a star could act as a heat engine and become unstable to pulsation (Eddington 1917, 1926). If the driving from a pulsational excitation mechanism in a star is strong enough to overcome local damping effects, a star will resonate in its natural oscillation modes, which are determined by the physics of stellar structure. Therefore, the observation and modelling of the conditions within stellar interiors, such as density, pressure and temperature, is of paramount importance so that we can understand how and why stars pulsate and the implications for stellar evolution. Asteroseismology, from the Greek meaning *star tremors* or *star quakes*, is the study of stellar structure and evolution from the observation and modelling of stellar pulsation. A thorough text on asteroseismology is given by Aerts et al. (2010).

The requirement of any heat engine is that heat is gained in the compression part of the cycle, with the thermal energy being converted into mechanical work. For Eddington's piston-like driving mechanism inside a star, a source of opacity provides the required instability to drive the heat engine, so it is referred to as the opacity or kappa (κ) mechanism in asteroseismology. The simplest case of driving

from the κ mechanism in a star is radial pulsation, with increased levels of opacity in the stellar atmosphere that block the outward flow of radiation. The blocked flux causes a layer of gas to heat up, which increases the internal pressure such that the layer expands to return to equilibrium with its surroundings. Eventually the gas within the layer will become ionised, reducing the local opacity so that the layer is no longer opaque and the radiation flows through again. Having expanded beyond its equilibrium point and no longer being heated, the radial layer cannot support the weight of the overlying stellar atmosphere and contracts once again. The contraction allows the ionised gas to recombine and absorb the stellar flux, regenerating the source of opacity once again. Thus, a piston-like driving mechanism is created with heat being gained upon compression and energy being released upon expansion of a layer of gas in a star's atmosphere.

Since the time of Eddington (1917, 1926), pulsations driven by the κ mechanism have been found in variable stars across the Hertzsprung–Russell (HR) diagram, which is shown schematically in Fig. 1.1. The hatched regions in this figure indicate a different type of pulsating star and its location in the HR diagram, with each group labelled by name and coloured approximately by spectral type. The nature of the driving mechanism in the various types of pulsator is specific to the structure of the stars within each group, with the κ mechanism operating in the regions with diagonal hatching. Asteroseismology has been applied to all the types of pulsating star shown in Fig. 1.1, and has allowed their interiors to be probed to varying levels of success (see e.g., Aerts et al. 2010).

Asteroseismology is a rapidly expanding field within astronomy with far-reaching implications both observationally and theoretically. The success of asteroseismology in recent years has been driven by significant improvements in techniques and instrumentation. This is particularly because of the high quality data produced from space telescopes that have been operating in the last decade. These space telescopes have
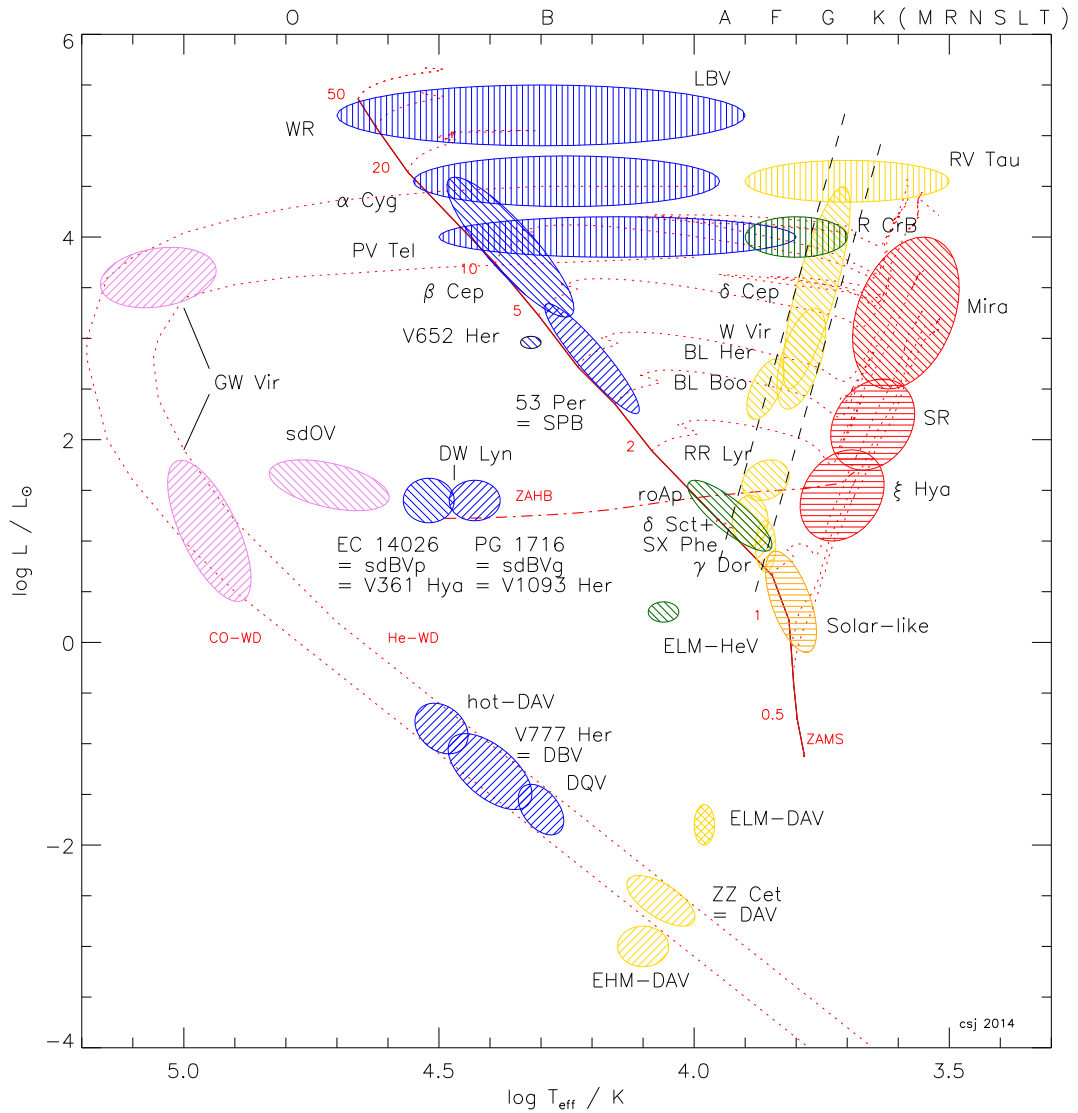
Figure 1.1: A schematic HR diagram for pulsating stars, demonstrating the various types of stars for which asteroseismology is possible. The main sequence is indicated by a solid red line and the boundaries of the classical instability strip are indicated by the long-dashed lines. Evolutionary tracks for different stellar masses are shown as dotted lines, and pulsators are coloured by their approximate spectral type. The κ mechanism operates in the regions with diagonal hatching, with the direction indicating if the dominant pulsations are p modes (\\\ ) or g modes (///), whereas horizontally hatched regions ($\equiv$) indicate stars with stochastically excited pulsations. Figure from Jeffery & Saio (2016), their figure 1.

enabled us to probe further and deeper into the physics that determines whether a star is unstable to pulsation, and have also vastly increased our understanding of stellar structure and evolution.

1.1.1   Pulsation modes

There are two main types of pulsation modes. The first are acoustic modes, or sound waves, for which pressure is the restoring force and hence are called p modes. These pulsations have vertical gas motions and are most sensitive to the surface conditions within a star. The other main type of pulsation modes are gravity modes, for which buoyancy or gravity is the restoring force and hence are called g modes. The gas motions of g modes can be horizontal and vertical, and are most sensitive to the conditions near the core of a star[1]. All g-mode pulsations are evanescent in a convectively unstable layer as defined by the Schwarzschild criterion, which causes runaway buoyancy and not oscillatory motion. On the other hand, p-mode pulsations can be supported in convectively unstable layers provided that the pulsation driving is stronger than the damping.

The coherent driving of pulsations in a star produces standing waves that are trapped within a pulsation cavity. Stars usually have spherical symmetry, with a displacement node at their centres and the surface acting as an anti-node. The standing waves inside a star are described by spherical harmonics using three quantum indices: n is the radial order or overtone number, ℓ is the angular degree (number of surface nodes), and m is the azimuthal order ($|m|$ is the number of surface nodes that are lines of longitude). The simplest example of a radial p mode is the fundamental radial mode where $\{n, \ell, m\} = 0$. In this mode of pulsation, the entire radius of a star expands and contracts over the pulsation cycle. Thus, the fundamental radial mode is a measure of the average density of a star, because the pulsation wave

---

[1]with the exception of pulsating white dwarf stars, in which the g modes are trapped in the surface layers.

travels from the stellar surface to the core and back again throughout the pulsation cycle.

Analogous to musical instruments, the next overtone is called the first overtone radial mode where $n = 1$ and $\{\ell, m\} = 0$, which has a displacement node that is a concentric shell within the star. In this mode of pulsation, the layers above and below the nodal shell expand and contract in anti-phase. For higher radial orders, further concentric shells are nodes within a star.

There also exist solutions to the equations of motion for a pulsating star where $\ell \geq 1$, which are called non-radial modes. The simplest non-radial mode is an axisymmetric dipole mode with $\ell = 1$ and $m = 0$, for which the equator separating the northern and southern hemispheres is a node. In this mode of pulsation, the northern hemisphere heats and expands whilst the southern hemisphere cools and contracts and vice versa, with no change in cross-sectional area of the star from a distant observer's point of view. A three-dimensional representation of octupole ($\ell = 3$) pulsation modes with different values of m viewed from different inclination angles, i, are shown in Fig. 1.2, in which red and blue represent the regions on the stellar surface that are moving in (heating) and moving out (cooling), respectively, at a given time.

The various radial and non-radial pulsations for both p and g modes can be interpreted using wave propagation diagrams. An example of such a diagram in two dimensions for pulsation modes in the Sun is shown in Fig. 1.3, with the left panel containing a selection of p modes and the right panel containing a single g mode. A radial p mode is represented by the straight line in Fig. 1.3, whose pulsation cavity is the radius of the star, as the pulsation wave travels from the stellar surface to the core and back again.

For the case of a non-radial p mode, the depth of the pulsation cavity is determined by refraction. Since pulsations are standing waves they are sensitive to

Inclination angle (deg)
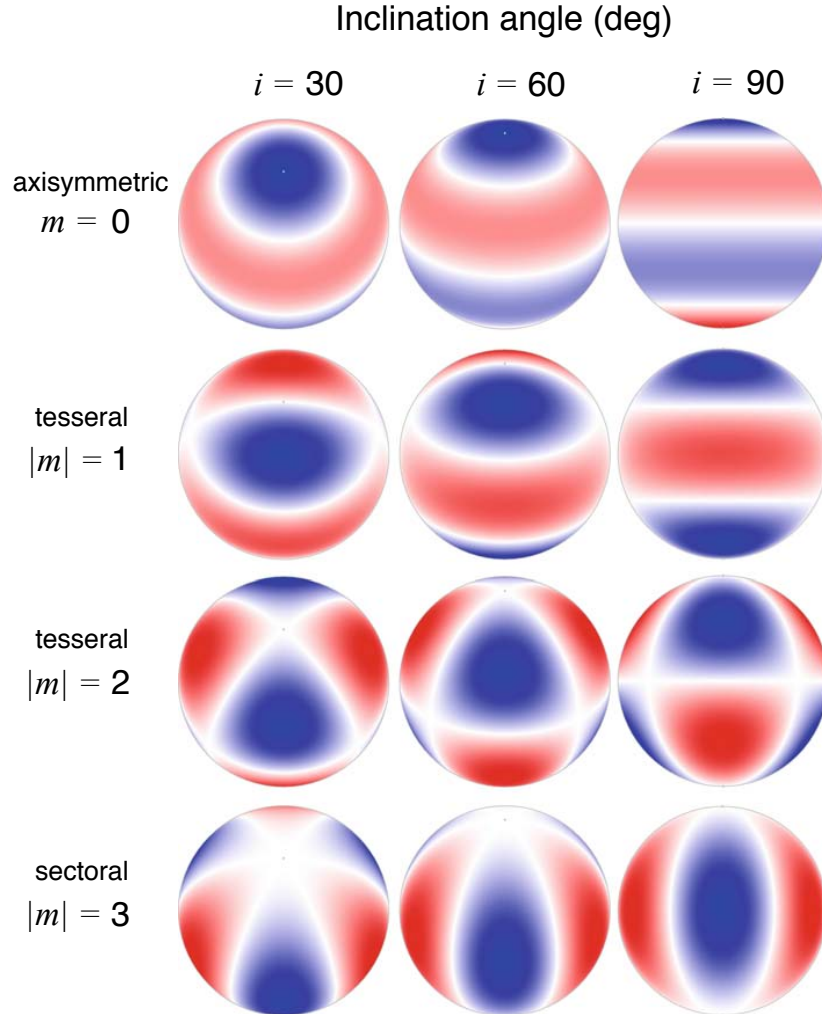
Figure 1.2: Snapshot of the radial component of the $\ell = 3$ octupole modes. The columns show the modes from different viewing angles; the left column is for an inclination of the pulsation pole of 30 deg, the middle column is for 60 deg, and the right column is for 90 deg. The white bands represent the positions of the surface nodes; red and blue represent sections of the star that are moving in (out) and/or heating (cooling) at any given time, then vice versa. The top row shows the axisymmetric octupole mode ($\ell = 3, m = 0$) where the nodes lie at latitudes ± 51 deg and 0 deg. The second row shows the tesseral (meaning $0 < |m| < \ell$) $\ell = 3$, $m = \pm 1$ mode with two nodes that are lines of latitude and one that is a line of longitude. The third row is the tesseral $\ell = 3$, $m = \pm 2$ mode, and the bottom row shows the sectoral mode (meaning $\ell = |m|$) with $\ell = 3$, $m = \pm 3$. Figure and caption from Aerts et al. (2010), their figure 1.4. Reproduced with permission from Springer.
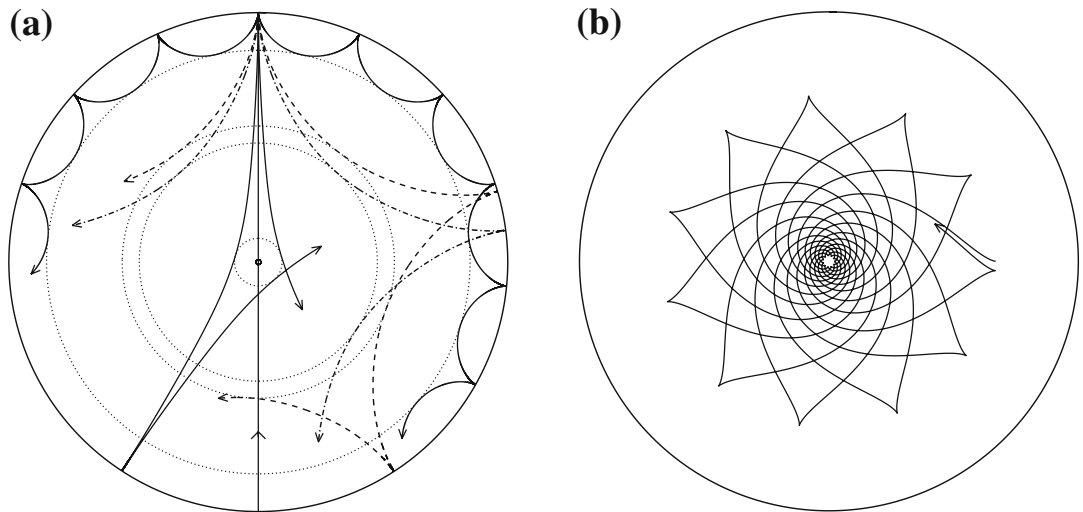
Figure 1.3: Propagation of rays of sound or gravity waves in a cross-section of the solar interior. The acoustic ray paths (a) are bent by the increase in sound speed with depth until they reach the inner turning point (indicated by the dotted circles) where they undergo total internal refraction, at the distance r_t. At the surface the acoustic waves are reflected by the rapid decrease in density. Rays are shown corresponding to modes with frequency 3000 μHz and degrees (in order of increasing penetration depth) $\ell = 75, 25, 20$ and 2; the line passing through the centre schematically illustrates the behaviour of a radial mode. The gravity-mode ray path (b) corresponds to a mode of frequency 190 μHz and degree 5. Figure and caption from Cunha et al. (2007), their figure 5. Reproduced with permission from Springer.

the conditions within the star, specifically the local adiabatic sound speed $c(r)$. As a non-radial pulsation wave travels inwards from the stellar surface, it encounters an increasing temperature and density gradient, hence a higher value of $c(r)$. This causes the wave to travel faster and to be continuously refracted. The depth to which a pulsation wave probes is called its turning radius, r_t, which is defined outwards from the core and is proportional to $\sqrt{\ell(\ell+1)}$. Therefore, higher degree modes have larger values of r_t, thus have smaller acoustic cavities and are more sensitive to the stellar surface.

The upper turning point of the pulsation cavity is defined by reflection at the stellar surface, at which a pulsation wave encounters a sharp density gradient. The highest frequency pulsation that can be supported in a star defines an acoustic cut-off frequency, and thus the upper limit of the acoustic cavity. Pulsations with frequencies above the acoustic cut-off are not trapped inside the stellar interior and do not provide a boundary condition for the creation of a standing wave.

The schematic of standing waves for the Sun in Fig. 1.3 demonstrates the sensitivity of the p modes to the surface conditions and the g mode to the core conditions within a star. Therefore, for stars that pulsate in g and p modes, the physical conditions throughout the stellar interior can be probed, which has been utilised to determine the surface-to-core rotation profile in main sequence B, A and F stars using asteroseismology (Kurtz et al. 2014; Saio et al. 2015; Triana et al. 2015; Murphy et al. 2016; Schmid & Aerts 2016).

Mixed modes

For a star on the zero-age main sequence (ZAMS), there is a clear separation in the pulsation cavities of g and p modes, with the lowest frequency p mode (i.e., the fundamental radial mode) having a larger frequency than the highest frequency

g mode. As a star ages and evolves off the ZAMS, the g-mode pulsation cavity extends to higher frequencies as a result of an increasing buoyancy frequency, known as the Brunt-Väisälä frequency (Aerts et al. 2010). It was first discovered by Osaki (1975) that this leads to a form of mode interaction called mixed modes, which are pulsations that have g-mode characteristics in the stellar interior and p-mode characteristics in the stellar envelope. The interaction of g and p mode properties takes place through a sequence of avoided crossings, which allow the modes to interact whilst maintaining their independent characters (Osaki 1975).

Therefore, the evolutionary state of a star, specifically if it is near the ZAMS or terminal-age main sequence (TAMS) can influence its pulsational properties and the presence of mixed modes in its amplitude spectrum. Mixed modes are typically found in stars that have evolved off the main sequence and are undergoing hydrogen shell burning, because the large density gradient outside the core couples the g- and p-mode pulsation cavities (Aerts et al. 2010).

Asymptotic pulsation modes

For high radial order pulsation modes that satisfy $n >> \ell$, p modes become approximately equally spaced in frequency and g modes become approximately equally spaced in period, which is known as the asymptotic regime of pulsation (Tassoul 1980; Gough 1986). Asymptotic pulsation modes create regularities in the amplitude spectrum of a pulsating star, which simplifies mode identification. Deviations from the regular spacings in frequency and period for p and g modes, respectively, have been utilised to study physics within the interiors of intermediate-mass stars, such as chemical mixing (Miglio et al. 2008) and rotation (Bouabid et al. 2013; Van Reeth et al. 2015b, 2016).

1.1.2 What is amplitude modulation?

The oscillations of a star can be detected using two main methods. The first method is to use photometry to measure the periodic changes in surface flux, which are caused by variations in surface temperature, and create a light curve for a star. The second method is to use spectroscopy to measure the displacement variations of the stellar surface and create a time series of radial velocity measurements. The common practice in asteroseismology is to use Fourier analysis to calculate an amplitude (or power) spectrum from a time series and extract the frequencies, amplitudes and phases of the detectable pulsation modes.

Non-continuous observations produce large gaps in a stellar time series and consequently complex window patterns in an amplitude spectrum, which makes it difficult to study pulsating stars. Despite this and the generally high levels of noise in ground-based observations, some δ Sct stars have been shown to oscillate with pulsation modes that varied in amplitude over time spans of months and years (Breger 2000b, 2009, 2016). This raises the question of what physical mechanism is causing the modulation of pulsation mode amplitudes in δ Sct stars. There are few published examples of δ Sct stars that exhibit amplitude modulation and it is difficult to draw any meaningful conclusions from so few examples. A useful case study of amplitude modulation in a δ Sct star observed from the ground is 4 CVn (Breger 2000b, 2009, 2016), which is discussed further in section 1.5.

A space telescope on the other hand can provide nearly continuous observations with a duty cycle close to 100 per cent, and a high photometric precision. The dawn of space telescopes useful for asteroseismology provides strong motivation for studying δ Sct stars in more detail. In this thesis, observations from the *Kepler* Space Telescope (Borucki et al. 2010) are used to study amplitude modulation and its possible causes using an ensemble of approximately 1000 δ Sct stars.

1.2   The delta Scuti stars

The δ Sct stars are the most common group of pulsators among the A and F stars and have been studied since the discovery of their variability about a century ago (Campbell & Wright 1900; Fath 1935; Colacevich 1935). In this section, a review of δ Sct stars is presented, including a historical overview, a summary of their physical properties and a discussion of the dominant pulsation excitation mechanism. Note that the chemically peculiar stars found in a similar location to the δ Sct stars in the HR diagram are discussed in section 1.3.2, with the current section focusing on the pulsations in δ Sct stars. Reviews of the physical properties of δ Sct stars are also given by Breger (2000a), Aerts et al. (2010) and Murphy (2014).

1.2.1   Historical overview

The first detection of variability in a δ Sct star was made by Campbell & Wright (1900), who studied nine purported spectroscopic binaries using radial velocity measurements. Campbell & Wright (1900) provided no explanation for the variability, but simply noted it. A few decades later, Fath (1935) and Colacevich (1935) used photometry and radial velocity measurements, respectively, to accurately determine the period of the variability in the star δ Sct itself. They placed it in the variable star group β Canis Majoris, which are today known as β Cep stars (Aerts et al. 2010). The few stars in this group had large photometric amplitudes as ground-based observations were restricted by high noise levels that created a strong selection bias. It was Eggen (1956) who first suggested that a new and separate type of variable star exists, of which δ Sct was the eponymous member. As instrumentation improved, lower levels of noise and an improved duty-cycle allowed more pulsating stars similar to δ Sct to be discovered and added to the group (Breger 1979).

The majority of discoveries throughout the early era of δ Sct research were based

on studying high-amplitude radial pulsation modes. One of the important conclusions from these studies was made by Breger & Bregman (1975), who calculated pulsation constants (see section 1.2.5) for radial pulsation modes in δ Sct stars and compared them to the predicted values from stellar models created by Cox et al. (1972). From the observations, it was discovered that hotter δ Sct stars typically have higher pulsation mode frequencies (Breger & Bregman 1975).

The focus of δ Sct research expanded to include the study of non-radial pulsation modes, with improved instrumentation allowing dozens, and sometimes hundreds, of low amplitude pulsations to be detected in many δ Sct stars (Baglin et al. 1973; Breger 1979). From a larger number of stars it was demonstrated that most δ Sct stars pulsate in low amplitude non-radial modes in addition to high-amplitude radial modes. Theoretical pulsation models were not limited by instrumentation and predicted a rich spectrum of p, g and mixed modes for δ Sct stars (Dziembowski et al. 1995), but only a few stars were observed to pulsate in high-degree modes ($\ell \leq 20$), for example τ Peg (Kennelly et al. 1998) and 4 CVn (Breger 2000b, 2009).

Today, the δ Sct stars represent a diverse group of stars that host a range of pulsational behaviour. The rich spectrum of pulsation modes excited in these stars offer the potential of probing physics at different depths using asteroseismology, which emphasises that δ Sct stars are useful for studying stellar structure and evolution in a transition region between low- and high-mass stars (Breger 2000a).

1.2.2   Physical properties

The δ Sct stars are Population I stars with spectral types between A2 and F2 (Rodríguez & Breger 2001). This places them within the mass range of $1.5 \leq M \leq$ 2.5 M$_\odot$ and within the effective temperature range of $6900 \leq T_{\text{eff}} \leq 8900$ K whilst on the ZAMS, although more evolved δ Sct stars can be as cool as $T_{\text{eff}} \simeq 6300$ K (Uytterhoeven et al. 2011). The δ Sct stars are found at the intersection of the main

sequence and the classical instability strip in the HR diagram, which is shown by a green hatched region in Fig. 1.1. Using ground-based observations, Rodríguez & Breger (2001) were able to constrain the location of δ Sct stars in the HR diagram by defining observational blue and red edges of the classical instability strip. Calibrated values of absolute visual magnitude M_{V}, colour $B - V$, and effective temperature T_{eff} for main sequence dwarfs (i.e., luminosity class V) around spectral type A are given in Table 1.1, which cover the expected range for δ Sct stars.

The δ Sct stars are often referred to as intermediate-mass stars as they lie in a transition region between early- and late-type stars (i.e., high- and low-mass stars), with the separation commonly defined at a spectral type of G0 (Gray & Corbally 2009). This separation is useful because it also corresponds to the lower limit in stellar mass, specifically $M \simeq 1.1$ M$_\odot$, for a main sequence star to have a convective core. Therefore, the pulsations in δ Sct stars provide the opportunity to study stellar structure and evolution in the interesting transition region from radiative cores and thick convective envelopes in low-mass stars ($M \lesssim 1$ M$_\odot$) to large convective cores and radiative envelopes in high-mass stars ($M \gtrsim 2$ M$_\odot$). Concurrently, the δ Sct stars also represent a transition in luminosity from the high amplitude radial pulsators, such as Cepheid variables, and the non-radial multiperiodic pulsators within the classical instability strip (Breger 2000a). Most δ Sct stars cross the instability strip on approximately horizontal tracks (Breger 2000a), which places them in the core hydrogen or hydrogen shell-burning stage of stellar evolution (Aerts et al. 2010).

Many δ Sct stars are multiperiodic pulsators with numerous radial and non-radial modes with pulsation periods of order a few hours (Uytterhoeven et al. 2011), but can be as short as 15 min (Holdsworth et al. 2014a). However, one of the difficulties encountered when studying δ Sct stars is the issue of mode identification, which is discussed further in section 1.2.5. If pulsation modes can be identified, the rich amplitude spectra of δ Sct stars allow stellar structure to be studied in great detail

Table 1.1: Observed parameters of the main sequence stars similar in spectral type to the δ Sct stars. Values of the absolute visual magnitude, M_V, which are calibrated to spectral type, are from Gray & Corbally (2009), with values of colour, $B - V$, taken from Fitzgerald (1970). Calibrated values of effective temperature, T_{eff}, were taken from Bessell (1979) and rounded to the nearest 50 K, with some values interpolated using the colour-temperature relations from Gray (2005).

Spectral Type	M_V (mag)	$B - V$ (mag)	T_{eff} (K)	Comment
B8	0.0	-0.11	12 000	
B9	0.7	-0.07	11 000	
A0	1.4	-0.01	10 000	
A1	1.6	0.02	9500	
A2	1.9	0.05	9000	
A3	2.0	0.08	8800	δ Sct blue edge
A4		0.12	8500	
A5	2.1	0.15	8250	
A6	2.2	0.17	8100	
A7	2.3	0.20	7850	γ Dor blue edge
A8	2.4	0.27	7400	
A9	2.5	0.30	7250	
F0	2.6	0.32	7100	
F1	2.8	0.34	7000	δ Sct red edge
F2	3.0	0.35	6950	
F3	3.1	0.41	6650	
F4	3.3	0.42	6600	
F5	3.4	0.45	6500	γ Dor red edge
F6	3.7	0.48	6350	

for both main sequence and post-main sequence stars.

1.2.3 Pulsational instability: driving versus damping

There are several mechanisms that can drive pulsation in stars across the HR diagram, but pulsational instability is always a balance between the driving and damping processes within a star, which are dependent on stellar structure. The temperature gradient within a star's envelope is a strong function of the effective temperature. As one transitions up the main sequence from late- to early-type stars, the depth of the surface convective envelope rapidly decreases, thus the ratio of the convective flux to total flux also decreases. This transition in stellar structure from low-mass stars with thick envelopes with energy transport dominated by convection to intermediate-mass stars with thin surface convective envelopes is shown in Fig. 1.4. The top panel of Fig. 1.4 shows the temperature range within the stellar envelope that is unstable to convection as a hatched region, as a function of effective temperature. The bottom panel of Fig. 1.4 shows the fraction of the convective flux to the total flux, as a function of effective temperature. Therefore, stars within the temperature range $7000 \leq T_{\mathrm{eff}} \leq 9000$ K, i.e., the early-F and late-A stars, represent a transition in stellar structure for which convection goes from being the dominant energy transport mechanism to a negligible contribution to the surface flux, respectively.

This change in stellar structure is the underlying cause of pulsation in the classical instability strip in the HR diagram and has been discussed in detail by Pamyatnykh (1999, 2000), Christensen-Dalsgaard (2000) and Aerts et al. (2010). The boundary between the adiabatic inner region and the non-adiabatic surface of the stellar envelope is defined as the *transition region*, in which the gradient of the flux $\delta L/L$ is not constant (Aerts et al. 2010). If the energy contained within the stellar material is large enough to cause a significant positive or negative perturbation to
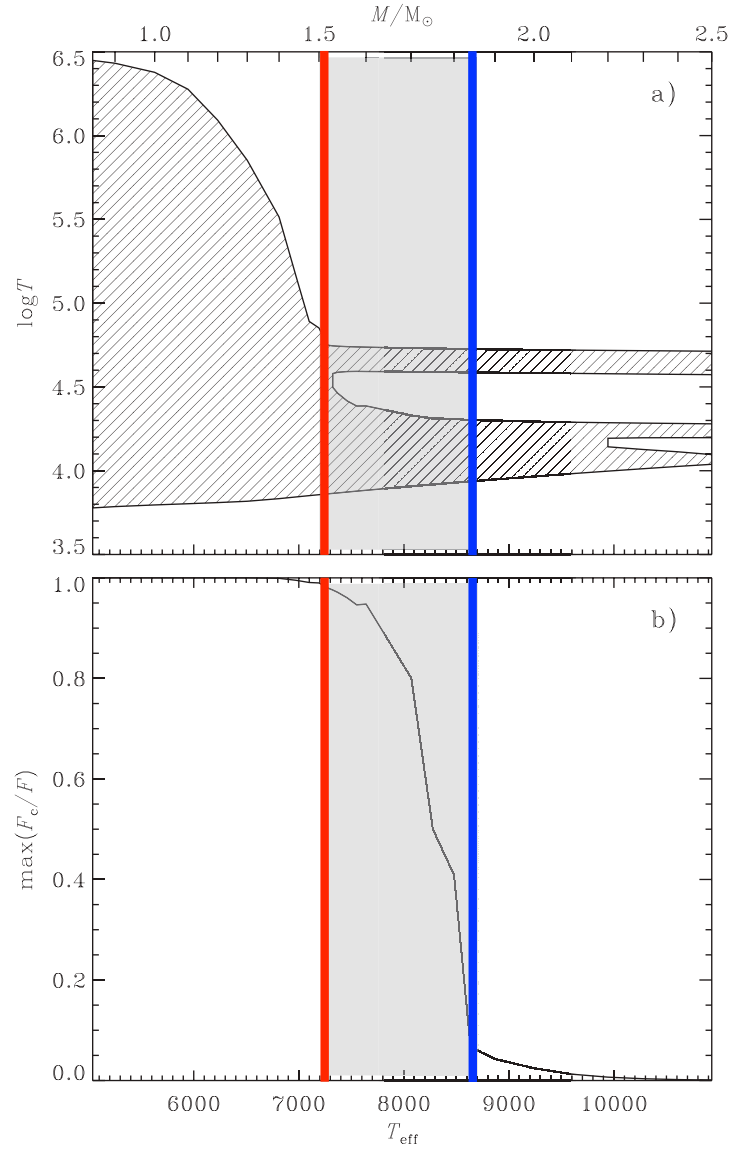
Figure 1.4: The structure of the stellar envelope in intermediate-mass ZAMS stars. The hatched region in the upper panel represents the temperatures within the stellar envelope that are unstable to convection as a function of T_{eff} (lower abscissa) and stellar mass (upper abscissa). The lower panel shows the fraction of flux that is transported by convection in the envelope as a function of T_{eff}. The cool and hot boundaries of the classical instability strip are shown by red and blue lines, respectively, which defines a transition region in between. Figure adapted from Christensen-Dalsgaard (2000), his figure 3. Reproduced with permission from AS-PCS.

the flux, i.e., δL, then it can contribute to damping or driving, respectively. The classical instability strip in the HR diagram corresponds to stars within a small range of effective temperature, such that an effective driving mechanism occurs at the same depth as the transition region, which defines hot and cool edges shown as blue and red lines in Fig. 1.4, respectively.

Pulsations in δ Sct stars are self-excited by the κ mechanism, resulting in a rich spectrum of predominantly low-overtone radial and non-radial p modes (Breger 2000a). The ionisation layers of H and He I at $T \simeq 15\,000$ K are too close to the surface and are not believed to play an important role, whereas the He II ionisation layer at $T \simeq 48\,000$ K provides increased opacity which is able to block the outward flow of radiation (Cox 1963; Chevalier 1971). Consequently, pulsations in δ Sct stars follow Eddington's heat engine cycle as discussed in section 1.1, with layers of gas in the stellar envelope periodically expanding and contracting about an equilibrium point to allow radiation to reach the stellar surface. The asymptotic relations of Tassoul (1980) are not applicable to the low-overtone p modes observed in δ Sct stars, which make mode identification difficult in these stars. Methods for identifying pulsation modes in δ Sct stars are discussed in section 1.2.5.

Synthetic amplitude spectra generated using theoretical pulsation models of δ Sct stars are only able to reproduce observations in a schematic sense, with models often predicting many more pulsation modes excited than are observed. For example, Dziembowski (1977b) calculated that high-degree modes ($\ell \leq 1000$) can be excited in a δ Sct star in the centre of the classical instability strip. However, it is not clear how observations of δ Sct stars with similar effective temperatures, structure and evolutionary state can have significantly different amplitude spectra. What physics determines which pulsation modes are excited, what their amplitudes are and how different pulsation modes interact with each other? A mode selection mechanism is clearly at work within δ Sct stars, as some stars pulsate in only a few radial

modes whereas others pulsate in dozens (sometimes hundreds) of radial and non-radial modes (Breger 2000a). Similarly, pulsation mode amplitudes in δ Sct stars can exceed 0.1 mag, whilst others are of the order of a few μmag. There is a diverse range of observed behaviour in δ Sct stars, so it is also possible that multiple mode selection mechanisms occur simultaneously within a star, or different mechanisms are dominant in different regions of the classical instability strip in the HR diagram. The nature of what causes the diversity of pulsational behaviour in these stars is one of the goals of asteroseismology and motivates the continued study of these stars.

Theoretical models are able to reproduce the observational blue and red edges of the classical instability strip with differing levels of success, and thus if a star is stable or unstable to pulsation (Pamyatnykh 1999; Houdek 2000; Dupret et al. 2004, 2005; Grigahcène et al. 2010a). At the blue edge ($T_{\mathrm{eff}} \simeq 8800$ K), the temperature of a star is too high to support a deep enough driving layer within the star, such that the He II ionisation zone is too shallow where the density of the stellar medium is insufficient to excite pulsation (Pamyatnykh 1999, 2000; Christensen-Dalsgaard 2000; Houdek 2000; Dupret et al. 2004, 2005). Thus, damping wins over driving at the blue edge and a star is returned to stability. Whereas at the red edge ($T_{\mathrm{eff}} \simeq 6900$ K), a star is returned to stability as the surface convective envelope becomes substantial enough such that convection damps the pulsations (Christensen-Dalsgaard 2000; Houdek 2000; Dupret et al. 2004, 2005). At the red edge, the κ mechanism is unable to overcome the damping from convection making the red edge more difficult to determine theoretically than the blue edge (Pamyatnykh 1999; Houdek 2000; Dupret et al. 2004, 2005). The interplay of convection and pulsation is crucial for our understanding of the red edge, with models including time-dependent convection with different treatments of mixing-length theory often needed to accurately match observations (Houdek et al. 1999b; Houdek 2000; Dupret et al. 2005; Grigahcène et al. 2005; Houdek & Dupret 2015).

It is important to note that the structure of a star does change throughout its evolution, including whilst it is on the main sequence (see figure 3.6 from Aerts et al. 2010). Most δ Sct stars evolve across the classical instability strip on approximately horizontal tracks, so a star can be unstable to pulsation at the ZAMS and not be unstable to pulsation at the TAMS, and vice versa (Breger 2000a).

Stochastic excitation of pulsation modes

Despite their thin convective envelopes, theoretical models of δ Sct stars predict that stochastically driven pulsations should be excited in these stars (Houdek et al. 1999a; Samadi et al. 2002). These authors used the time-dependent non-local mixing-length formalism for convection from Gough (1977) to study the stability of solar-like oscillations in δ Sct stars near the red edge of the classical instability strip. It was found that turbulence from the surface convection zone was sufficient to excite all the eigenmodes within a frequency range and excite solar-like oscillations to observable amplitudes (Houdek et al. 1999a; Samadi et al. 2002). However, dedicated observations have been unsuccessful in detecting solar-like oscillations in δ Sct stars (e.g., Antoci et al. 2013).

A claim of finding stochastically excited p modes in the δ Sct star HD 187547 (KIC 7548479) using data from the *Kepler* Space Telescope was made by Antoci et al. (2011), but a later analysis of the same star with a longer data set revealed that turbulent pressure operating in the H I zone was instead responsible (Antoci et al. 2014). In stars with solar-like oscillations, the turbulent motions in the thick convective envelope have random phases and produce stochastic driving (see section 1.4.2). Whereas, turbulent pressure, or the perturbation to the momentum flux associated with a convectively unstable region (Houdek 2000), is able to produce coherent driving in δ Sct stars. Driving from turbulent pressure in a δ Sct star is able to excite higher radial order ($7 \leq n \leq 10$) pulsation modes (Houdek 2000),

and is analogous to driving from the κ mechanism operating in the He II ionisation zone. For the case of the δ Sct star HD 187547, it was shown using theoretical models how the phase lag between the response of the turbulent pressure to an incoming pulsation wave or density perturbation creates coherent driving of high frequency pulsation modes (Antoci et al. 2014). The study by Antoci et al. (2014) of HD 187547 emphasises the importance of the interplay between convection and pulsation in δ Sct stars, especially for those with significant surface convection zones.

1.2.4   Non-linear effects

In any simple oscillatory motion, for example a spring or a swinging pendulum, there is no dependency of the amplitude on the oscillation period in the linear regime. Thus we have no prediction of the pulsation amplitudes in variable stars using linear models. The role of non-linearity in classical pulsators has been discussed in the literature for some time (e.g., Stellingwerf 1975a,b). However, the use of non-linear pulsation models to study δ Sct stars led to the problem now known as *'The Main Sequence Catastrophe'* — models predicted that pulsation amplitudes would grow exponentially and become large enough to cause the outer layers of a star to exceed the escape velocity (Stellingwerf 1980). Therefore, the pulsation mechanism would cause a star's outer layers to overcome the force of gravity and be dispersed from the star. This is similar to the late thermal pulses caused by repeated onsets of helium shell-burning in stars with masses between $2.3 \leq M \leq 9$ M$_\odot$ as they ascend the asymptotic giant branch (Aerts et al. 2010). Since observations of δ Sct stars do not have significant mass-loss rates on the main sequence and typically pulsate with amplitudes of order a few mmag, some physics is clearly missing from the pulsation models.

A solution may lie in introducing stronger damping effects deep within a star,

since the interactions between modes and the convection zone itself are not understood (Saio & Cox 1980). Alternatively, a non-linear mode selection and/or amplitude saturation mechanism is needed to limit the growth of mode amplitudes to explain observations (Dziembowski 1982). The mechanism(s) that determine the amplitudes of pulsation modes are largely unknown (see e.g., Nowakowski 2005), but a mechanism is needed to reproduce observations. This demonstrates the synergy needed between theory and observations and the motivation for further study of these stars.

1.2.5 Mode identification

A requirement of asteroseismology is to measure the frequency of pulsation modes, and identify modes in terms of their radial order n, angular degree ℓ and azimuthal order m. In the following subsections, different techniques for pulsation mode identification are discussed in the context of δ Sct stars.

Scaling relations

Mode identification is simplified for stars that pulsate in high-overtone p modes, because the pulsation modes are approximately equally spaced in frequency from being in the asymptotic regime (Tassoul 1980; Gough 1986). The separation in frequency between consecutive overtone radial modes is known as the large separation $\Delta\nu$. Therefore, if multiple high overtone radial modes are excited then a comb-like pattern of frequencies is observed in the amplitude spectrum.

Pulsation modes in δ Sct stars are typically low radial order, thus are not in the asymptotic regime. This makes it difficult to identify pulsation modes from the lack of obvious patterns in their amplitude spectra. For a few δ Sct stars, however, radial modes have been identified from observing the large frequency separation. The δ Sct star FG Vir was found to contain regularities in its amplitude spectrum that were

conjectured to be caused by the separation between consecutive overtones of radial modes (Breger et al. 2009).

Period ratios

The period ratios of high-amplitude pulsation modes can be used to identify radial modes in δ Sct stars. The period ratio of the first overtone to fundamental radial mode for δ Sct stars is between $0.756 \leq P_1/P_0 \leq 0.787$, and subsequent ratios are $0.611 \leq P_2/P_0 \leq 0.632$ and $0.500 \leq P_3/P_0 \leq 0.525$ for the second and third radial overtones, respectively (Stellingwerf 1979). Caution is advised when applying this mode identification technique as mode trapping in the stellar envelope (Dziembowski & Krolikowska 1990) or moderate to rapid rotation can lead to ambiguities in stars with a high density of pulsation modes in their amplitude spectra (see e.g., Breger & Pamyatnykh 2006).

Pulsation constants

Pulsation modes can also be identified by calculating pulsation constants using

$$Q = P\sqrt{\frac{\bar{\rho}}{\bar{\rho}_\odot}} \, , \tag{1.1}$$

where Q is the pulsation constant in days, P is the pulsation period in days, and $\bar{\rho}$ is the mean stellar density, which is normalised to the solar value $\bar{\rho}_\odot$. Eq. 1.1 can be re-written as

$$\log\, Q = \log\, P + \frac{1}{2}\log\, g + \frac{1}{10}M_{\text{Bol}} + \log\, T_{\text{eff}} - 6.454 \, , \tag{1.2}$$

where $\log g$ is the surface gravity in cgs units, M_{Bol} is the Bolometric absolute magnitude and T_{eff} is the effective temperature in K. A value of M_{Bol} can be calculated using T_{eff} and $\log g$ values in comparison with the Pleiades main sequence stars or,

for example, using the calibrations given in Table 1.1.

Typical values of pulsation constants for the fundamental, first and second-overtone radial p modes in δ Sct stars lie between $0.022 \leq Q \leq 0.033$ d (Breger & Bregman 1975). The pulsation constant can be used to identify the overtone number, n, of radial modes (Stellingwerf 1979), but the calculation using Eqn 1.2 is strongly dependent on the stellar parameters used, particularly log g. For example, Breger (1990b) quotes fractional uncertainties in Q values as high as 18 per cent, which could cause a first overtone radial mode to be confused for either the fundamental or second overtone radial mode. Therefore, caution is advised when applying this method of mode identification.

1.2.6 HADS stars

McNamara (2000) defined the subgroup of high amplitude δ Sct (HADS) stars as radial pulsators with asymmetric light curves, large pulsation amplitudes and pulsation periods between 1 and 6 hr. The HADS stars are found in a narrow region within the classical instability strip with effective temperatures between $7000 \leq T_{\mathrm{eff}} \leq 8000$ K and are typically slow rotators with rotational velocities of $v \sin i \lesssim 40$ km s^{-1} (McNamara 2000; Rodríguez et al. 2000). HADS stars are typically characterised as δ Sct stars with peak-to-peak light amplitudes exceeding 0.3 mag (McNamara 2000), but have similar characteristics to evolved pulsators in the classical instability strip. For example, approximately 40 per cent of HADS stars pulsate in the fundamental and first overtone radial modes (McNamara 2000).

The similarities between HADS stars and evolved pulsators in the classical instability strip resulted in the HADS stars having a long history of being called transitionary objects and being compared to Cepheid variables (see section 1.4.4). Perhaps the most obvious similarity is the non-sinusoidal shape of the light curves, with the changes between maxima and minima light excursions being similar to

Cepheid variables and RRab stars (McNamara 2000). Another similarity is that many of the double-mode HADS stars observed in the Large Magellanic Cloud have the same period ratios as Cepheid variables (Poleski et al. 2010), and also follow the same Period-Luminosity relationship (Soszyński et al. 2008). Therefore, it is perhaps not surprising that the HADS stars have been historically thought of as dwarf Cepheids in the literature. For example, Eggen (1976) originally referred to δ Sct stars as ultrashort-period Cepheids (USPC).

It was conjectured by Petersen & Christensen-Dalsgaard (1996), that HADS stars are in a post-main sequence stage of evolution, which creates a physical parameter space that allows HADS stars to pulsate at much higher pulsation amplitudes than main sequence δ Sct stars. Such an evolutionary state would create large changes in stellar structure over a relatively short period of time (Breger 2000a), but it remains unclear if *all* HADS stars are in a post-main sequence stage of evolution. Alternatively, Breger (2000a) conjectured that slow rotation is a requirement for high-amplitude pulsations for stars within the classical instability strip. It is unclear if the term HADS should be used other than phenomenologically, and if there is a physical distinction in the structure or pulsational excitation mechanism of HADS stars compared to their low-amplitude δ Sct counterparts.

The main advantage of studying HADS stars is the simplification of mode identification through period ratios because of their high amplitudes and low mode density in their amplitude spectra. Statistical studies of intermediate-mass stars have shown that HADS stars are rare, making up less than one per cent of all stars within the classical instability strip (Lee et al. 2008). Clearly the HADS stars are interesting because they are able to pulsate at much higher amplitudes than δ Sct stars, which implies a physical difference in the structure and evolutionary stage of these stars.

1.2.7 SX Phoenicis stars

SX Phoenicis (SX Phe) stars are Population II variable stars located within the classical instability strip in the HR diagram, but are found below the ZAMS for Population I stars. They have similar pulsation periods to δ Sct stars, but have large pulsation amplitudes, low metallicities and large spatial motions, and were proposed as a separate class of object by Frolov & Irkaev (1984). The SX Phe stars are mostly found in globular clusters or dwarf galaxies and are considered blue stragglers because they are brighter and bluer than the cluster population. The origin of such objects may be from mass transfer in binary systems or the collision of two stars (Eggen & Iben 1989).

Since their definition, SX Phe stars have been observed to be multiperiodic pulsators with many low-amplitude non-radial modes in addition to high amplitude radial modes (Olech et al. 2005). Therefore, the pulsation mode frequencies and amplitudes are not enough to distinguish δ Sct and SX Phe stars, so confirmation of low metallicity and high spatial motion is often needed (Nemec & Mateo 1990; Balona & Nemec 2012).

A well-studied SX Phe star using data from the *Kepler* Space Telescope is KIC 11754974, which was shown to pulsate with frequencies between $16 \leq \nu \leq 25$ d^{-1}, one of which had an amplitude greater than 60 mmag (Murphy et al. 2013a). From the frequency analysis, Murphy et al. (2013a) demonstrated that KIC 11754974 was in a 343-d binary system and constrained the mass of the SX Phe primary and non-pulsating secondary to 1.53 M$_\odot$ and 0.63 M$_\odot$, respectively. The authors confirmed KIC 11754974 as a SX Phe star using asteroseismic modelling, and because spectroscopic observations indicated that the star was metal-poor throughout its interior, as opposed to exhibiting only a surface abundance anomaly (Murphy et al. 2013a).

1.3 The inhomogeneous A stars

The A stars are possibly the most diverse spectral type of all stars in the HR diagram, as the group contains many different aspects of physics including rotation, pulsation, magnetic fields and chemical peculiarities. These properties and the interplay amongst them have been studied to varying levels of success, but they are clearly important for our understanding of stellar structure and evolution. The previous section focussed on discussing pulsations in A stars – i.e., the δ Sct stars – but in this section the diversity of all A stars is discussed for completeness. The incidence of non-pulsating stars in the classical instability strip is discussed in section 1.3.1, the different types of chemically peculiar A stars in 1.3.2, and rotation among the A stars in the context of *Kepler* data is discussed in section 1.3.3.

1.3.1 The incidence of non-pulsating A stars

The results from statistical studies of a large number of A and F stars by Uytterhoeven et al. (2011) and Balona & Dziembowski (2011) showed that the majority of A stars observed by the *Kepler* Space Telescope are not pulsating above the detection threshold. The lack of pulsation in chemically peculiar stars is not surprising (see section 1.3.2), but the lack of pulsation in a chemically normal star within the classical instability strip is puzzling.

To test the purity of the classical instability strip to pulsation, Murphy et al. (2015a) searched for a non-pulsating chemically normal star within the classical instability strip using high-resolution spectroscopy and photometry from the *Kepler* Space Telescope. The search for such a star resulted in finding only one, specifically KIC 6128236 (HD 184521), which has stellar parameters of $T_{\mathrm{eff}} = 7000 \pm 100$ K, $\log g = 3.5 \pm 0.1$ and $v \sin i = 106 \pm 2$ km s^{-1} and a spectral type of F0V derived from a detailed spectroscopic analysis (Murphy et al. 2015a). It should be noted that the definition of whether a star is pulsating or not is dependent on the choice of

detection threshold, with an amplitude threshold of 50 μmag used by Murphy et al. (2015a) in their study. The lack of pulsation in KIC 6128236 remains a challenge to pulsation theory (Murphy et al. 2015a).

On the other hand, it has not been definitively established if *all* of the non-pulsating stars that lie within the classical instability strip are chemically peculiar. Further work is still needed to address this.

1.3.2 Chemically peculiar A stars

Chemical peculiarities in A stars come in many flavours, which are characterised by common features in spectroscopic observations. These include the non-magnetic, metallic-lined Am stars, the magnetic Ap stars, the rapidly oscillating Ap stars and the λ Boo stars. In the following subsections, these chemically peculiar stars are discussed in the context of pulsating A stars.

Am stars

The first description of Am stars was provided by Titus & Morgan (1940), and later expanded by Conti (1970) and Smith (1971a,b), who characterised Am stars as slow rotators having a difference of at least five spectral subclasses between their Ca K line strength and their metallic line strengths. An example of a spectral classification for an Am star is kA3hA9mF1 V, which was taken from Murphy et al. (2015a). The Am stars are the most common type of A star, with approximately 50 per cent of A stars at a spectral type of A8 being classified as Am stars (Smith 1973). Marginal Am stars (denoted as Am:) are those that show less than five subclasses between their Ca K line strength and their metallic line strengths (Cowley et al. 1969; Kurtz 1978), but are still significantly different to normal A star abundance patterns. A thorough review of the classification of Am stars using spectroscopy is given by Gray & Corbally (2009).

CHAPTER 1

Am stars are often found in close binary systems (Abt 1961; Abt & Levy 1985), with at least 60 per cent of all known Am stars in binary systems (Murphy 2014; Smalley et al. 2014), which is significantly higher than the binary fraction of approximately 35 per cent for all A stars (Abt 2009; Duchêne & Kraus 2013; Moe & Di Stefano 2016). The short orbital periods of Am stars are between $1 \leq P_{\mathrm{orb}} \leq 10$ d (Abt 1967), and are sufficient to tidally brake Am stars into being slow rotators. The slow rotation allows gravitational settling and radiative diffusion to occur in Am stars, with different metallic species rising from radiative levitation or sinking from gravity based on the number of absorption lines (Baglin et al. 1973). Mixing caused by turbulence would prevent the separation of atomic species, but this is negligible in the slowly rotating Am stars (Slettebak 1954, 1955), so transition metals form clouds near the stellar surface and are observed as overabundance anomalies.

It was thought that Am stars cannot pulsate with high mode amplitudes, because atomic diffusion depletes helium from the He II ionisation zone preventing driving by the κ mechanism (Baglin et al. 1973). Observations of Am stars from the ground were in agreement with theoretical predictions of the lack of pulsation in Am stars (Breger 1970). The first classical Am star found to pulsate was HD 1097 by Kurtz (1989), after many attempts to find such a star (e.g., Kurtz 1976). More recently, it has been shown by Smalley et al. (2011) that approximately 14 per cent of all known Am stars pulsate with amplitudes of order 1 mmag, showing that these stars are more complicated than previously thought.

An attempt at understanding how Am stars pulsate from the κ mechanism operating in the metal bump (or 'Z bump') in opacity was made by Richer et al. (2000), and by introducing stronger mixing mechanisms by Turcotte et al. (2000) and Théado et al. (2009). Pulsations in marginal Am stars can be understood using diffusion theory because residual helium in the He II ionisation zone is able to excite pulsations through the κ mechanism. Similarly, pulsations in evolved Am

stars (known as ρ Pup stars) can also be understood, as the evolutionary changes to stellar structure in these stars allow the He II ionisation zone to be replenished with helium. A thorough review of pulsations in Am stars is given by Kurtz (2000).

Ap stars

Chemically peculiar A stars, denoted as Ap stars, are much rarer and constitute only 10 per cent of all A stars (Wolff 1968). The Ap stars have strong dipolar global magnetic fields, which range from 300 G (Aurière et al. 2004) to as large as 34 kG in Babcock's star (HD 215441; Babcock 1960). The magnetic field in an Ap star is misaligned with the rotation axis, with the angle between the magnetic and rotation axes, known as the angle of obliquity (Stibbs 1950).

The Ap stars are slow rotators with rotation periods that can be larger than several decades (Mathys 2015), with very few Ap stars known to exist in close binary systems (Abt & Snowden 1973). The slow rotation in Ap stars is believed to be caused be the interaction of the magnetic field with the circumstellar disk during the pre-main sequence contraction phase, which effectively brakes the star (Stępień 2000).

The slow rotation and the presence of a strong magnetic field causes stratification in the atmosphere and often leads to chemical spots on the surface of an Ap star (Stibbs 1950), which can be stable for many decades and thus used to determine the rotation period of the star. These chemical spots are caused by atomic diffusion with the strong magnetic field trapping ions within the stellar atmosphere (see Kochukhov 2011 and references therein). These atmospheric overabundances are rare-earth elements, such as strontium, europium or chromium, and can be as large as 10^6 times solar values.

CHAPTER 1

roAp stars

The rapidly oscillating Ap (roAp) stars were first discovered by Kurtz (1982), and represent a subgroup of pulsating A stars that contain many complex aspects of physics. They are located within a small region near the main sequence within the classical instability strip (Cunha 2002), and pulsate with periods between 6 and 23 min with photometric amplitudes as large as 20 mmag in the B band (Kurtz 1990; Holdsworth et al. 2014b). The exact nature of the pulsational driving mechanism is not known in these stars, but it is thought that the κ mechanism operating in the hydrogen ionisation zone is responsible for the high-overtone roAp pulsations, although this may not be true for all roAp stars (Cunha et al. 2013). The roAp stars are rare, with only around 60 confirmed stars known, which is a few per cent of the known Ap stars (Holdsworth et al. 2014a; Smalley et al. 2015). Similarly to the Ap stars, the roAp stars are rarely found in binary or multiple systems (e.g., Schöller et al. 2012).

The most remarkable property of roAp stars is that they provide the opportunity to study pulsations in the presence of a strong magnetic field within a chemically peculiar star. Even though the roAp stars are located within the classical instability strip (Cunha 2002), they do not pulsate in low-overtone p modes, because the dipolar magnetic field is strong enough to suppress low overtone δ Sct pulsation modes (Saio 2005). In a roAp star, the pulsation axis is nearly aligned with the magnetic field axis, which are misaligned with the rotation axis — this is known as the oblique pulsator model (Kurtz 1982; Bigot & Dziembowski 2002; Bigot & Kurtz 2011), which allows the pulsations to be viewed from different orientations as the star rotates.

The lambda Boötis stars

The λ Boo stars are a rare class of Population I stars between late-B and early-F in spectral type which make up a total of approximately 2 per cent of A stars. They

are classified by having underabundant Fe-peak elements and approximately solar values of lighter elements, for example C, N and O (Gray & Corbally 2009). A study by Paunzen et al. (2002b) revealed that λ Boo stars are found at all stages of stellar evolution, suggesting that the mechanism that causes the underabundant Fe-peak elements occurs continuously throughout an intermediate-mass star's lifetime.

Most λ Boo stars found within the classical instability strip are on the main sequence or pre-main sequence and are observed to pulsate in p modes (Paunzen et al. 2002a). Therefore, there is no clear distinction between δ Sct stars and λ Boo stars from their observed pulsation mode frequencies, but asteroseismology is able to determine if a star is metal-weak throughout its interior or if the underabundances are limited to the star's atmosphere (e.g., Murphy et al. 2013a). It has been suggested that the chemically peculiar nature of λ Boo stars is caused by accretion by a star from the interstellar medium (see Murphy et al. 2015b and references therein). A thorough review and updated catalogue of known λ Boo stars is provided by Murphy et al. (2015b).

1.3.3   Rotation in A stars

Eponymously named after Robert Kraft, the *Kraft Break* divides the main sequence into slowly rotating low-mass stars and fast-rotating high-mass stars (Kraft 1967), with the boundary occurring at approximately spectral type F5 ($M \simeq 1.3$ $M_\odot$). Rotation is extremely important in high- and intermediate-mass stars, as it facilitates the mixing of chemical abundances (Zahn 1992; Talon et al. 1997). The distribution in the rotational velocities of A stars has been described as bimodal (Abt & Morrell 1995) with two populations of A stars: the fast-rotating chemically normal stars and the slowly rotating chemically peculiar stars. If the chemically peculiar stars are excluded, A and F stars generally lie above the Kraft Break and have rotational velocities that typically lie between $100 < v \sin i < 250$ km s^{-1} (Zorec & Royer

2012). The distribution of the fast rotating A stars peaks at A5, with stars at this spectral type rotating at approximately two-thirds of their break-up velocity (Royer et al. 2007).

An extensive study of rotation in A stars was carried out by Zorec & Royer (2012), who demonstrated that the distribution is more complex than simple bimodal populations of slowly rotating chemically peculiar stars and fast-rotating chemically normal stars. The probability density distribution for rotational velocities as a function of stellar mass in the range $1.6 \leq M \leq 3.5$ M$_\odot$ taken from Zorec & Royer (2012) is shown in Fig. 1.5. The rotational velocities of stars with masses between 1.6 and 2.5 M$_\odot$ – i.e., the A and F stars – only increase by a small amount over their main sequence lifetime (Zorec & Royer 2012). A recent thorough review of rotation among intermediate-mass stars is given by Murphy (2014).

The δ Sct stars are generally considered moderate or fast rotators (Breger 2000a), with rotational velocities that can be as high as 300 km s^{-1} (see e.g., KIC 8054146; Breger et al. 2012). From a high-resolution spectroscopic study of bright *Kepler* A and F stars, Niemczura et al. (2015) determined a mean rotational velocity of $v \sin i \simeq 134$ km s^{-1}, which supports the view that intermediate-mass stars are generally moderate rotators. However, some δ Sct stars have been confirmed as very slow rotators. For example, the δ Sct star 44 Tau (HD 26322) was determined to have a rotational velocity of $v \sin i = 3 \pm 2$ km s^{-1} (Zima et al. 2006), and the δ Sct star KIC 11145123 was determined to have a surface rotation period of approximately 100 d, which can be converted into a rotational velocity of $v_{\mathrm{eq}} \simeq 1$ km s^{-1} (Kurtz et al. 2014). Clearly there is a diverse range in rotational velocities among the δ Sct stars, which plays an important role when interpreting their amplitude spectra.
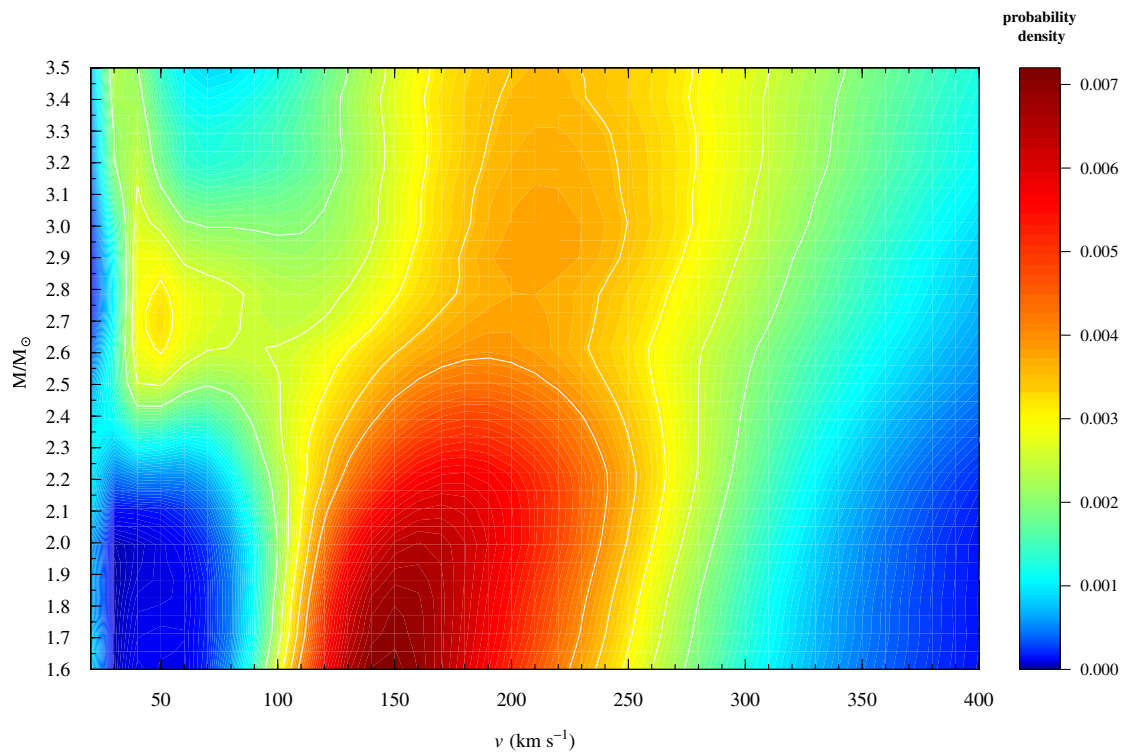
Figure 1.5: The contour of deprojected rotational velocities of chemically normal A stars excluding binary systems for the stellar mass range of $1.6 \leq M \leq 3.5$ M$_\odot$, which corresponds to an approximate spectral type range of F0 to B8, respectively. The fewest stars are found in the dark blue regions with a larger number of stars found in the dark red regions. Figure from Zorec & Royer (2012), their figure 7. © ESO; reproduced with permission from A&A.

CHAPTER 1

The effects of rotation on pulsation

Discussed by Ledoux (1951) and later by Dziembowski & Goode (1992), Goupil et al. (2000) and Aerts et al. (2010), the rotational splitting of a non-radial mode for the rest frame of an observer is commonly given by

$$\nu_{n\,\ell\,m} = \nu_{n\,\ell\,0} + m\left(1 - C_{n\ell}\right)\frac{\Omega}{2\pi} + D_{\mathrm{L}}\frac{m^2\Omega^2}{2\pi\nu_{n\,\ell\,0}}\;, \qquad (1.3)$$

where $\nu_{n\,\ell\,m}$ is the observed frequency, $\nu_{n\,\ell\,0}$ is the unperturbed frequency ($m = 0$), Ω is the angular velocity such that $\frac{\Omega}{2\pi}$ is the rotation frequency, $C_{n\ell}$ is the Ledoux constant, and D_{L} is a coefficient that depends on the character of a pulsation mode (Saio 1981; Dziembowski & Goode 1992). The sign convention in Eqn 1.3 follows Aerts et al. (2010), and is chosen such that positive values of m are prograde modes that travel in the direction of rotation, and modes with negative values of m are retrograde modes that travel against the direction of rotation.

Therefore, as shown by Eqn 1.3, rotation lifts the degeneracy of a non-radial pulsation mode into its $2\ell + 1$ components, which are observed as a multiplet in the amplitude spectrum. The splitting among the component frequencies of this multiplet is nearly exact but not perfectly in the cases of moderate and fast rotation because second-order effects act as an additional perturbation to the component frequencies (Goupil et al. 2000; Pamyatnykh 2003). For example, the Coriolis force in a rotating star acts against the direction of rotation and causes predominantly vertical variations to become circular (Aerts et al. 2010). The chosen sign convention in Eqn 1.3 results in prograde modes ($m > 0$) having higher frequencies than the central $m = 0$ component of the multiplet in the rest frame of an observer.

Using the slowly rotating δ Sct star 44 Tau as an example, a rotational splitting of approximately $0.02\,\mathrm{d}^{-1}$ is expected for this star (Breger et al. 2009). For most δ Sct stars, which are moderate and fast rotators, the amplitude spectrum can become

forest-like with much larger and asymmetric rotational splittings. This complicates the issue of mode identification and the detection of rotationally split non-radial pulsation modes.

Radial differential rotation

In the last few years, asteroseismology has been used to measure the radial rotation profile of stellar interiors throughout different stages of stellar evolution, from main sequence stars (Kurtz et al. 2014; Saio et al. 2015; Triana et al. 2015; Murphy et al. 2016; Schmid & Aerts 2016) to subgiant and red giant stars (Beck et al. 2012; Mosser et al. 2012; Deheuvels et al. 2012, 2014, 2015). The studies of interior rotation in these stars have revealed many interesting and unexpected results. The studied main sequence stars have almost uniform rotation, such that they are rotating approximately as a solid body. Moreover, these main sequence stars are slow rotators for their spectral type, but this is likely a selection effect, as it is easier to identify slowly rotating stars from the smaller rotational splitting in their amplitude spectra. See Aerts (2015) for a thorough review of interior rotation results obtained using asteroseismology.

Let us take the example of KIC 11145123 studied by Kurtz et al. (2014), which is a hybrid star pulsating in many g- and p-mode frequencies. The amplitude spectrum for KIC 11145123 is shown in Fig. 1.6, which shows a clear distinction in the g- and p-mode frequencies in this star. The authors used Eqn 1.3 to determine an upper constraint on the core rotation period of $P_{\text{core}} \geq 105.13 \pm 0.02$ d using $C_{n\ell} \simeq 0.5$ for the high-overtone g modes, and a lower constraint on the surface rotation period of $P_{\text{surface}} \leq 98.57 \pm 0.02$ d using $C_{n\ell} \simeq 0.03$ for the p modes (Kurtz et al. 2014). Therefore, the surface of this star is rotating slightly, but significantly, faster than the core. To understand a star on the main sequence with only a small gradient in its radial rotation profile, a physical mechanism other than viscosity is required
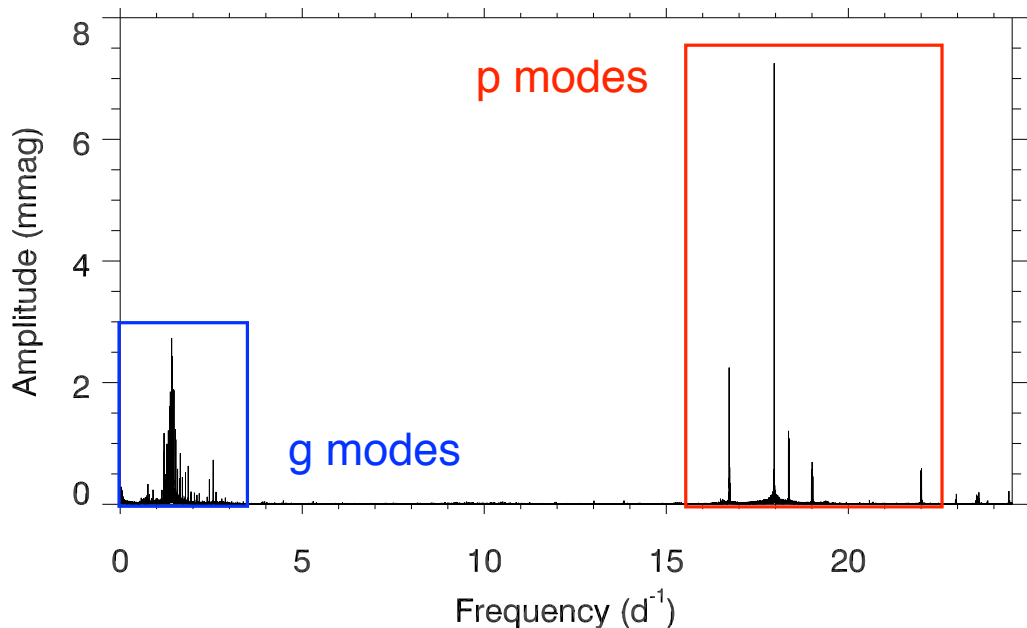
Figure 1.6: Core-to-surface rotation in KIC 11145123. The distinct g- and p-mode frequency regimes are clearly separated in the amplitude spectrum.

to redistribute angular momentum (Kurtz et al. 2014). What physical mechanism can cause such a rotation profile in a star? Further observations of similar stars are needed to help constrain theoretical models.

The investigation by Blomme et al. (2011) of three O stars observed by the CoRoT mission (Auvergne et al. 2009) found an excess of red noise in their amplitude spectra, which has been recently interpreted in terms of internal gravity waves (IGWs) in these stars (Aerts & Rogers 2015). These IGWs are able to efficiently transport angular momentum throughout a star, especially in stars with large convective cores and radiative envelopes (Rogers et al. 2013). Of the currently known main sequence stars with almost uniform rotation, perhaps the most remarkable is the Slowly Pulsating B (SPB) star KIC 10526294 studied by Triana et al. (2015). The authors studied a series rotationally split dipole modes that were almost equally spaced in period, and asteroseismically modelled the star to determine the radial

rotation profile. Their analysis indicated that the stellar envelope was not only rotating slightly faster than the core but was rotating in the opposite direction (Triana et al. 2015). It was shown by Rogers (2015) using numerical models that angular momentum transport by convectively-driven IGWs can not only cause uniform rotation in intermediate- and high-mass stars, but also explain counter-rotating cores and envelopes in a star, for example, KIC 10526294 (Triana et al. 2015). This is an exciting prospect that can be tested for many high-mass stars using asteroseismology in the near future.

1.4 Pulsations across the HR diagram

As shown by Fig. 1.1, pulsations can occur throughout all stages of stellar evolution, from pre-main sequence to the white dwarf cooling track. However, observations of the pulsation mode frequencies are not enough to fully classify a pulsating star, as other types of pulsators may have similar pulsation periods. Therefore, the fundamental parameters such as mass, effective temperature (or by proxy spectral type or colour) are also needed for a complete definition, and so that a star can be placed in the HR diagram. In the current section, a general discussion of different variable stars is provided in the context of amplitude modulation of pulsation modes.

1.4.1 The gamma Doradus stars

The gamma Doradus (γ Dor) stars were first considered a unique class of pulsating star about two decades ago (Balona et al. 1994; Kaye et al. 1999). They have similar effective temperatures and luminosities to δ Sct stars and are located on or near the main sequence in the HR diagram (Handler 1999; Uytterhoeven et al. 2011). The γ Dor stars are difficult to study from the ground because their long ($P \simeq 1$ d) pulsation periods are similar to the interval between nightly observations. They also

often have a high density of pulsation modes in their amplitude spectra resulting in beat periods of several months to years. Therefore, it is difficult to resolve individual pulsation modes in these stars without long-term continuous observations of order a few years.

With so few γ Dor stars known from ground-based observations, the largest increases in the number of these stars have come from space-based telescopes. For example, Handler (1999) used multi-colour Hipparcos photometry to study 70 γ Dor stars, which at the time was an increase in the number of known γ Dor stars by more than a factor of two. Whilst on the ZAMS, Handler (1999) found that γ Dor stars lie between $7200 \leq T_{\text{eff}} \leq 7700$ K and between $6900 \leq T_{\text{eff}} \leq 7500$ K if they are more evolved. A more complete sample of pulsating A and F stars was obtained by the *Kepler* Space Telescope, from which Uytterhoeven et al. (2011) found that most γ Dor stars were between F5 and A7 in spectral type and between $6500 \leq T_{\text{eff}} \leq 7800$ K in effective temperature.

Pulsations in γ Dor stars are driven by the flux blocking mechanism, which operates at the base of the surface convection zone (Guzik et al. 2000; Dupret et al. 2004, 2005; Grigahcène et al. 2005). At the boundary between the radiative envelope and the surface convection zone, there is an abrupt change in the dominant mechanism for energy transport. The large opacity gradient at this boundary causes luminosity to be blocked in the radiative zone. The surface convective zone is not able to adapt quickly enough to transport the increased flux causing the luminosity to be periodically blocked (Guzik et al. 2000). The theory of the flux blocking mechanism makes the assumption that fluctuations in convection are negligible throughout the pulsation cycle, because the local convective timescale at the base of the convection zone is similar to, or longer than, the pulsation period (Grigahcène et al. 2005). Thus, only stars with a non-negligible surface convection zone can be unstable from the flux blocking mechanism. Guzik et al. (2000) estimates that the optimum depth
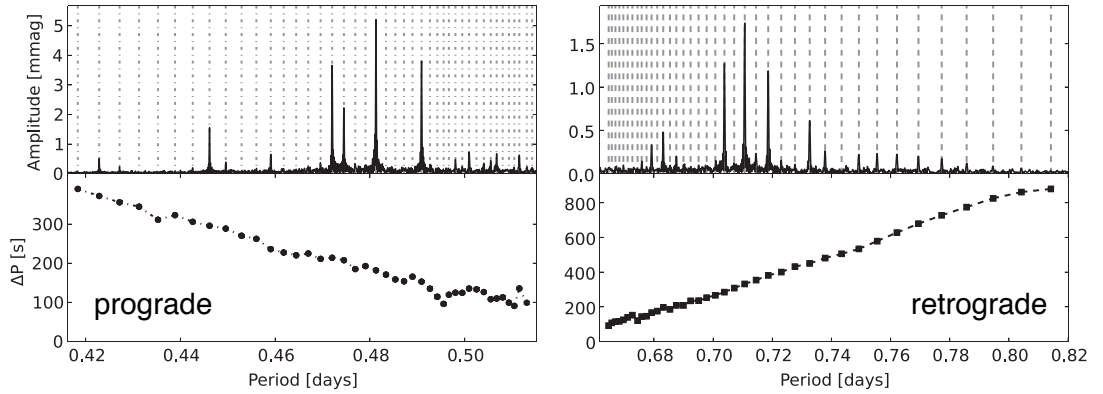
Figure 1.7: The asymptotic g-mode period spacing patterns in the γ Dor star KIC 8375138. The top panels show the amplitude spectrum using 4 yr of LC *Kepler* data. The bottom-left panel shows the prograde dipole modes identified as circles, and the bottom-right panel shows the retrograde dipole modes as squares. The vertical dashed grey lines are the expected location of the series (or comb) of pulsation mode frequencies. Figure adapted from Van Reeth et al. (2015b), their figure 4. © AAS; reproduced with permission from author and AAS.

of the convection zone as a fraction of the stellar radius should be $\simeq 0.975$, with larger convective envelopes creating large enough damping to suppress the pulsations. Therefore, the flux blocking mechanism is dominant in a narrow transition region between solar-type and δ Sct stars in the HR diagram (Guzik et al. 2000; Dupret et al. 2005).

The buoyancy-driven, high-order non-radial g modes produced by the flux blocking mechanism have periods that range between 8 hr and 3 d (Kaye et al. 1999; Balona et al. 2011a; Uytterhoeven et al. 2011). These high-order g modes follow the asymptotic approximation (Tassoul 1980; Gough 1986), such that g modes of the same degree are equally spaced in period for consecutive radial orders. The observed g modes and the departure from the equal period spacing have allowed the physical conditions deep within the stellar interior, such as chemical mixing (Miglio et al. 2008) and rotation (Bouabid et al. 2013; Van Reeth et al. 2015a, 2016), to be probed in many γ Dor stars. Excellent examples of γ Dor stars observed by the

Kepler Space Telescope to have 'combs' of g modes that are almost equally spaced in period are given by Van Reeth et al. (2015b, 2016). The gradient of the period spacing, ΔP, against the pulsation period, P, indicates the direction of the pulsation wave relative to the stellar rotation (Bouabid et al. 2011), with the example of KIC 8375138 taken from Van Reeth et al. (2015b) shown in Fig. 1.7. A positive gradient indicates retrograde motion and a negative gradient indicates prograde motion, with the gradient itself indicating the magnitude of the rotation.

On the other hand, many more γ Dor stars do not show regularities in their amplitude spectra consistent with asymptotic g modes that are approximately equally-spaced in period. The γ Dor stars are promising targets to study using asteroseismology with many new and exciting discoveries expected in the near future. Although the focus of this thesis is on amplitude modulation in δ Sct stars, the non-linearity of a selection of γ Dor stars observed by the *Kepler* Space Telescope is discussed in section 6.4.

1.4.2   Solar-type stars

Helioseismology is the specific application of studying oscillations in our nearest star — the Sun. Pulsations in the Sun are driven by stochastic turbulence in the convective envelope that simultaneously drives and damps the Sun to resonate in its natural oscillation modes (Goldreich & Keeley 1977a,b; Balmforth & Gough 1990), but the κ mechanism has also been shown to play a minor role (Balmforth 1992). These stochastically driven oscillations, often called solar-like oscillations, are expected in stars with thick convective envelopes and are predicted to be excited in stars as massive as 1.6 $M_{\odot}$ (Houdek et al. 1999a). Turbulence causes all the eigenmodes within a particular frequency range to be excited, so a roughly Gaussian peak of low-amplitude pulsation modes is observed. The centre of the Gaussian distribution is centred on a particular frequency, which is denoted $\nu_{\max}$. In the Sun,

the value of $\nu_{\max}$ is approximately 3 mHz, with pulsation periods ranging between approximately 3 and 15 min (Aerts et al. 2010).

Since the discovery that the Sun is a pulsating star, helioseismology has been used to study its interior (see e.g., Gough & Toomre 1991 and Christensen-Dalsgaard et al. 1996), including the determination of the depth of the convective envelope to be 0.287 ± 0.003 R$_\odot$ (Christensen-Dalsgaard et al. 1991). Helioseismic inversions of observed pulsation modes in the Sun have also allowed the internal rotation profile for a large fraction of the solar radius to be measured (Schou et al. 1998; Korzennik & Eff-Darwich 2011). The strong rotational shear at the base of the solar convection zone, termed the tachocline by Spiegel & Zahn (1992), is believed to be responsible for the 11-yr Schwabe activity cycle, causing a dynamic solar magnetic field that modulates the frequencies and amplitudes of the solar pulsation modes (Chaplin et al. 2000, 2007). Thus, the periodic changes in the frequencies and amplitudes of pulsation modes can be used as a proxy for magnetic activity in the Sun, and possibly other solar-type stars (Chaplin et al. 2011a). This concept has been applied to solar-type stars observed by CoRoT and the *Kepler* Space Telescope (see Régulo et al. 2016).

The p mode pulsations excited from convective turbulence in solar-type stars are high radial order, thus are in the asymptotic regime and are approximately equally spaced in frequency (Tassoul 1980; Gough 1986). The frequency spacing between consecutive radial order modes of the same angular degree, known as the large frequency separation, $\Delta\nu$, creates a similar comb-like pattern of pulsation modes in the amplitude spectra of these stars. Empirical scaling relations from the observables $\Delta\nu$ and $\nu_{\max}$ have allowed stellar parameters such as mass and radius to be determined (Kjeldsen & Bedding 1995). The scaling relations have been shown to be very robust with masses and radii of these stars accurate to less than three per cent in the best cases (Chaplin & Miglio 2013). These have been applied

to hundreds of solar-type stars (Chaplin et al. 2011b, 2014) and thousands of red giant stars (Stello et al. 2009; Huber et al. 2011), with a thorough review given by Chaplin & Miglio (2013).

1.4.3   Pulsating B stars

Understanding the physics at work within massive stars ($M \geq 9$ M$_\odot$) is an important goal for asteroseismology as these stars are important in stellar evolution theory. They also play a crucial role in the evolution of galaxies because they are supernovae progenitors that chemically enrich the interstellar medium. It was originally discussed by Maeder & Meynet (2000) how the insight of the internal rotation and possible mixing processes are of vital importance in understanding the evolution of these stars. The variety of pulsations in massive stars is interesting as the structure of these stars is similar across a wide range of stellar masses and effective temperatures, between the ZAMS and the TAMS (McNamara et al. 2012).

There are two main types of pulsating B star, the β Cep stars that pulsate in p and g modes and the Slowly Pulsating B (SPB) stars that pulsate in g modes (Aerts et al. 2010). The instability regions of these stars overlap in the HR diagram (Miglio et al. 2007; Paxton et al. 2015), thus hybrid stars of both pulsator type are expected and have been observed (e.g., Handler 2009; Degroote et al. 2012). The instability regions for high-mass stars have been investigated using the stellar evolution and modelling code `MESA` (Paxton et al. 2011, 2013, 2015), and are shown in Fig. 1.8. The `MESA` models calculated by Paxton et al. (2015) use different opacity tables, OPAL[2] and OP[3], with the latter shifting the instability regions to higher luminosities, a result also noted by Pamyatnykh (1999) and Miglio et al. (2007). There is also a very clear distinction between the SPB and the δ Sct instability regions, with theoretical models predicting that the κ mechanism is unable to excite pulsations

---

[2]Opacity Project at Livermore, for more information see Iglesias & Rogers (1996)
[3]The Opacity Project, for more information see Seaton et al. (1994)
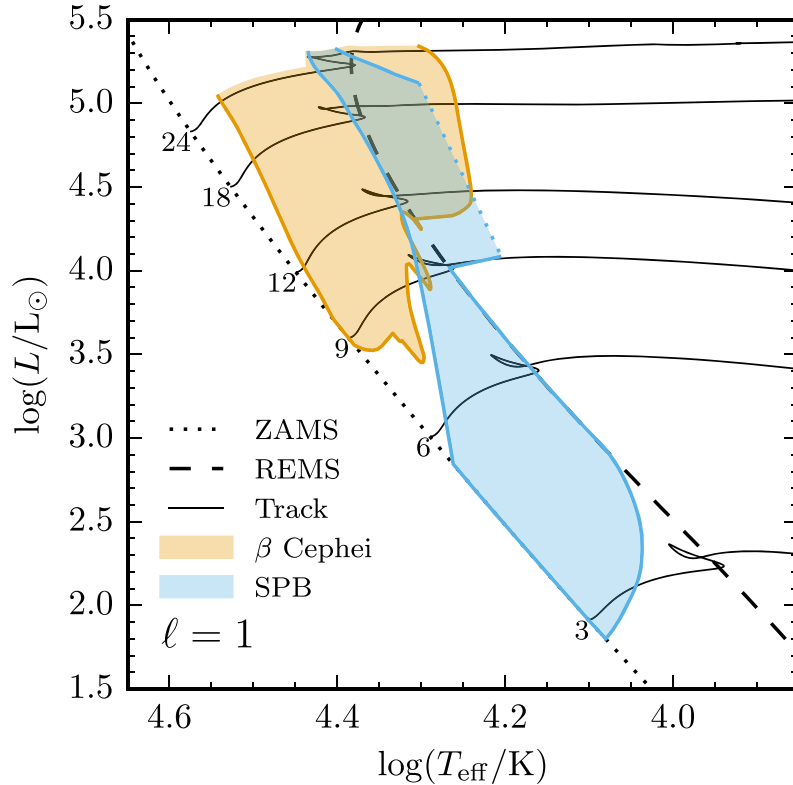
Figure 1.8: A theoretical HR diagram for the upper main sequence. The instability regions for β Cep and SPB stars calculated using `MESA` for dipole ($\ell = 1$) modes are shown in orange and blue, respectively. The zero-age main sequence (ZAMS) and red edge of the main sequence (REMS), or TAMS, are shown as dotted and dashed lines, respectively, and various evolutionary tracks are shown as solid black lines labelled by stellar mass in units of $M_\odot$. Figure from Paxton et al. (2015), their figure 11. © AAS; reproduced with permission from author and AAS.

in this gap (Pamyatnykh 1999).

A preliminary analysis of B stars observed by the *Kepler* Space Telescope was conducted by Balona et al. (2011b), who found that 15 of 48 B stars were pulsating. A follow-up study was performed by McNamara et al. (2012), who selected all stars observed by *Kepler* with effective temperatures above 10 000 K and within the region on a colour-magnitude diagram that is expected for a B star. This led to a total of 252 B stars, which were classified as β Cep, SPB, or a hybrid (McNamara et al. 2012). There were also subdwarf B and white dwarf stars, and targets that had

variability caused by rotation (spots) or binarity included in the sample (McNamara et al. 2012). Further analysis of more than 100 late-B stars observed by *Kepler* was conducted by Balona et al. (2015a) and extended to early-B stars by Balona (2016b), who focussed on the occurrence of low frequency variability in these stars. These low frequencies were often found to be non-periodic and interpreted to be caused by rotational modulation, suggesting that spots generated by magnetic fields can exist in stars with radiative envelopes (Balona et al. 2015a; Balona 2016b).

beta Cephei stars

The β Cep stars are high-mass ($8 \leq M \leq 18$ M$_\odot$) Population I stars, pulsating in g and p modes (Stankov & Handler 2005; Aerts et al. 2010). Pulsation modes in β Cep stars are excited by the κ mechanism operating in the Z bump in opacity at $T \simeq 200\,000$ K, which causes low-order radial and non-radial p modes with periods between 2 and 8 hr to become unstable (Dziembowski & Pamyatnykh 1993b). However, this is not a complete explanation of mode excitation in β Cep stars as observations have revealed that these stars also pulsate in g modes with periods of order a few days (Handler et al. 2004; Degroote et al. 2012). To explain the excitation of g modes by the κ mechanism, an overabundance of Iron in the driving zone needs to be assumed, which was demonstrated by Pamyatnykh et al. (2004) for the β Cep star ν Eridani, but the exact nature of g-mode excitation in these stars remains unclear.

Slowly Pulsating B stars

The group of Slowly Pulsating B (SPB) stars was originally defined by Waelkens (1991), with seven Population I B stars with spectral types between B3 and B9. The SPB stars are high-mass stars ($2 \leq M \leq 7$ M$_\odot$) with pulsation periods typically between 1 and 3 d, which similarly to γ Dor stars are difficult to study from the

ground without long-term multi-site observations. It is important to note that without an effective temperature estimate, the time series alone does not distinguish a γ Dor star from a SPB from the similar pulsation mode frequencies.

Pulsations in SPB stars are excited by the κ mechanism operating in the Z bump, which produces high-order low-degree g modes (Dziembowski et al. 1993). A large increase in the number of SPB stars was facilitated by the Hipparcos mission (e.g., Aerts et al. 1999), which allowed pulsation mode properties to be extracted and compared to predictions from theory that these stars pulsate in predominantly dipole modes (De Cat & Aerts 2002; Townsend 2005).

1.4.4 Evolved stars

In this section, RR Lyrae stars, Cepheid variables, white dwarfs and sdB stars are discussed in the context of amplitude modulation of their pulsation modes.

RR Lyrae stars

RR Lyrae (RR Lyr) stars are Population II classical pulsators with masses less than 1 $M_\odot$ that are in a post-giant stage of evolution on the horizontal branch (Breger 2000a; Aerts et al. 2010). RR Lyr stars were first classified by Bailey (1902) phenomenologically into subgroups of 'a', 'b' and 'c'. Since then, the 'a' and 'b' subgroups have been consolidated into what are now known as RRab stars, which have non-sinusoidal light curves with the dominant light variations caused by the fundamental radial mode. The 'c' subgroup contains RR Lyr stars which have sinusoidal light curves predominantly caused by the star pulsating in the first-overtone radial mode. The RR Lyr stars have been studied extensively since their discovery (e.g., Preston 1959; Stellingwerf 1975a), with more than 38 000 RR Lyr stars discovered in the bulge of the Milky Way (Soszyński et al. 2014).

RR Lyr stars are not purely periodic and exhibit a quasi-periodic form of amplitude and phase modulation that was first discovered by Blažko (1907), and is today known as the Blazhko effect (TSesevich 1953). The cause of the Blazhko effect in RR Lyr stars remains an unsolved problem but is a well-known example of pulsational non-linearity in asteroseismology. Another characteristic in the pulsation modes in RR Lyr stars is period doubling, which was predicted by Moskalik & Buchler (1990) as half-integer resonances (e.g., 3:2, 9:2) between radial overtones and the fundamental radial mode. In the light curve, period doubling appears as alternating maxima and minima in the brightness of the light excursions, which is shown in the bottom panel of Fig. 1.9. In the amplitude spectrum, period doubling appears as half-integer frequencies (sub-harmonics) in the form of $f(n + \frac{1}{2})$ where f is the frequency of the period-doubled pulsation mode (Moskalik & Buchler 1990; Kolenberg et al. 2010b; Kolláth et al. 2011). Period doubling is now believed to be ubiquitous in RR Lyr stars, with the first detection made in RR Lyr itself (KIC 7198959) and two other RRab stars observed by the *Kepler* Space Telescope (Kolenberg et al. 2010a; Szabó et al. 2010). A thorough review of period doubling and the Blazhko effect in RR Lyr stars is given by Szabó et al. (2014).

Cepheid variables

There are two flavours of Cepheid variables, which are referred to as type I and type II Cepheids in the literature. Cepheid variables are stars that are crossing the classical instability strip in the core helium burning stage of stellar evolution, or are stars in a post red giant stage of evolution that are crossing the classical instability strip for a second time (Aerts et al. 2010).

Type I Cepheids are also known as classical Cepheids and are Population I stars, which typically pulsate in the fundamental radial mode and can have amplitudes as large as 1 mag. They are evolved giant or supergiant stars with spectral types
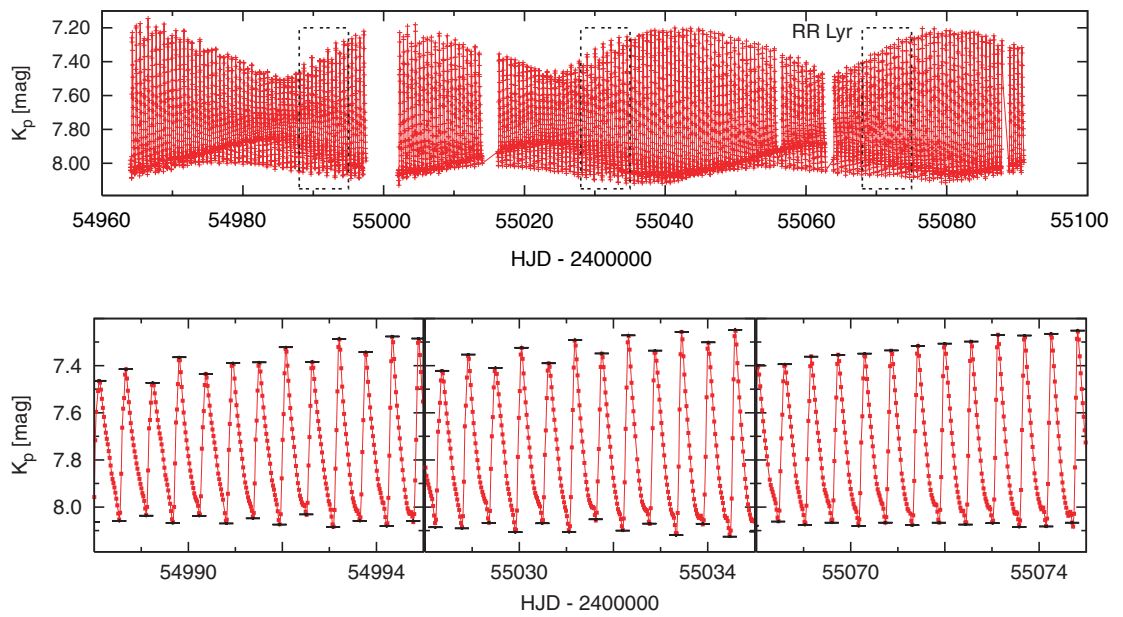
Figure 1.9: The Blazhko effect and period doubling in RR Lyr (KIC 7198959). The top panel shows the long-term quasi-periodic ($P \simeq 40$ d) amplitude modulation known as the Blazhko effect in RR Lyr using data from the *Kepler* Space Telescope. The bottom panel shows a zoom-in of the three dashed-edge boxes from the panel above, in which the transient period doubling effect can be seen. Figure adapted from Szabó et al. (2010), their figures 3 and 4.

between F5 and G5 (Aerts et al. 2010). Typical pulsation periods are between 1 and 50 d, with the longer period Cepheids located in the top-right part of the classical instability strip. Similarly to RRab stars, the light curves of type I Cepheids are non-sinusoidal caused by their high-amplitude and non-linear pulsations, with maximum brightness occurring approximately at the epoch of minimum radial velocity of the stellar surface. Some Cepheids pulsate in the first or second radial overtone in addition to the fundamental radial mode and are known as double-mode Cepheids, so further properties of these star such as mass and radius can be determined from the period ratio of the observed modes (Petersen 1973).

Type II Cepheids are Population II stars, which are crossing the classical instability strip as they transition from the horizontal branch to the asymptotic giant branch. They typically pulsate in the fundamental or first overtone radial mode, with excitation from the κ mechanism operating in the hydrogen and helium ionisation zones (see e.g., Bono et al. 1997). Unlike their type I cousins, type II Cepheids are not a homogenous group of stars, with subgroups defined by the observed pulsation periods: BL Herculis stars pulsate with periods between 1 and 5 d, W Virginis stars pulsate with periods between 10 and 20 d, and RV Tauri stars pulsate with periods longer than 20 d (Aerts et al. 2010). An extensive review of type II Cepheids is given by Wallerstein (2002).

Amplitude modulation has also been observed among Cepheid variables (see e.g., Breger 1981). A study of double-mode Population I Cepheids in the LMC, which pulsate in the first and second overtone radial modes has revealed that approximately 19 per cent of these stars exhibited variable pulsation mode amplitudes (Moskalik et al. 2006; Moskalik & Kołaczkowski 2009). This quasi-periodic form of amplitude modulation is similar to the Blazhko effect observed in RR Lyr stars, but had periods longer than 700 d. Furthermore, the amplitude modulation of the two radial overtone modes in a Cepheid are always anti-correlated, such that the

maxima of one radial mode coincides with the minima of the other (Moskalik & Kołaczkowski 2009). Blazhko models were unable to explain the observations of amplitude modulation in these double-mode Cepheid variables, and it was proposed that the resonant interaction of radial and non-radial modes may be responsible (Moskalik & Kołaczkowski 2009).

Sub-dwarf B stars

The subdwarf B (sdB) stars are low luminosity B stars with masses below 0.5 $M_{\odot}$, effective temperatures between $28\,000 \leq T_{\mathrm{eff}} \leq 35\,000$ K and which have weak He I lines in their spectra (Kilkenny 2007; Aerts et al. 2010). The sdB stars are in an unusual stage of stellar evolution having experienced significant mass loss on the red giant branch, which strips the star of its envelope leaving a helium core. The sdB stars are found between the giant branch and the extreme horizontal branch in the HR diagram, which is indicated by the dashed-dot line in Fig. 1.1, and they are progenitors of white dwarf stars.

The first sdB star observed to pulsate was EC 14026 with a pulsation period of 144 s and an amplitude of 12 mmag, which was discovered by Kilkenny et al. (1997, 1998) and is labelled in the HR diagram given in Fig. 1.1. Since their discovery, many variable sdB (sdBV) stars have been observed to pulsate with g, p or mixed modes with periods between 80 and 600 s and amplitudes between 1 and 300 mmag (Kilkenny 2007). The g mode sdBV stars are slightly cooler than the p mode sdBV stars, so these stars are analogous the SPB and β Cep stars, and also the γ Dor and δ Sct stars. Pulsations in sdBV stars are driven by the κ mechanism operating in the Z bump with predominantly low-overtone non-radial p modes of $\ell = 3$ or 4 being excited (Fontaine et al. 2003; Jeffery & Saio 2006a), but g modes of $\ell = 3$ or 4 can also be excited (Jeffery & Saio 2006b). An observational review of variable sdB stars is given by Kilkenny (2007).

CHAPTER 1

Amplitude variations from one observing season to another were first noted for the prototype sdBV star by Kilkenny et al. (1997), and in other sdBV stars since (Kilkenny et al. 2007). Using follow-up observations of a selection of sdBV stars, Kilkenny (2010) re-analysed longer data sets and found that amplitude modulation is common amongst these stars with periods of days to years. However, there were large gaps in the data sets so Kilkenny (2010) cautioned that the observed amplitude variability may be the result of beating of unresolved frequencies and may not have been astrophysical.

White dwarfs

All stars with masses below $M \lesssim 9$ $M_\odot$ will eventually become white dwarf stars, with the white dwarf cooling tracks ranging from $200\,000$ K to cooler than 5000 K, as shown in Fig. 1.1. Traditionally, white dwarf stars are categorised spectroscopically into different groups. For example, the DB and DA groups contain white dwarf stars with similar spectral classifications to main sequence B and A stars, respectively — the spectra of DB white dwarfs have few hydrogen lines and are dominated by helium lines, whereas the spectra of DA white dwarfs are dominated by hydrogen lines (Aerts et al. 2010).

The three main groups of white dwarf stars known to pulsate are the variable DO stars (DOV; also known as GW Vir stars), the variable DB stars (DBV; also known as V777 Her stars), and the variable DA stars (DAV; also known as ZZ Cet stars). These groups lie in the effective temperature ranges of $75\,000 \leq T_{\mathrm{eff}} \leq 170\,000$ K, $22\,000 \leq T_{\mathrm{eff}} \leq 28\,000$ K and $11\,000 \leq T_{\mathrm{eff}} \leq 12\,000$ K, respectively (Fontaine & Brassard 2008). The hottest variable white dwarf stars, the DOV stars, are exclusively low-degree ($\ell < 2$) high-order multiperiodic g mode pulsators; this has allowed asteroseismic studies to constrain rotation periods and inclinations, magnetic field strengths and atmospheric stratification in these stars (Fontaine &

Brassard 2008; Winget & Kepler 2008). The pulsations in variable white dwarf stars are thought to be excited from outflowing energy being impeded from partial ionisation zones of the main elements in the stellar envelope (Fontaine & Brassard 2008; Winget & Kepler 2008), although pulsations in DAV have also sometimes been referred to as convective driving in the literature (Brickhill 1990, 1991a,b). Thorough reviews of pulsating white dwarfs are given by Fontaine & Brassard (2008) and Winget & Kepler (2008).

A fourth and relatively new group of white dwarf stars are the hot DQ stars, which were discovered by Dufour et al. (2007). The hot DQ stars have carbon-dominated atmospheres (Dufour et al. 2007, 2008), with only a few of these stars known to pulsate (Montgomery et al. 2008; Barlow et al. 2008; Dufour et al. 2009). The low-degree g-mode pulsations in variable hot DQ stars (DQV stars) are also thought to be driven by a surface partial-ionisation zone (Fontaine et al. 2008).

Amplitude modulation and non-linearity in the form of harmonics and combination frequencies are well-documented for pulsating white dwarfs (Fontaine & Brassard 2008; Winget & Kepler 2008). For example, combination frequencies in variable white dwarfs were extensively studied by Brickhill (1992b) and Wu (2001), who demonstrated mathematically that any variability in parent pulsation modes should be mirrored by similar variability in their combination frequencies. This concept and its application to pulsations in δ Sct and γ Dor stars is discussed further in chapter 6.

1.5   4 CVn: a case study of amplitude modulation in a delta Scuti star

The variability of the δ Sct star 4 CVn (HD 107904) was first discovered by Jones & Haslam (1966), and the star has been extensively studied since, with 26 independent pulsation mode frequencies and many more combination frequencies discovered (Breger et al. 1990, 1999; Breger 2000b, 2009; Schmid et al. 2014; Breger 2016). This makes it one of the longest-studied δ Sct stars, with observations covering a few decades. Many of the pulsation modes in 4 CVn show frequency and amplitude variations, some of which can be explained by a mode coupling mechanism (Breger 2000b), the beating of two close frequencies (Breger 2009), or have an unknown cause (Breger 2016).

The problems associated with studying amplitude modulation from the ground were epitomised by Breger (2000b) in his study of 4 CVn. Intermittent observations between 1966 and 1997 allowed the amplitudes of pulsation modes to be studied over a long time span, but the large gaps between observation runs and high levels of noise introduced an instrumental bias towards extracting only high amplitude pulsation modes. His results are shown graphically in Fig. 1.10, in which a single p mode at $\nu = 7.375$ d^{-1} decreased in amplitude from 15 mmag in 1974 to 4 mmag in 1976 and to 1 mmag in 1977, after which a phase jump occurred and the mode began increasing in amplitude again (Breger 2000b). Other pulsation modes were found to be coupled to the variable pulsation mode at $\nu = 7.375$ d^{-1}, and Breger (2000b) concluded that energy was being transferred between pulsation modes by a mode coupling mechanism. A more exhaustive list of other possible causes of amplitude modulation in the pulsation mode at $\nu = 7.375$ d^{-1} discussed by Breger (2000b) are summarised below.

(i) **Beating:** a simple beating model was indicated by the observed phase change,
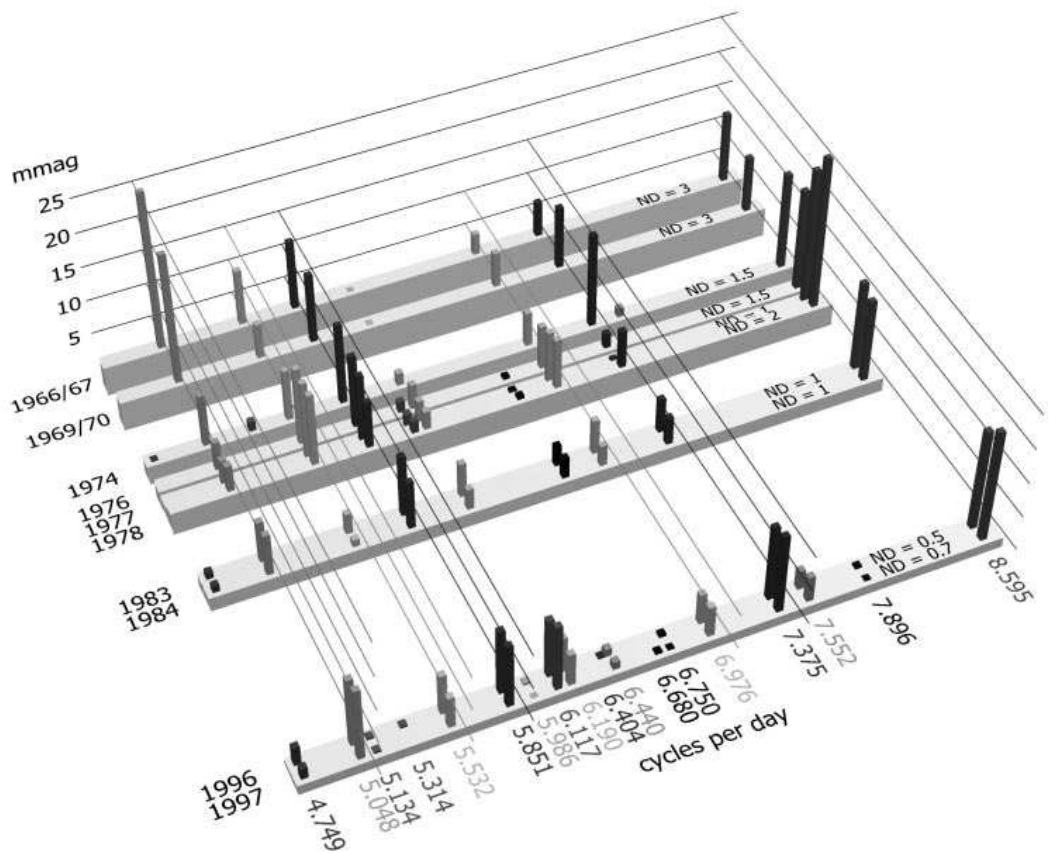
Figure 1.10: Amplitude modulation in the δ Sct star 4 CVn with observations covering 1966 – 1997. The noise level of each data set is given by ND in units of mmag, so only peaks with amplitudes above these values are shown. Figure from Breger (2000b), his figure 5.

which suggested that unresolved modes of similar frequency and amplitude were beating against each other. However, the poor quality of the beating model and the lack of a half-cycle phase change, which was required for the beating model, resulted in Breger (2000b) rejecting the beating hypothesis.

(ii) **Mode re-excitation:** multiple pulsation modes, including $\nu = 7.375$ d^{-1}, were observed to decay in amplitude and then soon afterwards were re-excited with a random phase. The observed phase change supported the hypothesis of the amplitude modulation being caused by changeable driving or damping in the star (Breger 2000b).

(iii) **Stellar cycle:** the apparent periodic behaviour of the pulsation mode amplitude could be evidence of a stellar activity cycle, as cyclic periodicity in mode amplitude cannot be explained by stellar evolution, especially on time-scales of order a few decades (Breger 2000b).

With more data, Breger (2009) concluded that the observed variability in pulsation mode amplitudes could be fitted with a period of several decades — longer than the current data set for the star. Without observing even a single cycle for this pulsation mode, it was difficult to test the stellar activity cycle hypothesis.

Schmid et al. (2012) obtained spectroscopic data of 4 CVn from the 2.1-m Otto Struve telescope at McDonald observatory in Texas throughout 2010 and 2011. A total of 767 spectra with a signal-to-noise ratio of greater than 200, a resolving power greater than $R = 60\,000$, covering the wavelength range of $4200 < \lambda < 4800$ Å were used to study line profile variations in 4 CVn, with the star discovered to be in a binary system with an orbital period of $P_{\rm orb} = 124.3$ d (Schmid et al. 2012).

A couple of years later, Schmid et al. (2014) performed a follow-up spectroscopic analysis of 4 CVn, using spectroscopic data collected between 2008 and 2011 from the McDonald observatory. The binarity of 4 CVn was confirmed with the orbital

CHAPTER 1

Table 1.2: Stellar parameters of the δ Sct 4 CVn from the spectroscopic analysis of Schmid et al. (2014).

P_{orb} (d)	e	T_{eff} (K)	$\log g$ (cgs)	[m/H] (dex)	$v_{\mathrm{eq}} \sin i$ (km s^{-1})
124.44 ± 0.03	0.311 ± 0.003	6875 ± 120	3.30 ± 0.35	-0.05 ± 0.15	109 ± 3

and stellar parameters determined from the spectroscopic analysis by Schmid et al. (2014) given in Table 1.2. The high resolution of the spectroscopy allowed mode identification to be performed, with a resolution of at least $R = 40\,000$ needed to determine the order and degree of a pulsation mode (Aerts et al. 2010). After removing the binary signature, further amplitude and phase variability of order 1 yr remained in pulsation modes (Schmid et al. 2014). A few pulsation modes varied quasi-sinusoidally in amplitude that was explained by the beating of two mode frequencies spaced closer than the frequency resolution (Schmid et al. 2014). However, modes that varied on timescales longer than 1 yr could not be ruled out as single pulsation modes with intrinsic amplitude modulation (Schmid et al. 2014).

Recently, Breger (2016) revisited the analysis of 4 CVn including further photometry taken between 2005 – 2012, and studied mode coupling in this star. He concluded that the energy associated with variable pulsation modes in 4 CVn was not transferred to any other visible pulsation modes, thus the amplitude modulation in 4 CVn remains an unsolved problem.

4 CVn remains one of the longest- and best-studied δ Sct stars from the ground. With the dawn of space telescopes, however, a vast increase in the number and quality of photometric observations of δ Sct stars have allowed amplitude modulation to be investigated in greater detail than is possible from the ground. In this thesis, I present the results from my statistical study of 983 δ Sct stars that were observed continuously by the *Kepler* Space Telescope for over 4 yr, and specifically the incidence of amplitude modulation in this ensemble of stars.

Chapter 2

The *Kepler* space photometry revolution

2.1 Introductory remarks

In the last few decades, the field of asteroseismology has rapidly expanded and become a widely-known area within astronomy, primarily because of the launch of space-based telescopes. The MOST (Walker et al. 2003) and CoRoT (Auvergne et al. 2009) missions provided a wealth of data on a variety of pulsating stars and paved the way for the more recent *Kepler* Space Telescope (Borucki et al. 2010). These space missions were overwhelmingly successful for asteroseismology and their data remain of great use to this day. Consequently, the decade between the launch of the MOST telescope and the end of the *Kepler* mission has become known as the start of the *Space Photometry Revolution*[1]. An argument can certainly be made that the biggest advances in asteroseismology have been for stars with solar-like oscillations, especially in red giant stars, with $\sim 14\,000$ being observed by *Kepler*

---

[1]This was the title of the CoRoT-3/KASC7 conference held in 2013, the first conference I attended as a postgraduate student. The conference website is http://corot3-kasc7.sciencesconf.org. At this meeting, I presented a poster and my conference proceedings were published in the European Physical Journal Web of Conferences (EPJWC; Bowman & Kurtz 2015).

alone (Chaplin & Miglio 2013). Even though asteroseismology of δ Sct stars was possible from the ground, our understanding of these stars has also undoubtedly improved from high-quality space photometry.

This chapter provides an overview of the *Kepler* Space Telescope and its data in section 2.2, with the specifics of Fourier analysis of stellar time series discussed in section 2.3. Section 2.4 contains an overview of how I created my *Kepler* data catalogues, which have formed the basis of many research projects for myself and my collaborators.

2.2 The *Kepler* Space Telescope

The *Kepler* Space Telescope was launched on 7 March 2009 and positioned into a 372.5-d Earth-trailing orbit (Borucki et al. 2010). The field of view covered approximately 115 deg^2 in the constellations of Cygnus and Lyra and *Kepler* observed approximately 200 000 stars at an unprecedented photometric precision of a few μmag (Koch et al. 2010). The field of view was chosen with the CCD array positioned so that the brightest stars lie in the gaps between CCD modules, with most stars having apparent magnitudes in the *Kepler* passband between $10 \leq$ Kp ≤ 14 mag. The primary goal of *Kepler* was to locate Earth-like planets in the habitable zone of their host star using the transit method (Borucki et al. 2010), but these data have also been extremely useful to asteroseismology.

To date, the *Kepler* mission has obtained transit signals for approximately 4700 candidate exoplanets (Borucki et al. 2011), of which more than 3300 have been observed using follow-up spectroscopy and confirmed as exoplanets[2]. On the other hand, an argument can be made that *Kepler* was more successful for stellar astronomy with more discoveries and advances made in asteroseismology than exoplanet

---

[2]an up-to-date catalogue is available at: http://exoplanetarchive.ipac.caltech.edu

science. *Kepler* has validated theoretical predictions and made many new and unexpected discoveries. For example, approximately 2900 eclipsing binary systems[3] were observed by *Kepler* (Prša et al. 2011), which allowed the theoretical prediction of tidally induced pulsations made by Kumar et al. (1995) to be tested. Tidal pulsations were first observed in stars in eccentric binary systems using *Kepler* data, creating a group of stars known colloquially as *'Heartbeat stars'*, because of the characteristic shapes of their light curves resembling an echocardiogram (Thompson et al. 2012; Hambleton et al. 2013; Hambleton 2016).

2.2.1 *Kepler* instrumentation

The design of the *Kepler* instrument maximises the search for solar-type stars, hence the wavelength response peaks at ~ 6000 Å. The wavelength response function for the *Kepler* telescope is plotted in Fig. 2.1 with Johnson filters from Johnson & Morgan (1953) also plotted for comparison (for an extensive review of standard photometric techniques, see Bessell 2005). Using Wien's law, the peak in the *Kepler* response function corresponds to the λ_{max} for a star with an effective temperature of approximately $T_{\mathrm{eff}} \simeq 5000$ K. Therefore, *Kepler* is optimised for studying F, G and K stars. Consequently, *Kepler* observations of oscillations in A stars are suppressed in amplitude from the instrument's passband, but can be corrected for by comparison to other observations (Bowman et al. 2015). This is demonstrated for the δ Sct star KIC 7106205 in chapter 3.

One of the disadvantages to consider when using broad-band photometry is the restriction of mode visibility (Aerts et al. 2010). Observations from space telescopes such as *Kepler* are often only sensitive to detecting low-degree ($\ell \leq 2$) pulsation

---

[3]an up-to-date catalogue is available at: http://keplerebs.villanova.edu
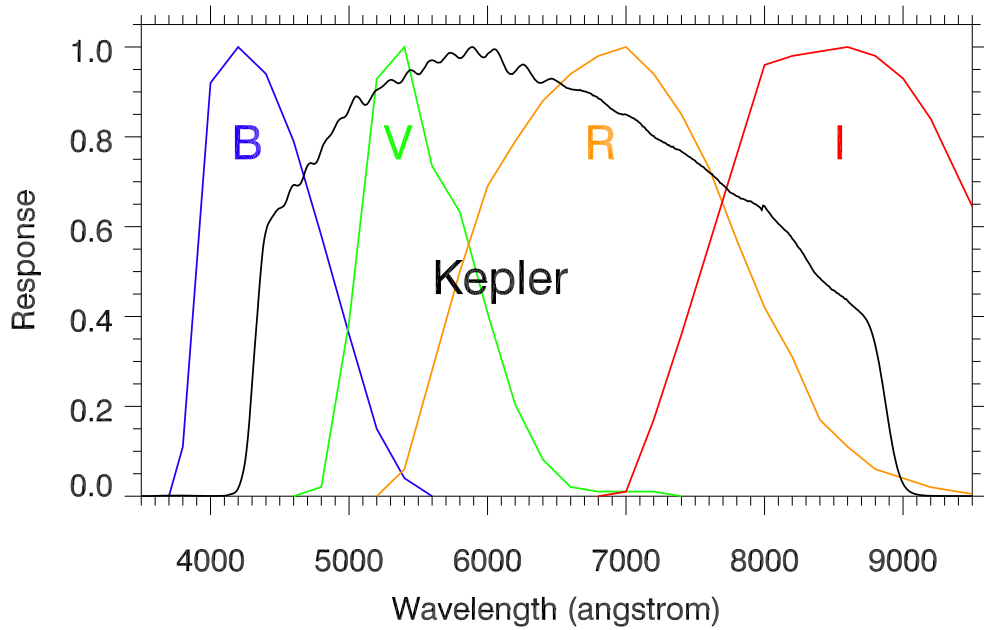
Figure 2.1: The normalised wavelength response function for the *Kepler* instrument is plotted as the solid black line and Johnson *B*, *V*, *R* and *I* filters taken from Johnson & Morgan (1953) are shown as coloured solid lines for comparison.

modes, because the amplitudes of high-degree modes are only excited to small amplitudes (Balona & Dziembowski 1999), and because of geometrical cancellation effects (Dziembowski 1977a).

2.2.2 *Kepler* **data characteristics**

Kepler data are available in long and short cadence (hereafter called LC and SC, respectively), which were created from multiple 6.02-s exposures, each with 0.52-s readout times (Gilliland et al. 2010). The LC data comprised 270 exposures creating a total integration time of 29.45 min, which allowed approximately 170 000 simultaneous observations (Jenkins et al. 2010). The SC data comprised nine exposures creating a total integration time of 58.5 sec, which was chosen to increase the temporal resolution, thus increase the number of data points per exoplanet transit of a star. From the limited amount of data storage on board the spacecraft, only 512
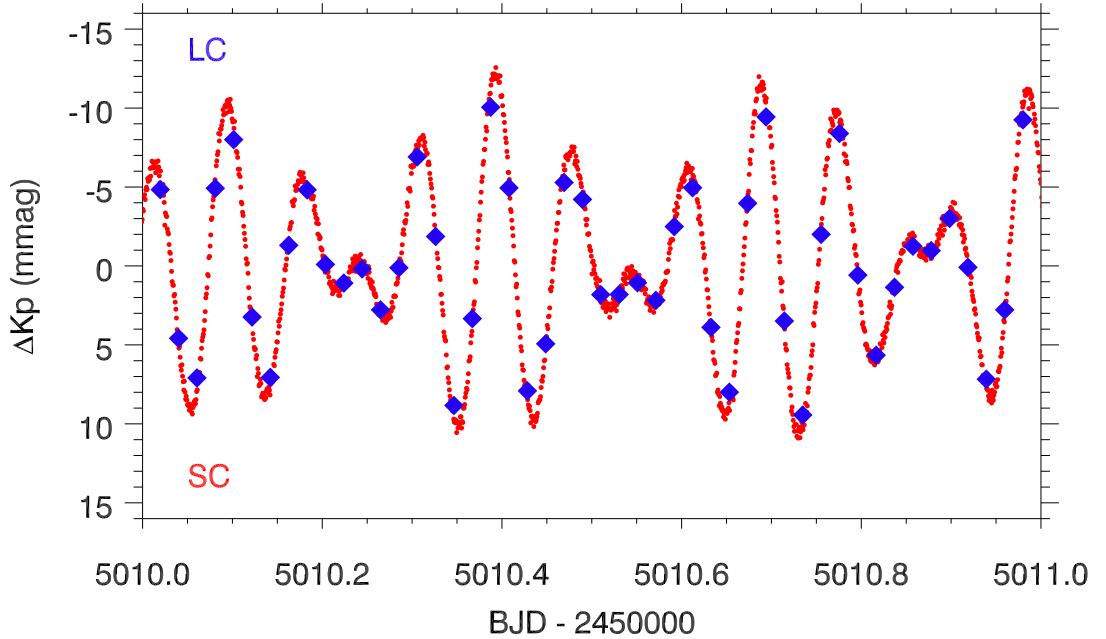
Figure 2.2: Comparison of LC and SC *Kepler* data spanning 1 d for the δ Sct star KIC 7106205. The SC data have a cadence of 58.5 sec and the LC data have a cadence of 29.45 min.

stars were observed with SC at any one time (Gilliland et al. 2010). To demonstrate the difference in temporal resolution between LC and SC data, the light curves spanning 1 d of the δ Sct star KIC 71060205 using LC and SC data are shown as blue diamonds and red circles, respectively, in Fig. 2.2.

To keep its solar panels pointing towards the Sun, the *Kepler* spacecraft had to roll 90 degrees approximately every 93 d — i.e., one quarter of the *Kepler* orbit. The *Kepler* CCD was designed with four-fold symmetry, so a star rotated on the focal plane four times in a *Kepler* year, which is divided into four quarters of LC data. Each quarter was then divided into three months and so SC data are labelled with a quarter and month number. *Kepler* data were stored on board the spacecraft and downloaded to Earth approximately every 31 d. Therefore, *Kepler* data are available as SC months and LC quarters, corresponding to approximately 31 d and 93 d, respectively. At the end of the main *Kepler* mission in May 2013, there was

a total of 18 LC data quarters each approximately 93 d in length, but Q0, Q1 and Q17 were approximately 10, 30 and 30 d, respectively. The length of the complete data set is 1470.5 d, which is just over 4 yr.

Approximately one per cent of all the targets observed by *Kepler* were allocated for asteroseismic research (Gilliland et al. 2010), with a 1-yr proprietary access period given to the *Kepler* Asteroseismic Science Consortium (KASC) via the *Kepler* Asteroseismic Science Operations Center[4]. Today, all *Kepler* light curves in both raw and reduced formats are publicly available from the Mikulski Archive for Space Telescopes (MAST)[5], and are available in two formats. The first type are the raw or unprocessed light curves that are produced using Simple Aperture Photometry (SAP), and the second type are the reduced light curves that are created using a multi-scale Maximum A Prior Pre-Search Data Conditioning (msMAP PDC) pipeline developed by the *Kepler* Science Office — see Smith et al. (2012) and Stumpe et al. (2012) for more details.

The main advantages of using the reduced light curves from the msMAP PDC pipeline over the SAP light curves include: data quarters have been automatically stitched together; the removal of outlying data points; and the removal of systematic sources of instrumental noise. The *Kepler* science pipeline has been developed to optimise the light curves for the detection of exoplanet transit signals and can suppress the amplitudes of long period signals ($P \geq 10$ d). The pipeline does not, however, modify the frequencies of these long-period signals, so the difference for asteroseismology of high-frequency pulsators, such as δ Sct stars, is negligible. Murphy (2014) provided a detailed overview of *Kepler* data being used for asteroseismology research.

---

[4]KASOC website: http://www.kasoc.phys.au.dk
[5]MAST website: http://archive.stsci.edu/kepler/

2.2.3 The *Kepler* Input Catalogue

Approximately 200 000 targets stars were selected to be observed by *Kepler*, with the specific selection criteria discussed by Koch et al. (2010). These targets were characterised with values of T_{eff}, log g and [Fe/H] using *griz* and 2MASS *JHK* broad-band photometry prior to the launch of the telescope and were collated into the *Kepler* Input Catalogue (KIC; Brown et al. 2011). Since the end of the nominal *Kepler* mission, Huber et al. (2014) revised the stellar parameters for the $\sim$200 000 *Kepler* targets and concluded that a colour-dependent offset exists compared to other sources of photometry (e.g., Sloan). This resulted in KIC temperatures for stars hotter than $T_{\mathrm{eff}} \gtrsim 6500$ K being, on average, 200 K lower than temperatures obtained from Sloan photometry or the infrared flux method (Pinsonneault et al. 2012). Also, log g values for hot stars were overestimated by up to 0.2 dex. Huber et al. (2014) stress that the T_{eff}, log g and [Fe/H] values and their respective uncertainties should not be used for a detailed analysis on a star-by-star basis, as they are only accurate in a statistical sense.

2.2.4 The failure of module 3

Approximately 2 yr into the *Kepler* mission, two CCD arrays located on module 3 failed. This resulted in approximately 4/21 of *Kepler* targets not being observed every fourth quarter after this point, because of the rotation of the telescope 90 degrees every $\sim$93 d. These stars, commonly known as module 3 stars, have significant gaps in their light curves causing more complex window patterns in their amplitude spectra.

2.2.5 K2

In May 2013 the *Kepler* Space Telescope suffered the failure of a second reaction wheel. With only two remaining reaction wheels, the telescope could no longer

maintain the necessary level of still-pointing without the significant expenditure of fuel. An ingenious solution was devised by NASA, in which the field of view was repositioned to point in the direction of the ecliptic, such that torques from the solar radiation pressure were minimised and a smaller amount of fuel was needed to maintain the field of view (Howell et al. 2014). Consequently, the mission parameters have changed and a new mission called K2, *Kepler*'s second light, is underway. K2 data are divided into campaigns, each approximately 80 d in length, with each new campaign observing a variety of targets, including young stars and star-forming regions; supernovae, white dwarfs and the Galactic centre (Howell et al. 2014).

Analysis of K2 data has proved fruitful. Discoveries have included a rare triple-mode RR Lyrae star, EPIC 201585823, with currently only 12 such objects known (Kurtz et al. 2016); an in-depth asteroseismic analysis of O stars for the first time (Buysschaert et al. 2015); and the continued success in finding exoplanets (Vanderburg et al. 2016). The future is bright for K2 asteroseismology and many interesting discoveries are expected in the next few years. Even though the *Kepler* mission has been redesigned and the telescope is no longer observing the original target stars, the 4 yr of high-quality data will remain a gold mine for scientific discoveries and investigation for many years to come.

2.3   Fourier analysis of stellar time series

The fundamental data of asteroseismology are the pulsation mode frequencies, which are extracted from time series photometry using Fourier analysis. The Fourier transform (FT) allows one to move from the time domain into the frequency domain by use of

$$F(\nu) = \int_{-\infty}^{+\infty} x(t)e^{2\pi i\nu t}dt \ , \tag{2.1}$$

in which $x(t)$ is a continuous infinite function. The principle of Fourier analysis is

that any function can be represented by a summation of sine and cosine functions. In reality, stellar time series are not infinitely long nor are they continuous functions, so the discrete Fourier transform (DFT) described by Deeming (1975) is implemented for finite and discrete data sets. The calculated amplitude spectrum is also convolved with the spectral window of the data set, which is defined by gaps in the data and deviations from a regular cadence (Deeming 1975).

Using the DFT described by Deeming (1975), an amplitude spectrum is calculated using

$$A_i = \left(\frac{2}{N}\right) \sqrt{\left(\sum_{j=0}^{N} x_j(t) \sin(2\pi\nu_i t_j)\right)^2 + \left(\sum_{j=0}^{N} x_j(t) \cos(2\pi\nu_i t_j)\right)^2} \ , \qquad (2.2)$$

where A_i is the amplitude at the frequency ν_i, calculated from the summation of sine and cosine signals for the discrete time series $x(t)$ with N data points.

2.3.1 The Nyquist frequency

The Nyquist frequency is the highest frequency that is not undersampled for a given sampling frequency, and is defined as

$$\nu_{\mathrm{Nyq}} = \frac{1}{2\Delta t} \ , \qquad (2.3)$$

where Δt is the cadence of a discrete data set. For LC *Kepler* data this corresponds to a value of $\nu_{\mathrm{Nyq}} = 24.47$ d^{-1} and for SC data this is 727.35 d^{-1}. The Nyquist frequency is commonly used as an upper limit in frequency when calculating the amplitude spectrum of a discrete data set because frequencies outside of the range $0 \le \nu \le \nu_{\mathrm{Nyq}}$ are undersampled and subject to aliasing.

It has been demonstrated that pulsation mode frequencies in δ Sct stars typically lie between $4 \le \nu \le 50$ d^{-1} (Grigahcène et al. 2010a; Uytterhoeven et al. 2011;

Balona & Dziembowski 2011), thus can exceed the LC *Kepler* Nyquist frequency. Before the advent of the super-Nyquist asteroseismology technique by Murphy et al. (2013b), care was needed when extracting frequencies from an amplitude spectrum near or above LC Nyquist frequency because they may be aliases of undersampled frequencies above the Nyquist frequency.

Super-Nyquist asteroseismology

It was shown by Murphy et al. (2013b) using the super-Nyquist asteroseismology (sNa) technique, that real and alias frequencies of pulsation modes can be easily identified in an amplitude spectrum when using *Kepler* data. *Kepler* data were sampled at a regular cadence onboard the spacecraft, but Barycentric time stamp corrections were made to correct for the difference in light arrival time of the photons to the barycentre of the Solar system and to the telescope, respectively, resulting in a non-constant cadence (Murphy et al. 2013b). Thus, Nyquist aliases are subject to periodic frequency (phase) modulation with a period equal to the *Kepler* satellite's orbital period of 372.5 d, and consequently have a multiplet structure split by the *Kepler* orbital frequency in an amplitude spectrum (Murphy et al. 2013b). The total integrated power is the same for a real peak and its alias multiplet in an amplitude spectrum, but the power of an alias is spread between the central component of the multiplet and its super-Nyquist sidelobes, resulting in a central component with a smaller amplitude when compared to the real peak (Murphy et al. 2013b). Therefore, using the sNa technique, real and alias frequencies can often be identified without the need to calculate an amplitude spectrum beyond the LC Nyquist frequency.

To demonstrate the sNa technique described by Murphy et al. (2013b), the amplitude spectra for simultaneous LC and SC observations of the HADS star KIC 5950759 have been plotted in the left panel of Fig. 2.3. This HADS star acts as
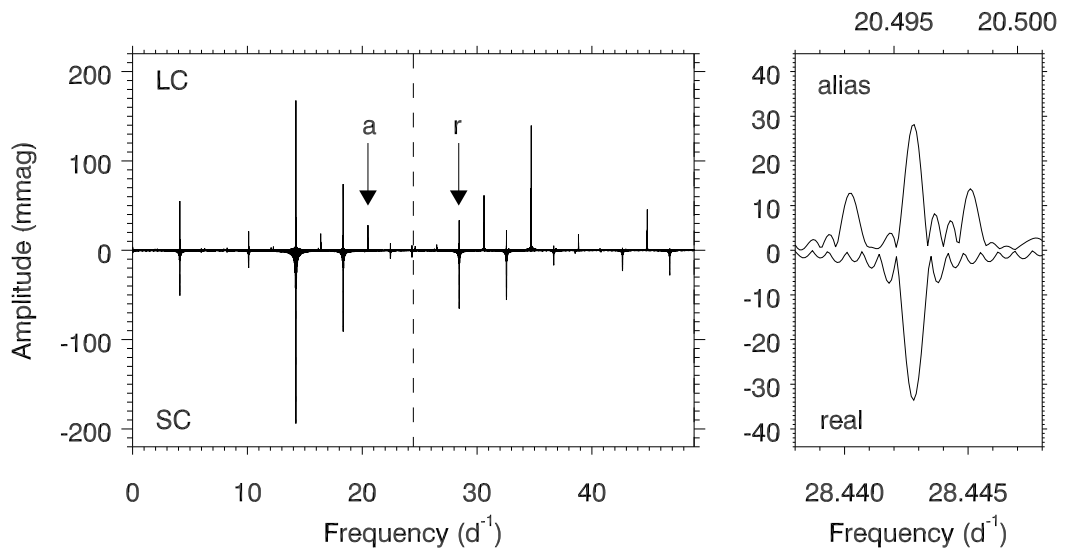
Figure 2.3: Demonstration of super-Nyquist asteroseismology using the amplitude spectrum of the HADS star KIC 5950759. Real and alias peaks associated with the harmonic of the fundamental radial mode are marked by 'r' and 'a', respectively, in the LC amplitude spectrum in the left panel. The LC Nyquist frequency is indicated by the vertical dashed line and the SC amplitude spectrum is shown below for comparison. The right panel contains inserts of the LC amplitude spectrum showing the real peak below and the alias peak above. The alias peak is easily identified as its multiplet structure is split by the *Kepler* orbital frequency. Some peaks that exist in the SC amplitude spectrum do not appear in the LC amplitude spectrum as they lie close to the LC sampling frequency and are heavily suppressed in amplitude. Figure from Bowman et al. (2016), their figure 2.

a useful example because of the high S/N of its pulsation modes and because simultaneous LC and SC observations are available. The LC and SC amplitude spectra for KIC 5950759 both show the fundamental radial mode at $\nu_1 = 14.221372$ d^{-1}, and its harmonic $2\nu_{1,\mathrm{r}} = 28.442744$ d^{-1} labelled 'r' for real, which lies above the LC Nyquist frequency indicated by a vertical dashed line in Fig. 2.3. The alias of the harmonic $2\nu_{1,\mathrm{a}} = 20.496203$ d^{-1} can also be seen in the LC amplitude spectrum in Fig. 2.3 and is labelled 'a'. The right panel in Fig. 2.3 shows a zoom-in of the amplitude spectrum using LC data, showing the multiplet structure split by the *Kepler* satellite's orbital frequency of the alias peak in the top panel, compared to the real peak shown below for comparison. Note also, how the amplitude of the alias peak is smaller than the real peak in the LC amplitude spectrum, as predicted by Murphy et al. (2013b).

2.3.2 Frequency resolution

It is important to note that SC *Kepler* data does provide a higher temporal resolution, as shown by Fig. 2.2, but does not provide a higher frequency resolution compared to LC observations. The frequency resolution of a data set is given by the Rayleigh resolution criterion of

$$\sigma\left(\nu\right) = \frac{1}{\Delta T} \ , \tag{2.4}$$

where $\sigma\left(\nu\right)$ and ΔT are the frequency resolution and the length of the data set, respectively. A longer time series results in a smaller frequency resolution, which is represented by the width of the peak in an amplitude spectrum.

This is demonstrated in Fig. 2.4, in which amplitude spectra for time series spanning 30 d, 90 d, 1 yr and 4 yr for a pulsation mode frequency at $\nu = 10.0323$ d^{-1} have been plotted for comparison. As can be seen in Fig. 2.4, the width of the peak is smaller for longer time series following Eqn 2.4. For the 4-yr *Kepler* data set, a
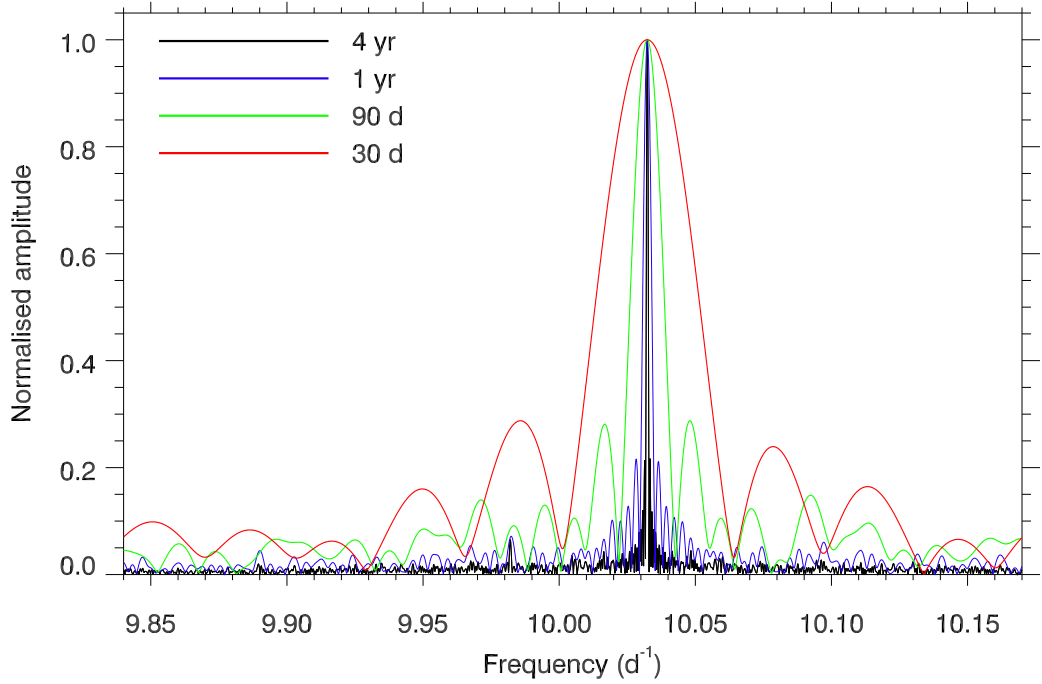
Figure 2.4: Demonstration of frequency resolution using four different lengths of observations for the pulsation mode frequency at $\nu = 10.0323$ d^{-1} in the δ Sct star KIC 7106205. With a longer time series, a better frequency resolution is obtained, which corresponds to the width of the peak in the amplitude spectrum.

frequency resolution of 0.00068 d^{-1} ($\simeq 8$ nHz) is obtained.

2.3.3 Amplitude visibility function

It was discussed in section 2.3.2 how the length of a data set determines the frequency resolution in an amplitude spectrum and is independent of the cadence, such that the width of a peak in an amplitude spectrum is the same for both LC and SC observations of the same length. However, the longer integration times of the LC data reduce the amplitudes of peaks in an amplitude spectrum compared to SC data, which is also a strong function of frequency. The exact functional form of the amplitude suppression caused by integration time is given by the amplitude visibility function in Eqn 2.5. The derivation of this equation is given below and
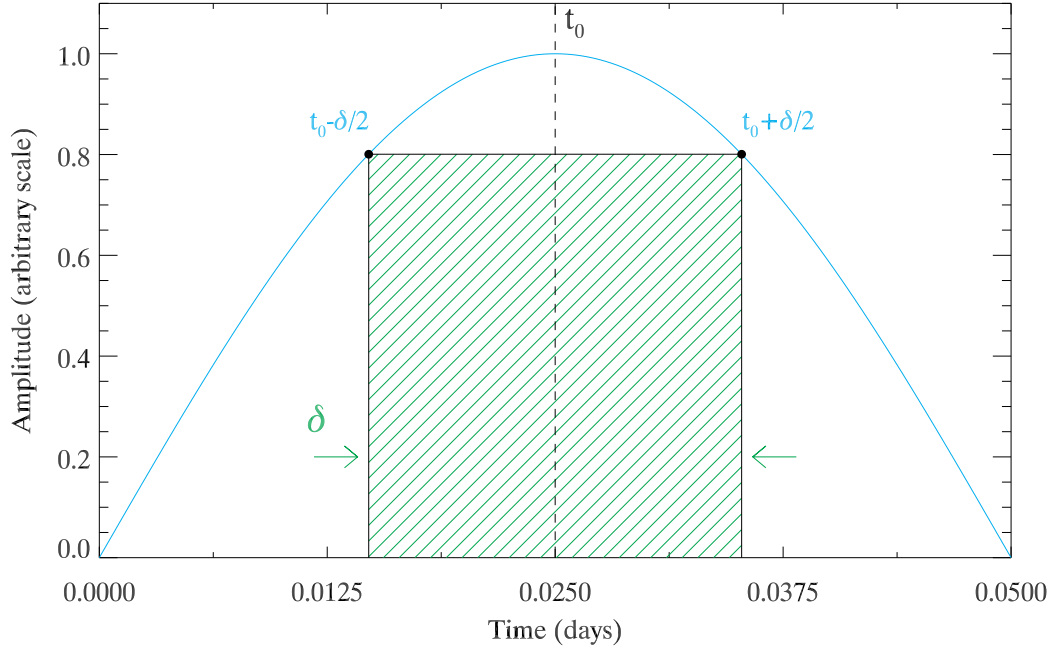
Figure 2.5: Demonstration of how longer integration times lead to an underestimate in amplitude of a periodic signal. A frequency of $\nu = 10.0$ d^{-1} is shown as the solid blue line and the interval between consecutive data points is given by δ, which is symmetric from a reference time, t_0, and has been chosen to emulate the LC *Kepler* sampling frequency. With a shorter integration time, δ, less amplitude suppression occurs as the height of the rectangle increases and approaches the true amplitude of unity in this example. Figure from Murphy (2014), his figure 1.4.

was described by Murphy (2014).

In Fig. 2.5 a periodic flux variation of frequency $\nu = 10.0$ d^{-1} is shown by the solid blue line and the interval between consecutive data points in LC *Kepler* data is shown by the width of the green-hatched rectangle, δ. The height of the rectangle is the area divided by its width, thus for the same frequency signal a shorter sampling would produce a taller and narrower rectangle in Fig. 2.5. Assuming that the $\nu = 10.0$ d^{-1} signal is periodic and has the form $\cos(\omega t)$, then the height of the

rectangle, H, is given by:

$$H = \frac{1}{\delta} \int_{t_0 - \frac{\delta}{2}}^{t_0 + \frac{\delta}{2}} \cos(\omega t) dt$$

$$= \frac{1}{\delta} \frac{1}{\omega} \left\{ \sin \left[\omega \left(t_0 + \frac{\delta}{2} \right) \right] - \sin \left[\omega \left(t_0 - \frac{\delta}{2} \right) \right] \right\} .$$

This can be re-written using the trigonometric identity $\sin(X+Y) = \sin X \cos Y + \cos X \sin Y$, as:

$$H = \frac{1}{\delta} \frac{1}{\omega} \left[\sin(\omega t_0) \cos \left(\frac{\omega \delta}{2} \right) + \cos(\omega t_0) \sin \left(\frac{\omega \delta}{2} \right) \right.$$

$$\left. - \sin(\omega t_0) \cos \left(\frac{\omega \delta}{2} \right) + \cos(\omega t_0) \sin \left(\frac{\omega \delta}{2} \right) \right]$$

$$= \frac{1}{\omega \delta} \left[2 \cos(\omega t_0) \sin \left(\frac{\omega \delta}{2} \right) \right]$$

$$= \cos(\omega t_0) \operatorname{sinc} \left(\frac{\omega \delta}{2} \right) .$$

Using the relationship between angular frequency and period, $\omega = \frac{2\pi}{P}$, with P being the period of the signal, and that the time interval between consecutive data points is related to the number of data points per cycle, $\delta = \frac{P}{n}$, the above can be rewritten as

$$A = A_0 \operatorname{sinc} \left(\frac{\pi}{n} \right) , \tag{2.5}$$

where A is the observed amplitude, A_0 is the true amplitude and n is the number of data points per pulsation cycle. From the relationship in Eqn 2.5, it can be seen that higher frequency signals are, on average, more heavily suppressed in amplitude, but only exactly integer multiples of the sampling frequency are completely suppressed, which is shown graphically in Fig. 2.6. Therefore, from the shorter integration times, SC data will produce a higher amplitude peak for a given frequency compared to LC data.
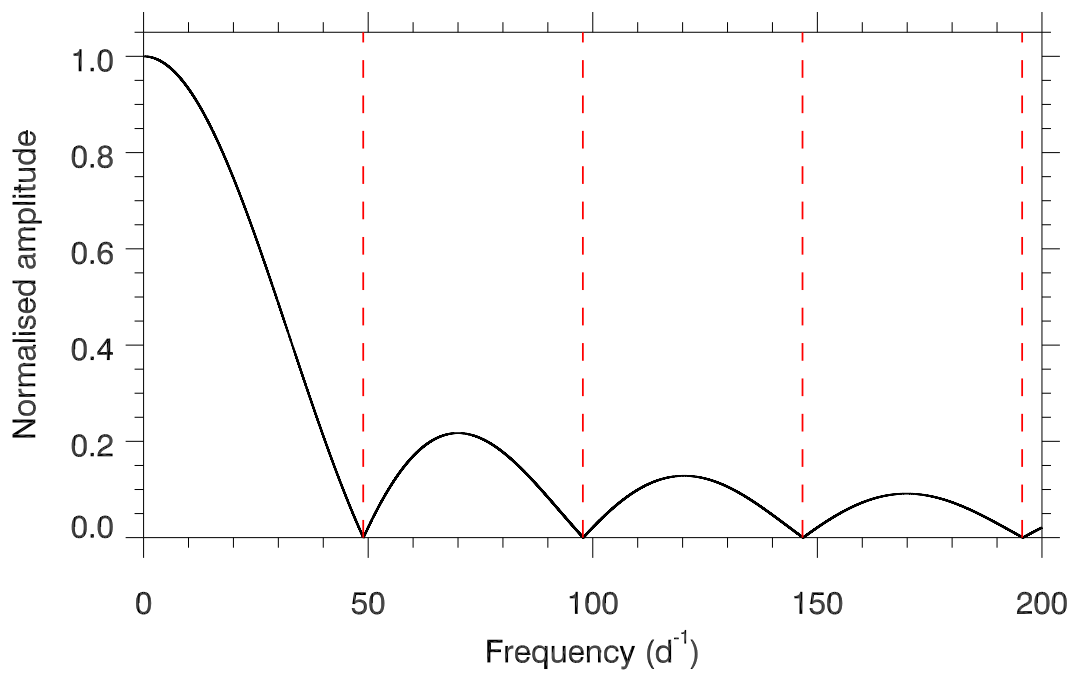
Figure 2.6: The amplitude visibility function as a function of frequency for LC *Kepler* data. Higher frequencies are suppressed heavily in amplitude because there are fewer data points per pulsation cycle, n, but only frequencies equal to integer multiples of the sampling frequency are completely suppressed. The vertical red dashed lines indicate integers of the LC sampling frequency $\nu_{\mathrm{samp}} = 48.9 \ \mathrm{d}^{-1}$.

2.4   *Kepler* data catalogues

One of the first tasks undertaken as part of this thesis was to identify all the pulsating A and F stars, specifically the δ Sct stars, observed by the *Kepler* Space Telescope. Although the *Kepler* instrument is optimised for observing solar-type stars, several thousand A and F stars were included in the 200 000 target stars. In this section, the downloading and processing of light curves for all A and F stars, and the methodology of producing my *Kepler* data catalogues is discussed.

2.4.1   Creating data catalogues

To create a statistical ensemble of δ Sct stars, the light curves produced by the msMAP PDC pipeline (Stumpe et al. 2012; Smith et al. 2012) for all *Kepler* targets with effective temperatures between $6400 \leq T_{\mathrm{eff}} \leq 10\,000$ K in the KIC were downloaded from MAST. The extracted time series were stored locally in the format of reduced Barycentric Julian Date (BJD $-\,2\,400\,000$) and stellar magnitudes, which were normalised for each quarter of LC and month of SC data to be zero in the mean. This resulted in approximately 10 400 stars within this T_{eff} range. Examples of the file format for the first LC quarter and first SC month of the fictitious star KIC 1234567 are

    kic001234567_Q00_LC.txt   and   kic001234567_Q00_M1_SC.txt .

The time series were separated into temperature bins for parallelised computing with the number of stars in each temperature bin shown in Table 2.1. The range of the temperature bins is somewhat arbitrary, but was chosen to create bins with similar number of stars and type of pulsator. For example, the overlapping region of the δ Sct and γ Dor instability regions is approximately between $6800 \leq T_{\mathrm{eff}} \leq 8000$ K, and so it was important to separate these stars into three groups. Similarly, the hot

Table 2.1: The number of stars downloaded from MAST for each temperature bin as listed in the KIC (Brown et al. 2011) is given, indicating fewer hot stars than cool stars.

KIC temperature (K)	Number	Spectral Type	Comment
$9000 \leq T_{\mathrm{eff}} < 10\,000$	329	A1 – A3	
$8000 \leq T_{\mathrm{eff}} < 9000$	907	A3 – A6	δ Sct blue edge
$7500 \leq T_{\mathrm{eff}} < 8000$	912	A6 – A7	γ Dor blue edge
$7000 \leq T_{\mathrm{eff}} < 7500$	1587	A8 – F0	
$6800 \leq T_{\mathrm{eff}} < 7000$	1129	F0 – F2	δ Sct red edge
$6600 \leq T_{\mathrm{eff}} < 6800$	1752	F3 – F4	
$6500 \leq T_{\mathrm{eff}} < 6600$	1754	F4 – F5	γ Dor red edge
$6400 \leq T_{\mathrm{eff}} < 6500$	2025	F5 – F6	
TOTAL	**10 395**		

δ Sct and cool γ Dor stars have separate groups. Thus, considering that typical uncertainties for stars with $T_{\mathrm{eff}} \simeq 6500$ K and $T_{\mathrm{eff}} \simeq 9000$ K are approximately $\pm\,150$ and $\pm\,400$ K, respectively, all the stars within a bin can be considered as having the same effective temperature.

An automated pipeline was created to calculate the amplitude spectrum for each LC quarter for each star. The method for calculating the Fourier transform of a discrete data series is described in detail by Deeming (1975), and was optimised for speed by Kurtz (1985). These tools were checked and found to be consistent with the frequency software package `PERIOD04` (Lenz & Breger 2005).

2.4.2 *Kepler* data catalogue extract

The light curves and amplitude spectra have been collated into a series of PDF catalogues, one for each of the effective temperature bins given in Table 2.1. At the top of each page in a data catalogue, a star's unique *Kepler* ID number starting with the characters KIC (*Kepler* Input Catalogue) and its stellar parameters listed in the KIC (Brown et al. 2011) are given. Next to the KIC ID number, the LC data quarter number is also given. The light curve is shown in the top panel, which have all been

set to be zero in the mean and have ordinate units of mmag. The middle panel shows the LC amplitude spectrum calculated out to the Nyquist frequency, and the bottom panel shows a zoom-in of the low-frequency regime in the amplitude spectrum at the same ordinate scale but a smaller abscissa scale. The frequency range of $0 \leq \nu \leq 6$ d^{-1} was chosen to plot the g mode frequency regime separately as many δ Sct stars have peaks in the low-frequency regime (see e.g., Grigahcène et al. 2010a; Uytterhoeven et al. 2011; Balona 2011). The ordinate scale in every page (i.e., for all LC data quarters) of each star is kept fixed, thus one can see changes in amplitude of the pulsation modes more easily.

The following two pages are extracts from my $6800 \leq T_{\mathrm{eff}} \leq 7000$ K *Kepler* data catalogue showing Q0 and Q17 for the δ Sct star KIC 7106205. Scrolling through the *Kepler* data quarters on separate pages of my catalogues allowed KIC 7106205 to be quickly identified as a δ Sct star with significant amplitude modulation, and motivated the analysis of this star by Bowman & Kurtz (2014), which is discussed in chapter 3. Specifically, it was the significant decrease in the amplitude of the peak at $\nu \simeq 13.5$ d^{-1} from Q0 to Q17 that caught my attention.

kic7106205 Q00

Teff= 6967
log(g)= 4.052
Radius= 1.775 $R_{\odot}$

$[Fe/H]$= -0.012
Contam= 0.005
Kep Mag= 11.455
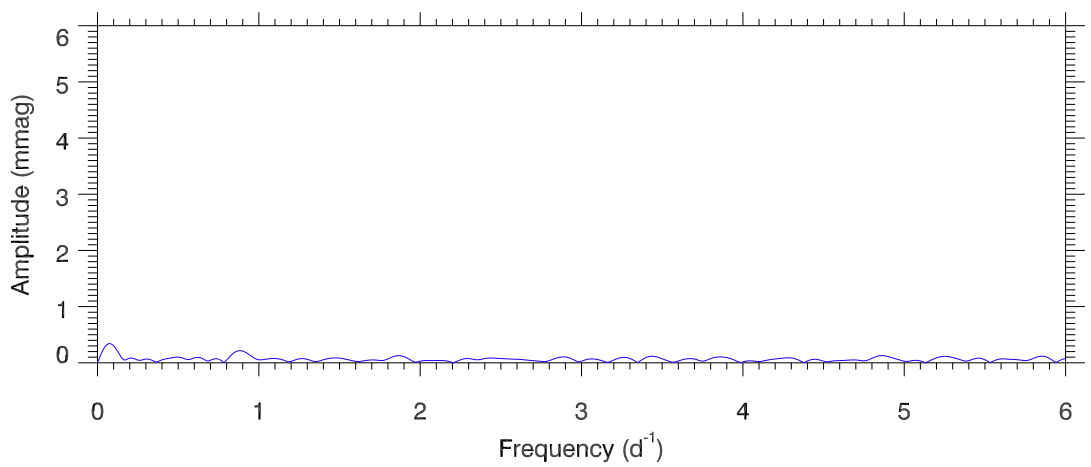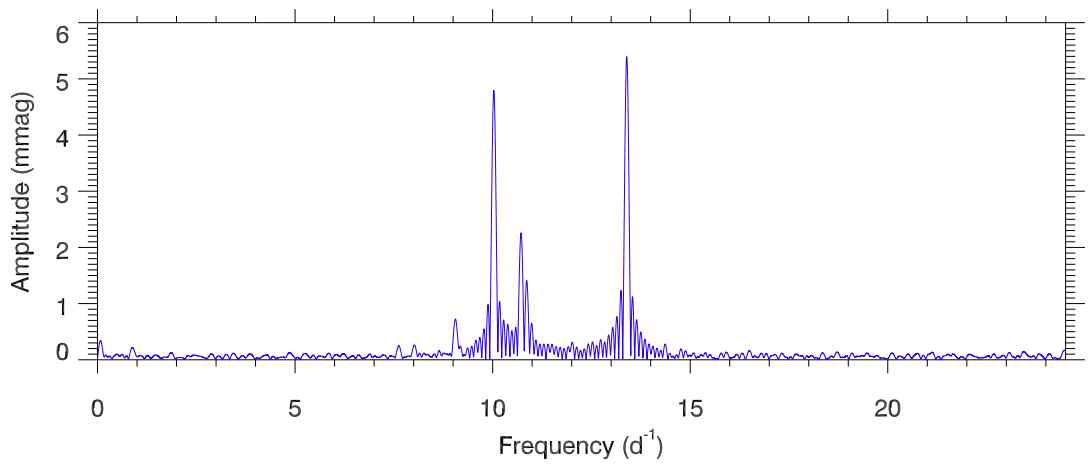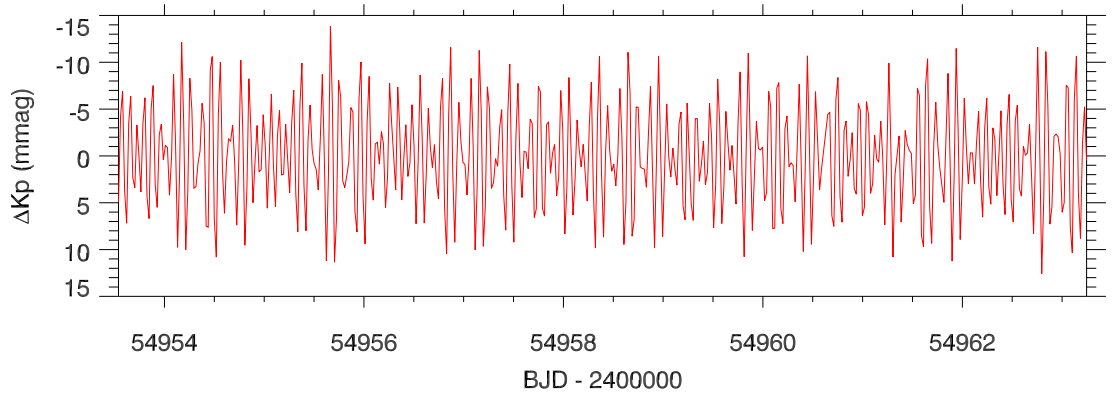
kic7106205 Q17

Teff= 6967
log(g)= 4.052
Radius= 1.775 $R_\odot$

$[Fe/H]$= -0.012
Contam= 0.005
Kep Mag= 11.455
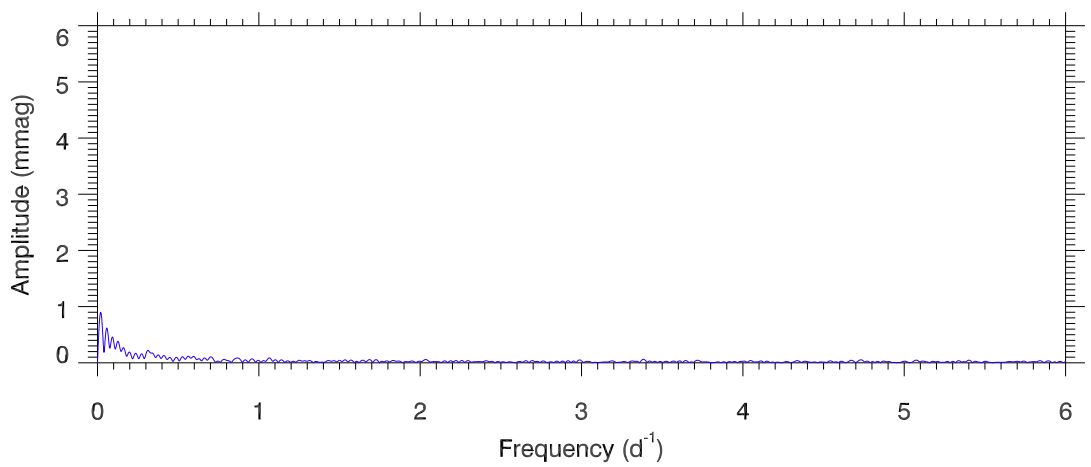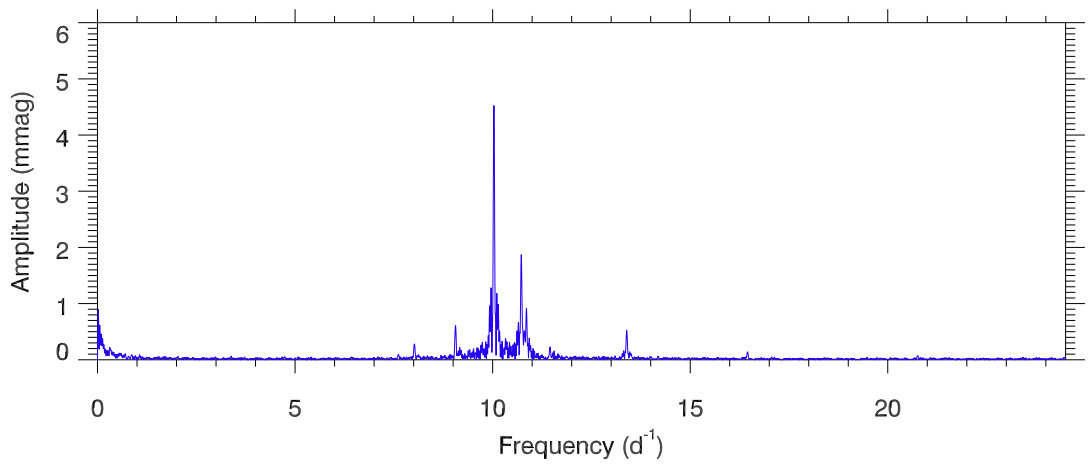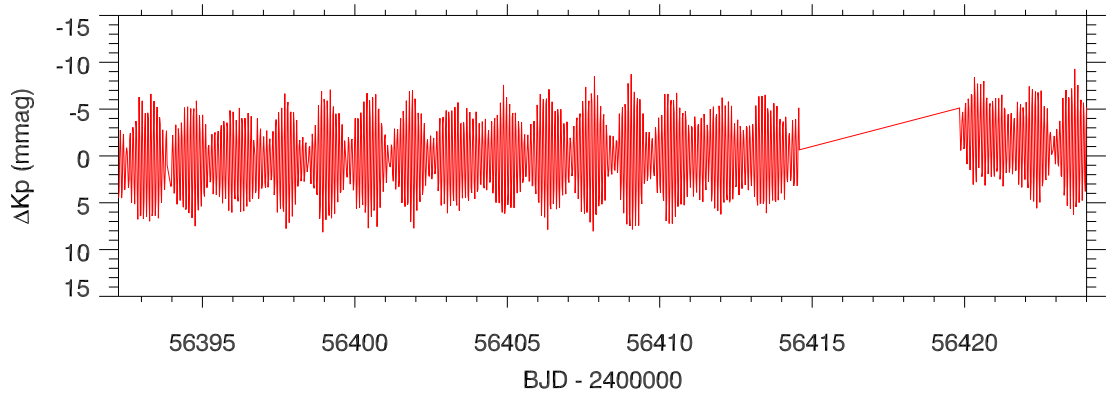
2.5 Discussion

The advent of space-based telescopes in the last decade such as MOST (Walker et al. 2003), CoRoT (Auvergne et al. 2009) and *Kepler* (Borucki et al. 2010), has become known as the Space Photometry Revolution. The *Kepler* Space Telescope provided high photometric precision, high duty cycle and data spanning years for 200 000 stars (Koch et al. 2010). Although the mission was designed to find Earth-like exoplanets orbiting solar-type stars using the transit method, these data have also been extremely useful for studying pulsating stars using asteroseismology.

In this chapter, a review of *Kepler* instrumentation has been provided, including a discussion of the main differences in SC and LC data and the implications for asteroseismology. Specifically, the 29.5-min integration time of LC *Kepler* data may have the same frequency resolution for the same length of SC data according to the Rayleigh resolution criterion, but it was shown that the amplitude suppression from the longer integration time is an important factor to consider when calculating an amplitude spectrum. From the complete 4-yr *Kepler* data set, a frequency resolution of $0.00068\,\mathrm{d}^{-1}$ ($\simeq 8\,\mathrm{nHz}$) and an amplitude precision of order a few μmag is obtained, which are important for studying the changes in the pulsation modes over time – i.e., frequency and amplitude modulation – in pulsating stars such as δ Sct stars.

In this chapter, it was discussed how a total of approximately 10 400 stars with effective temperatures between $6400 \leq T_{\mathrm{eff}} \leq 10\,000$ K observed by *Kepler* were downloaded and processed into *Kepler* data catalogues. These catalogues represent a valuable tool for quickly and efficiently identifying different types of pulsating stars observed by *Kepler*, as one is able to simply search for pulsation modes in the frequency range of interest. The ordinate axis of the amplitude spectra was chosen to be fixed for each LC quarter of each star, such that significant amplitude modulation in δ Sct stars could easily be identified.

The usefulness of these data catalogue was demonstrated for the δ Sct star

CHAPTER 2

KIC 7106205 in section 2.4.2, which led to the study of amplitude modulation in this star by Bowman & Kurtz (2014) and Bowman et al. (2015) presented in chapter 3. The *Kepler* data catalogues discussed in this chapter will remain of great use for years to come, as the 4-yr length of *Kepler* data will not be surpassed in the foreseeable future.

Chapter 3

KIC 7106205 — an archetypal delta Scuti star with amplitude modulation

3.1 Introductory remarks

In this chapter, the published studies of the δ Sct star KIC 7106205 by Bowman & Kurtz (2014) and Bowman et al. (2015) are presented in sections 3.2 and 3.3, respectively. KIC 7106205 represents a special case study that allows energy conservation of pulsation modes to be studied in a δ Sct star with significant amplitude modulation, and provided motivation to extend this analysis to an ensemble of δ Sct stars.

Only a single pulsation mode exhibits amplitude modulation in KIC 7106205 whilst all other statistically significant modes remain constant in amplitude, such that the visible pulsation energy budget is not conserved over the 4-yr *Kepler* data set (Bowman & Kurtz 2014). Ground-based data from the Wide Angle Search for Planets (WASP; Pollacco et al. 2006) are used to extend the study of KIC 7106205

and it is shown that the majority of the amplitude modulation in this variable pulsation mode occurred prior to the launch of the *Kepler* Space Telescope (Bowman et al. 2015). It is clear from these studies that time spans of years and decades are important in δ Sct stars (Bowman & Kurtz 2014; Bowman et al. 2015), with the 4-yr *Kepler* data set providing only a blink-of-an-eye insight into the physics at work in these stars.

3.2 Pulsational frequency and amplitude modulation in the δ Sct star KIC 7106205

In this section, the research paper by Bowman & Kurtz (2014) is presented, which was published in Monthly Notices of Royal Astronomical Society in October 2014. I performed the frequency analysis of KIC 7106205, which led to the discovery of significant amplitude modulation in this δ Sct star. I created specialised amplitude and phase tracking routines which allowed the frequency and amplitude modulation of multiple pulsation modes in KIC 7106205 to be studied. I wrote the majority of the publication and D. W. Kurtz contributed to the discussion and editing of the paper.

Pulsational frequency and amplitude modulation in the δ Sct star KIC 7106205

Dominic M. Bowman[★] and Donald W. Kurtz

Jeremiah Horrocks Institute, University of Central Lancashire, Preston PR1 2HE, UK

ABSTRACT

Analysis of the *Kepler* δ Sct star KIC 7106205 showed amplitude modulation in a single pressure mode, whilst all other pressure and gravity modes remained stable in amplitude and phase over the 1470 d length of the data set. The *Kepler* data set was divided into a series with time bins of equal length for which consecutive Fourier transforms were calculated. An optimum fixed frequency, calculated from a least-squares fit of all data, allowed amplitude and phase of each pulsation mode for each time bin to be tracked. The single pressure mode at $\nu = 13.3942$ d^{-1} changed significantly in amplitude, from 5.16 ± 0.03 to 0.53 ± 0.06 mmag, but also varied quasi-sinusoidally in phase, with a characteristic period similar to the length of the data set. All other p and g modes were stable in both amplitude and phase, which is clear evidence that the visible pulsation mode energy is not conserved within this star. Possible causes of the observed amplitude and phase modulation and the missing mode energy are discussed.

Key words: asteroseismology – stars: individual: KIC 7106205 – stars: oscillations – stars: variables: δ Scuti.

1 INTRODUCTION

The recent revolution in space photometry, facilitated by the *MOST*, *CoRoT* and *Kepler* space missions, has dramatically improved our understanding for a variety of different types of stars. The vast increase in high-quality data has driven remarkable advances into understanding both convection and the mechanisms that drive stellar pulsations in A- and F-type variable stars (Guzik et al. 2000; Dupret et al. 2004, 2005), i.e. the δ Sct and γ Dor stars.

Asteroseismology is a rapidly expanding field of astrophysics, in which stellar pulsations and the internal structures of stars are studied from periodic changes in brightness and radial velocity of their surfaces. With more than 4 yr of high duty-cycle data from the *Kepler* space telescope, we are able to probe frequency and amplitude modulation of pulsation modes in δ Sct and γ Dor stars. The high-precision values of frequency, amplitude and phase for individual pulsation modes in *Kepler* stars yield cleaner and richer amplitude spectra than can be obtained from a ground-based telescope and, most importantly, a better insight into the various pulsation excitation mechanisms.

A little more than a decade ago, Rodríguez & Breger (2001) commented in their catalogue of δ Sct and related stars, that '*severe selection effects exist*' in ground-based observations, which made any analysis requiring high-precision values, such as mode identification, difficult. However, *Kepler* data are not limited by many of

the observational biases encountered when using ground-based surveys, such as poor signal-to-noise and aliasing caused by large gaps in the data. In this paper, we demonstrate the superiority of space photometry, and in particular *Kepler* data, for asteroseismology and the study of pulsational amplitude modulation.

1.1 The *Kepler* mission

The *Kepler* space telescope, launched in 2009 March, has recorded photometric observations of more than 190 000 stars at the µmag precision level (Koch et al. 2010). The *Kepler* telescope is in a 372.5 d Earth-trailing orbit and the field of view covered approximately 115 deg^2 in the constellations of Cygnus and Lyra. The primary goal of the *Kepler* mission was to locate Earth-like planets in the habitable zone of their host star using the transit method (Borucki et al. 2010).

The main mission came to an end in 2013 May when the telescope lost the function of a second reaction wheel that was vital for the still-pointing of the spacecraft. Since the failure, the mission parameters have been changed and the telescope is now observing in the plane of the ecliptic, because in this position solar torques can be balanced so that spacecraft drift can be controlled with minimum loss of propellant (Howell et al. 2014). The new mission has been named 'K2', and provides a variety of targets, such as young stars and star-forming regions, supernovae, white dwarfs and the Galactic Centre (Howell et al. 2014). The telescope may no longer be collecting data on the original target list, but there is more than 4 yr of high-quality

★ E-mail: dmbowman@uclan.ac.uk

data available to study on a variety of different stellar objects – a goldmine for scientific discoveries.

Kepler data are available in two formats, long and short cadence (hereafter called LC and SC, respectively). *Kepler's* primary mission goal required a short integration time in order to maximize the number of data points for each transit of a planet in front of its host star. This was achieved by the SC data, which had an integration time of 58.5 s. However, this limited the number of stars that were observed at this cadence to 512 at any one time (Gilliland et al. 2010). LC data had an integration time of 29.5 min and consequently, the maximum number of LC targets was 170 000 (Jenkins et al. 2010). Therefore, a compromise between the number and temporal resolution of *Kepler* targets was chosen for a given observing time. Most target stars were chosen to fulfil *Kepler's* primary goal of detecting planetary transits, but approximately 1 per cent of all targets were reserved solely for asteroseismology (Gilliland et al. 2010).

LC data are grouped in quarters, denoted by Q[n], where $n =$ 0–17, which lasted for approximately 93 d, although Q0, Q1 and Q17 were approximately 10, 30 and 30 d, respectively. SC data are denoted by Q[n]M[m], where $m = 1$, 2 or 3. Every quarter, *Kepler* had to roll 90 deg in order to keep its solar panels pointing towards the Sun and the radiator for keeping it cool pointing into deep space. Therefore, a star rotated its position on the focal plane four times throughout an entire *Kepler* year. For a detailed review concerning the differences in SC and LC asteroseismology using *Kepler* data and also the differences in the data processing pipelines, see Murphy (2012).

1.2 Delta Scuti stars

Delta Scuti stars are the most common group of pulsating A-type stars, which lie at the intersection of the main sequence and the classical instability strip on the Hertzsprung–Russell (HR) diagram. Whilst on the main sequence, they range from A2 to F0 in spectral type and lie between $7000 \leq T_{\rm eff} \leq 9300$ K (Uytterhoeven et al. 2011).

The δ Sct pulsations are excited by the κ-mechanism, which operates in the He II ionization zone, and consequently pressure (p) modes and gravity (g) modes are observed (Chevalier 1971). The changes in opacity, and therefore pressure, of a parcel of gas relative to its surroundings are analogous to a piston in a heat engine cycle. The result is a periodic expansion and reduction in the radius of the parcel of gas giving rise to the nomenclature of pressure modes. Typical periods for p-mode pulsations in δ Sct stars range from 15 min to 5 h (Uytterhoeven et al. 2011). See Breger (2000a) for a thorough review of δ Sct stars.

1.3 Gamma Doradus stars

Gamma Doradus stars have only been recognized as a distinct category of pulsating objects in the last two decades (Kaye et al. 2000). They have similar effective temperatures and luminosities to δ Sct stars such that both types of star occupy overlapping regions on the HR diagram (Uytterhoeven et al. 2011). Most γ Dor stars observed by *Kepler* lie on the main sequence and range between F5 and A7 in spectral type and between $6500 \leq T_{\rm eff} \leq 7800$ K (Uytterhoeven et al. 2011). However, using *Hipparcos* photometry, Handler (1999) found that γ Dor stars lie between $7200 \leq T_{\rm eff} \leq 7700$ K, which illustrates that a difference in the definition of the red edge of the instability strip can cause confusion between distinguishing

γ Dor and δ Sct stars. Therefore, knowledge of the star's pulsation frequencies is essential in order to classify the pulsator type.

Even though they have similar spectral parameters to δ Sct stars, pulsations observed in γ Dor stars are driven by a different mechanism: the flux modulation or flux blocking mechanism (Guzik et al. 2000; Dupret et al. 2004; Grigahcène et al. 2005). Pulsation driving requires the local convective time-scale at the base of the convection zone to be similar to, or longer than, the pulsation period such that convection cannot adapt quickly enough to damp the pulsations (Guzik et al. 2000). These buoyancy-driven, g-mode pulsations have much longer periods than p modes observed in δ Sct stars and range between 8 h and 3 d (Uytterhoeven et al. 2011).

1.4 Hybrid stars

Due to the unprecedented photometric precision, high duty-cycle and length of *Kepler* data, more pulsation modes have been observed in a variety of stellar types than was previously possible. Some stars have been found to exhibit modes in both the γ Dor regime ($\nu < 4\,{\rm d}^{-1}$) and the δ Sct regime ($\nu \geq 5\,{\rm d}^{-1}$). Attempts have been made to catalogue the many different types of behaviour that these stars present. For example, it has been suggested that δ Sct/γ Dor hybrids and γ Dor/δ Sct hybrids are two distinct groups (Grigahcène et al. 2010).

Classifying a hybrid star often requires a visual inspection of the light curves for the star, which can be a lengthy process. Nonetheless, it is clear that a significant fraction of A- and F-type stars exhibit at least some form of hybrid behaviour. The once separate groups of γ Dor and δ Sct stars overlap more than was previously thought as some stars show pulsations excited by the two different mechanisms (Uytterhoeven et al. 2011). From analysis of the complete *Kepler* data set catalogue, at least 23 per cent of all A- and F-type stars can be classed as hybrid stars (Uytterhoeven et al. 2011).

These stars are ideal test candidates to study pulsation energy conservation between the p and g modes, and also between the modes and the driving zones, for both opacity and convective driving. If, for example, the visible pulsation energy is conserved within a star, then any decrease in mode amplitude in one or more modes would result in any number of other modes increasing in amplitude and vice versa. This concept has not been thoroughly investigated before now, and it is important to understand whether a star's pulsation energy budget is constant, especially on such a short time-scale as 4 yr. If a star does not conserve its pulsation energy, then it may be transferred to either the convection or ionization driving zones, or to another damping region.

2 AMPLITUDE MODULATION

The vast number of stars available to study within the *Kepler* data set has allowed the variety of observed stellar pulsations to be probed. Prior to space-based missions that were useful to asteroseismology, ground-based observations of variable stars had been limited to observing pulsations with amplitudes larger than a few mmag. Even so, some δ Sct stars contained some constant and some extremely variable pulsation modes (Breger 2009). There are few examples of stars that demonstrate this behaviour, and some case studies are given below.

From theoretical studies of δ Sct stars, mode-coupling is expected between different combinations of frequencies (Dziembowski 1982). Parametric resonance instability can occur in which the instability of a linearly driven mode at ν_1 causes the growth

of two modes at ν_2 and ν_3 such that $\nu_1 \approx \nu_2 + \nu_3$, satisfying the resonance condition (Dziembowski 1982). The decay of either a linearly driven p or g mode into two g modes is most likely as linearly driven modes usually have low radial orders (Dziembowski 1982). Observationally, this is difficult to confirm due to the extremely low g-mode amplitudes and the complexities of different mode-coupling mechanisms at work within a star. However, with the high precision of the *Kepler* data, we can now begin to address this question.

2.1 Case studies

In a recent paper, Breger & Montgomery (2014) analysed a rapidly rotating A-type star, KIC 8054146, and observed mode-coupling of two 'parent' modes that produced a single 'child' mode, as predicted by the resonance condition given by Dziembowski (1982). The amplitude changes of a combination mode are predicted to follow the product of the amplitude changes in the two parent modes, which was subsequently used to identify which modes were the parent and child modes (Breger & Montgomery 2014). KIC 8054146 contained 349 statistically significant frequencies in the range $0 < \nu \leq 200\,\mathrm{d}^{-1}$, including three separate 'families' of frequencies whose amplitude variations of the low-frequency members correlated with the high-frequency ones (Breger & Montgomery 2014). Thus, energy seemed to be conserved between the visible pulsation modes in KIC 8054146.

Analysis of the δ Sct star 4 CVn over 40 yr showed modes that appeared and disappeared unpredictably, which illustrated mode stability in A-type stars (Breger 2000b, 2009). A single p mode at $\nu = 7.375\,\mathrm{d}^{-1}$ decreased in amplitude from 15 mmag in 1974 to 4 mmag in 1976 and to 1 mmag in 1977, after which a phase jump occurred and the mode began increasing in amplitude again (Breger 2000b). Observations suggested that other frequencies were strongly coupled to the $\nu = 7.375\,\mathrm{d}^{-1}$ mode and Breger (2000b) speculated that power was being transferred between modes by mode-coupling and suggested a few plausible possibilities as follows.

(i) *Mode beating*: a simple beating model is supported by the observed phase change, which suggested that two modes of similar frequency and amplitude were beating against each other. However, the poor quality of the fit from this model led to this hypothesis being rejected (Breger 2000b).

(ii) *Re-excitation*: the mode decayed and soon afterwards was re-excited with a completely random phase. However, this does not require the phase change of half a cycle that was observed (Breger 2000b).

(iii) *Stellar cycle*: the apparent periodic behaviour of the mode amplitude could be evidence of a stellar cycle as cyclic periodicity in mode amplitude cannot be explained by stellar evolution (Breger 2000b).

With more data, Breger (2009) found that the mode variability could be fitted with a period of decades – far longer than the current data set available for the star. Therefore, without seeing even a single cycle for this mode, it was difficult to test the stellar cycle hypothesis. Therefore, the amplitude modulation in 4 CVn remains an unsolved problem.

A different form of amplitude modulation was seen in the Am star KIC 3429637 (HD 178875), which showed continual growth in mode amplitude across 2 yr of the *Kepler* data set (Murphy et al. 2012). It was shown that two of the three most prominent modes grew in amplitude, whilst the other decreased – changes in all three

modes required different functional forms. Murphy et al. (2012) demonstrated that this was not an instrumental effect, as all modes would decrease or increase with the same functional form if the modulation was instrumental. Murphy et al. (2012) concluded that real-time evolution of the star across 2 yr of observations was seen. As the star evolved, the changes in the different pulsation cavities modulated the observed pulsation amplitudes (Murphy et al. 2012).

Even though they may act as useful case studies, it is difficult to draw conclusions concerning amplitude modulation from a few stars, conclusions that may have been speculative and specific to the case study in question. This is strong motivation for studying this phenomenon in detail using the much larger number of stars showing amplitude modulation within *Kepler* data. Clearly, it is important to understand the various interactions between different pulsation modes, even those that are driven by different excitation mechanisms, which reinforces the importance of studying hybrid stars and understanding the stellar pulsations they produce. To that end, the following hypothesis has been tested: Is the visible pulsation energy conserved within KIC 7106205? From this, an investigation of energy conservation and mode-coupling followed.

3 DATA RETRIEVAL: FROM STAR TO SCREEN

In order to maximize the number of case studies of amplitude modulation, and to create a catalogue of modulated δ Sct and γ Dor stars, a data retrieval and processing method has been automated for all stars between $6500 \leq T_{\mathrm{eff}} \leq 20\,000$ K in the *Kepler* Input Catalogue (KIC; Brown et al. 2011). Since *Kepler*'s launch, the resultant photometric time series have been through several versions of the different data processing pipelines, the latest being the multiscale Maximum A Posteriori (msMAP) implementation of the Pre-search Data Conditioning (PDC) module.[1] Data are available from MAST[2] in FITS file format, which were downloaded for stars between $6500 \leq T_{\mathrm{eff}} \leq 20\,000$ K in the KIC and stored locally. These FITS files were then processed to produce time series in reduced Barycentric Julian Date (BJD – 2400000) and normalized magnitudes for each quarter of LC and month of SC data for every star. A pipeline for producing Fourier transforms for each quarter of LC data was also automated and stars that met the criteria of significant amplitude modulation of at least one pulsation mode were flagged for further study.

The light curve of KIC 7106205 in the top-left panel of Fig. 1 shows reduction in the amplitude of variability of the star on a time-scale less than the length of the data set, which spans a total of 1470 d (4 yr). No data points have been deleted and no gaps have been interpolated in the time series for this star.

The KIC parameters for KIC 7106025 and the revised values from Huber et al. (2014), with their respective errors, are given in Table 1. The values of T_{eff} (6900 K) from both of these catalogues are consistent and characterizes KIC 7106205 as an early F-type star. KIC 7106205 demonstrates a conclusion stated in Huber et al. (2014) that stars with $T_{\mathrm{eff}} \leq 7000$ listed in the original KIC have robust values for T_{eff}. The revised values of $\log g$ and metallicity are sourced from spectroscopy and demonstrate the inconsistencies between spectroscopy and photometry for deriving $\log g$ and metallicity values.

In their overview of A- and F-type stars, Uytterhoeven et al. (2011) classify KIC 7106205 as a pure δ Sct star (i.e. shows no

---

[1] Kepler data notes: https://archive.stsci.edu/kepler/data_release.html
[2] MAST website: http://archive.stsci.edu/kepler/
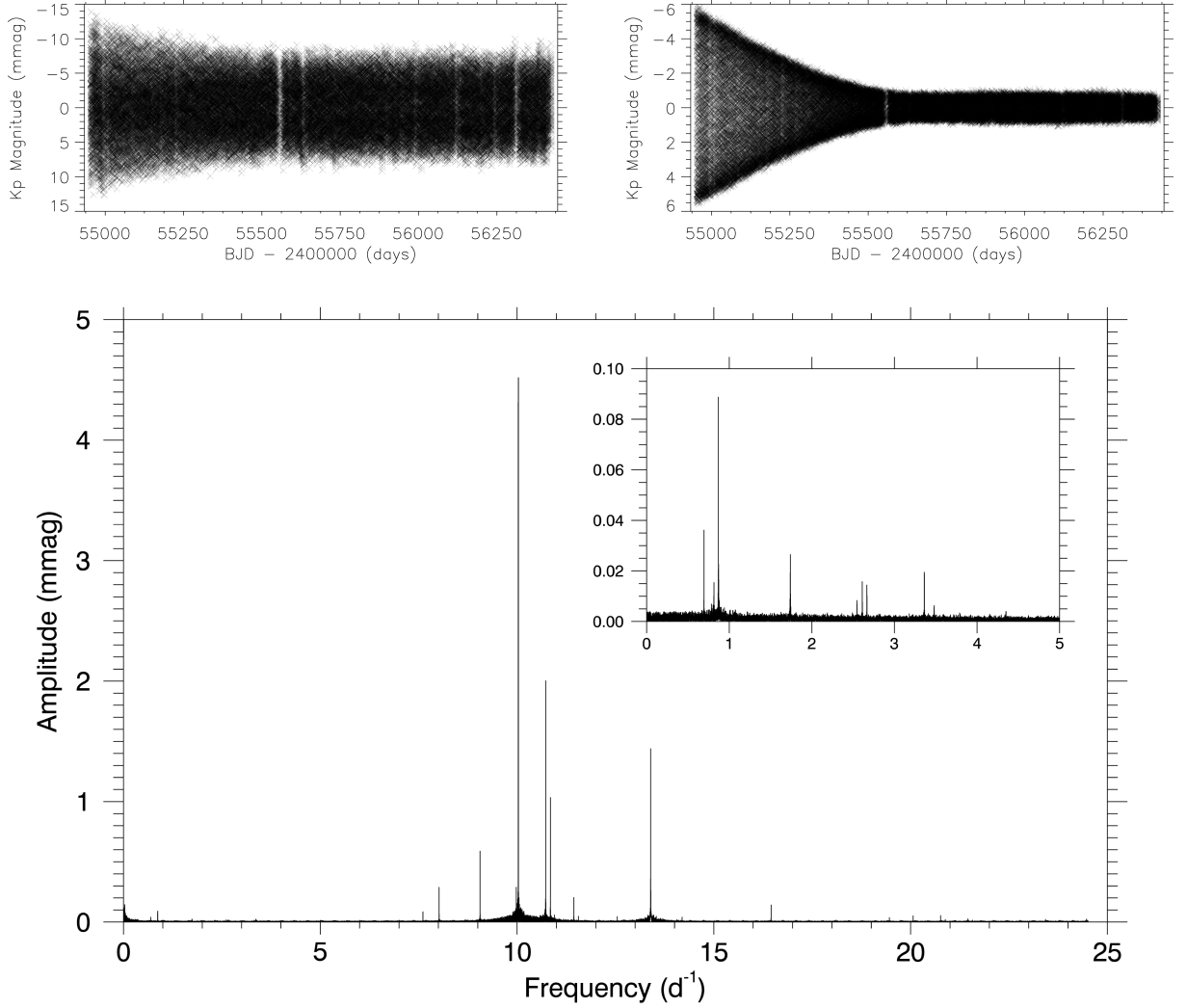
Figure 1. Top-left panel: the light curve of all LC *Kepler* data for KIC 7106205. Top-right panel: the light curve of KIC 7106205 with all significant peaks pre-whitened down to 8 µmag except for $\nu = 13.3942$ d^{-1}. Bottom panel: the discrete Fourier transform of all LC *Kepler* data for KIC 7106205 out to the Nyquist frequency of 24.51 d^{-1}. The subplot in the bottom panel shows the g-mode frequency regime which contains several low-amplitude frequencies.

Table 1. Stellar parameters listed for KIC 7106205 in the KIC (Brown et al. 2011) and the revised values given in Huber et al. (2014).

	$T_{\rm eff}$ (K)	$\log g$ (cm s^{-2})	[Fe/H] (dex)	Radius (R$_\odot$)	$m_{\rm v}$ (mag)	Contamination (per cent)
KIC (Brown et al. 2011)	6960 ± 150	4.05 ± 0.15	-0.01 ± 0.15	1.78 ± 0.89	11.46	0.005
Revised KIC (Huber et al. 2014)	6900 ± 140	3.70 ± 0.15	0.32 ± 0.15	3.23 ± 0.61	–	–

evidence of hybrid behaviour) and also a possible binary system. However, the analysis done by Uytterhoeven et al. (2011) used only Q0 and Q1 of the *Kepler* data set and as such, the resultant frequency resolution with only 40 d of data was 0.025 d^{-1} ($\approx$ 30 µHz). With 1470 d of LC data available for KIC 7106205, consisting of 65 308 data points, the frequency resolution was 6.8×10^{-4} d^{-1} ($\approx$ 8 nHz), and thus frequencies from stars with 1470 d of *Kepler* data are well-resolved. As for possible binarity, the target pixel files were also extracted from MAST, and it was clear that there was negligible contamination from background sources. Contrary to Uytterhoeven

et al. (2011), we found in this analysis that KIC 7106205 is a single star. There is no evidence of the pulsational frequency modulation that would be found in a binary system (Shibahashi & Kurtz 2012).

The Nyquist frequency of LC *Kepler* data is $1/(2\Delta t) = 24.51$ d^{-1}, where $\Delta t = 29.5$ min is the cadence of the data. On board *Kepler*, the data were regularly sampled, but due to the orbit of the spacecraft, barycentric corrections were made to the time series in order to correct for the difference in light arrival time of the photons to the barycentre of the Solar system and to the telescope, respectively (Murphy, Shibahashi & Kurtz 2013). This correction modified the

Table 2. Frequencies with their associated amplitudes, phases with respective errors, extracted using a least-squares fit of 1470 d of data for KIC 7106205. Linear combination frequencies are labelled and pulsation constants are given for the identified real frequencies. The table only gives the g- and p-mode frequencies with amplitudes ≥ 0.01 mmag and ≥ 0.1 mmag, respectively.

	ν (d^{-1})	Amplitude (mmag)	Phase (rad)	Comment	Pulsation constant (d)
g_1	0.6949	0.036 ± 0.006	0.231 ± 0.153	$g_1 = g_8 - g_7$	$Q = 0.3247$
g_2	0.8153	0.016 ± 0.006	2.993 ± 0.357	$g_2 = g_8 - g_5$	$Q = 0.2767$
g_3	0.8697	0.089 ± 0.006	2.986 ± 0.063		$Q = 0.2594$
g_4	1.7397	0.027 ± 0.006	-3.029 ± 0.209		$Q = 0.1297$
g_5	2.5464	0.008 ± 0.006	2.014 ± 0.659	$g_5 = g_8 - g_2$	$Q = 0.0886$
g_6	2.6108	0.016 ± 0.006	-2.280 ± 0.349		$Q = 0.0864$
g_7	2.6669	0.015 ± 0.006	-1.791 ± 0.381	$g_7 = g_8 - g_1$	$Q = 0.0846$
g_8	3.3618	0.020 ± 0.006	0.487 ± 0.284	$g_8 = g_7 + g_1$	$Q = 0.0671$
p_1	8.0193	0.291 ± 0.006	-1.612 ± 0.019		$Q = 0.0281$
p_2	9.0588	0.591 ± 0.006	-2.940 ± 0.009		$Q = 0.0249$
p_3	9.9821	0.291 ± 0.006	-3.160 ± 0.019		$Q = 0.0226$
p_4	10.0324	4.525 ± 0.006	1.602 ± 0.001	$p_4 = p_5 - g_1$	$Q = 0.0225$
p_5	10.7273	2.009 ± 0.006	-2.257 ± 0.003	$p_5 = p_4 + g_1$	$Q = 0.0210$
p_6	10.8477	1.036 ± 0.006	0.065 ± 0.005	$p_6 = p_4 + g_2$	$Q = 0.0208$
p_7	11.4421	0.205 ± 0.006	-1.008 ± 0.027		$Q = 0.0197$
p_8	16.4530	0.144 ± 0.006	0.382 ± 0.034		$Q = 0.0137$
p_{mod}	13.3942	1.444 ± 0.006	-1.007 ± 0.004	$p_{mod} = p_4 + g_8$	$Q = 0.0168$
				$p_{mod} = p_5 + g_7$	
				$p_{mod} = p_6 + g_5$	

time stamps in the time series to be in BJD and resulted in a cadence which was not constant. An advantage of the unequally spaced data allows one to easily identify Nyquist aliases using super-Nyquist asteroseismology (Murphy et al. 2013).

4 A FOURIER VIEW

When analysing asteroseismic data, a normal approach is to use all data in a single Fourier transform, which maximizes the signal-to-noise ratio and frequency resolution. In the following subsections, we explain the differences and advantages between using all data simultaneously compared to dividing the data into time bins, when performing a Fourier analysis of *Kepler* data.

All the amplitude spectra produced in the analysis of KIC 7106205 were discrete Fourier transforms and the method for calculating these numerically is described in detail in Deeming (1975). The mid-point of the entire time series, $t_0 = 2455688.77$ (BJD), was chosen as the zero-point in time when calculating every amplitude spectrum, in order to estimate phase errors accurately over 1470 d when applying non-linear least-squares fitting in other parts of the analysis. For the time-based approach, a bin length of 50 d was chosen, which was a compromise between temporal and frequency resolution. Note that changing the bin length to another value between 30 and 100 d did not significantly alter the results, but only the number of data points in Fig. 4. The mid-point of each 50 d time bin was used as the time value label on the *x*-axis in all plots. The step size in frequency in the amplitude spectrum was defined as $1/(20T)$, where T is the length of each data set in days, so that every peak was fully resolved. All of the above steps ensured that the resultant values of frequency, amplitude and phase were reliable and consistent throughout the analysis, but also that they were of

sufficient accuracy to have been used as input into a least-squares fit.

4.1 All data simultaneously

The amplitude spectrum for all LC data for KIC 7106205 is shown in the bottom panel of Fig. 1. As discussed in Section 1.4, there are two frequency regimes: g modes have frequencies $\nu < 4\,\mathrm{d}^{-1}$ and p modes have frequencies $\nu > 5\,\mathrm{d}^{-1}$. The amplitude spectrum of KIC 7106205 contains many p modes that are clearly visible because of their high amplitudes compared to the noise level. Due to these strong p-mode amplitudes, the g modes were drowned in the noise and associated window patterns of the p modes. In order to see the g modes easily, frequencies outside of the g-mode regime were pre-whitened down to 3 μmag. The strongest eight g modes and nine p modes were used throughout the analysis of KIC 7106205 and are given in Table 2. Since this was not a peak bagging exercise, throughout this paper we refer to *all peaks* as the 17 peaks given in Table 2, as these have strong amplitudes for their respective frequency regime, i.e. $A \geq 0.1$ mmag for p modes and $A \geq 0.01$ mmag for g modes.

The most prominent pulsation mode has a frequency of 10.0324 d^{-1} with an amplitude of 4.525 ± 0.006 mmag. In order to establish whether this mode was stable in frequency and amplitude, the peak was pre-whitened with a sinusoidal function, given as equation (1), where y is the resultant pre-whitened function, A_i is the amplitude, ν_i is the optimized frequency obtained from the non-linear least-squares fit, ϕ_i is the phase in radians and t is the time normalized to the centre of the data set, specifically $t_0 = 2455688.77$ (BJD). The index i refers to a particular mode:

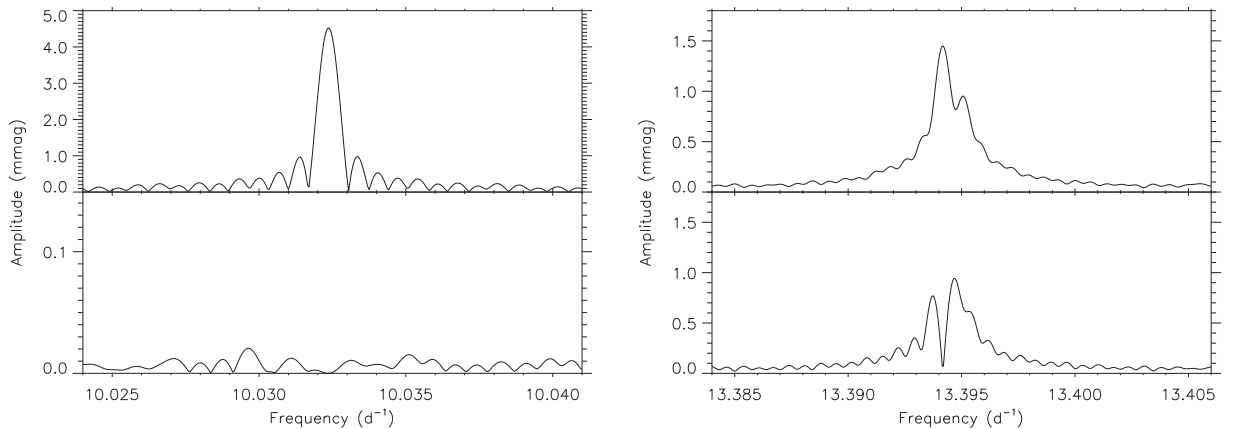$$y = A_i \cos(2\pi\nu_i(t - t_0) + \phi_i). \tag{1}$$

Figure 2. The left-hand panel shows the amplitude spectrum for the strongest stable pulsation mode at $\nu = 10.0324$ d^{-1} and the right-hand panel shows the amplitude spectrum for the modulated pulsation mode at $\nu = 13.3942$ d^{-1}. The top and bottom parts of each panel show the amplitude spectrum before and after pre-whitening, respectively, for each pulsation frequency. Note the change of *y*-axis scale for the stable mode and the fixed *y*-axis scale for the modulated mode.

The amplitude spectrum of the residuals of this fit was calculated and used to examine what periodicity remained within the data after a frequency had been removed from the associated time series. This process was performed for all peaks and it was found that all modes were stable down to at most 10 µmag, except for $\nu = 13.3942$ d^{-1}. A resultant pre-whitened light curve is given in the top-right panel of Fig. 1, in which the significant amplitude modulation of the remaining mode can be seen.

In the pre-whitened amplitude spectrum, the pulsation mode at $\nu = 13.3942$ d^{-1} is not a resolved single peak, which is shown on the right-hand side of Fig. 2. For comparison, the strongest stable frequency at $\nu = 10.0324$ d^{-1} is shown on the left-hand side of Fig. 2. The top and bottom panels are before and after pre-whitening each peak, respectively. The remaining mode amplitude after pre-whitening the peak at $\nu = 13.3942$ d^{-1} was approximately 1 mmag, which was the result of the peak being unresolved over the length of the 1470 d data set. A single frequency value output from a least-squares fit of all the data was unable to remove the various frequencies and corresponding amplitudes produced by this mode over 1470 d. Hence, mode amplitude remains after pre-whitening – a clear result of amplitude modulation. Since the p mode changed in frequency and amplitude over the length of the data set, when all data were used in the amplitude spectrum, an unresolved peak was seen. It is important to note that this is the only pulsation mode that showed this behaviour and all others were stable in frequency and amplitude, remarkably stable to parts-per-million. This establishes that δ Sct stars can have modes stable to this high precision over 4 yr.

4.2 Dividing the data into 50 d segments

The data were divided into 30 bins, each 50 d (except for the last one which was 20 d) in length, which allowed amplitude and phase to be tracked for all modes against time. An amplitude spectrum was calculated for each bin, and the resultant values of amplitude and phase optimized using a least-squares fit with fixed frequency. This showed that the amplitude of the p mode at 13.3942 d^{-1} decreased over the 1470 d data set, from 5.161 ± 0.031 to 0.528 ± 0.055 mmag. This is clearly demonstrated in the right-hand panel of Fig. 3, in which a section of the amplitude spectrum containing the modulated p mode and other stable modes was tracked throughout the entire

data set. The left-hand panel of Fig. 3 shows the g-mode regime tracked throughout the 1470 d data set. The g modes do show small variations in amplitude, but these are negligible. They also show no phase variation and thus are considered to be stable in both amplitude and phase, as any amplitude modulation is within the errors calculated from the least-squares fit.

The fixed frequency for each mode used for tracking amplitude and phase throughout the data set was obtained from a least-squares fit using the frequency, amplitude and phase of the peak from the high-resolution amplitude spectrum for all data as input parameters. The values of amplitude and phase were then optimized using this fixed frequency for each time bin in turn. The corresponding amplitude and phase values for the mode at 13.3942 d^{-1} for each 50 d bin of data are given in Table 3 and shown graphically in the right-hand column of Fig. 4. The same method for tracking amplitude and phase for all other frequencies given in Table 2 was performed. The results for the mode at 10.0324 d^{-1} are included in the left-hand column of Fig. 4 for comparison. 1σ uncertainties for values of amplitude and phase are given in Tables 2 and 3, and shown in Fig. 4, which were calculated from the least-squares fitting routine.

It is clear that the amplitude of the 13.3942 d^{-1} mode dropped significantly and the phase changed over the length of the data set, while all other mode frequencies were stable in both amplitude and phase. We now discuss the implications of these observations.

5 DISCUSSION

The hypothesis proposed in Section 2 concerning amplitude modulation has been successfully tested: Is the visible pulsation energy conserved in KIC 7106205?

Small changes in amplitude were observed in the g modes, but these changes were negligible as the errors on amplitudes were relatively much larger on smaller values. Moreover, the changes in g-mode amplitudes were not sufficient to explain the significant decrease in amplitude of the mode at $\nu = 13.3942$ d^{-1}. Since the modulated mode was decreasing in amplitude, one would expect the g-mode amplitudes to increase, if energy were to be conserved between the visible pulsation modes. Since, the negligible variation in the g-mode amplitudes also show a slight decrease in amplitude over the data set, the energy from the mode at $\nu = 13.3942$ d^{-1} is not being transferred to the g modes.
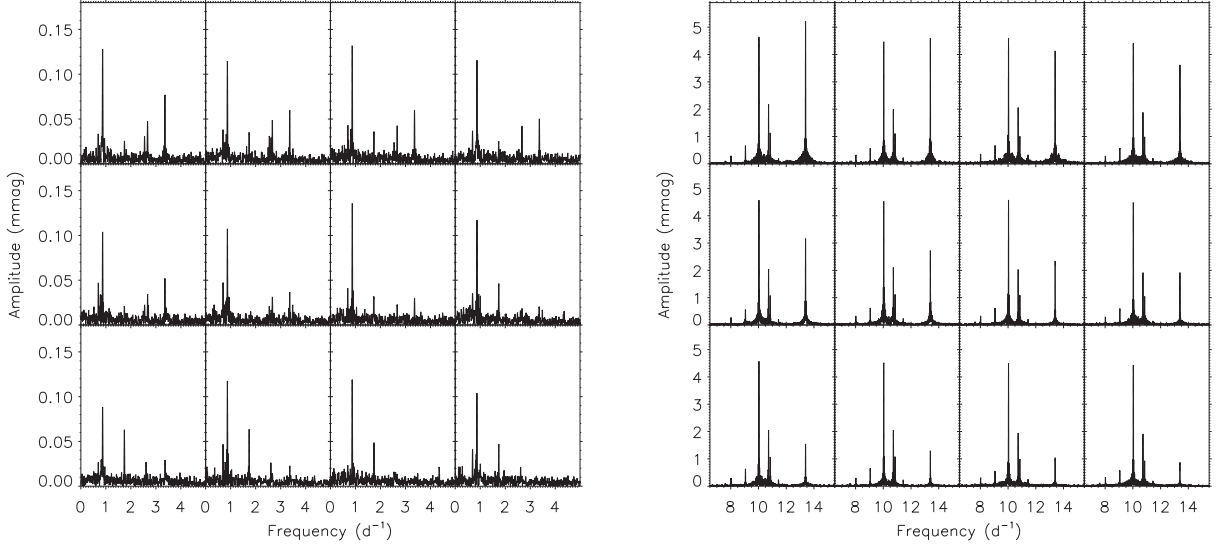
Figure 3. Going from left to right, row by row, the left- and right-hand panels show the amplitude spectra for consecutive bins of 50 d of *Kepler* data for KIC 7106205 for the g-mode and p-mode regimes, respectively. The *y*-axis range is kept fixed in both panels, in order to show the slight modulation in g-mode amplitudes and the significant reduction in amplitude of the p mode at $\nu = 13.3942 \ \mathrm{d}^{-1}$ in each successive amplitude spectrum. All other p modes remain stable in frequency and amplitude.

Table 3. Amplitude and phase values optimized using a least-squares fit analysis for a fixed frequency of $13.3942 \ \mathrm{d}^{-1}$ for each 50 d time bin, where N is the number of data points in each time bin. The phases are all with respect to the time zero-point $t_0 = 2455688.77$ (BJD).

Mid-point of bin BJD − 2400000 (d)	N	Amplitude (mmag)	Phase (rad)
54978.53	2121	5.161 ± 0.031	-1.284 ± 0.006
55028.53	2258	4.634 ± 0.030	-1.184 ± 0.006
55078.53	2208	4.113 ± 0.030	-1.096 ± 0.007
55128.53	2339	3.607 ± 0.029	-1.003 ± 0.008
55178.53	2179	3.126 ± 0.030	-0.908 ± 0.010
55228.53	2178	2.716 ± 0.030	-0.824 ± 0.011
55278.53	2283	2.295 ± 0.030	-0.744 ± 0.013
55328.54	2287	1.907 ± 0.030	-0.686 ± 0.016
55378.54	2315	1.576 ± 0.029	-0.656 ± 0.019
55428.54	2379	1.300 ± 0.029	-0.651 ± 0.022
55478.54	2312	1.037 ± 0.029	-0.669 ± 0.028
55528.05	2307	0.850 ± 0.029	-0.731 ± 0.035
55586.43	1391	0.705 ± 0.038	-0.858 ± 0.054
55628.54	2078	0.633 ± 0.031	-0.972 ± 0.049
55678.54	2390	0.599 ± 0.029	-1.125 ± 0.048
55728.55	2200	0.598 ± 0.030	-1.230 ± 0.050
55777.89	2310	0.603 ± 0.029	-1.304 ± 0.049
55828.66	2272	0.618 ± 0.030	-1.340 ± 0.048
55878.10	2031	0.632 ± 0.031	-1.345 ± 0.050
55929.93	2116	0.645 ± 0.031	-1.336 ± 0.048
55978.55	2077	0.653 ± 0.031	-1.309 ± 0.048
56028.54	2332	0.661 ± 0.029	-1.270 ± 0.044
56078.52	2335	0.647 ± 0.029	-1.219 ± 0.045
56128.53	1945	0.640 ± 0.032	-1.170 ± 0.050
56178.54	2379	0.626 ± 0.029	-1.120 ± 0.046
56228.54	1985	0.603 ± 0.032	-1.074 ± 0.053
56278.53	2387	0.575 ± 0.029	-1.011 ± 0.050
56328.53	1808	0.558 ± 0.033	-0.950 ± 0.059
56378.54	2062	0.545 ± 0.031	-0.910 ± 0.057
56413.77	663	0.528 ± 0.055	-0.869 ± 0.104

Table 2 lists the frequencies, amplitudes and phases with respective errors of the g and p modes used in this analysis. It also labels the frequencies most likely to be combination frequencies. The pulsation constants were calculated using equation (2):

$$\log Q = \log P + \frac{1}{2}\log g + \frac{1}{10}M_{\mathrm{Bol}} + \log T_{\mathrm{eff}} - 6.454, \qquad (2)$$

where P is the pulsation period in days, M_{Bol} is the bolometric magnitude (a value of $M_{\mathrm{Bol}} = 1.2$ was calculated using T_{eff} and $\log g$ in comparison with the Pleiades main sequence) and other parameters have their usual meanings with values taken from Huber et al. (2014). The modulated p mode at $\nu = 13.3942 \ \mathrm{d}^{-1}$ is subject to combination effects, but since the g-mode amplitudes are so small and their variation is negligible, it is unlikely that these combination effects are the cause of the significant amplitude modulation. The strongest pulsation frequency at $\nu = 10.0324 \ \mathrm{d}^{-1}$ has a pulsation constant of $Q = 0.0225$ d, which suggests that it is a first or second radial overtone mode (see Stellingwerf 1979). The modulated mode at $\nu = 13.3942 \ \mathrm{d}^{-1}$ has a pulsation constant of $Q = 0.0168$ d which suggests that it is a third or fourth radial overtone mode. Since none of the p modes have Q-values greater than the 0.033 d expected for the radial fundamental mode, there is no evidence of any mixed modes.

From the amplitude spectrum of all data, we found that the amplitudes of the eight highest p and eight highest g modes were stable to at most 10 μmag, and a single modulated mode at $13.3942 \ \mathrm{d}^{-1}$ was unstable. Amplitude and phase values, optimized by least-squares fitting, for a fixed frequency were also tracked across 1470 d and found to be stable for all modes except $\nu = 13.3942 \ \mathrm{d}^{-1}$. The most important point to note is that KIC 7106205 is a star that contains pulsation modes, stable in frequency and amplitude to remarkable levels of precision, but also contains a single pulsation mode that is not. This behaviour is astrophysical and is not an instrumental effect. If this were an instrumental effect, one would expect all modes to decrease (or increase) in amplitude by the same amount over the length of the data set. Since a significant decrease in amplitude of the pulsation mode at $\nu = 13.3942 \ \mathrm{d}^{-1}$ was observed and all
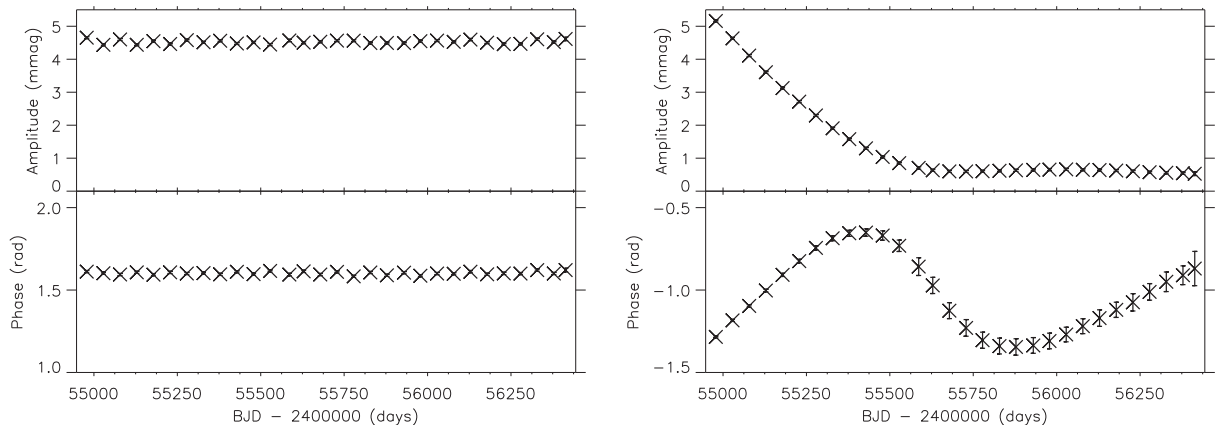
Figure 4. The left-hand panel contains amplitude and phase plots for the strongest stable mode at a fixed frequency of 10.0324 d^{-1} over 1470 d. The right-hand panel contains amplitude and phase plots for the modulated mode at a fixed frequency of 13.3942 d^{-1} over 1470 d. The x-axis is the mid-point of each 50 d time bin in BJD – 2400000 d and phase values were calculated relative to the mid-point of the 1470 d time series. 1σ uncertainties for amplitude and phase values are also plotted, which were calculated from the least-squares fitting routine. The error bars are generally smaller than the data points. Note the y-axis scales are the same for both modes.

other modes were stable in frequency and amplitude, it is concluded that the visible pulsation energy was not conserved. In the following subsections, the possible causes of the amplitude modulation and quasi-sinusoidal phase variation are discussed.

5.1 Causes of decreasing mode amplitude

Analysis of KIC 7106205 showed a single mode that decreased in amplitude by an order of magnitude, on a time-scale less than 1470 d, with all other modes remaining stable in amplitude and phase. This star is an example of a hybrid star within the *Kepler* data set with p and g modes, but also both stable and unstable pulsation modes, among which visible energy is not conserved. The energy from this modulated mode has gone somewhere other than into the visible pulsation modes, as all other modes were observed to be stable in frequency and amplitude. The following are possible causes of the amplitude modulation observed in KIC 7106205.

(i) *Energy is lost to the convection or ionization zone*: the energy may have been lost to the convection zone or He II ionization zone, both of which are driving regions in δ Sct and γ Dor stars. This suggests that driving and damping are unstable processes on the time-scale studied for some pulsation modes, but not for others. We conjecture that this is a function of the structure of the mode cavity with respect to the driving zones, particularly the positions of the radial nodes. Modelling studies might shed some light on this conjecture, and further observational studies of the *Kepler* hybrid stars will illuminate the range of mode stability characteristics observationally. Similar behaviour was reported by Breger (2000a) from ground-based study of the δ Sct star 4 CVn. KIC 7106205 demonstrates how much more clearly we can examine mode stability with the nearly continuous, high-precision *Kepler* 4 yr data.

(ii) *Mode beating*: the change in amplitude of the modulated p mode at $\nu = 13.3942$ d^{-1} is unlikely to be the result of unresolved frequencies beating. The amplitude spectrum of the full 1470 d data set shows a broad peak not consistent with only two unresolved modes; hence, a hypothesis of beating of unresolved mode frequencies would require more than two. That is further supported by the apparently non-periodic behaviour of the amplitude variability,

coupled with the quasi-sinusoidal phase variability. This case is not similar to that of 4 CVn, where Breger (2000b) did suggest beating of unresolved mode frequencies. Finally, for mode frequencies to be unresolved in the 1470 d full *Kepler* data set, they have to be closer in frequency than 8 nHz. It is an unresolved question whether two mode frequencies can be this close in a pulsating star and still maintain their independent characters. Modelling studies are needed to address this question.

(iii) *Stellar evolution*: pulsations are the result of the balance between the driving and damping mechanisms in a star. Could the modulation of the $\nu = 13.3942$ d^{-1} mode be the result of evolutionary changes in the structure of KIC 7106205, which lies close to the red edge of the δ Sct instability strip (Uytterhoeven et al. 2011)? The answer to that question is not known, but for it to be true, the pulsation cavities would need to be finely tuned for all other modes to show the high level of stability observed.

(iv) *Mode-coupling*: as mentioned in Section 2, theory of δ Sct star pulsations predicts mode-coupling that can affect pulsation frequencies. Dziembowski (1982) derived a parametric resonance condition of $\nu_1 \approx \nu_2 + \nu_3$, in which a low radial order, linearly driven mode, ν_1, is able to decay into two other modes, ν_2 and ν_3. The most likely outcome is two g modes with low amplitudes. If the g modes are not observable, then this hypothesis cannot be verified. Small and negligible changes in amplitude were seen in the low-amplitude g modes present in KIC 7106205. However, the only combination frequencies that included the mode at $\nu = 13.3942$ d^{-1} do not exclusively involve two g modes that satisfy $\nu_1 \approx \nu_2 + \nu_3$. Moreover, the small amplitudes of the observed g modes cannot explain the amplitude modulation seen in the mode at $\nu = 13.3942$ d^{-1} according to the parametric resonance theory of Dziembowski (1982), as the amplitudes of the coupled modes need to be comparable. No growth of g mode amplitudes was observed. Breger & Montgomery (2014) do observe parent–daughter mode-coupling in *Kepler* data of the unusual δ Sct star KIC 8054146, but we see no similar behaviour in KIC 7106205. We consider it unlikely that mode-coupling to g modes that are not visible in the amplitude spectrum is an explanation for the changes in the 13.3942 d^{-1} mode. However, we cannot rule our coupling to high-degree (high-ℓ) modes that are not visible in broad-band photometry. A hypothesis of mode-coupling to

unobservable high-degree modes is not testable with *Kepler* data. This does not contradict our conclusion that we have tested the hypothesis of energy conservation in *observable* modes.

5.2 Quasi-sinusoidal phase variations

A remarkable outcome of this analysis was the sinusoidal variation in phase of the p mode at a fixed frequency of $\nu = 13.3942\,\text{d}^{-1}$. This cannot be the result of frequency modulation in a binary system (Shibahashi & Kurtz 2012), since that would affect all pulsation frequencies and would not generate amplitude modulation. The changes in the $13.3942\,\text{d}^{-1}$ mode are internal to the star. A magnetic cycle with changes confined to the thin surface convection zone might conceivably affect only the highest radial overtone mode. However, the existence of lower amplitude modes with even higher frequencies, such as the one at $\nu = 16.4530\,\text{d}^{-1}$ listed in Table 2, argues against this.

We know that the pulsation frequencies in the Sun are variable over the solar cycle (Chaplin et al. 2000, 2007), but whether such an effect is possible in δ Sct stars is unknown. In the case of KIC 7106205, the lack of any indication of periodicity in the amplitude modulation of the $13.3942\,\text{d}^{-1}$ mode does not support a hypothesis of cyclic behaviour, and we note that for the phase variation there is only one cycle that may, or may not continue to vary quasi-sinusoidally. The possibly periodic nature of this variation suggests that the mode may become re-excited in the future and start to increase in amplitude once again, but with only a single cycle observed, this is very speculative. This was not observed in the amplitude and phase variations of 4 CVn, as the re-excited pulsation mode in that star was preceded by a phase shift of half a cycle (Breger 2000b, 2009). Quasi-sinusoidal phase variation was also observed in pulsation modes in KIC 8054146, which Breger & Montgomery (2014) interpreted as mode-coupling, since they could observe the coupled modes in that star. We cannot do that for KIC 7106205. We therefore reach no conclusion about the quasi-sinusoidal phase variation of the $13.3924\,\text{d}^{-1}$ mode, but simply note it.

6 CONCLUSIONS

KIC 7106205 is an ideal case study of a δ Sct star that exhibits amplitude modulation because only a single pulsation mode is modulated over the length of the data set, whilst all other modes remained highly stable in both frequency and amplitude. We showed that this amplitude modulation is astrophysical, not instrumental. A single p mode at $\nu = 13.3942\,\text{d}^{-1}$ decreased in amplitude from 5.161 ± 0.031 to 0.528 ± 0.055 mmag over 1470 d. The missing mode power was not seen to increase the amplitude of any existing p or g mode, nor did it excite any new visible modes in either of the low- or high-frequency regime. Hence, we conclude that the visible pulsation energy is not conserved in KIC 7106205.

There are two possible explanations for the lost mode energy: mode-coupling or loss of mode energy to the convection zone and/or the pulsational p mode driving He II ionization zone. We suggested that mode-coupling to g modes is not a likely explanation, as even though g modes are visible in hybrid stars such as KIC 7106205, none of the g modes observed meet the criteria specified in Dziembowski (1982). We cannot rule out coupling to high-degree modes that are not visible in broad-band photometry. Breger (2000b) speculated that power can be transferred between pulsation modes by a mode-coupling mechanism but was unable to completely explain the amplitude modulation observed in 4 CVn. Similarly, Breger

& Montgomery (2014) concluded that a mode-coupling mechanism was operating in KIC 8054146, in which amplitude and phase variation of many different modes was observed. A similar mode-coupling mechanism could be at work within KIC 7106205 and such effects are important if one is to fully understand the mechanisms that excite pulsation modes and the physics that governs hybrid stars within the instability strip. Alternatively, if mode-coupling is not the explanation, then the lost energy must have been transferred somewhere in the star; whether this is caused by a decrease in driving in the He II ionization zone or an increase in damping elsewhere is not known.

Stellar evolution theory and convection models predict that real-time evolution of a star can be observed with a data set as short as a few years. Murphy et al. (2012) analysed a ρ Puppis star, in which two pulsation modes grew in amplitude over the time span of the data set. They concluded that the growth in mode amplitude might be the result of the pulsation driving zone being driven deeper within the He II ionization zone, which is predicted by stellar evolution models for this star. Therefore, the star was evolving in real time over the 2 yr of observations. Since a decline in mode amplitude was observed in KIC 7106205, it is unlikely that this is the same effect. It does mean that stellar evolution can operate on short time-scales, of the order of years, but does not provide support for the amplitude modulation being caused by the outer layers of KIC 7106205 altering the pulsation cavity for the $13.3942\,\text{d}^{-1}$ mode. The mode at $13.3942\,\text{d}^{-1}$ is not the highest overtone observed in KIC 7106205, it is unlikely that stellar evolution is the solution to the amplitude modulation seen, as a higher frequency mode at $\nu = 16.4530\,\text{d}^{-1}$ was observed to be stable.

Both mode-coupling to high-degree modes and energy being lost to a damping region could explain the amplitude modulation seen in KIC 7106205. The analysis of the star does not distinguish which is more likely, only that the energy lost from the modulated mode was not transferred to any of the existing observed pulsation modes. In reality, both solutions could be operating in congruence, as both are feasible solutions to the observed amplitude modulation, which further complicates the issue of testing the hypothesis of energy conservation between pulsation modes.

These conclusions are speculative, but this is a step towards understanding the phenomenon of amplitude modulation within δ Sct and γ Dor stars using the *Kepler* data set. What is certain is that the hypothesis concerning energy conservation between visible pulsation modes has been successfully tested and proved not to be the case in KIC 7106205. This problem of mode stability is widely observed in pulsating stars. For stochastically driven, solar-like and red giant pulsators, there is no problem understanding changes in mode amplitude and phase, given the stochastic nature of the driving. For heat engine pulsators, the situation is unclear.

REFERENCES

Borucki W. J. et al., 2010, Science, 327, 977
Breger M., 2000a, in Breger M., Montgomery M., eds, ASP Conf. Ser. Vol. 210, Delta Scuti and Related Stars. Astron. Soc. Pac., San Francisco, p. 3
Breger M., 2000b, MNRAS, 313, 129

Breger M., 2009, in Guzik J. A., Bradley P. A., eds, AIP Conf. Proc. Vol. 1170, Stellar Pulsation: Challenges for Theory and Observation. Am. Inst. Phys., New York, p. 410

Breger M., Montgomery M. H., 2014, ApJ, 783, 89

Brown T. M., Latham D. W., Everett M. E., Esquerdo G. A., 2011, AJ, 142, 112

Chaplin W. J., Elsworth Y., Isaak G. R., Miller B. A., New R., 2000, MNRAS, 313, 32

Chaplin W. J., Elsworth Y., Miller B. A., Verner G. A., New R., 2007, ApJ, 659, 1749

Chevalier C., 1971, A&A, 14, 24

Deeming T. J., 1975, Ap&SS, 36, 137

Dupret M.-A., Grigahcène A., Garrido R., Gabriel M., Scuflaire R., 2004, A&A, 414, L17

Dupret M.-A., Grigahcène A., Garrido R., Gabriel M., Scuflaire R., 2005, A&A, 435, 927

Dziembowski W., 1982, Acta Astron., 32, 147

Gilliland R. L. et al., 2010, PASP, 122, 131

Grigahcène A., Dupret M.-A., Gabriel M., Garrido R., Scuflaire R., 2005, A&A, 434, 1055

Grigahcène A. et al., 2010, Astron. Nachr., 331, 989

Guzik J. A., Kaye A. B., Bradley P. A., Cox A. N., Neuforge C., 2000, ApJ, 542, L57

Howell S. B. et al., 2014, PASP, 126, 398

Handler G., 1999, MNRAS, 309, L19

Huber D. et al., 2014, ApJS, 211, 2

Jenkins J. M. et al., 2010, ApJ, 713, L120

Kaye A. B., Handler G., Krisciunas K., Poretti E., Zerbi F. M., 2000, in Szabados L., Kurtz D., eds, ASP Conf. Ser. Vol. 203, IAU Colloq. 176: The Impact of Large-Scale Surveys on Pulsating Star Research. Astron. Soc. Pac., San Francisco, p. 426

Koch D. G. et al., 2010, ApJ, 713, L79

Murphy S. J., 2012, MNRAS, 422, 665

Murphy S. J., Grigahcène A., Niemczura E., Kurtz D. W., Uytterhoeven K., 2012, MNRAS, 427, 1418

Murphy S. J., Shibahashi H., Kurtz D. W., 2013, MNRAS, 430, 2986

Rodríguez E., Breger M., 2001, A&A, 366, 178

Shibahashi H., Kurtz D. W., 2012, MNRAS, 422, 738

Stellingwerf R. F., 1979, ApJ, 227, 935

Uytterhoeven K. et al., 2011, A&A, 534, A125

This paper has been typeset from a TeX/LaTeX file prepared by the author.

3.3 Combining WASP and *Kepler* data: the case of the δ Sct star KIC 7106205

Space-based photometry offers unprecedented photometric precision and a high duty-cycle, which is useful for asteroseismology. However, the financial expenditure needed to build, launch and support such missions is large and so these missions often do not last for more than a few years. One of the major advantages of ground-based telescopes is the relatively small maintenance and support costs, and the accessibility that can extend the lifetime of a telescope if a problem occurs. For studying variable stars, the pulsation mode frequencies are the main data parameters, so high frequency resolution from long observations is preferable. In section 3.2, it was shown that 4 yr of *Kepler* data was not long enough to resolve the amplitude modulation in the δ Sct star KIC 7106205 (Bowman & Kurtz 2014), so data from a ground-based telescope have been used to extend the observations of this star.

The Wide Angle Search for Planets (WASP) project is a wide-field survey based at two observing sites that aims to find transiting exoplanets (Pollacco et al. 2006). The instruments use broad-band filters of $400 - 700$ nm for observations, with the WASP wavelength response function plotted in comparison to *Kepler* passband in Fig. 3.1. The WASP observations of the δ Sct star KIC 7106205 from 2007 provided the opportunity to study amplitude modulation in this star 2 yr prior to the launch of the *Kepler* Space Telescope. However, the instrumentation differences between WASP and *Kepler* meant that the WASP data needed to be calibrated before it could be included in the analysis of KIC 7106205. Specifically, the WASP data needed to be calibrated for the difference in integration time, wavelength passband and dilution in the WASP aperture from neighbouring stars, with full details of the methodology given by Bowman et al. (2015). Further details of the WASP project are given by Pollacco et al. (2006).
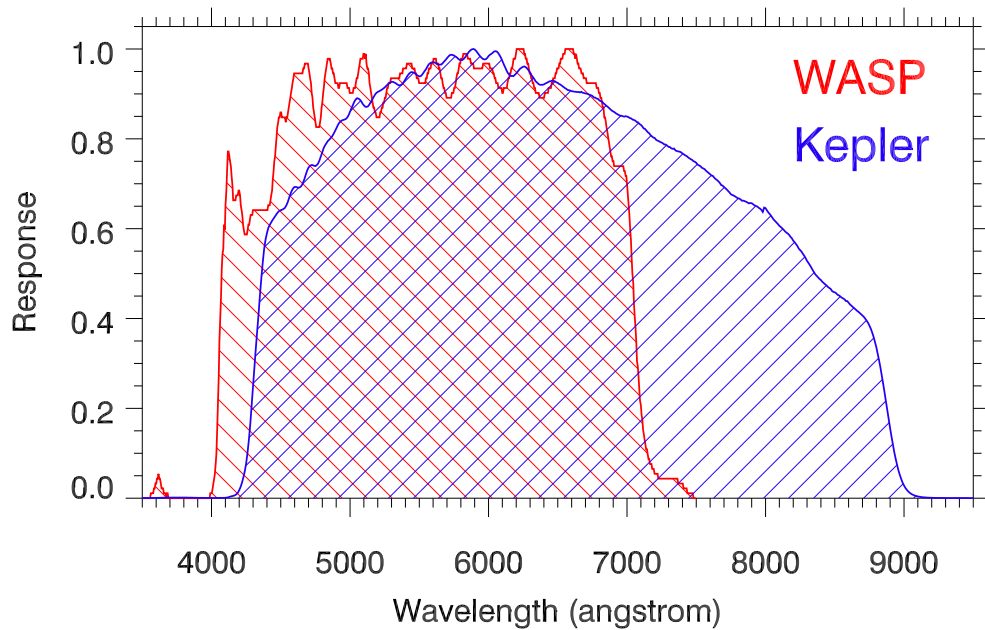
Figure 3.1: The normalised wavelength response functions for the *Kepler* and WASP instruments are plotted as the blue and red hatched regions, respectively.

In this section, the research paper by Bowman et al. (2015) is presented, which was published in Monthly Notices of Royal Astronomical Society in May 2015. I led and co-ordinated the project, including the frequency analysis and calibration of the WASP data for the δ Sct star KIC 7106205. The WASP data were kindly contributed by D. L. Holdsworth, who assisted in the frequency analysis and calibration, and also contributed to the writing of sections 1.2, 3 and 4 in the paper. D. W. Kurtz provided guidance throughout the project and contributed to the discussion and editing of the paper.

Combining WASP and *Kepler* data: the case of the δ Sct star KIC 7106205

Dominic M. Bowman,[1][*] Daniel L. Holdsworth[2] and Donald W. Kurtz[1]

[1]*Jeremiah Horrocks Institute, University of Central Lancashire, Preston PR1 2HE, UK*
[2]*Astrophysics Group, Keele University, Staffordshire ST5 5BG, UK*

ABSTRACT

Ground-based photometric observations from Wide Angle Search for Planets (WASP) have been calibrated, scaled and combined with *Kepler* observations of the δ Sct star KIC 7106205, allowing us to extend the time base of the study of the unexplained amplitude and frequency variation of a single pressure mode at $\nu = 13.3942\,\mathrm{d}^{-1}$ by 2 yr. Analysis of the combined data sets, spanning 6 yr, show that the amplitude modulation in KIC 7106205 has a much larger range than a previous study of the *Kepler* data alone indicated. The single pressure mode decreased from 11.70 ± 0.05 mmag in 2007, to 5.87 ± 0.03 mmag in 2009, and to 0.58 ± 0.06 mmag in 2013. Observations of the decrease in mode amplitude have now been extended back 2 yr before the launch of *Kepler*. With observations over a longer time span, we have been able to further investigate the decrease in mode amplitude in KIC 7106205 to address the question of mode amplitude stability in δ Sct stars. This study highlights the usefulness of the WASP data set for extending studies of some *Kepler* variable stars.

Key words: asteroseismology – stars: individual: KIC 7106205 – stars: oscillations – stars: variables: δ Scuti.

1 INTRODUCTION

The *Kepler* mission photometric data set spans 4 yr for over 190 000 stars, with precision in the measurement of the amplitudes of pulsating stars of the order of a few μmag. While these data provide unprecedented views of the light variations in variable stars, many stars are not purely periodic, and we wonder what happened for these stars before the *Kepler* data set started and after the *Kepler* data set ended. In this paper, we demonstrate how including ground-based photometric data, specifically from the Wide Angle Search for Planets (WASP) project, alongside *Kepler* data allows us to study the multiperiodic δ Sct star KIC 7106205 (TYC 3129-879-1; 1SWASPJ191157.46+424022.6) over a longer time span than the 4 yr of the *Kepler* data set – a total of 6 yr in this case. Our aim is to investigate the unusual frequency and amplitude modulation in only a single pulsation frequency, discovered by Bowman & Kurtz (2014), and to test if this behaviour is present in other observations of this star, specifically the WASP data set.

Periodic changes in the surface brightness and measurements of radial velocities of pulsating stars allow us to probe stellar interiors and have driven remarkable advances in understanding the mechanisms that drive pulsations in variable stars, especially δ Sct stars (e.g. Dupret et al. 2004, 2005). The δ Sct stars lie at the intersection of the main sequence and the classical instability strip on the Hertzsprung–Russell diagram (Uytterhoeven et al. 2011). The

pulsations are driven by the κ-mechanism, in which changes in opacity set up a piston-like change in the radius of a shell of gas in the He II ionization zone (Chevalier 1971). Consequently, low-order p modes are excited, with typical periods of 15 min to 5 hr (Uytterhoeven et al. 2011). See Breger (2000) and Murphy (2014) for reviews of δ Sct stars.

Pulsational frequency and/or amplitude modulation are observed in a variety of stellar types, e.g. solar-like stars (Chaplin et al. 2000, 2007), δ Sct stars (Bowman & Kurtz 2014; Breger & Montgomery 2014), roAp stars (Holdsworth et al. 2014b; Kurtz et al. 1997), and white dwarfs (Winget et al. 1991). For stochastically driven pulsators, the short mode lifetimes are easy to explain, given the nature of the driving and damping mechanisms that are competing within the star. However, no theory exists that can explain the diversity of behaviours observed, especially in the classical pulsators, e.g. the δ Sct stars (see Breger & Montgomery 2014 and references therein).

1.1 The *Kepler* mission

The *Kepler* space telescope was launched in 2009 March and observed more than 190 000 stars at high photometric precision and high duty-cycle (Koch et al. 2010). The primary goal of the mission was to observe Earth-like planets within the habitable zone of their host star using the transit method (Borucki et al. 2010). A total of 4 yr (1470 d) of observations were collected, covering a 115 deg² field of view in the constellations of Cygnus and Lyra. Observations, taken in the passband of 420–900 nm (Koch et al. 2010), were made in two modes, long cadence (LC) of 29.5 min, and short

[*] E-mail: dmbowman@uclan.ac.uk

cadence of 58.5 s (Gilliland et al. 2010). These excellent data have also proved invaluable for studying pulsating stars. A frequency resolution of 7.9 nHz (0.00068 d^{-1}) is obtained when calculating the Fourier transform of all 1470 d of *Kepler* observations, so only since the end of the main mission has it been possible to study frequency modulation in δ Sct stars at this precision, and to study amplitude modulation over this time span.

1.2 The WASP project

The WASP project is a two-site wide-field survey for transiting exoplanets (Pollacco et al. 2006). The instruments are located at the Observatorio del Roque de los Muchachos on La Palma and at the Sutherland Station of the South African Astronomical Observatory (SAAO), and achieved first light in 2003 and 2005, respectively. The instruments consist of eight 200-mm, f/1.8 Canon telephoto lenses mounted in a 2 × 4 configuration. Each is backed by an Andor CCD of 2048 × 2048 pixels, allowing a pixel size of about 14 arcsec. Observations are made through broad-band filters of 400–700 nm for the eight lenses. The data pass through a reduction pipeline correcting for primary and secondary extinction, the colour-response of the instrument, the zero-point, and atmospheric extinction. The pipeline is optimized for G stars. The data are also corrected for instrumental systematics using the SYSREM algorithm of Tamuz, Mazeh & Zucker (2005).

The observing strategy of WASP provides two consecutive 30 s exposures at a given pointing, before moving to the next available field; fields are typically revisited every 10 min. Such a strategy has enabled the discovery of many types of variable stars, from low-frequency binary stars (Smalley et al. 2014), to high-frequency pulsating A stars (Holdsworth et al. 2014a). For further details of the WASP project and the techniques used for the detection of pulsations, we refer the reader to Pollacco et al. (2006) and Holdsworth et al. (2014a), respectively.

1.3 Mode-coupling in δ Sct stars

The δ Sct stars demonstrate diverse pulsational behaviour, but no theory exists to describe all the phenomena observed, especially variable pulsation amplitudes. Mode-coupling is predicted between frequencies in δ Sct stars (Dziembowski 1982), specifically parametric resonance in which the instability of a linearly driven mode at ν_1 causes the growth of two modes at ν_2 and ν_3, such that $\nu_1 \approx \nu_2 + \nu_3$. The most likely outcome of these non-linear effects is the decay in amplitude of a linearly driven p mode, as such modes usually have low radial orders, and the growth of two g modes (Dziembowski 1982; Nowakowski 2005). These g modes can become trapped in a pulsation cavity close to the core of the star and are therefore invisible at the stellar surface. Thus, these are considered *internal* g modes.

Observationally, the resonant mode-coupling predictions of Dziembowski (1982) and Nowakowski (2005) are difficult to test using broad-band photometry alone, as high-degree (high-ℓ) p modes and internal g modes have small amplitudes at the surface of the star. On the other hand, studies of variable amplitudes of modes of low degree ($\ell \leq 2$) are relatively easy as a consequence of their higher visibility.

2 PREVIOUS STUDY OF KIC 7106205

KIC 7106205 is a multiperiodic δ Sct star that was studied by Bowman & Kurtz (2014) using *Kepler* data. They tracked amplitude

and phase at fixed frequency for 16 significant pulsation modes over the 1470 d time span of the *Kepler* data set. All pulsation frequencies were found to be remarkably stable except for $\nu_{\text{mod}} = 13.3942 \, \text{d}^{-1}$, which decreased in amplitude from 5.87 ± 0.03 mmag in 2009 to 0.58 ± 0.06 mmag in 2013, corrected for the *Kepler* integration time (see equation 1). The pulsation constant of ν_{mod} indicates it is likely a third or fourth radial overtone mode. Higher frequencies (i.e. higher overtones) were observed to be stable, thus the observed modulation was not constrained to the surface of the star (Bowman & Kurtz 2014).

The loss of mode energy of ν_{mod} was not observed to excite any new frequencies or to be transferred to any existing frequencies. Therefore, it was concluded that energy was lost to a damping region within the star or transferred to either high-ℓ p modes or two internal g modes via the parametric resonance instability. Both outcomes would result in modes that are invisible at the stellar surface using broad-band photometry.

The 1470-d light curve for KIC 7106205 and the subsequent amplitude spectrum are given in the top and bottom panels of Fig. 1, respectively. The amplitude spectrum illustrates that KIC 7106205 contains only a modest number of pulsation frequencies. Table 1 provides the stellar parameters of KIC 7106205 from both the *Kepler* Input Catalogue (KIC; Brown et al. 2011) and the revised values given in Huber et al. (2014).

3 METHOD: COMBINING THE DATA

The instrumental differences between *Kepler* and WASP require the data to be corrected before a direct comparison of the data sets can be made. The pulsation amplitude correction from the difference in integration times for each data set is calculated using

$$A = A_0 \text{sinc} \left(\frac{\pi}{n} \right), \tag{1}$$

where A and A_0 are the observed and corrected amplitudes, respectively, and n is the number of data points per pulsation cycle (Murphy 2014).

3.1 Using the HADS star KIC 9408694 for calibration

A calculation of the effect on the measurement of pulsation amplitude caused by the passband differences between *Kepler* and WASP was conducted using a high-amplitude δ Sct (HADS) star. The HADS stars are a subgroup of δ Sct stars that are found in the central region of the instability strip (McNamara 2000). They generally have pulsation amplitudes greater than approximately 0.3 mag and pulsate in fundamental and first overtone radial modes (e.g. see Balona et al. 2012). A HADS star was chosen for the passband calibration, as the signal-to-noise ratio is extremely high for high-amplitude pulsations. Moreover, the particular pulsation mode did not vary in amplitude over time span of the 4-yr *Kepler* data set. The HADS star used was KIC 9408694, which has a well-resolved dominant peak at 5.6611 d^{-1}. A 1-d sample of *Kepler* and WASP over plotted light curves and the amplitude spectra of KIC 9408694 in 2009 and 2010 for both instruments are shown in Fig. 2.

The HADS star is not isolated in the WASP aperture, but the background objects are 3 mag fainter and added only a small amount of flux to the photometry. The dilution suffered by the target star can be calculated by comparing the flux of the target star and contaminating stars such that

$$\text{Dilution} = \left[1 - \left(\frac{F_{\text{T}}}{F_{\text{T}} + F_{\text{C}}} \right) \right] \times 100, \tag{2}$$
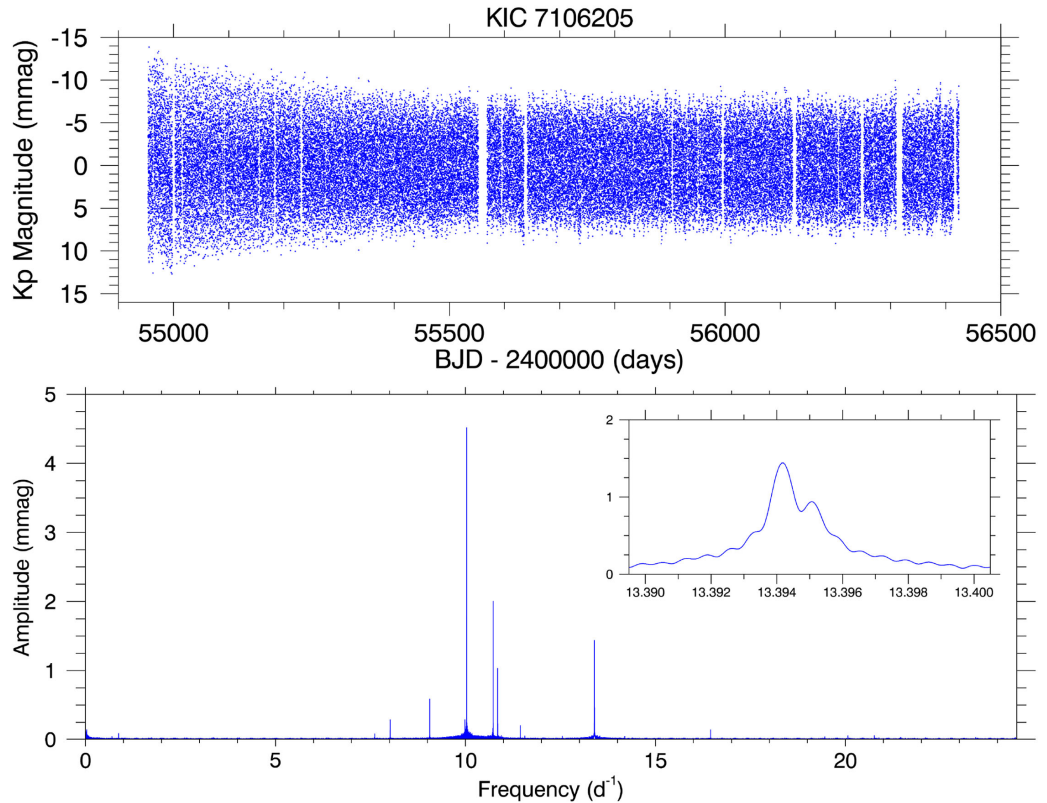
Figure 1. The 1470 d *Kepler* light curve for the δ Sct star KIC 7106205 is given in the top panel and the bottom panel is the amplitude spectrum, calculated out to the LC Nyquist frequency. The sub-plot in the bottom panel shows a zoomed-in view of the modulated mode $\nu_{mod} = 13.3942 \, \mathrm{d}^{-1}$.

Table 1. Stellar parameters listed for KIC 7106205 in the KIC (Brown et al. 2011) and the revised values given in Huber et al. (2014).

	T_{eff} (K)	$\log g$ (cm s^{-2})	[Fe/H] (dex)	K_{p} mag (mag)
KIC	6960 ± 150	4.05 ± 0.15	-0.01 ± 0.15	11.46
Revised	6900 ± 140	3.70 ± 0.15	0.32 ± 0.15	

where F_{T} is the flux of the target and F_{C} is the combined flux of the contaminating stars (Holdsworth, in preparation). The dilution for the HADS star KIC 9408694 was calculated to be 14 per cent (i.e. the observed amplitude is reduced by 1.1400).

Simultaneous WASP and *Kepler* observations of KIC 9408694 were made in 2009 and 2010. The data from WASP and *Kepler* were truncated to the same time period and analysed to determine their pulsation amplitudes, $A_{0_{\mathrm{W}}}$ and $A_{0_{\mathrm{K}}}$, respectively. The difference in the derived amplitudes (after optimizing using linear least squares, correcting for dilution in the WASP data and integration time effects in both data sets) is solely a result of the difference in the passbands and the ratio allows one data set to be scaled for comparison to the other. The average of the ratio ($A_{0_{\mathrm{K}}}/A_{0_{\mathrm{W}}}$) for the two years was 0.9242, i.e. the *Kepler* data show amplitudes 7.58 per cent smaller than those of the WASP data due to the filter differences, which is an expected result for an A star given the filter responses.

3.2 Application to the δ Sct star KIC 7106205

In the WASP data, KIC 7106205 was observed for three seasons, 2007, 2009, and 2010. Due to the large pixel size of the WASP instrument, the star suffers from contamination from other sources in the photometric aperture (see Figs 3 and 4). Therefore, a dilution correction factor must also be calculated before comparison can be made with *Kepler* data. Simultaneous observations by WASP and *Kepler* of KIC 7106205 in 2009 show the ν_{mod} peak.

To perform the comparison, the *Kepler* data were truncated to the same time period as the WASP data, and the pulsation peak ν_{mod} was extracted from both data sets, optimized by linear least squares and then corrected for the different integration times as described previously. This gave a corrected WASP amplitude of $A_{0_{\mathrm{W}}} = 2.77$ mmag and a *Kepler* amplitude of $A_{0_{\mathrm{K}}} = 5.18$ mmag.

To calculate the dilution effect in KIC 7106205, the *Kepler* peak was transformed into the WASP passband, giving the expected WASP amplitude if no dilution occurred, A_{exp}. The ratio, therefore, between A_{exp} and $A_{0_{\mathrm{W}}}$ is a result of the dilution of other stars in the aperture; this is calculated to be 2.0212. Alternatively, if equation (2) is used, a dilution factor of 1.7098 is obtained. The difference in this value and the direct comparison of the two data sets is possibly due to the bleeding of light from other nearby bright stars into the extracted pixels. Therefore, we conclude that the most reliable method is to compare the pulsation amplitudes from both instruments, as this includes any residual effect and corrects for it along with the dilution.
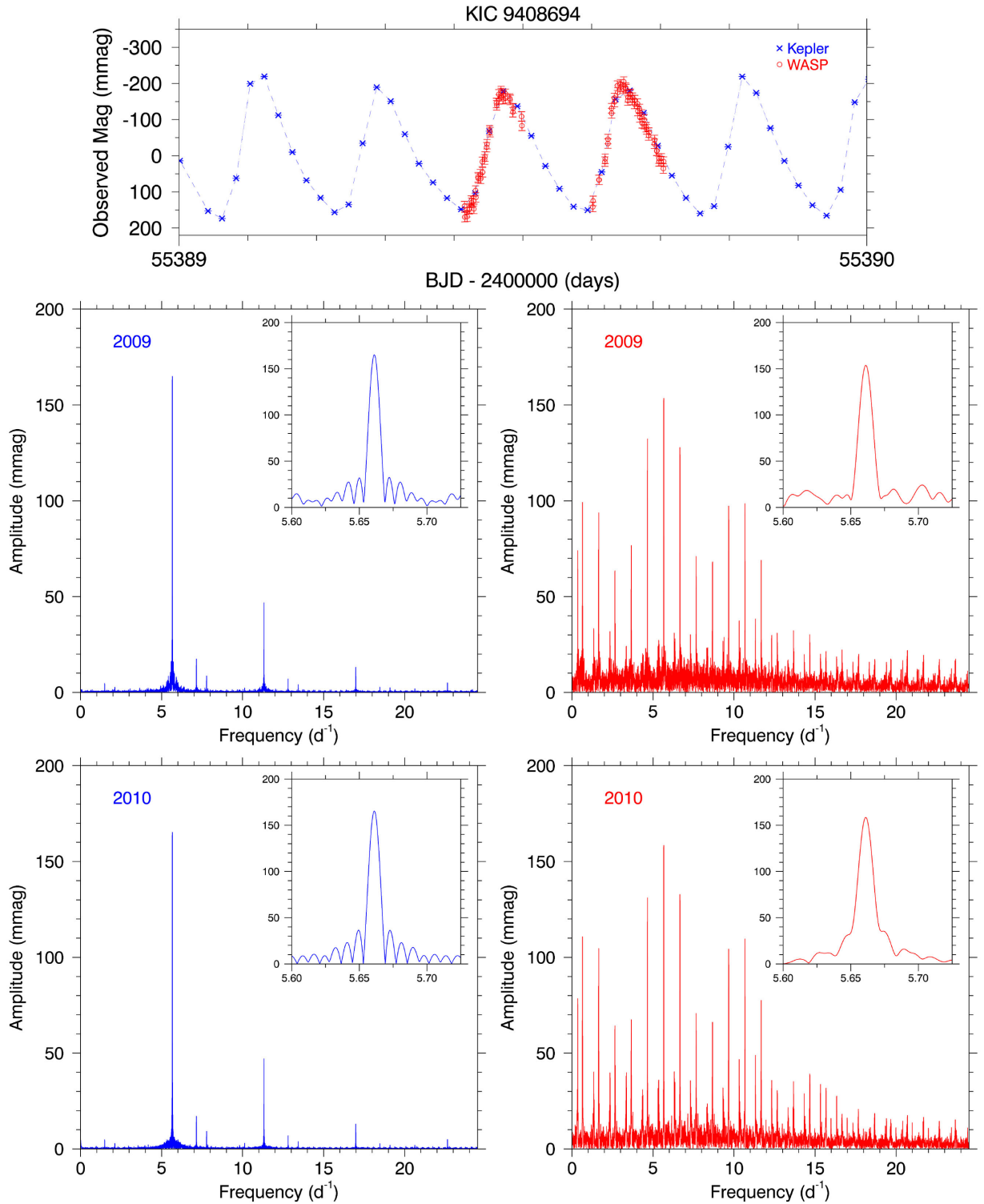
Figure 2. A 1-d sample showing simultaneous WASP and *Kepler* observations of the HADS star KIC 9408694 is given in the top panel. The left- and right-hand columns are the amplitude spectra, calculated out to the *Kepler* LC Nyquist frequency, for the *Kepler* (blue) and WASP (red) time series, respectively, in which 2009 and 2010 are the top and bottom rows. The sub-plots in the bottom panels show a zoomed-in view of the mode at $\nu = 5.6611\,\mathrm{d}^{-1}$, used for calculating the *Kepler* and WASP passband differences.
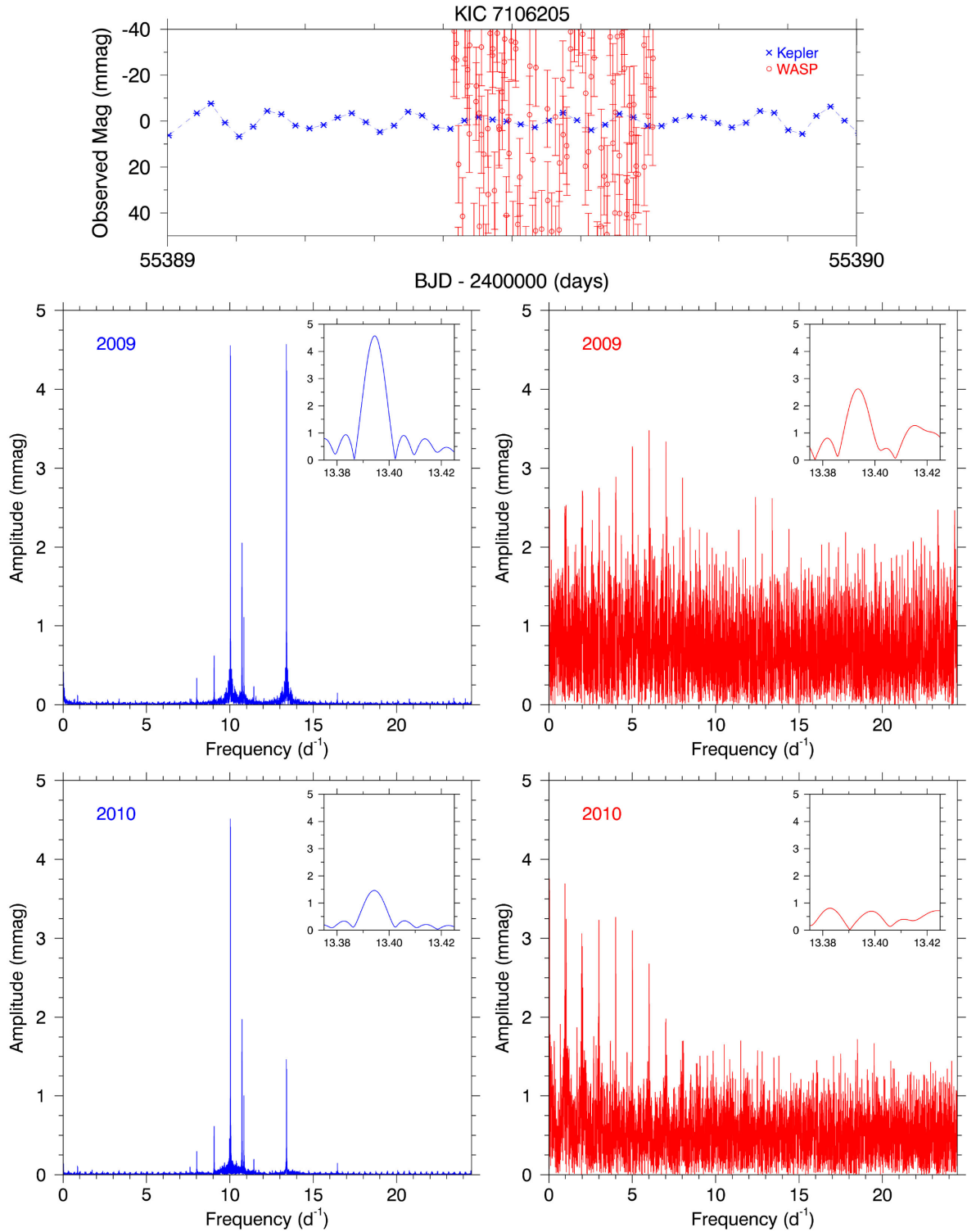
Figure 3. A 1-d sample showing simultaneous WASP and *Kepler* observations of the δ Sct star KIC 7106205 is given in the top panel, in which the larger scatter of WASP observations due to a higher point noise is clearly seen. The left- and right-hand columns are the amplitude spectra, calculated out to the *Kepler* LC Nyquist frequency, for the *Kepler* (blue) and WASP (red) time series, respectively, in which 2009 and 2010 are the top and bottom rows. The sub-plots in panels show a zoomed-in view of the modulated mode $\nu_{\mathrm{mod}} = 13.3942\,\mathrm{d}^{-1}$.
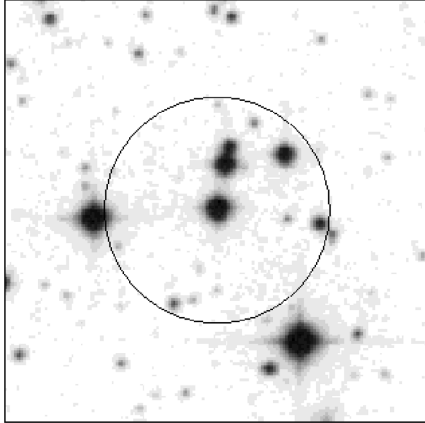
Figure 4. The photometric aperture (dark circle) for KIC 7106205 in the WASP data showing multiple sources of contamination. The aperture is 48 arcsec (3.5 WASP pixels) in radius. Image from Digitized Sky Survey (DSS).

Figure 5. The amplitude spectrum of the 2007 WASP data for KIC 7106205, calculated out to the *Kepler* LC Nyquist frequency. The sub-plot shows a zoomed-in view of ν_{mod}. Note the difference in *y*-axis scale compared to the amplitude spectra given in Fig. 3, illustrating the large decrease in mode amplitude between 2007 and 2009.

Figure 6. Corrected and calibrated values of amplitude of ν_{mod} in KIC 7106205 for *Kepler* (in 50 d bins) and WASP (single 66.1-d bin) data, marked as blue crosses ($\times$) and a red circle ($\bigcirc$), respectively. 1σ errors are calculated from the least-squares fit at fixed frequency of $13.3942\,\mathrm{d}^{-1}$, but are generally smaller than the data points.

Fig. 3 shows the 2009 and 2010 *Kepler* and WASP data used for the calibration study of KIC 7106205. The top panel shows an example of simultaneous observations by WASP and *Kepler* in 2009. The bottom-left column shows the amplitude spectra of the *Kepler* 2009 and 2010 data, with the bottom-right column showing the amplitude spectra of the same two of the three seasons of available WASP data, as in the *Kepler* data.

Unfortunately, the 2010 WASP data do not show the ν_{mod} peak. The amplitude of ν_{mod} in the 2010 *Kepler* data is 1.46 mmag, and correcting this for integration time gives $A_{0_K} = 1.66$ mmag. The passband difference and dilution factor in KIC 7106205 of 2.0212, and the WASP integration time correction means that we would expect an amplitude of 0.87 mmag in the 2010 WASP data. Despite being above the nominal detection limit of 0.50 mmag (Holdsworth et al. 2014a), ν_{mod} is not observed in the 2010 WASP data due to higher photometric noise.

The 2007 WASP data set for KIC 7106205 is 66.1 d in length and consists of 3322 data points. Fig. 5 shows the amplitude spectrum of the 2007 WASP data, from which the amplitude of ν_{mod} was extracted, optimized by linear least squares at a fixed frequency of $13.3942\,\mathrm{d}^{-1}$ and then corrected using the methodology described previously. Due to the higher levels of noise present in WASP data compared to *Kepler* data, it is not possible to track amplitude changes in all pulsation modes and so we were unable to perform an analysis of all the frequencies listed in Bowman & Kurtz (2014). However, ν_{mod} has a sufficiently high amplitude that it can be extracted from the 2007 WASP observations and calibrated to find its corrected amplitude.

4 RESULTS

The 66.1 d of 2007 WASP data for KIC 7106205 were combined into a single data bin, so that the highest possible frequency resolution ($0.015\,\mathrm{d}^{-1}$) was obtained when calculating a discrete Fourier transform. The amplitude was obtained by optimizing the amplitude and phase using a least-squares fit, which was normalized to the centre of the 1470 d *Kepler* data set, specifically $t_0 = 2455688.77$ (BJD), and at the fixed frequency of $13.3942\,\mathrm{d}^{-1}$. This ensures that values of amplitude can be compared to the analysis of Bowman & Kurtz (2014).
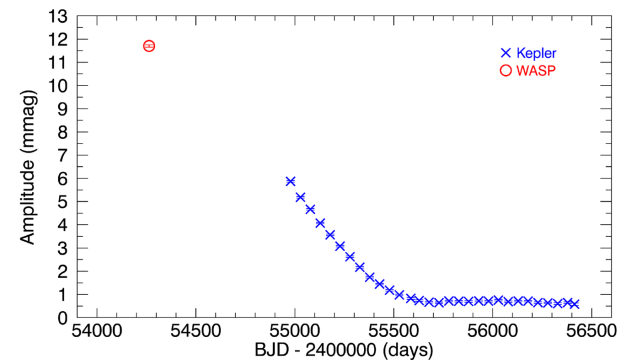
The resultant amplitude from the least-squares fit was calibrated, as described in previous sections for integration time, dilution from other stars and passband differences (in that order). A corrected amplitude of 11.70 ± 0.05 mmag was obtained for ν_{mod} and is shown graphically in Fig. 6, which contains the single calibrated WASP data point alongside 1470 d of *Kepler* data for KIC 7106205 adapted from Bowman & Kurtz (2014). The inclusion of the WASP data point illustrates that the amplitude of ν_{mod} appears to have been steadily decreasing since at least 2007.

It should also be noted that if a non-linear least-squares fit of the 2007 WASP data of KIC 7106205 is performed, values of $\nu = 13.3924\,\mathrm{d}^{-1}$ and a corrected amplitude of 11.88 ± 0.06 mmag are obtained, which would increase the amplitude of ν_{mod} by 0.18 mmag in 2007. Therefore, ν_{mod} may also have been exhibiting

frequency modulation since 2007 along with the amplitude modulation shown in Fig. 6.

The result of the non-linear least-squares fit of the 2009 WASP data is within the errors of the frequency obtained from *Kepler* data and thus is compatible with the fixed frequency that we use. The difference of $0.0018\,\mathrm{d}^{-1}$ between the frequencies obtained from the linear and non-linear fits of the 2007 WASP data is smaller than our resolution limit, and so we conclude that the linear least-squares fit using $\nu_{\mathrm{mod}} = 13.3942\,\mathrm{d}^{-1}$ is the correct approach. The linear least-squares fit allows us to study the amplitude modulation in KIC 7106205, but we cannot explore the frequency modulation due to the poor frequency resolution.

5 CONCLUSIONS

This work highlights the success of utilizing ground-based photometry, specifically WASP, to support *Kepler* observations. We have calibrated and combined the data sets and have increased the total length of the observations of KIC 7106205 and its pulsational amplitude modulation to 6 yr. A single p mode was extracted from the WASP observations, specifically $\nu_{\mathrm{mod}} = 13.3942\,\mathrm{d}^{-1}$, and has been shown to decrease in amplitude from 11.70 ± 0.05 mmag in 2007, to 5.87 ± 0.03 mmag in 2009, and to 0.58 ± 0.06 mmag in 2013. We agree with the conclusions of Bowman & Kurtz (2014), that the observed amplitude modulation in the single pulsation frequency can be explained by either a loss of mode energy to a damping region within the star; or to either invisible high-ℓ p modes or two *internal* g modes facilitated by the parametric resonance instability.

We are unable to extend the study of amplitude modulation in KIC 7106205 prior to 2007 using WASP data, as there are no previous observations of the star in the data archive. We have demonstrated that the amplitude of ν_{mod} after 2009 is too small to be detected above the typical WASP noise level and moreover, there are no observations of KIC 7106205 after 2010.

The methodology we have developed for combining WASP and *Kepler* data can also be used to study other stars, provided that the time series overlap at some point thus allowing for the passband and dilution corrections to be made. It requires time and careful analysis to find stars that exhibit amplitude modulation, but also if they are present in the WASP data set.

The majority of the significant decrease in mode amplitude of a single pulsation frequency in KIC 7106205 occurred prior to the launch of the *Kepler* mission. Therefore, it is important to remember that the *Kepler* observations provide an extremely high quality, yet small *snapshot* of 4 yr of data, which is a mere blink of an eye insight into the stellar physics at work within this star. Time spans of the order of a decade may be more significant in δ Sct stars than was previously thought and analyses of these so-called *coherent* pulsators should take this into account. Modelling studies are needed if we are to understand the mechanisms that cause such strong changes in pulsation mode amplitude on time-scales of several years.

REFERENCES

Balona L. A. et al., 2012, MNRAS, 419, 3028
Borucki W. J. et al., 2010, Science, 327, 977
Bowman D. M., Kurtz D. W., 2014, MNRAS, 444, 1909
Breger M., 2000, in Breger M., Montgomery M., eds, ASP Conf. Ser. Vol. 210, Delta Scuti and Related Stars. Astron. Soc. Pac., San Francisco, p. 3
Breger M., Montgomery M. H., 2014, ApJ, 783, 89
Brown T. M., Latham D. W., Everett M. E., Esquerdo G. A., 2011, AJ, 142, 112
Chaplin W. J., Elsworth Y., Isaak G. R., Miller B. A., New R., 2000, MNRAS, 313, 32
Chaplin W. J., Elsworth Y., Miller B. A., Verner G. A., New R., 2007, ApJ, 659, 1749
Chevalier C., 1971, A&A, 14, 24
Dupret M. A., Grigahcène A., Garrido R., Gabriel M., Scuflaire R., 2004, A&A, 414, L17
Dupret M. A., Grigahcène A., Garrido R., Gabriel M., Scuflaire R., 2005, A&A, 435, 927
Dziembowski W., 1982, Acta Astron., 32, 147
Gilliland R. L. et al., 2010, PASP, 122, 131
Holdsworth D. L. et al., 2014a, MNRAS, 439, 2078
Holdsworth D. L., Smalley B., Kurtz D. W., Southworth J., Cunha M. S., Clubb K. I., 2014b, MNRAS, 443, 2049
Huber D. et al., 2014, ApJS, 211, 2
Koch D. G. et al., 2010, ApJ, 713, L79
Kurtz D. W., van Wyk F., Roberts G., Marang F., Handler G., Medupe R., Kilkenny D., 1997, MNRAS, 287, 69
McNamara D. H., 2000, in Breger M., Montgomery M., eds, ASP Conf. Ser. Vol. 210, Delta Scuti and Related Stars. Astron. Soc. Pac., San Francisco, p. 373
Murphy S. J., 2014, PhD thesis, Jeremiah Horrocks Institute, University of Central Lancashire
Nowakowski R. M., 2005, Acta Astron., 55, 1
Pollacco D. L. et al., 2006, PASP, 118, 1407
Smalley B. et al., 2014, A&A, 564, A69
Tamuz O., Mazeh T., Zucker S., 2005, MNRAS, 356, 1466
Uytterhoeven K. et al., 2011, A&A, 534, A125
Winget D. E. et al., 1991, ApJ, 378, 326

This paper has been typeset from a TeX/LaTeX file prepared by the author.

3.4 Spectroscopic analysis of KIC 7106205

To support the photometric analysis of the δ Sct star KIC 7106205, spectroscopic follow-up observations were made with the Intermediate dispersion Spectrograph and Imaging System (ISIS) on the William Herschel Telescope (WHT). This telescope is part of the Isaac Newton Group (ING)[1] and is located at the Spanish Observatorio del Roque de los Muchachos of the Instituto de Astrofísica de Canarias on the island of La Palma. The spectral resolution of ISIS/WHT at 4000 Å using a 1 arcsec slit is given by $R = \frac{\lambda}{\Delta\lambda} \simeq 2000$, which is sufficient to classify the spectral type of A and F stars and determine an approximate value for the effective temperature, and constrain surface gravity and rotational velocity by comparing the observed spectrum to synthetic spectra.

A total of 23 δ Sct stars, which included KIC 7106205, were observed using ISIS/WHT between 30 March 2016 and 24 May 2016, with the right ascension, declination, apparent visual magnitude, SIMBAD classification and date of observations given in Table 3.1.

3.4.1 Spectral classification

The ISIS/WHT spectrum for KIC 7106205 was reduced using STARLINK software[2], which included cleaning of cosmic rays, de-biasing and flat-fielding. The normalised spectrum for the wavelength range $3800 \leq \lambda \leq 4600$ Å for the δ Sct star KIC 7106205 is shown in Fig. 3.2, along with MK standard F0 V and F2 V stars above and below, respectively, for comparison. The spectral classification of KIC 7106205 closely followed the prescription of Gray & Corbally (2009).

It was discussed in section 1.3.2 how a significant fraction of A stars are Am stars, which are defined as having a difference of at least five spectral subclasses between

---

[1]ING website: http://www.ing.iac.es
[2]STARLINK website: http://starlink.eao.hawaii.edu/starlink/

Table 3.1: Parameters of the 23 δ Sct stars observed using ISIS/WHT at epoch J2000.0 with a classification taken from the SIMBAD[†] data base if available.

KIC ID	RA	Dec	m_V	classification	Date Observed
3429637	19:08:38.04	+38:30:31.96	7.72	δ Sct	30/03/2016
5964173	19:32:12.82	+41:16:23.68	12.04	δ Sct	20/05/2016
6357702	19:18:46.72	+41:44:21.34	11.27		20/05/2016
6590403	19:05:53.36	+42:02:14.50	10.55	δ Sct	30/03/2016
6848661	19:07:53.77	+42:21:41.98	11.55		30/03/2016
7106205	19:11:57.46	+42:40:22.89	11.38		30/03/2016
7217483	19:45:57.87	+42:45:23.17	10.54		21/05/2016
7533694	19:34:12.91	+43:07:03.54	10.29	δ Sct	24/05/2016
7830684	19:38:14.07	+43:34:10.67	12.07	δ Sct	20/05/2016
8177748	19:43:13.01	+44:05:53.81	11.76	rot var	20/05/2016
8196840	20:03:12.94	+44:04:03.99	11.81	δ Sct	21/05/2016
8246833	19:45:18.48	+44:08:03.85	11.98		21/05/2016
8386122	19:52:56.59	+44:23:24.84	10.45		21/05/2016
9156808	19:30:53.18	+45:33:12.75	11.29	δ Sct	20/05/2016
9353572	19:43:58.62	+45:53:54.74	10.51	δ Sct	21/05/2016
9408694	19:34:45.59	+45:54:16.32	11.48	δ Sct	20/05/2016
9642894	19:16:18.08	+46:21:16.03	11.27	δ Sct	30/03/2016
9700322	19:07:50.71	+46:29:11.93	12.61	δ Sct	30/03/2016
9773094	19:31:35.93	+46:35:19.48	11.37		30/03/2016
10273384	19:26:19.52	+47:23:36.72	11.68	δ Sct	20/05/2016
11513155	19:38:32.33	+49:26:40.09	11.19	star	20/05/2016
11661993	19:27:55.76	+49:45:43.37	9.33	δ Sct	24/05/2016
12117689	19:40:37.23	+50:38:31.47	11.74	star	20/05/2016

[†] http://simbad.u-strasbg.fr/simbad/

the Ca K line strength and the metallic line strengths (Conti 1970; Smith 1971a,b). It does not take more than a cursory study of the spectrum of KIC 7106205 in Fig. 3.2 to note the similar line strengths of the Ca II K and hydrogen lines (Hϵ, Hδ and Hγ), indicating that the Ca II K line strength is normal for a star of spectral type F0 V. On the other hand, the Sr II and Ca I lines in KIC 7106025 appear stronger than in the chemically-normal standard stars shown above and below in Fig. 3.2. Thus KIC 7106205 does have small, yet significant, differences between its Ca II K and metal line strengths and can be classified as a marginal Am star (i.e., Am:). This is not surprising considering the large fraction of A stars that are Am and Am: stars (Conti 1970; Smith 1971a,b).

The low-to-medium resolution of the ISIS/WHT spectrum for KIC 7106205 means that the spectral type of F0 V determined from its hydrogen line strengths is consistent with the effective temperature of $T_{\mathrm{eff}} = 6900 \pm 150$ K listed in the KIC for this star. However, the resolution of the spectrum was insufficient to determine precise values of the rotational velocity and surface gravity of KIC 7106205, but these were constrained to $v \sin i \leq 100$ km s^{-1} and $\log g \simeq 4$ (cgs), respectively. Therefore, the spectroscopic analysis of KIC 7106205 indicates that this star is likely a slow rotator for a δ Sct star and confirms it is near the red edge of the classical instability strip in the HR diagram.

The spectroscopic analysis of KIC 7106205 indicates that this δ Sct star is not a classical Am star, because it does not have a difference of at least five spectral subclasses between its Ca II K and metal lines. It does have a few relatively strong metal lines for a F0 V star and so can be considered an Am: star, although it should be noted that the spectrum of KIC 7106205 is noisier than the standard stars given in Fig. 3.2. It appears that chemical peculiarity does not offer a solution to why the δ Sct star KIC 7106205 exhibits amplitude modulation.

Further work is needed in analysing similar stars, including the remaining stars
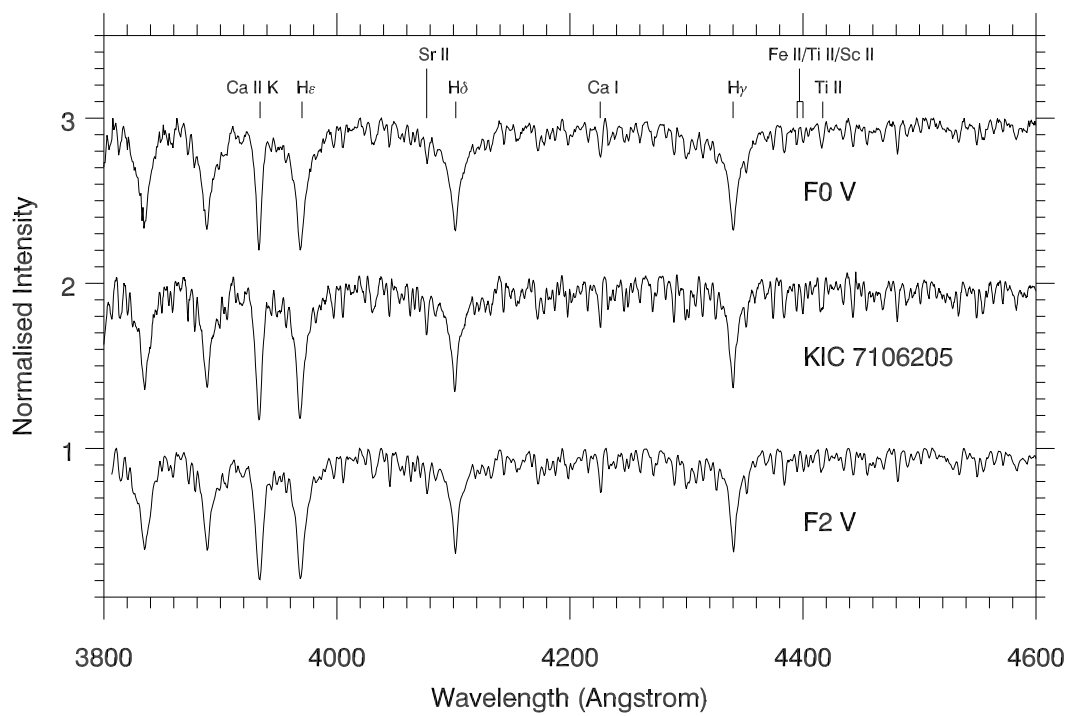
Figure 3.2: Normalised spectrum of the δ Sct star KIC 7106205, in the wavelength range $3800 \leq \lambda \leq 4600$ Å. The spectra above and below are F0 V and F2 V MK standard stars, respectively, taken from Gray & Corbally (2009).

given in Table 3.1, to establish if chemical peculiarities in A stars are related to amplitude modulation of pulsation modes in δ Sct stars, especially since it is only a recent discovery that a significant fraction of Am stars have been observed to pulsate (Smalley et al. 2011).

3.5 Discussion

The analysis of the δ Sct star KIC 7106205 revealed that a single p mode with a frequency of $\nu_{\mathrm{mod}} = 13.3942$ d^{-1} decreased in amplitude by more than a factor of 20 over 6 yr (Bowman & Kurtz 2014; Bowman et al. 2015). WASP data for KIC 7106205 were calibrated to *Kepler* observations by correcting for the difference in instrument integration times, passband differences and dilution effects and included alongside *Kepler* observations. This allowed the amplitude and frequency modulation of ν_{mod} to be extended back to 2007, 2 yr prior to the launch of the *Kepler* Space Telescope. The amplitude and phase tracking routine used to study the variability of ν_{mod} showed that the mode amplitude changed from 11.70 ± 0.05 mmag in 2007, to 5.87 ± 0.03 mmag in 2009, and to 0.58 ± 0.06 mmag in 2013 (Bowman et al. 2015). A modified version of figure 6 from Bowman et al. (2015) is given in Fig. 3.3, which shows the combined WASP and *Kepler* observations of the observed amplitude modulation in ν_{mod} for both WASP observing seasons. The significance of the amplitude modulation in KIC 7106205 is emphasised since all other pulsation modes in this star had constant frequencies and amplitudes over the 4-yr *Kepler* data set, thus the mode energy associated with the decrease in amplitude of ν_{mod} was not transferred to any other visible pulsation mode, nor was it observed to excite a new pulsation mode by a mode coupling mechanism (Bowman & Kurtz 2014).

A spectroscopic analysis of KIC 7106205 using a classification-resolution spectrum obtained from ISIS/WHT has revealed that KIC 7106205 does not show the necessary difference of at least five spectral subclasses between its Ca II K and metal
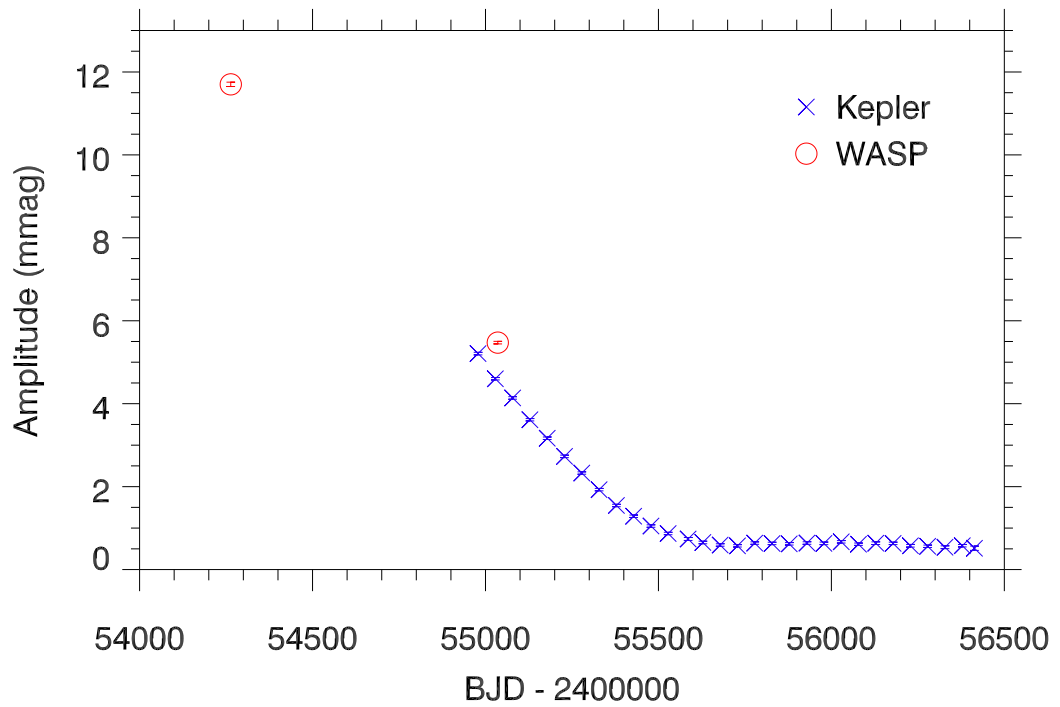
Figure 3.3: Corrected and calibrated values of amplitude modulation in the pulsation mode $\nu_{\mathrm{mod}} = 13.3942\,\mathrm{d}^{-1}$ in KIC 7106205 for *Kepler* (in 50-d bins) and WASP (single 66.1-d bin) data, shown as blue crosses ($\times$) and red circles ($\circ$), respectively. 1σ errors are calculated from the least-squares fit at fixed frequency, but are generally smaller than the data points. Figure adapted from Bowman et al. (2015), their figure 6.

line strengths to be defined as a classical Am star. KIC 7106205, however, does have relatively strong Sr II and Ca I metal lines for a F0 V star so can be considered an Am: star. The lack of strong chemical peculiarities in this star implies that this is unrelated to the observed amplitude modulation. The spectroscopic analysis of KIC 7106205 has also shown that this star is likely a slow rotator near the red edge of the classical instability strip in the HR diagram. The spectroscopic classification of F0 V determined from comparison of the hydrogen line strengths of KIC 7106205 to standard stars from Gray & Corbally (2009) is consistent with the KIC and Huber et al. (2014) values for KIC 7106205 of $T_{\rm eff} \simeq 6900 \pm 150$ K.

The functional form of the observed amplitude modulation in KIC 7106205 is not consistent with stochastic excitation. On the other hand, mode coupling to high-degree modes or internal g modes, beating of multiple unresolved close-frequency pulsation modes and energy being lost to a damping region are all possible explanations of the amplitude modulation observed in KIC 7106205. The analysis of this δ Sct star by Bowman & Kurtz (2014) and extended using WASP observations by Bowman et al. (2015) does not distinguish which of these possibilities is most likely, only that the mode energy lost from $\nu_{\rm mod}$ was not transferred to any other observed pulsation modes. In reality, all of these mechanisms could be operating in congruence, as they are all feasible solutions to the observed amplitude modulation, which complicates the issue of testing the hypothesis of energy conservation amongst pulsation modes in a δ Sct star.

KIC 7106205 is a special case study – an archetypal example of amplitude modulation in a δ Sct star – that provides strong motivation to study amplitude modulation and energy conservation of pulsation modes in a large number of δ Sct stars, which is discussed in chapter 5.

Chapter 4

Kepler observations of

delta Scuti stars

4.1   Introductory remarks

This chapter focusses on the statistical properties of an ensemble of δ Sct stars observed by the *Kepler* Space Telescope. It was previously discussed in section 1.2.2 how the δ Sct stars are the most common type of pulsator among main sequence A and F stars, and are found in a transition region between low- and high-mass stars in the HR diagram. Before the advent of space telescopes, the δ Sct stars were well defined by the observational blue and red edges of the classical instability strip (Rodríguez & Breger 2001). These multiperiodic pulsators are interesting to study using asteroseismology, as the various pulsation modes are sensitive to different depths within a star.

In this chapter, the somewhat unexpected discovery of many δ Sct/γ Dor hybrid stars amongst the A and F stars observed by *Kepler* is discussed in section 4.2. In section 4.3, the so-called 'organ pipe' stars are discussed in the context of the incidence of low-frequency peaks in the amplitude spectra of δ Sct stars. In section 4.4,

an example of a star pulsating in g modes that lies in the no-man's land between the hot edge of the γ Dor instability region and the cool edge of the SPB instability region is provided. These stars have been termed 'hot γ Dor stars' in the literature (e.g., Balona 2014) and are a challenge to pulsation theory. In section 4.5, it is discussed how an ensemble of 983 δ Sct stars that were observed continuously by *Kepler* for 4 yr was created, which was large enough to characterise statistical properties of the δ Sct stars, including an evaluation of the observational blue and red edges of the classical instability strip. Section 4.7 discusses the correlations between the dominant pulsation mode frequency and stellar parameters using the ensemble of 983 δ Sct stars.

4.2 Hybrid stars

The theoretical instability regions of the δ Sct and γ Dor stars overlap in the HR diagram (Dupret et al. 2004). Hybrid pulsators from the δ Sct and γ Dor pulsational excitation mechanisms occurring simultaneously within a star were first predicted by Dupret et al. (2005), but only expected to comprise a small minority of A and F stars. Prior to the recent space photometry revolution, very few hybrid δ Sct/γ Dor stars were known (see e.g., Handler 2009). One of the first confirmed hybrid pulsators was HD 209295, which was studied by Handler & Shobbrook (2002b). Although the g- and p-mode frequencies in HD 209295 were confirmed to be from the same star, it was later shown that the g modes were tidally excited from the star being in an eccentric binary (Handler et al. 2002).

The *Kepler* mission data revealed that many δ Sct stars are in fact hybrid pulsators (Grigahcène et al. 2010a; Uytterhoeven et al. 2011; Balona 2011), exhibiting both p modes ($\nu \geq 5$ d^{-1}) and g modes ($\nu < 4$ d^{-1}). Attempts have been made to catalogue the different types of hybrid behaviour observed; for example, it has been suggested that δ Sct/γ Dor hybrids and γ Dor/δ Sct hybrids are two distinct groups

(Grigahcène et al. 2010a,b). These definitions were used to distinguish hybrid stars that have dominant pulsation modes in the δ Sct and γ Dor frequency regimes, respectively (Grigahcène et al. 2010a). Classifying hybrid stars into these subgroups using these definitions is some what of a pedantic exercise as it often requires visual inspection of the light curves and amplitude spectra of many stars, which can be a lengthy and subjective process. Currently it is not established whether there are any significant physical differences for why a hybrid star should exhibit higher amplitude pulsation modes in one frequency regime compared to the other. It is not clear whether the definitions of Grigahcène et al. (2010a) are distinct groups and so all hybrid stars in this thesis are considered a single pulsator type.

A statistical analysis of 750 A and F stars was carried out by Uytterhoeven et al. (2011) using 1 yr (Q0 – Q4) of LC *Kepler* data from the start of the mission. The authors discovered that 475 of these stars were pulsating in either g or p modes, with 171 stars (23 per cent) being classified as hybrid pulsators. The distributions of δ Sct, γ Dor and hybrid stars on a $T_{\mathrm{eff}} - \log g$ diagram from Uytterhoeven et al. (2011) are given in Fig. 4.1, which are shown as red squares, blue stars and black circles, respectively. The top panel in Fig. 4.1 shows the δ Sct, γ Dor and hybrid stars studied using ground-based observations and the bottom panel shows the stars studied by Uytterhoeven et al. (2011) using *Kepler* data for comparison. Using the high-quality *Kepler* data, Uytterhoeven et al. (2011) demonstrated that a significant fraction of A and F stars exhibit at least some form of hybrid behaviour and that the hybrid stars are not restricted to where the δ Sct and γ Dor instability regions overlap in the HR diagram.

The hybrid fraction from Uytterhoeven et al. (2011) can be considered a conservative estimate of the hybrid fraction amongst all δ Sct stars observed by *Kepler*. With the complete 4-yr data set, and subsequently improved frequency resolution and amplitude precision, many more δ Sct stars are observed to have low-frequency
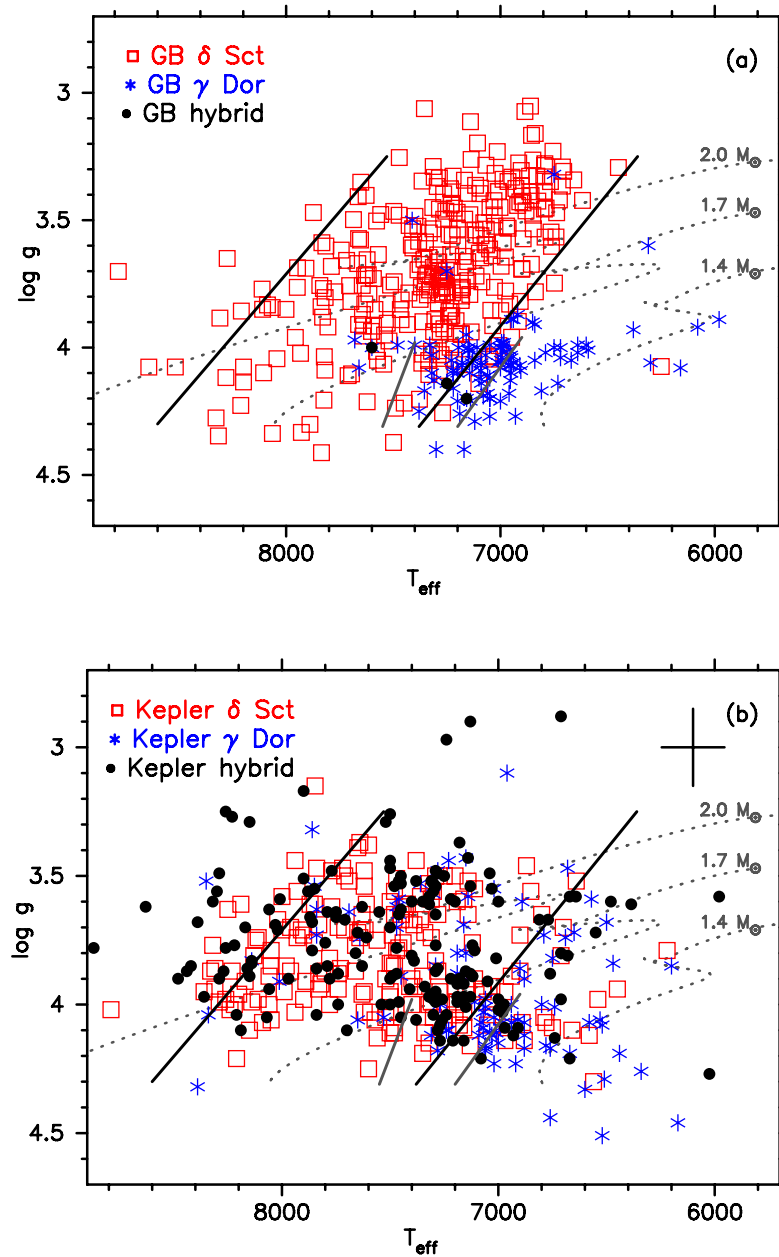
Figure 4.1: T_{eff} – log g diagrams for intermediate-mass pulsators. The top panel shows all the known δ Sct stars (shown as red squares), γ Dor stars (shown as blue stars) and hybrid stars (shown as filled black circles) observed using ground-based data. The bottom panels shows the same classifications of stars using the first 1 yr of *Kepler* data. The black and grey solid lines indicate the observational edges of the δ Sct and γ Dor instability regions taken from Rodríguez & Breger (2001) and Handler & Shobbrook (2002a), respectively, and the dotted lines represent evolutionary tracks. Figure from Uytterhoeven et al. (2011), their figure 10. © ESO; reproduced with permission from A&A.

peaks in their amplitude spectra, but it is not established if these are always caused by pulsation (Balona 2011; Balona & Dziembowski 2011; Balona 2014).

The hybrid stars offer the opportunity to study stellar structure throughout a star's interior, because the g modes excited from the flux blocking mechanism are sensitive to conditions near the core and the p modes excited by the κ mechanism are sensitive to conditions near the surface (Aerts et al. 2010). Understanding the multiperiodic hybrid stars is an exciting prospect for asteroseismology as one can make measurements of the radial rotation profile in main sequence stars (Kurtz et al. 2014; Saio et al. 2015; Keen et al. 2015; Triana et al. 2015; Murphy et al. 2016; Schmid & Aerts 2016).

Ideally, the hybrid stars could be used to study the pulsation excitation mechanisms directly, particularly the possible exchange of energy between pulsation modes excited by the different mechanisms. This idea was explored by Chapellier et al. (2012), who studied the interaction between 180 g-mode and 59 p-mode independent pulsation mode frequencies in the CoRoT hybrid star ID 105733033. The authors demonstrated that the p- and g-mode frequencies originated in the same star and that a coupling mechanism must exist to explain the observed mode interaction between the g- and p-mode frequency regimes (Chapellier et al. 2012).

4.2.1   Are all hybrid stars binaries?

Binarity may appear to be a simple solution to the discovery that the amplitude spectra of many δ Sct stars contain g-mode frequencies, which are associated with a pulsating companion star. The binary fraction of A stars is approximately 35 per cent (Abt 2009; Duchêne & Kraus 2013; Moe & Di Stefano 2016), so to first order this means that a non-negligible fraction of δ Sct stars are in binary systems. However, for most δ Sct stars in binary systems the companion is likely to have a mass too small for a g-mode pulsator such as a SPB or γ Dor star. Binarity cannot explain

all hybrid stars discovered by *Kepler*, because the binary fraction of δ Sct stars is similar to that of all A stars and of the order 30 per cent (S. Murphy, *private communication*). Therefore, the majority of δ Sct stars are in single star systems.

It has been demonstrated by Chapellier et al. (2012), Kurtz et al. (2014) and Van Reeth et al. (2015b) (and others) that not all hybrid stars are the result of binary systems with a δ Sct primary and γ Dor secondary, or vice versa. Hybrid stars have been confirmed as members of both single and multiple systems, with p mode frequencies from the κ mechanism and g mode frequencies from the flux blocking mechanism as predicted by Dupret et al. (2005), but in greater numbers in the *Kepler* data set than were anticipated.

4.2.2 Pure delta Scuti stars

Although there are many hybrid stars in the *Kepler* dataset, there are also pure δ Sct stars that show no significant low-frequency peaks in their amplitude spectra. Balona (2014) investigated the incidence of peaks in the γ Dor frequency regime using approximately 1800 δ Sct stars observed by *Kepler* for 1061 d (i.e., Q0 – Q12). He suggested that the majority of, if not all, δ Sct stars have low-frequency peaks in their amplitude spectra and the term hybrid should no longer be used as all δ Sct stars are hybrid stars (Balona 2014; Balona et al. 2015b). Whilst it is true that many δ Sct stars have low-frequency peaks in their amplitude spectra, it is not true that they all do. Furthermore, it is not established if the low-frequency peaks are always caused by pulsation in δ Sct stars.

An example of a δ Sct star with no g modes is KIC 5617488, with its amplitude spectrum given in Fig. 4.2. The sub-plot in the top-left corner of Fig. 4.2 contains a zoom-in of the low-frequency regime for this star, which shows a distinct lack of significant peaks in the typical g-mode frequency range of $0.3 \leq \nu \leq 4$ d^{-1}. A commonly used criterion for whether a peak in an amplitude spectrum is statistically
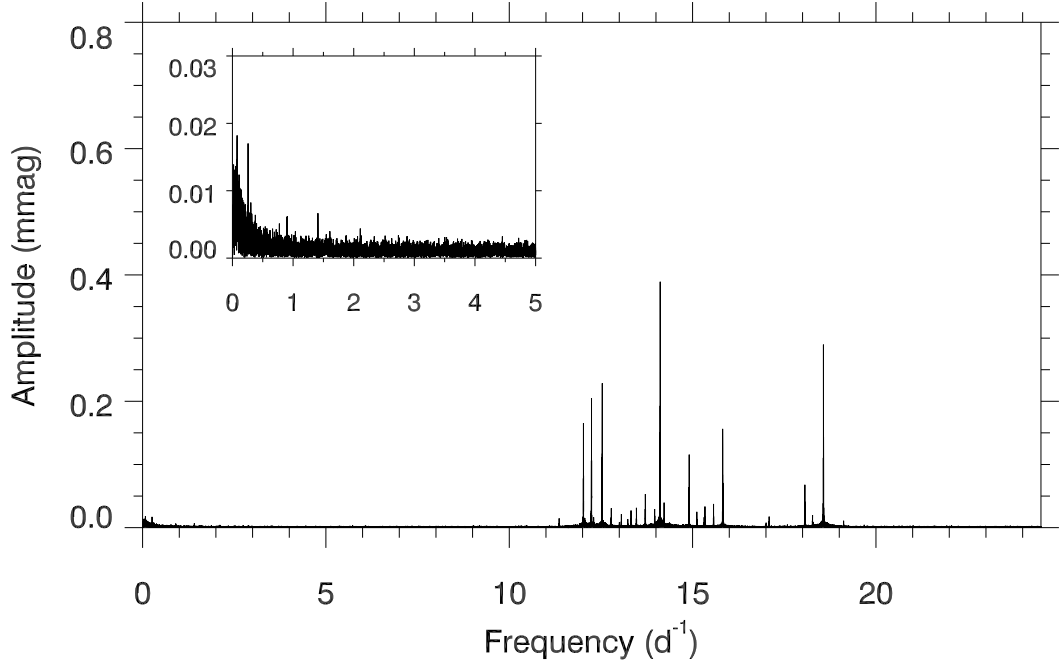
Figure 4.2: The amplitude spectrum of the pure δ Sct star KIC 5617488 with no statistically significant low-frequency peaks in its amplitude spectrum that can be confirmed as g-mode pulsation frequencies.

significant is if it has a signal-to-noise ratio in amplitude of $S/N \geq 4$ (Breger et al. 1993). The few peaks in the g-mode frequency regime for KIC 5617488 in Fig. 4.2 have amplitudes of order a few μmag, thus do not satisfy the statistical significance criterion from Breger et al. (1993). The low-frequency peaks in KIC 5617488 cannot be claimed to be statistically significant, let alone represent g-mode frequencies. Although they are uncommon, this is also demonstrably true for other δ Sct stars, thus pure δ Sct stars pulsating only in p modes do exist, which is contrary to the claim made by Balona (2014) and Balona et al. (2015b) that all δ Sct stars are hybrid stars.

Therefore, various studies of hybrid stars across a range of effective temperatures have shown that the majority of δ Sct stars have g mode pulsation frequencies, but not all do (Grigahcène et al. 2010a; Uytterhoeven et al. 2011; Balona 2011). Further work is needed to study the interplay between the flux blocking mechanism and the

κ mechanism in A and F stars, with a focus on understanding the observed minority of δ Sct stars pulsating in purely p modes.

4.3 Low frequencies in delta Scuti stars: the organ pipe stars

Many δ Sct stars in the *Kepler* data set have low-frequency peaks in their amplitude spectra (Balona & Dziembowski 2011; Balona 2014), but it is not established whether these frequencies are always caused by pulsation or the effects of rotation as claimed by Balona (2011, 2013), or have some other cause. For δ Sct stars that have high effective temperatures, $T_{\text{eff}} \geq 8000$ K, such that they are not found within the overlap of the δ Sct and γ Dor instability regions, these low frequencies are difficult to explain as g modes because these stars do not have a thick enough convective envelope to support the convective flux blocking excitation mechanism (Guzik et al. 2000; Dupret et al. 2004, 2005).

Balona et al. (2015b) investigated if increased sources of opacity within pulsation models of δ Sct stars were able to explain the low frequencies in terms of pulsation modes excited from the κ mechanism. Increasing the opacity at $T \simeq 115\,000$ K within the models by a factor of two caused low-degree modes at low frequency to be excited, but also decreased the range of pulsation mode frequencies such that the models were no longer consistent with observations (Balona et al. 2015b). It was suggested by Balona et al. (2015b) that non-linearity may be, at least in part, responsible for the incidence of low frequencies and the diversity in pulsational behaviour among δ Sct stars. This provides strong motivation for studying pulsations in δ Sct stars as a single population, but also individual stars so that insight of the excitation mechanisms, specifically non-linearity, can be gained.

In this section, a subgroup of δ Sct stars that have been called 'organ pipe'

stars is discussed. The organ pipe stars have a series of low-frequency peaks in their amplitude spectra, which are often highly variable in amplitude and phase in a chaotic manner. This coined the term organ pipe as the peaks appear and disappear in an amplitude spectrum throughout the *Kepler* data set, analogous to the various harmonics from an organ in a piece of music. Many δ Sct stars have these low frequencies, but since they often have low amplitudes they are not discovered until the high-amplitude pulsation modes and their window patterns are removed by pre-whitening. In this section, a case study using the organ pipe δ Sct star KIC 10407873 is used to demonstrate that these low-frequency peaks are not necessarily always caused by rotation.

Consider a simple model of a typical δ Sct star with a mass of $M = 1.8\,\mathrm{M}_\odot$ and a radius of $R = 2\,\mathrm{R}_\odot$. To first order, a slow rotator with $v \sin i \simeq 50\ \mathrm{km\,s^{-1}}$ would produce a rotational splitting of approximately 0.5 d^{-1}, a moderate rotator with $v \sin i \simeq 100\ \mathrm{km\,s^{-1}}$ would produce a rotational splitting of approximately 1.0 d^{-1}, and a fast rotator with $v \sin i \simeq 200\ \mathrm{km\,s^{-1}}$ would produce a rotational splitting of approximately 2.0 d^{-1}. Therefore, rotation can easily create complex amplitude spectra with only a few non-radial modes. Now let us consider a hypothetical δ Sct star which has two important properties:

(i) The δ Sct star pulsates in non-radial pulsation modes and is a moderate rotator, with the rotation splitting non-radial pulsation modes into their $2\ell + 1$ components. As discussed in section 1.3.3, the Ledoux constant is very small for p modes (e.g., $C_{n\ell} \simeq 0.03$; Kurtz et al. 2014); therefore, to first order, the surface rotation period can be directly inferred as the inverse of the frequency splitting of p modes in a δ Sct star.

(ii) The δ Sct star has surface features, let us call them starspots, which are co-rotating with the star's rotation period. If the modulation of the stellar flux by these starspots is large enough, then the frequencies associated with these

co-rotating features will be present in the light curve and amplitude spectrum of our hypothetical δ Sct star.

Thus, from the above two criteria, if a δ Sct star pulsates with a non-radial mode in the presence of rotation and has starspots on its surface, the rotation periods must agree to within some tolerance. KIC 10407873 is an ideal example of an organ pipe star, which is used to demonstrate that the low-frequency peaks in this star are not caused by rotation, as they are not consistent with the surface velocity obtained from a rotationally split non-radial mode.

4.3.1 KIC 10407873

The only significant p-mode frequencies in the amplitude spectrum of KIC 10407873 are a mixed mode triplet split by rotation. The KIC and Huber et al. (2014) stellar parameters for KIC 10407873 are given in Table 4.1, and its amplitude spectrum is shown in the top panel of Fig. 4.3. The triplet consists of three pulsation mode frequencies, $13.077173\,\mathrm{d}^{-1}$, $13.805580\,\mathrm{d}^{-1}$ and $14.520178\,\mathrm{d}^{-1}$, which have separations of $0.714598\,\mathrm{d}^{-1}$ and $0.728407\,\mathrm{d}^{-1}$. This means that the component frequencies of the triplet are not exactly equally split, as predicted for a rotationally split non-radial mode. A series of low amplitude peaks is also present at low frequency, specifically $0.977732\,\mathrm{d}^{-1}$, $1.954641\,\mathrm{d}^{-1}$ and $2.933393\,\mathrm{d}^{-1}$, which are not resolved sinc functions. The almost chaotic variability in the low-frequency peaks is shown graphically using a series of amplitude spectra in Fig. 4.4.

The amplitude and phase variability of the low frequency peaks and the triplet were tracked through the 4-yr *Kepler* data set using a similar method employed by Bowman & Kurtz (2014) to study amplitude modulation in the δ Sct star KIC 7106205 discussed in chapter 3. The results of the amplitude and phase tracking for the low frequency peaks and triplet of frequencies in KIC 10407873 are given in the bottom-left and bottom-right panels of Fig. 4.3, respectively. Clearly, the
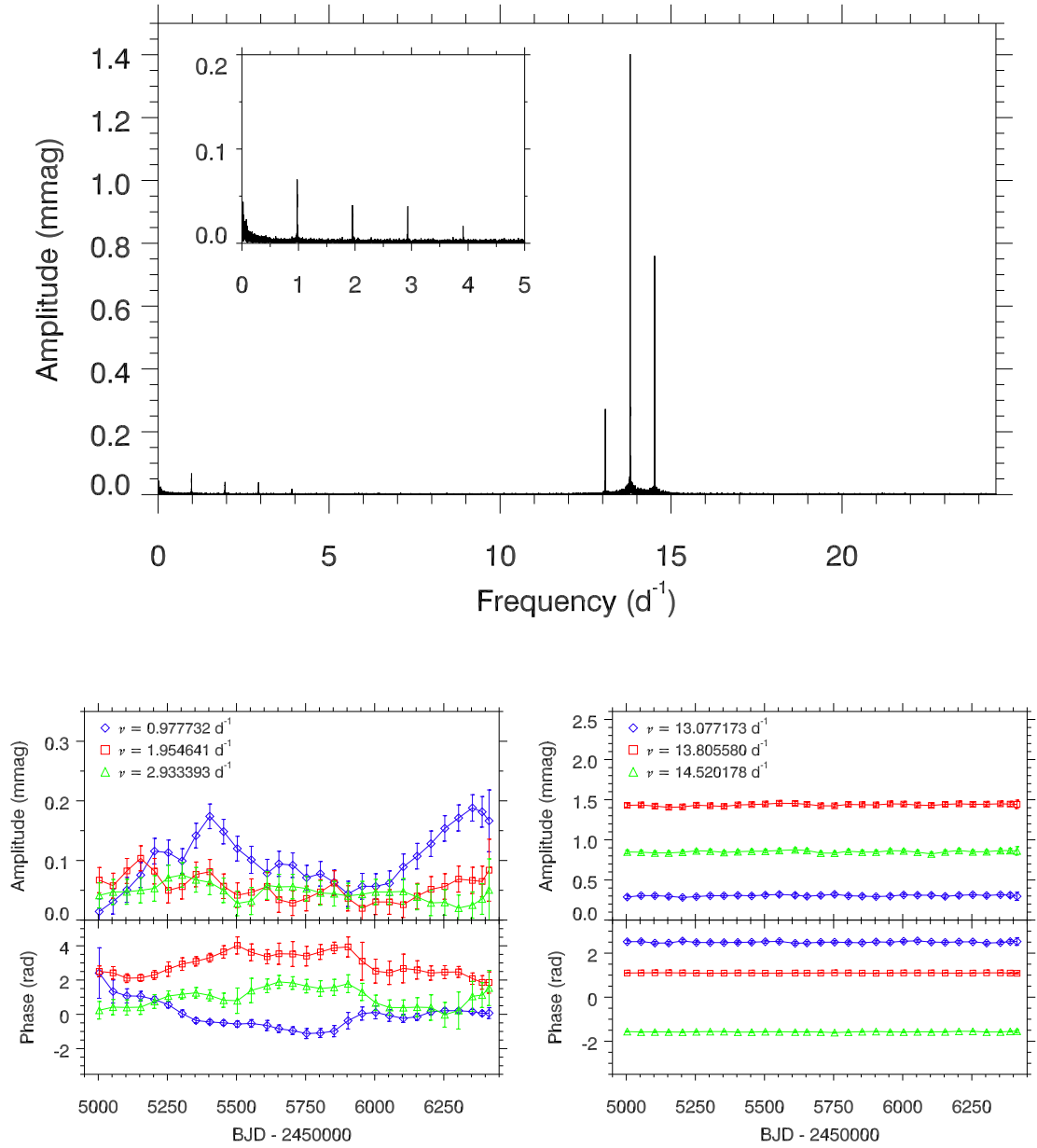
Figure 4.3: The amplitude spectrum of the star KIC 10407873 is given in the top panel, which contains a triplet of frequencies interpreted as a rotationally split dipole mode, and a series of peaks at low frequency that are unrelated to the rotation in this star. The bottom row shows the amplitude and phase variability of the the low frequency peaks and the triplet of frequencies in the left and right panels, respectively.
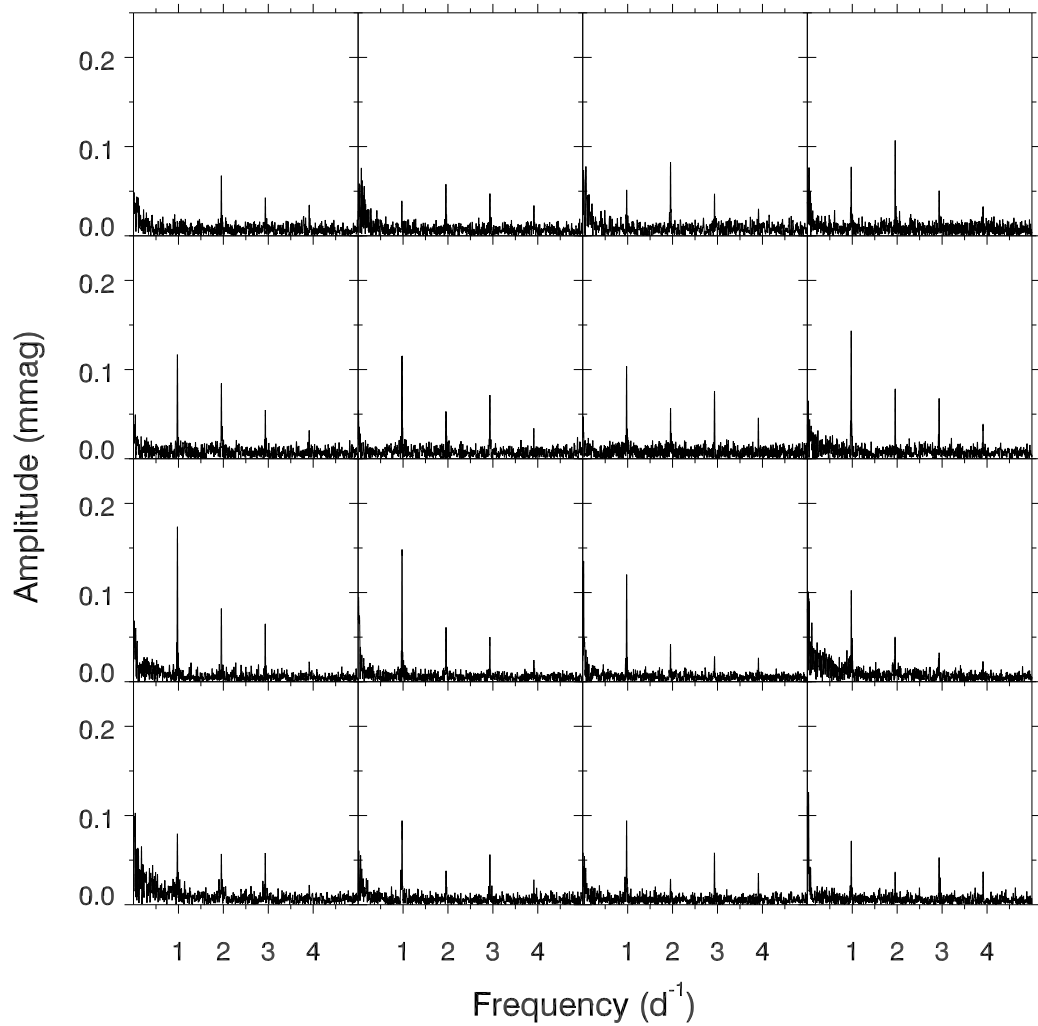
Figure 4.4: A series of amplitude spectra of the low-frequency peaks for the organ pipe star KIC 10407873 using 100-d bins with a 50-d overlap, which are ordered in time from left to right, row by row. Only the first 16 time bins are shown, which corresponds to the first 800 d of the *Kepler* data set. From one spectra to the next, the amplitudes of the low-frequency peaks change in a chaotic manner, hence coined the name organ pipes.

Table 4.1: Stellar parameters of the case study of the δ Sct star KIC 10407873 with low-frequency peaks called organ pipes in its amplitude spectrum.

	$T_{\rm eff}$ (K)	$\log g$ (cgs)	[Fe/H] (dex)
KIC (Brown et al. 2011)	7270 ± 250	3.42 ± 0.25	0.11 ± 0.25
Huber et al. (2014)	7510 ± 270	3.42 ± 0.28	0.07 ± 0.26

pulsation modes in the triplet are constant in amplitude and phase over time, but the low frequency peaks are not.

None of the frequencies in the triplet can be understood in terms of combination frequencies, because the splitting of the triplet is asymmetric and combination frequencies must be exactly equally-split as they are mathematical representations of non-linearity (see e.g., Kurtz et al. 2015). Moreover, the low-frequency peaks cannot be understood as combination frequencies of the triplet, because of the significant difference in frequency values. Therefore, the logical inference is that the triplet is likely a rotationally split dipole mode. From theoretical modelling, the central frequency of the triplet was matched to a mixed mode using a model of a 1.8-$M_\odot$ δ Sct star, but the asymmetry of the triplet was smaller than expected for the inferred rotation of this star (H. Saio, *private communication*). Using the simple model of a δ Sct star with a mass of 1.8 $M_\odot$, a radius of $R \simeq 2$ $R_\odot$, and the average of the rotational splitting in the triplet, 0.7215025 d^{-1}, a surface rotation velocity of $v_{\rm eq} \simeq 70$ km s^{-1} is indicated.

On the other hand, if the low-frequency peaks are assumed to represent harmonics of the star's rotation frequency caused by spot modulation, the rotational velocity calculated from the lowest-frequency is $v_{\rm eq} \simeq 100$ km s^{-1}, which implies that the triplet cannot be caused by rotation. These hypotheses are inherently mutually exclusive, unless spots on the surface of this star have significantly different rotational velocities than the value calculated from the rotationally split dipole modes.

For the low frequencies and the triplet to both be explained by rotation, a significant latitudinal differential rotation is needed in this star, which is unlikely.

The organ pipe star KIC 10407873 remains a useful case study for studying rotation and low frequency peaks in the amplitude spectra of δ Sct stars observed by the *Kepler* Space Telescope. Follow-up spectroscopy of KIC 10407873 and other organ pipe stars that have low-frequency peaks in their amplitude spectra is needed to determine a true surface rotational velocity and test if the low frequency peaks are caused by, or are unrelated to, the rotation of the star.

4.4 Hot gamma Doradus stars

In this section, stars that pulsate with only g-mode frequencies and lie between the cool edge of the SPB and the hot edge of the γ Dor instability regions are discussed. Balona (2014) identified a dozen of these stars in the *Kepler* data set, which have effective temperatures between $8100 \leq T_{\text{eff}} \leq 9200$ K and were pulsating purely in g modes. He termed these stars 'hot γ Dor stars' as they are located in a region of the HR diagram where neither the κ mechanism (Pamyatnykh 1999, 2000) or the flux blocking mechanism (Dupret et al. 2004, 2005) is predicted to excite g modes.

4.4.1 KIC 5130890

One such hot γ Dor star is KIC 5130890, which has an effective temperature and surface gravity that places it beyond the ZAMS blue edge of the classical instability strip, with the KIC and Huber et al. (2014) stellar parameters for KIC 5130890 given in Table 4.2. The amplitude spectrum of KIC 5130890 is shown in the bottom panel of Fig. 4.5, in which there only significant pulsation mode frequencies below $\nu < 5$ d^{-1} and are interpreted as g modes.

The simplest interpretation is that KIC 5130890 and other hot γ Dor stars have

Table 4.2: Stellar parameters of KIC 5130890, which is too hot to be within the γ Dor instability region and too cool to be within the SPB instability region.

	T_{eff} (K)	$\log g$ (cgs)	[Fe/H] (dex)
KIC (Brown et al. 2011)	9020 ± 350	4.03 ± 0.25	0.04 ± 0.25
Huber et al. (2014)	9250 ± 340	4.01 ± 0.24	0.07 ± 0.36
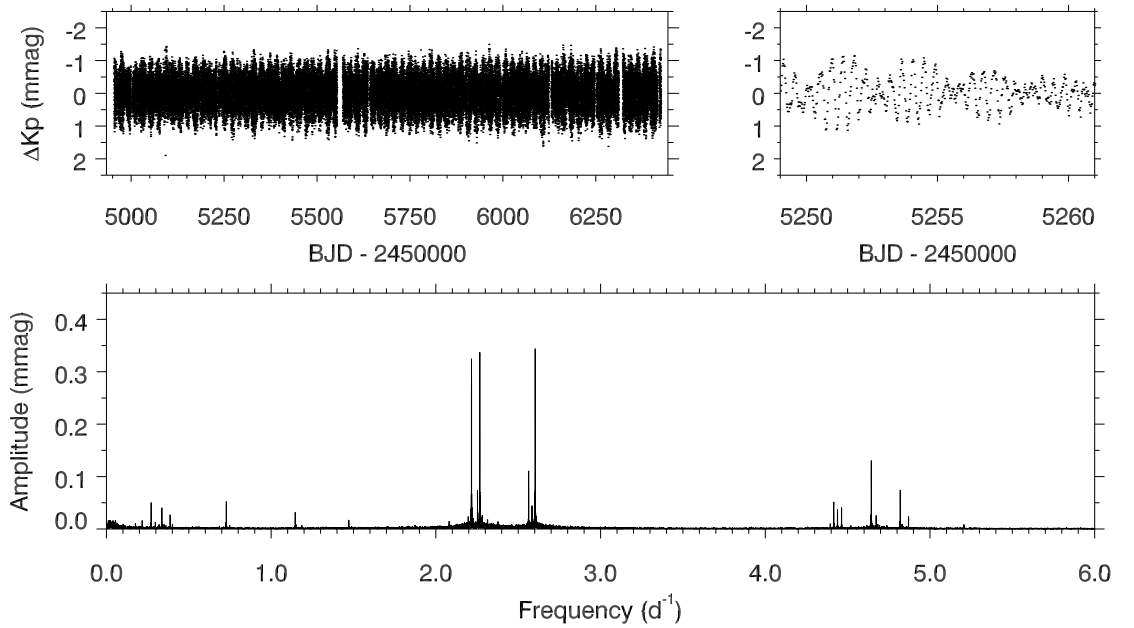
Figure 4.5: KIC 5130890 is a g mode pulsator characterised by an effective temperature that is too hot to place the star within the γ Dor instability region and too cool to place the star within the SPB instability strip. The 4-yr LC *Kepler* light curve is shown in the top-left panel and a 12-d insert of the LC light curve is shown in the top-right panel. The bottom panel is the LC amplitude spectrum between $0 \leq \nu \leq 6$ d^{-1}, which contains many g-mode frequencies.

incorrect T_{eff} values in the KIC and Huber et al. (2014) catalogues, which could be caused by the flux from the target star being contaminated from a background star. If, for example, the target star is a SPB star with $T_{\text{eff}} \simeq 11\,000$ K, then a cool contaminant star could dilute the target temperature to the observed T_{eff} value. A spectroscopic study of these hot γ Dor stars is needed for the determination of accurate effective temperatures.

On the other hand, if the effective temperature of KIC 5130890 and other hot γ Dor stars are accurate, and these stars are located outside of the SPB and γ Dor instability regions, then it is interesting how these stars can pulsate purely in g modes in a region in the HR diagram where g modes are not predicted to be excited (Pamyatnykh 1999, 2000; Dupret et al. 2004, 2005). Even though these hot γ Dor stars are rare, the discovery of pure g mode pulsators in the classical instability strip implies that our understanding of the interaction between the δ Sct and γ Dor excitation mechanisms is far from complete.

4.5 Creating an ensemble of delta Scuti stars

Using the *Kepler* data catalogues of $\sim$10 400 stars that were discussed in section 2.4.1, an ensemble of δ Sct stars was created of the stars that met *all* of the following criteria:

1. Characterised by $6400 \leq T_{\text{eff}} \leq 10\,000$ K in the KIC;

2. Observed continuously in LC from Q0 (or Q1) to Q17;

3. Contain peaks in the amplitude spectrum in the sub-Nyquist p-mode frequency regime ($4 \leq \nu \leq 24.5$ d^{-1}) with amplitudes greater than 0.10 mmag.

This resulted in 983 δ Sct and hybrid stars. This ensemble was created for two purposes. First so that the statistical properties of the δ Sct stars could be

investigated, which is discussed in the remaining sections of this chapter. Secondly, to study amplitude modulation in a large sample of δ Sct stars, which is discussed in chapter 5. The following paragraphs justify the motivation for each of the selection criteria.

The lower temperature limit of $T_{\mathrm{eff}} \geq 6400$ K was chosen because this is the observational red edge of the classical instability strip for δ Sct stars from Rodríguez & Breger (2001). The ZAMS red edge was calculated to be approximately 6900 K by Dupret et al. (2004), but cooler high-luminosity δ Sct stars are found below 6900 K and so the lower limit of 6400 K was chosen to include these targets. Few δ Sct stars are found between $6400 \leq T_{\mathrm{eff}} \leq 6500$ K, supporting this as the observational red edge defined by Rodríguez & Breger (2001). An upper limit of $T_{\mathrm{eff}} \leq 10\,000$ K was chosen to exclude pulsators that do not lie within the classical instability strip, such as SPB and β Cep stars (e.g., see Balona et al. 2011b and McNamara et al. 2012).

The use of LC data gives the largest number of stars that were observed over the longest possible time span of 4 yr. Only a small fraction of intermediate (and high) mass stars were observed in SC and even fewer for many consecutive SC months. Using LC data is motivated by previously studied δ Sct stars that exhibit amplitude modulation over time-scales of order years and decades (e.g., 4 CVn was observed to exhibit amplitude and frequency variability of order a few decades by Breger 2000b, 2016), and so complete data coverage over the maximum of 4 yr is most useful. It was also decided to exclude the stars that fall on module 3 of the *Kepler* CCD, because of the complicated window patterns in these stars.

The stars that contain pulsation mode frequencies within $4 \leq \nu \leq 24.5$ d^{-1} were selected because the LC Nyquist frequency is $\nu_{\mathrm{Nyq}} = 24.5$ d^{-1}. Although δ Sct stars can pulsate with frequencies higher than ν_{Nyq} (e.g., Holdsworth et al. 2014a), Nyquist alias peaks are subject to frequency (phase) variations and amplitude suppression

(Murphy et al. 2013b), thus real and alias frequency peaks can be identified without the need to calculate an amplitude spectrum beyond the Nyquist frequency.

It should be noted that this ensemble of 983 δ Sct stars includes many hybrid stars, but does not include any pure γ Dor stars because these stars do not pulsate in p modes with frequencies $\nu \geq 4 \, \mathrm{d}^{-1}$. Thus, when referring to this ensemble of 983 δ Sct stars, the terms δ Sct and hybrid can be used interchangeably, as the criteria given above selected stars that pulsate in p modes.

4.5.1 Ensemble limitations

It was discussed in section 2.3.3 and shown graphically in Fig. 2.6 how pulsation mode amplitudes are heavily suppressed for higher frequency signals and completely suppressed at integer multiples of the LC sampling frequency in *Kepler* data. Therefore, it is important to note that this ensemble of δ Sct stars is biased towards low pulsation mode frequencies, hence more evolved and cooler δ Sct stars. This is explored in more detail in section 4.7.

An example of a δ Sct star that was not included in the ensemble is KIC 10977859, which has an effective temperature of $T_{\mathrm{eff}} = 8180 \pm 170$ K (Huber et al. 2014) and pulsates with high frequency pulsation modes between $50 \leq \nu \leq 60 \, \mathrm{d}^{-1}$. KIC 10977859 was observed continuously by *Kepler* for 4 yr in LC and between Q8 – Q17 in SC, with the amplitude spectra for approximately 90 d of simultaneous LC and SC observations shown in the top and bottom panels of Fig. 4.6, respectively. The amplitude visibility function has resulted in significant amplitude suppression of this star's pulsation mode amplitudes from $A \simeq 1$ mmag in the SC amplitude spectrum to $A \simeq 0.2$ mmag in the LC amplitude spectrum.

To study the δ Sct star KIC 10977859, and other high frequency pulsators in the *Kepler* data set, it is necessary to use SC observations because the amplitude
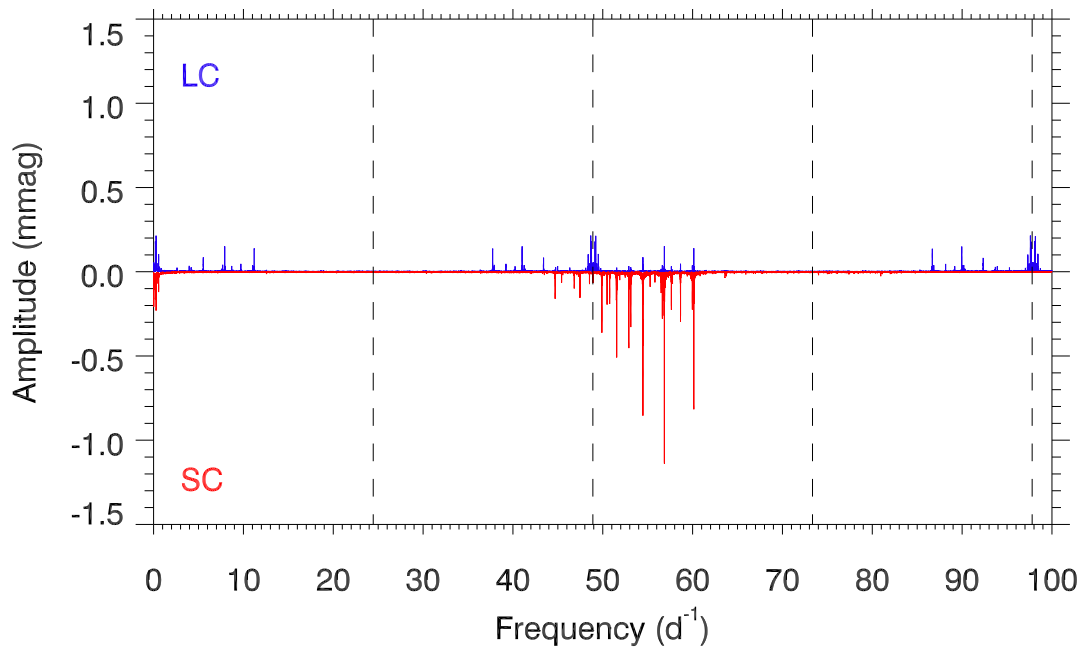
Figure 4.6: The LC and SC amplitude spectra for the δ Sct star KIC 10977859, calculated out to 100 d^{-1}, are shown in the top and bottom panels, respectively. Integer multiples of the LC Nyquist frequency are shown as vertical dashed lines. The pulsation mode frequencies between $50 \leq \nu \leq 60$ d^{-1} are clearly visible in the SC amplitude spectrum, but are heavily suppressed in the LC amplitude spectrum because of the longer integration time. Nyquist aliases of the pulsation mode frequencies can also be seen throughout the LC amplitude spectrum.

visibility function suppresses mode amplitudes at high frequency in LC data. Furthermore, amplitudes at integer multiples of the Nyquist frequency are completely suppressed when using LC data. Very few δ Sct stars were observed by *Kepler* in SC for more than a couple of consecutive months. As discussed previously, it was important to maximise both the number of stars in the ensemble and the length of observations to obtain the highest possible frequency resolution.

4.6 Revisiting the delta Scuti instability strip

The δ Sct stars are a diverse group of pulsators, with no obvious consistency in the number of excited pulsation modes, their amplitudes or range in observed frequencies. Balona & Dziembowski (2011) used a subset of 418 d of *Kepler* data (i.e., Q0 – Q5) to study 1568 δ Sct stars, particularly the occurrence of pulsation within the classical instability strip in the HR diagram. They concluded that no more than 50 per cent of stars between $7000 \leq T_{\mathrm{eff}} \leq 8000$ K in the *Kepler* data set were δ Sct stars. The lack of pulsation in chemically peculiar stars is not surprising, which explains why many A stars are not observed to pulsate; this was discussed in section 1.3.2.

In this section, the observed boundaries of the classical instability strip are revisited using the ensemble of 983 δ Sct stars that were observed continuously by *Kepler* for over 4 yr. The distribution of these stars in a T_{eff} – log g diagram using values from the KIC is shown in Fig. 4.7. In this figure, the location of each star is shown by a black cross, with stellar evolutionary tracks calculated from the ZAMS for 1.4, 1.8 and 2.2 $M_{\odot}$ stars shown as solid purple lines. The stellar evolutionary tracks were calculated using time-dependent convection (TDC) models and are courtesy of S. Murphy (*private communication*). The solid black lines in Fig. 4.7 indicate the observed blue and red edges of the classical instability strip from Rodríguez & Breger (2001), and the typical uncertainty for each star is shown by the error bar
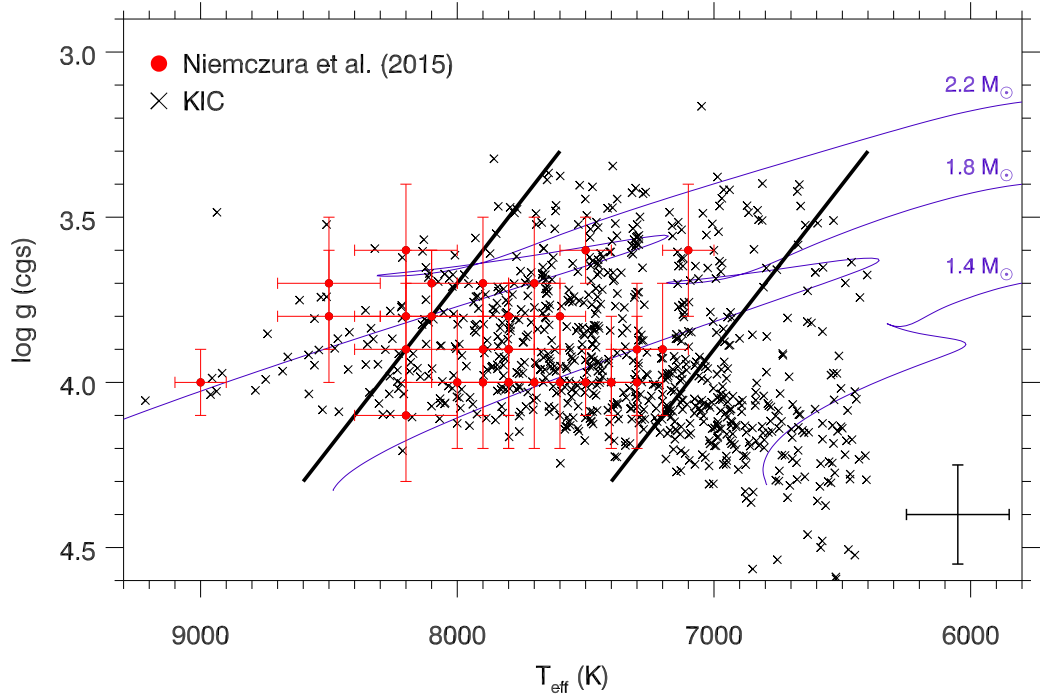
Figure 4.7: $T_{\rm eff}$ – log g diagram for the ensemble of 983 δ Sct stars. The distribution of KIC parameters for the ensemble of 983 δ Sct stars is shown as black crosses, with the typical point uncertainties shown by the error bars in the bottom right. The observational hot and cool borders of the classical instability strip are taken from Rodríguez & Breger (2001) and are shown as solid black lines. Stellar evolutionary tracks calculated using time-dependent convection (TDC) models, courtesy of S. Murphy (*private communication*), are shown as solid purple lines. A subgroup of δ Sct stars for which accurate spectroscopic values of $T_{\rm eff}$ and log g from Niemczura et al. (2015) are plotted as filled red circles.

in the bottom-right corner of the plot.

A study using high-resolution spectroscopic data from the HERMES spectrograph on the Mercator Telescope by Niemczura et al. (2015) characterised 117 bright (V $\leq$ 10 mag) A and F stars observed by the *Kepler* Space Telescope. Accurate values for fundamental stellar parameters including $T_{\rm eff}$, log g, rotational and microturbulent velocities and their respective uncertainties were determined for each star (Niemczura et al. 2015). The stars studied by Niemczura et al. (2015) that are included in the ensemble are shown as filled red circles in Fig. 4.7. Therefore, these

stars represent a subsample of all the δ Sct stars observed by *Kepler* for which accurate spectroscopic values of T_{eff} and log g are known, with uncertainties for individual stars that range between $100 \leq \sigma\left(T_{\mathrm{eff}}\right) \leq 200$ K and $0.1 \leq \sigma\left(\log g\right) \leq 0.2$ (cgs), respectively.

The majority of δ Sct stars in Fig. 4.7 are cooler than the blue edge of the classical instability strip, especially if the uncertainties in effective temperature are taken into account. In section 2.2.3, it was discussed how the effective temperatures listed in the KIC are accurate in a statistical sense, but are underestimated by approximately 200 K (Pinsonneault et al. 2012; Huber et al. 2014). This was also noted by Niemczura et al. (2015) in their study, and explains the systematic shift to higher temperatures for the stars in the Niemczura et al. (2015) subsample compared to the ensemble of 983 δ Sct stars. If this systematic error is included, then the majority of δ Sct stars in Fig. 4.7 are within 1σ of being within the classical instability strip. What is clear from the distribution of stars in Fig. 4.7 is that almost all δ Sct stars lie within the observational edges of the classical instability strip taken from Rodríguez & Breger (2001) if 3σ uncertainties in T_{eff} and log g are taken into account. For stars within the classical instability strip, it is not surprising that they are observed to pulsate for the reasons discussed in section 1.2.3.

On the other hand, a minority of δ Sct stars in the ensemble have effective temperatures that are hotter than the blue edge or cooler than the red edge of the classical instability strip by more than 3σ, so further investigation is needed to study these stars. There is also a high density of stars near the red edge in Fig. 4.7 indicating there is not an abrupt transition in temperature for whether a star is stable or unstable to pulsation by the κ mechanism. The edges of the instability strip from Rodríguez & Breger (2001) shown in Fig. 4.7 are purely observational, so could be moved to take into account the outlying δ Sct stars in the *Kepler* data set.

The majority of the δ Sct stars in Fig. 4.7 have surface gravities between $3.5 \leq$

log $g \leq 4.0$ with few stars around log $g \simeq 4.4$, thus the TAMS is better sampled than the ZAMS for δ Sct stars observed by the *Kepler* Space Telescope. This result was also found for the subsample of bright A and F stars studied by Niemczura et al. (2015) using spectroscopy.

In summary, it can be concluded that the observed blue and red edges from Rodríguez & Breger (2001) remain a reasonable indicator for the location of δ Sct stars observed by the *Kepler* Space Telescope. However, a few δ Sct stars lie beyond the blue edge of the classical instability strip, some of which have been studied spectroscopically by Niemczura et al. (2015) and have accurate effective temperatures and surface gravities. These stars will be interesting to study further, as they lie in a region where the excitation of p modes by the κ mechanism is not expected to occur (Pamyatnykh 1999, 2000; Dupret et al. 2005). Also, a significant fraction of δ Sct stars are located near the red edge of the classical instability strip and so the observed boundaries may need to be moved to take these stars into account.

4.7 Correlations in the stellar parameters of delta Scuti stars

In this section, correlations between pulsation and different stellar parameters are investigated using the ensemble of 983 δ Sct stars. The amplitude spectrum for each star in the ensemble was calculated to 98 d^{-1}, which is four times the LC Nyquist frequency, or twice the sampling frequency. The highest amplitude peak in the p mode frequency regime ($4 \leq \nu \leq 98$ d^{-1}) was extracted and values of frequency, amplitude and phase were optimised using non-linear least-squares.

In this analysis, only a single frequency is extracted per star to ensure that it is a pulsation mode frequency and not an Nyquist alias peak, as real pulsation mode frequencies have higher amplitudes than their Nyquist aliases (Murphy et al.

2013b). It was discussed in section 2.3.1 and demonstrated in Fig. 2.3 how the Barycentric time stamp corrections made to *Kepler* data produce a non-constant cadence, which causes Nyquist aliases to experience a periodic frequency modulation and amplitude suppression (Murphy et al. 2013b). Therefore, the frequency of the highest amplitude peak (i.e., the frequency of A_{max}) in the amplitude spectrum cannot be an alias of a pulsation mode frequency, as a real frequency has a larger amplitude (Murphy et al. 2013b).

The amplitude spectrum for each star is not corrected for the amplitude visibility function given in Eqn 2.5, because it would then be possible for Nyquist aliases to have higher amplitudes than pulsation mode frequencies. This is demonstrated graphically in Fig. 4.8 using the LC amplitude spectrum of the δ Sct star KIC 7106205. In this figure, integer multiples of the LC Nyquist frequency are shown as dashed lines and the amplitude visibility function is shown as a red line. The highest amplitude peak, which corresponds to a pulsation mode at $\nu = 10.0323 \ \mathrm{d}^{-1}$ is labelled 'r' for real, and its Nyquist aliases are labelled a_1, a_2 and a_3. If the amplitude spectrum is corrected for the amplitude visibility function, then the alias frequencies would have larger amplitudes than the real pulsation mode.

By not correcting the amplitude spectra of 983 δ Sct stars for the amplitude visibility function, it is ensured that the extracted frequency is a pulsation mode frequency and not a Nyquist alias frequency. The disadvantage of this approach is that the distribution of frequencies will be biased towards, on average, lower values, but this is a compromise that yields the most meaningful results.

Restricting this search to the p-mode frequency regime also ensures that variability from longer period phenomena such as rotation is excluded. The histogram for the distribution of the frequency of the highest amplitude pulsation mode is shown by the black region in Fig. 4.9, which demonstrates that the dominant pulsation mode frequency typically lies below $\nu \lesssim 40 \ \mathrm{d}^{-1}$ for most δ Sct stars. This agrees
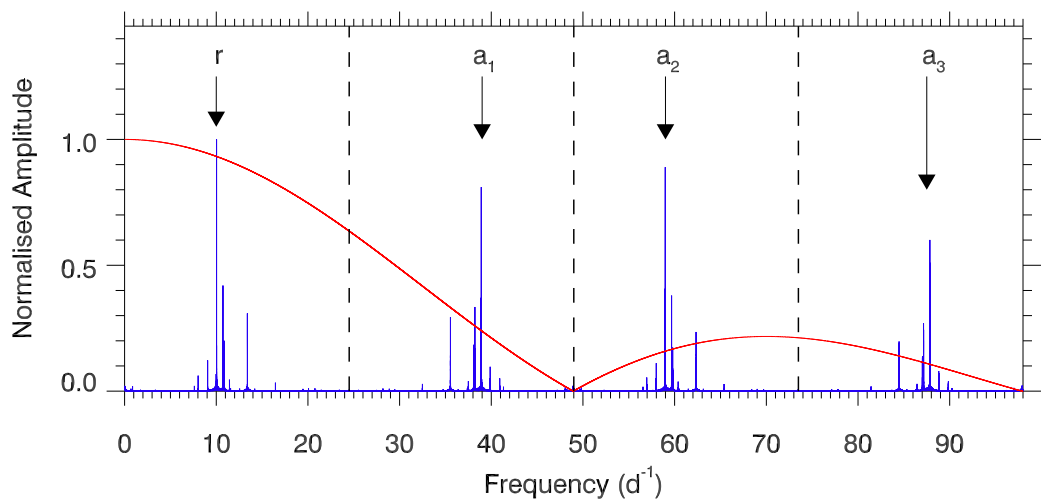
Figure 4.8: Application of amplitude visibility function using the δ Sct star KIC 7106205. The normalised amplitude spectrum using LC *Kepler* data has been calculated to four times the Nyquist frequency, with integer multiples of ν_{Nyq} shown as dashed lines. The highest amplitude peak, which corresponds to a pulsation mode at $\nu = 10.0323$ d^{-1} is labelled 'r' for real, and its Nyquist aliases are labelled with a_i. The normalised amplitude visibility is shown as a red solid line. If the amplitude spectrum was corrected for the amplitude visibility function, then the alias peaks, a_1, a_2 and a_3 would have higher amplitudes than the real peak, thus justifying why frequencies are extracted without correcting for the *Kepler* integration time.
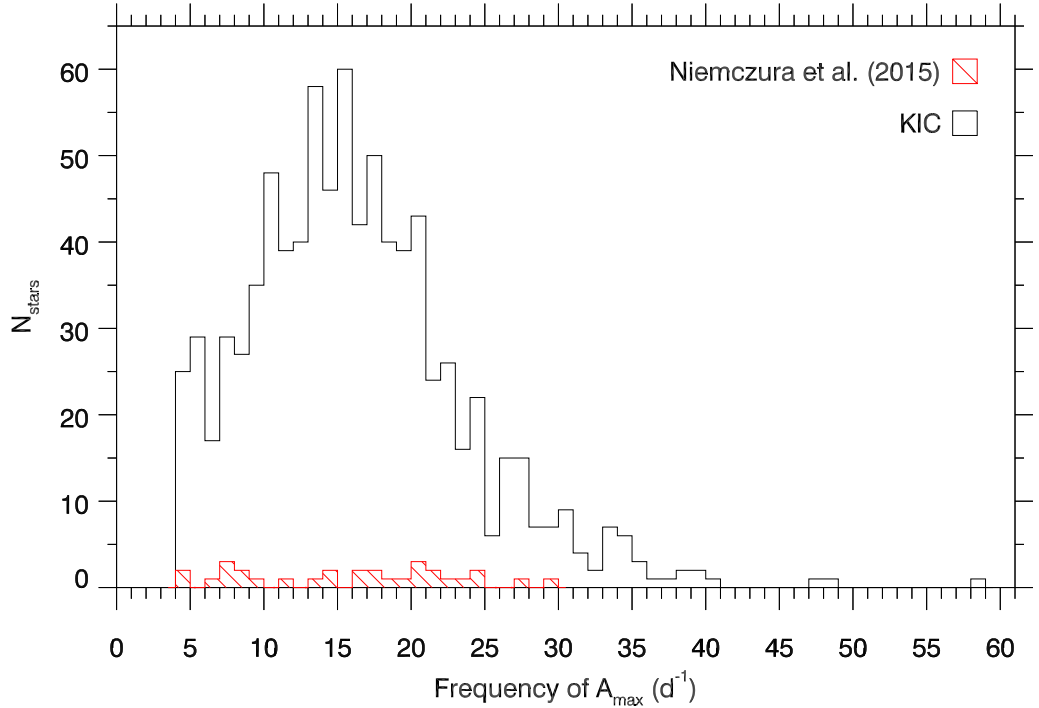
Figure 4.9: The histogram of the frequency of maximum amplitude for the ensemble of 983 δ Sct stars. The frequency of maximum amplitude is extracted from the frequency range of $4 \leq \nu \leq 98$ d^{-1}, and is optimised using non-linear least-squares fit to the data set for each star. The subgroup of bright A and F stars studied by Niemczura et al. (2015) is also plotted in red for comparison.

with the analysis by Balona & Dziembowski (2011). However, the bias introduced by the amplitude visibility function means that stars with pulsation modes at or near the *Kepler* sampling frequency have been included, and explains the dearth of δ Sct stars with frequencies $\nu \gtrsim 40$ d^{-1} in the *Kepler* data set.

4.7.1 Pulsation and effective temperature

A semi-empirical relationship exists between the effective temperature and the observed pulsation mode frequencies in a δ Sct star. As discussed in section 1.2.3, the depth of the He II ionisation zone is a function of T_{eff} in the stellar envelope. A hot δ Sct star near the blue edge will typically pulsate in higher radial overtone modes, resulting in higher pulsation mode frequencies (Pamyatnykh 1999,

2000; Christensen-Dalsgaard 2000; Dupret et al. 2004, 2005). Thus, hotter δ Sct stars typically have higher pulsation mode frequencies, a relationship that has been observed from the ground (see e.g., Breger & Bregman 1975; Breger 2000a).

Theoretically, there are predictions of where the δ Sct instability region is located in the HR diagram (Pamyatnykh 1999; Dupret et al. 2004, 2005; Grigahcène et al. 2010a), but the predictions depend on the numerical treatment of convection used in stellar models, especially for determining the red edge of the classical instability strip (see e.g., Dupret et al. 2004, 2005). Observationally, the blue and red edges are well-constrained using ground-based data (Rodríguez & Breger 2001), but with less accuracy when using space-based observations (Grigahcène et al. 2010a; Uytterhoeven et al. 2011; Balona & Dziembowski 2011; Bowman et al. 2016).

The frequency of the highest amplitude pulsation mode is plotted against T_{eff} using the KIC parameters for the ensemble of 983 δ Sct stars in Fig. 4.10. A linear regression of these two parameters, shown as a black line in Fig. 4.10, and a Pearson coefficient of $R = 0.282$ indicate a weak correlation between the frequency of the highest amplitude pulsation mode and effective temperature in δ Sct stars observed by the *Kepler* Space Telescope. The subsample of bright A and F stars from Niemczura et al. (2015) are also plotted in Fig. 4.10 as filled red circles for comparison, for which a separate linear regression is plotted as a red line.

The amplitude suppression of high frequency pulsation modes in LC *Kepler* data may explain why only a weak correlation was found between pulsation and effective temperature as very few δ Sct stars with pulsation mode frequencies above 40 d^{-1} are included in the ensemble of 983 δ Sct stars. For example, the δ Sct KIC 10977859 discussed in section 4.5.1 has an effective temperature of $T_{\text{eff}} = 8180 \pm 170$ K (Huber et al. 2014) and pulsates with pulsation mode frequencies between $50 \leq \nu \leq 60$ d^{-1}, so clearly at least one hot, high-frequency δ Sct star has not been included in the ensemble, which would improve the correlation in Fig. 4.10.

Figure 4.10: A linear regression of the frequency of maximum amplitude against T_{eff} using the KIC parameters for the ensemble of 983 δ Sct stars is shown as a black line. The Pearson coefficient is shown in the top-left corner of the plot indicating a weak correlation, and a typical error bar for each data point is shown in the bottom-right corner of the plot. The subsample of δ Sct stars for which accurate spectroscopic values of T_{eff} obtained from Niemczura et al. (2015) are plotted as filled red circles, with a separate linear regression of these values plotted as the red line.

Despite this, the observed correlation is in agreement with the expectation that hotter δ Sct stars have higher pulsation mode frequencies (Breger & Bregman 1975; Breger 2000a).

4.7.2 Pulsation and surface gravity

Another semi-empirical relationship exists between the evolutionary state and the observed pulsation mode frequencies in a δ Sct star. As discussed previously in section 1.1.1, the evolutionary state of a star influences its pulsations with post-main sequence stars exhibiting mixed modes (Osaki 1975), which are the result of the coupling of the g- and p-mode pulsation cavities (e.g., Lenz et al. 2010). The δ Sct stars are interesting as they include main sequence and post-main sequence stars, with models of δ Sct stars predicting that mixed modes can be excited in these stars (Dziembowski et al. 1995; Christensen-Dalsgaard 2000).

The evolutionary state of a star can be inferred from its $\log g$ value, with the more evolved stars having lower $\log g$ values. This is caused by the increase in radius after as star has evolved beyond the TAMS. Therefore, a more-evolved δ Sct star in a post-main sequence stage of stellar evolution will generally have lower pulsation mode frequencies than its ZAMS counterpart for a given effective temperature.

The frequency of the highest amplitude pulsation mode is plotted against $\log g$ using the KIC parameters for the ensemble of 983 δ Sct stars in Fig. 4.11. A linear regression of these two parameters, shown as a black line in Fig. 4.11, and a Pearson coefficient of $R = 0.075$ indicate almost no correlation between the frequency of the highest amplitude pulsation mode and surface gravity in δ Sct stars observed by the *Kepler* Space Telescope. The subsample of bright A and F stars from Niemczura et al. (2015) are also plotted in Fig. 4.11 as filled red circles for comparison, for which a separate linear regression is plotted as a red line. The lack of correlation in Fig. 4.11 is likely because of the previously discussed bias towards lower frequencies

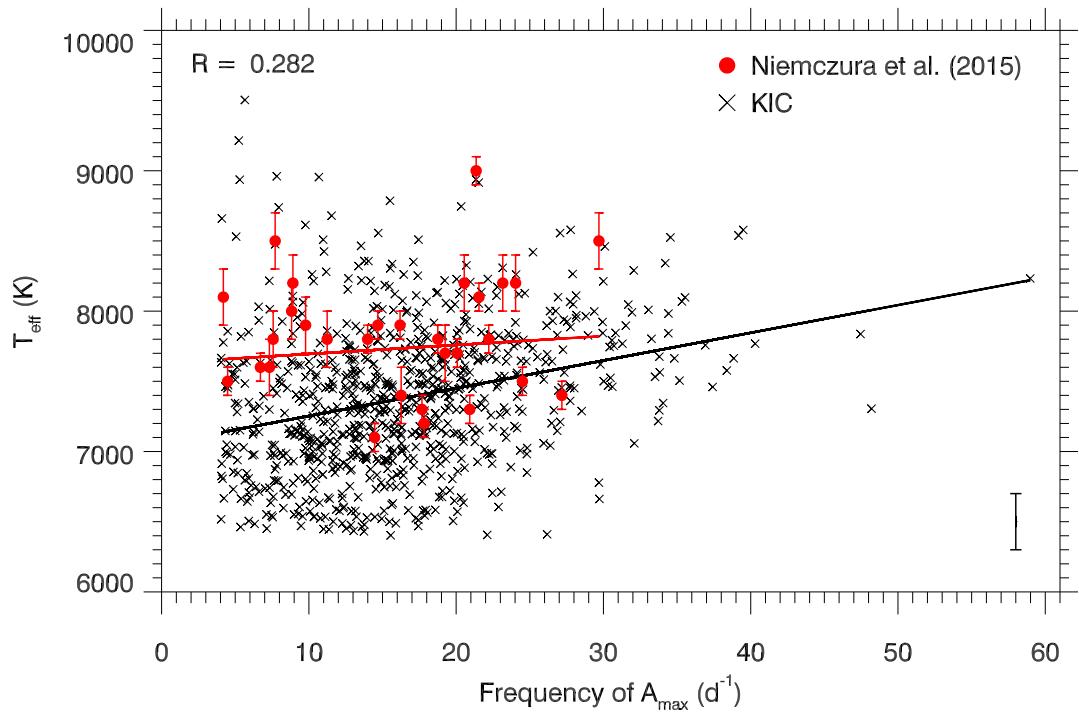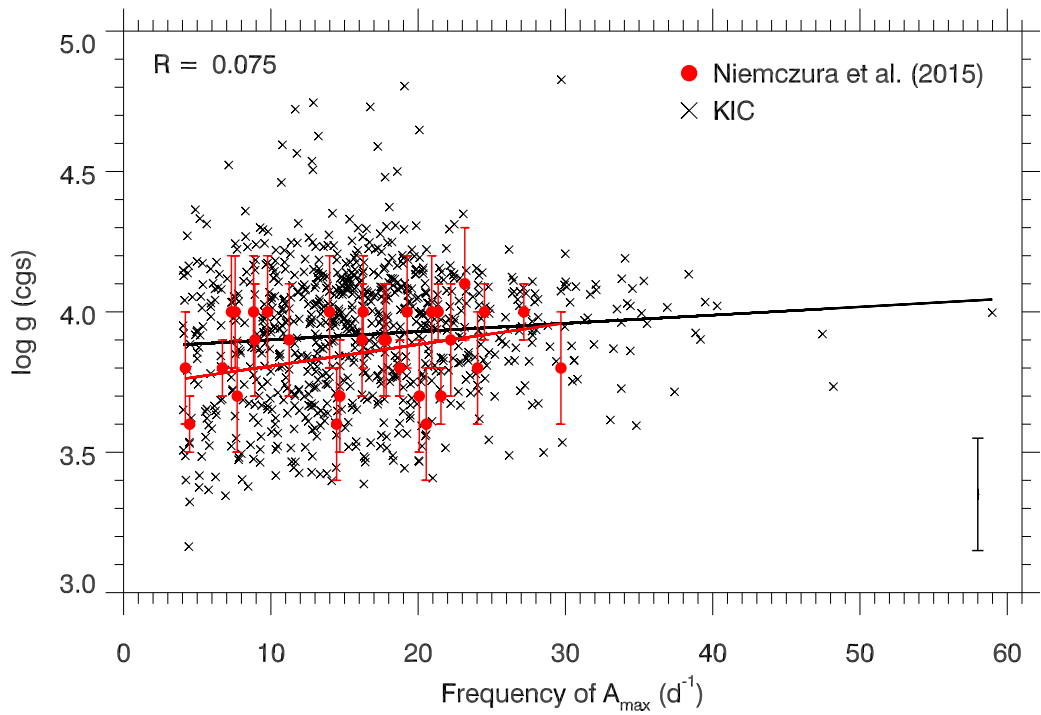Figure 4.11: A linear regression of the frequency of maximum amplitude against log g using the KIC parameters for the ensemble of 983 δ Sct stars is shown as a black line. The Pearson coefficient is shown in the top-left corner of the plot indicating almost no correlation, and a typical error bar for each of the data points is shown in the bottom-right corner of the plot. The subsample of δ Sct stars for which accurate spectroscopic values of log g obtained from Niemczura et al. (2015) are plotted as filled red circles, with a separate linear regression of these values plotted as the red line.

resulting in only a narrow range of extracted frequencies. Furthermore, there is degeneracy in the observed pulsation mode frequencies between evolved stars and cool main sequence stars, with both groups of δ Sct stars typically having lower pulsation mode frequencies.

4.7.3 Pulsation across the $T_{\mathrm{eff}} - \log g$ diagram

The relationships between pulsation and effective temperature, and pulsation and surface gravity are degenerate, making it difficult to distinguish cool main sequence δ Sct stars and evolved δ Sct stars. Therefore, using a $T_{\mathrm{eff}} - \log g$ diagram is a sensible way to investigate these correlations further. The ensemble of 983 δ Sct stars observed by *Kepler* are plotted in a $T_{\mathrm{eff}} - \log g$ in Fig. 4.12, which is colour-coded to denote the frequency of the highest amplitude pulsation mode. As expected, the δ Sct stars with higher pulsation mode frequencies ($\nu \geq 40$ d^{-1}) typically lie at higher effective temperatures in Fig. 4.12.

The ensemble of 983 δ Sct stars shown in Fig. 4.12 are divided into three populations and plotted separately in Fig. 4.13 for comparison. In this figure, the top, middle and bottom panels correspond to the stars with low-frequency pulsations ($4 < \nu < 18$ d^{-1}), mid-range pulsation frequencies ($18 < \nu < 32$ d^{-1}), and high-frequency pulsations ($32 < \nu < 60$ d^{-1}), respectively. Although, there is a dearth of high-frequency δ Sct stars, a shift from lower $\log g$ and T_{eff} to higher values of $\log g$ and T_{eff} can be seen from the top to bottom panels in Fig. 4.13.

The relationships between the frequency of the highest amplitude pulsation mode and the stellar parameters T_{eff} and $\log g$ presented in this thesis may not be completely representative of δ Sct stars, as only a single pulsation mode frequency was used for each star. Many δ Sct stars have a large range of pulsation mode frequencies, which is not taken into account in Figs 4.9 – 4.13. Moreover, the degeneracy between evolved and cool main sequence δ Sct stars complicates the method for
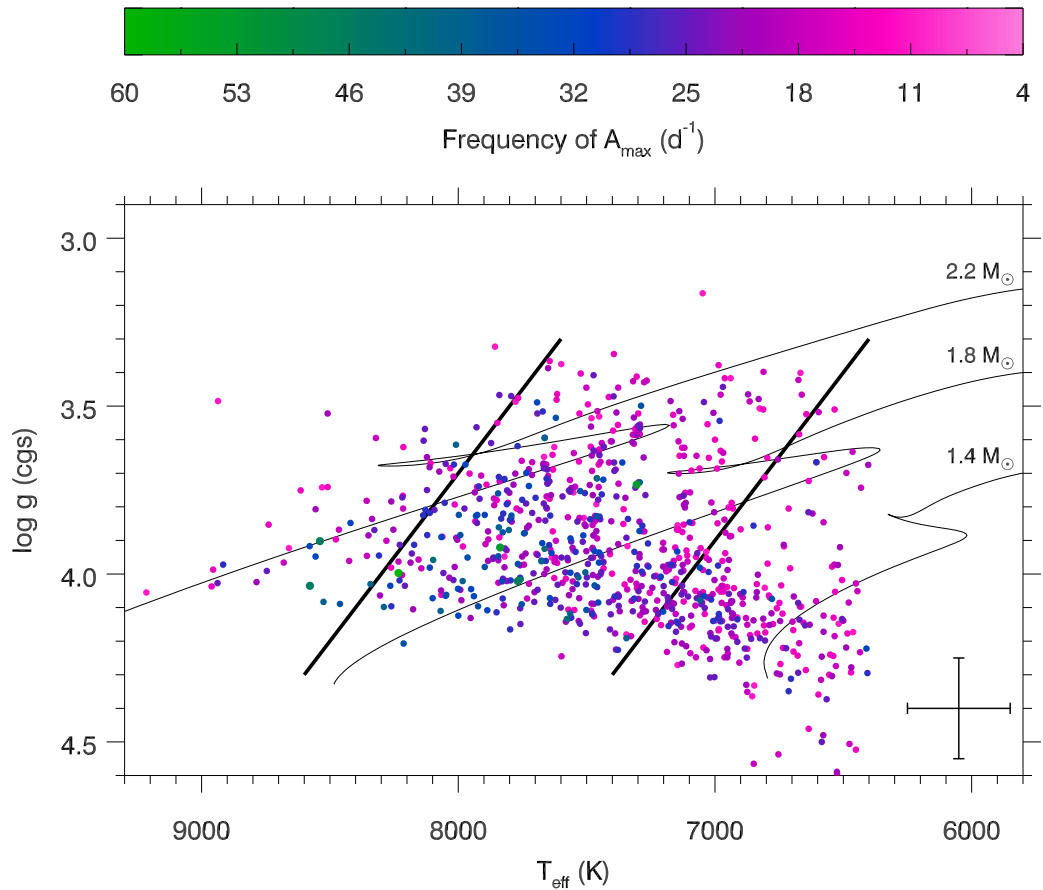
Figure 4.12: Pulsation across the T_{eff} – log g diagram. This figure is the same as Fig. 4.7, but each filled circle has been coloured by the frequency of its highest amplitude pulsation mode. High densities of δ Sct stars with low-frequency pulsations ($\nu \leq 25$ d^{-1}) are found near the ZAMS red edge and the TAMS, whereas δ Sct stars with high-frequency pulsations ($\nu > 25$ d^{-1}) are found closer to the blue edge.
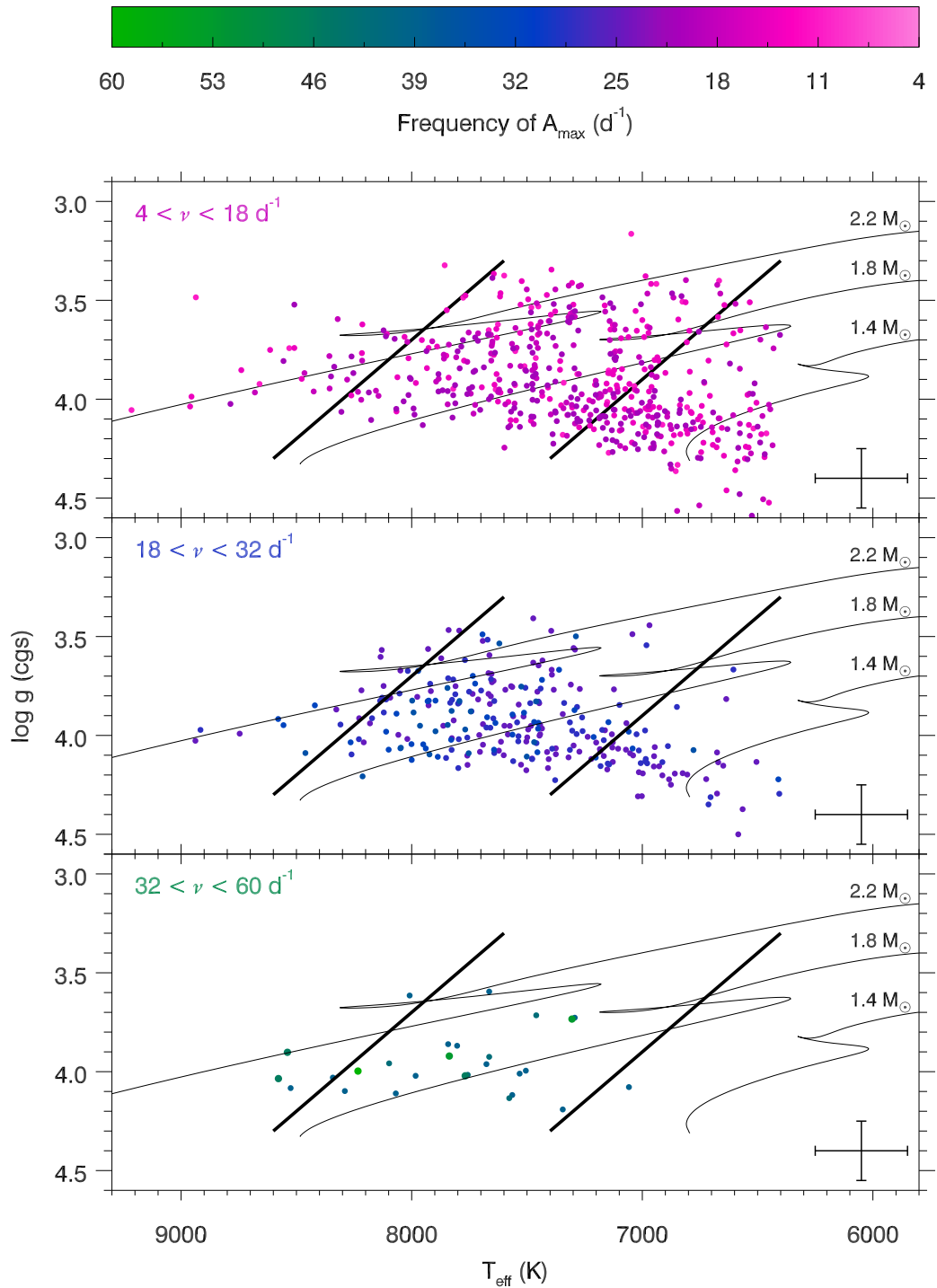
Figure 4.13: Distribution of pulsation across the $T_{\mathrm{eff}} - \log g$ diagram. This figure is similar to Fig. 4.12, but the ensemble of 983 δ Sct stars has been split into three populations based on the frequency of the highest amplitude pulsation mode. The top, middle and bottom panels show the $4 < \nu < 18 \ \mathrm{d}^{-1}$, $18 < \nu < 32 \ \mathrm{d}^{-1}$ and $32 < \nu < 60 \ \mathrm{d}^{-1}$ populations, respectively.

determining general properties of an ensemble of δ Sct stars. Nonetheless, the high-frequency δ Sct stars are typically located near the blue edge of the instability strip and the ZAMS as shown in Figs 4.12 and 4.13. This relationship has been predicted by theoretical models (Pamyatnykh 1999, 2000; Christensen-Dalsgaard 2000; Dupret et al. 2004, 2005) and studied using ground-based observations of δ Sct stars (Breger & Bregman 1975; Breger 2000a), and so the results presented in this thesis are consistent with previous analyses.

4.7.4 Pulsation and rotation

The frequency of the highest amplitude pulsation mode is plotted against $v \sin i$ using the subsample of δ Sct stars from Niemczura et al. (2015) in Fig. 4.14, for which accurate values of $v \sin i$ were obtained from high-resolution spectroscopy. The effects of rotation modify the pulsation mode frequencies of a star by lifting the degeneracy of non-radial modes into their $2\ell + 1$ components, but there is no expectation for either slow or fast rotating δ Sct stars to have dominant high or low pulsation mode frequencies, or vice versa. As shown in Fig. 4.14, there is no correlation between the rotational velocity of a δ Sct star and the frequency of the highest amplitude pulsation mode.

4.8 Discussion

From ground-based observations, the δ Sct stars are found on or near the main sequence within the classical instability strip, and are well-defined by the observational blue and red edges from Rodríguez & Breger (2001). The γ Dor stars are located in a nearby and overlapping region in the HR diagram (Dupret et al. 2004), but only a small minority of stars were predicted to be simultaneously unstable to both δ Sct
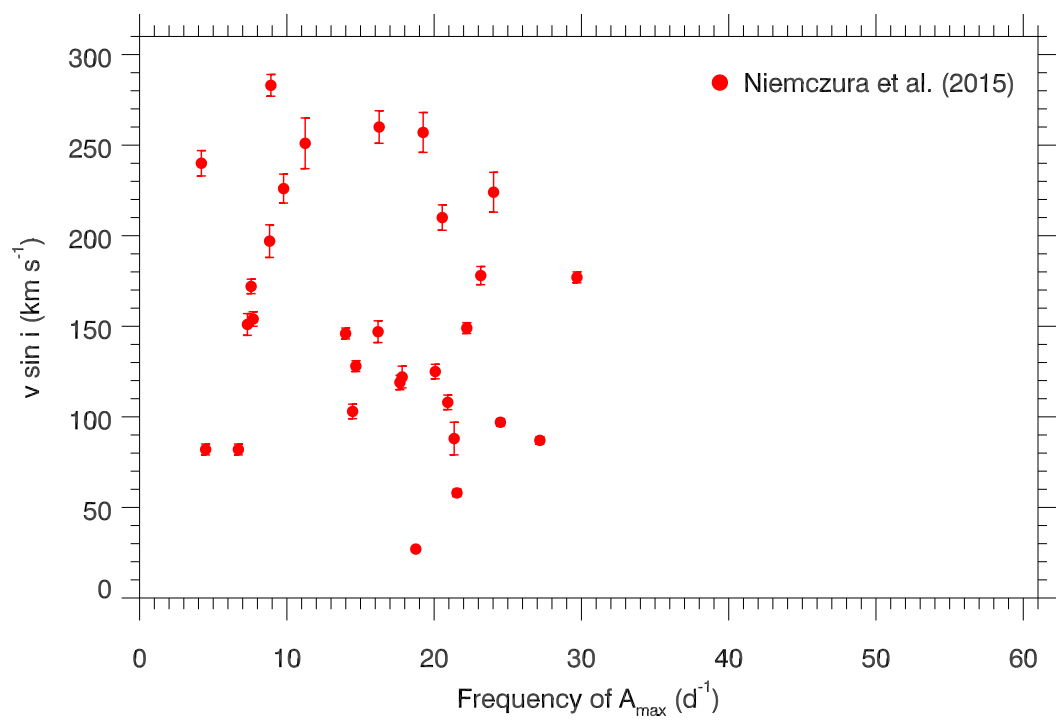
Figure 4.14: The frequency of the highest amplitude pulsation mode plotted against $v \sin i$ using the subsample of δ Sct stars from Niemczura et al. (2015), which reveals no correlation between these two parameters.

and γ Dor excitation mechanisms (Dupret et al. 2005). However, *Kepler* observations have revealed that many pulsating A and F stars are hybrid stars pulsating in both p and g modes (Grigahcène et al. 2010a; Uytterhoeven et al. 2011; Balona & Dziembowski 2011), which is shown in Fig. 4.1.

From the in-depth studies of individual hybrid stars, it has been shown that p modes from the κ mechanism and g modes from the flux blocking mechanism can be simultaneously excited and be intrinsic to a single star (see e.g., Chapellier et al. 2012 and Kurtz et al. 2014). Also, it has been shown that hybrid stars can exist in binary systems, with all pulsations originating in the primary (see e.g., Van Reeth et al. 2015b). Therefore, binarity does not offer a ubiquitous solution for why many δ Sct stars are hybrid pulsators. It has been suggested that all δ Sct stars are hybrid stars (Balona 2014; Balona et al. 2015b), but stars pulsating in purely p modes with no statistically significant peaks in the g-mode frequency regime do exist. This was demonstrated using KIC 5617488 in section 4.2.2.

In section 4.3, it was discussed how a diverse range of yet unexplained phenomena can exist in δ Sct stars, including the incidence of low-frequency peaks in δ Sct stars. These so-called organ pipe stars have a series of low-frequency peaks in their amplitude spectra that are highly variable in amplitude and phase throughout the *Kepler* data set, and it has been claimed that these low-frequency peaks are caused by rotation (Balona 2011, 2013). The δ Sct star KIC 10407873 was shown to contain a rotationally-split dipole mode, which was used to calculate a rotational velocity of $v_{\rm eq} \simeq 70~{\rm km\,s^{-1}}$ for this star. This value is not consistent with the rotational velocity of $v_{\rm eq} \simeq 100~{\rm km\,s^{-1}}$ calculated using the low-frequency peaks. Therefore, rotational modulation from starspots is not always the cause of low-frequency peaks in δ Sct stars. Further work is clearly needed to investigate the cause of these low-frequency peaks in δ Sct stars.

In this chapter, 4 yr of continuous *Kepler* data have been used to create an

ensemble of 983 δ Sct stars to study the statistical properties of these stars, including the correlations between the fundamental stellar parameters and the frequency of the highest amplitude pulsation mode in each star. The majority of the 983 δ Sct stars are located inside the classical instability strip, as shown in Fig. 4.7, especially if the uncertainties in T_{eff} and log g, and the 200 K systematic underestimation of KIC effective temperatures (Pinsonneault et al. 2012; Huber et al. 2014; Niemczura et al. 2015) are taken into account. However, a small fraction of stars are located outside the classical instability strip, and if the effective temperatures and surface gravities of these stars are accurate, then the observational blue and red edges from Rodríguez & Breger (2001) may need to be revised.

The correlations between the frequency of the highest amplitude pulsation mode and effective temperatures and surface gravities were investigated using the ensemble of 983 δ Sct stars in section 4.7. For a hot δ Sct star near the blue edge of the classical instability strip, a high effective temperature facilitates the excitation of higher overtone modes because the κ mechanism operating in the He II ionisation zone is closer to the surface of the star (Pamyatnykh 1999; Christensen-Dalsgaard 2000; Dupret et al. 2004, 2005). A linear regression of the frequency of the highest amplitude pulsation mode against effective temperature is shown in Fig. 4.10, which indicates a weak correlation between these two parameters. This relationship was also found in ground-based observations of δ Sct stars (Breger & Bregman 1975; Breger 2000a).

Similarly, there is an expectation for post-main sequence δ Sct stars to exhibit lower pulsation mode frequencies from the presence of mixed modes (Osaki 1975) and the increase in radius caused by stellar evolution. A linear regression of the frequency of the highest amplitude pulsation mode against surface gravity is shown in Fig. 4.11, which reveals no significant correlation between these parameters. However, the degeneracy in pulsation mode frequencies for cool main sequence and evolved stars

makes finding any correlation difficult.

In Figs 4.7, and $4.9-4.11$, a subsample of δ Sct stars from Niemczura et al. (2015) are also shown, for which accurate T_{eff} and $\log g$ values obtained from high-resolution spectroscopy are known. The spectroscopic observations of $v \sin i$ for the subsample of δ Sct stars from Niemczura et al. (2015) are plotted against the frequency of the maximum amplitude pulsation mode in Fig. 4.14, which shows no correlation between the frequency of the highest amplitude pulsation mode and rotational velocity in this subsample of δ Sct stars.

Chapter 5

Amplitude modulation in delta Scuti stars

5.1 Introductory remarks

The various causes of why δ Sct stars exhibit variable pulsation mode amplitudes (and/or frequencies) can be loosely grouped as intrinsic and extrinsic, i.e., those physical and interior to the star and those caused by external effects, respectively. The motivation for a statistical search for amplitude modulation in a large number of δ Sct stars, which is presented in this chapter, is primarily motivated by studies of the δ Sct star KIC 7106205 discussed in chapter 3. The *Kepler* data set offers the opportunity to test if this phenomenon is common among a large number of δ Sct stars. Further motivation comes from well-studied δ Sct stars observed from the ground. The δ Sct star 4 CVn, which was discussed in section 1.5, epitomises the diversity among all δ Sct stars, because it has been shown to be part of a binary system (Schmid et al. 2014), has beating of close-frequency pulsation modes (Breger & Bischof 2002), has a mode coupling mechanism (Breger 2000b), and exhibits amplitude modulation from an unknown mechanism (Breger 2016).

CHAPTER 5

In this chapter, inspired by the extensive literature on the δ Sct star 4 CVn and the previous analyses of KIC 71026205, two research questions are tested using the ensemble of 983 δ Sct stars discussed in chapter 4, which are:

(i) Is amplitude modulation common among δ Sct stars?

(ii) Is the pulsational energy budget conserved?

5.2 Amplitude modulation in δ Sct stars: statistics from an ensemble of *Kepler* targets

In this section, the research paper by Bowman et al. (2016) is presented, which was published in Monthly Notices of Royal Astronomical Society in August 2016. I created an automated amplitude and phase tracking pipeline that produced an amplitude modulation catalogue of 983 δ Sct stars observed by the *Kepler* Space Telescope. This catalogue is available as a PDF online and an electronic version of Table 1 has been placed on CDS. The beating and coupling models discussed in sections 5 and 6 of the paper, respectively, were created using a selection of example stars that I chose myself. I wrote the majority of the publication and D. W. Kurtz contributed to the discussion throughout. M. Breger contributed to the writing of sections 2.2 and 6, and S. J. Murphy kindly contributed the binary periods of the four stars identified as binaries in section 4.6, and contributed to the writing of section 2.3. All co-authors were involved in editing the paper.

Amplitude modulation in δ Sct stars: statistics from an ensemble study of *Kepler* targets

Dominic M. Bowman,[1]★ Donald W. Kurtz,[1] Michel Breger,[2] Simon J. Murphy[3,4] and Daniel L. Holdsworth[1]

[1]*Jeremiah Horrocks Institute, University of Central Lancashire, Preston PR1 2HE, UK*

[2]*Department of Astronomy, University of Texas, Austin, TX 78712, USA*

[3]*Sydney Institute for Astronomy (SIfA), School of Physics, The University of Sydney, NSW 2006, Australia*

[4]*Stellar Astrophysics Centre, Department of Physics and Astronomy, Aarhus University, Ny Munkegade 120, DK-8000 Aarhus C, Denmark*

ABSTRACT

We present the results of a search for amplitude modulation of pulsation modes in 983 δ Sct stars, which have effective temperatures between $6400 \leq T_{eff} \leq 10\,000$ K in the *Kepler* Input Catalogue and were continuously observed by the *Kepler Space Telescope* for 4 yr. We demonstrate the diversity in pulsational behaviour observed, in particular non-linearity, which is predicted for δ Sct stars. We analyse and discuss examples of δ Sct stars with constant amplitudes and phases; those that exhibit amplitude modulation caused by beating of close-frequency pulsation modes; those that exhibit pure amplitude modulation (with no associated phase variation); those that exhibit phase modulation caused by binarity; and those that exhibit amplitude modulation caused by non-linearity. Using models and examples of individual stars, we demonstrate that observations of the changes in amplitude and phase of pulsation modes can be used to distinguish among the different scenarios. We find that 603 δ Sct stars (61.3 per cent) exhibit at least one pulsation mode that varies significantly in amplitude over 4 yr. Conversely, many δ Sct stars have constant pulsation amplitudes so short-length observations can be used to determine precise frequencies, amplitudes and phases for the most coherent and periodic δ Sct stars. It is shown that amplitude modulation is not restricted to a small region on the HR diagram, therefore not necessarily dependent on stellar parameters such as T_{eff} or log g. Our catalogue of 983 δ Sct stars will be useful for comparisons to similar stars observed by K2 and TESS, because the length of the 4-yr *Kepler* data set will not be surpassed for some time.

Key words: asteroseismology – stars: oscillations – stars: variables: δ Scuti.

1 INTRODUCTION

Almost a century ago, Sir Arthur Eddington proposed that a star could act as a heat engine and become unstable to pulsation (Eddington 1917, 1926). For mono-periodic radial pulsators such as classical Cepheid variables and RR Lyrae stars (e.g. RRab stars using the classification of Bailey 1902), a piston-like driving mechanism in which layers of gas in the stellar atmosphere periodically expand and contract about an equilibrium point is relatively simple to envisage. Conversely, multiperiodic pulsators with many excited pulsation modes can be more complicated. The amplitude spectra of multiperiodic pulsators are often forest-like with a greater likelihood of mode interaction among the pulsation modes (e.g.

Chapellier et al. 2012). The reward of studying a multiperiodic pulsator is a greater insight into a star's interior, because different pulsation mode frequencies probe different depths within a star (e.g. Kurtz et al. 2014). The process of identifying and modelling pulsation mode frequencies is called asteroseismology, with an in-depth review given by Aerts, Christensen-Dalsgaard & Kurtz (2010).

1.1 Delta Sct stars

The multiperiodic pulsators known as delta Scuti (δ Sct) stars are the most common group of variable A and F stars, and are found at the intersection of the classical instability strip and main sequence on the Hertzsprung–Russell (HR) diagram. On the main-sequence, δ Sct stars typically range from A2 to F2 in spectral type (Rodríguez & Breger 2001) and within the effective temperature range of $6300 \leq T_{eff} \leq 8600$ K (Uytterhoeven et al. 2011). The δ Sct stars can

★E-mail: dmbowman@uclan.ac.uk

be considered intermediate-mass stars, as they lie in a transition-region from radiative cores and thick convective envelopes in low-mass stars ($M \lesssim 1\,\mathrm{M}_{\odot}$), to large convective cores and thin convective envelopes in high-mass stars ($M \gtrsim 2\,\mathrm{M}_{\odot}$). Concurrently, they also represent a transition from the high-amplitude radial pulsators, such as Cepheid variables, and the non-radial multiperiodic pulsators within the classical instability strip (Breger 2000a).

Pulsations in δ Sct stars are excited by the κ-mechanism operating in the He II ionization zone at $T \sim 50\,000$ K (Cox 1963; Chevalier 1971) producing low-order pressure (p) modes. Typical pulsation periods observed in δ Sct stars are of order a few hours (Breger 2000a), but can be as short as 15 min (Holdsworth et al. 2014). Hotter δ Sct stars generally have shorter pulsation periods (i.e. higher pulsation mode frequencies) than cooler δ Sct stars. Pulsational instability is a balance between driving and damping within a star; for example, the depth of the convective envelope is predicted to be large enough at the red edge of the classical instability strip to damp the δ Sct pulsations (Christensen-Dalsgaard 2000; Houdek 2000; Grigahcène et al. 2010). Thorough reviews of δ Sct stars are provided by Breger (2000a), Aerts et al. (2010) and Murphy (2014).

The evolutionary state of a star, specifically if it is near the zero-age main-sequence (ZAMS) or terminal-age main-sequence (TAMS), can influence its pulsational characteristics. The δ Sct stars are interesting as they lie on and beyond the main sequence and so experience large changes in their interiors in a relatively short period of time after the hydrogen in their cores is exhausted. Evolved stars often are observed to show a form of mode interaction called mixed modes, which are pulsation modes that exhibit gravity (g) mode characteristics near the core and p-mode characteristics near the surface (Osaki 1975). Mixed modes are often observed in evolved stars because the large density gradient outside the core couples the g- and p-mode pulsation cavities (e.g. Lenz et al. 2010). For a given T_{eff}, a more-evolved δ Sct star near the TAMS will generally have lower pulsation mode frequencies than its ZAMS counterpart.

Another strong influence on stellar pulsations is rotation. The Kraft Break (Kraft 1967) divides the main sequence into slowly rotating low-mass stars and fast-rotating high-mass stars, with the boundary occurring at approximately spectral type F5 ($M \simeq 1.3\,\mathrm{M}_{\odot}$). If the chemically peculiar Am and Ap stars are excluded, A and F stars lie above the Kraft Break and have typical values between $150 < v\sin i < 200$ km s^{-1} (Zorec & Royer 2012). From a high-resolution spectroscopic study of bright *Kepler* A and F stars, a mean $v\sin i$ value of 134 km s^{-1} was obtained by Niemczura et al. (2015). Therefore, δ Sct stars are generally considered moderate, and often, fast rotators (Breger 2000a). Rotation lifts the degeneracy of a non-radial ($\ell > 0$) pulsation mode into its $2\ell + 1$ components, which are observed as a multiplet with nearly exact splitting among its component frequencies (Pamyatnykh 2003).

The relationship between rotation and mode density is demonstrated by the high-amplitude δ Sct (HADS) stars. The HADS stars were first classified by McNamara (2000), who defined a sub-group of slowly rotating δ Sct stars with peak-to-peak light amplitude variations of more than 0.3 mag. These HADS stars have few pulsation mode frequencies in their amplitude spectra, with the dominant light variation usually being associated with the fundamental radial mode (McNamara 2000). The slow rotation seems to be a requirement for high-amplitude pulsations (Breger 2000a). The HADS stars are found in a very narrow region within the classical instability strip with effective temperatures between $7000 \leq T_{\mathrm{eff}} \leq 8000$ K (McNamara 2000), and offer an opportunity to study non-linearity in high-amplitude pulsations for which mode identification is rela-

tively simple. We explore the non-linearity of HADS stars observed by *Kepler* in Section 4.6.

1.2 Hybrid stars

Near the red edge of the classical instability strip and the main sequence on the HR diagram, is another group of variable stars called gamma Doradus (γ Dor) stars, which pulsate in high-order low-degree non-radial g modes driven by the convective flux blocking mechanism operating at the base of the convective zone (Guzik et al. 2000; Dupret et al. 2005). Typical g-mode pulsation frequencies in a γ Dor star lie between $0.3 < \nu < 3$ d^{-1} (Uytterhoeven et al. 2011). Reviews of γ Dor stars are provided by Balona, Krisciunas & Cousins (1994), Kaye et al. (2000) and Aerts et al. (2010).

The theoretical instability regions of the δ Sct and γ Dor stars have been shown to overlap on the HR diagram (Dupret et al. 2004). Hybrid pulsators from the δ Sct and γ Dor pulsational excitation mechanisms occurring simultaneously within a star were first predicted by Dupret et al. (2005), but only expected to comprise a small minority of A and F stars. The *Kepler* mission data revealed that many δ Sct stars are in fact hybrid pulsators (Balona 2011; Uytterhoeven et al. 2011), exhibiting both p and g modes. Although it is common for the amplitude spectra of δ Sct stars to contain low-frequency peaks, it is not established whether these frequencies are always caused by pulsation, the effects of rotation or have some other cause. Often low-frequency peaks in δ Sct stars can be associated with combination frequencies of high-frequency pulsation modes.

Understanding the multiperiodic hybrid stars is an exciting prospect for asteroseismology as one can gain insight into subsurface conditions, such as measurements of the rotation profile in main-sequence stars (Kurtz et al. 2014; Keen et al. 2015; Saio et al. 2015; Schmid et al. 2015; Triana et al. 2015; Murphy et al. 2016). Ideally, the hybrid stars could be used to study the pulsation excitation mechanisms directly, particularly the possible exchange of energy between pulsation modes excited by the different mechanisms. This idea was explored by Chapellier et al. (2012), who studied the interaction between 180 g-mode and 59 p-mode independent pulsation frequencies in the CoRoT hybrid star ID 105733033. The authors demonstrated that the p- and g-mode frequencies originated in the same star and that a coupling mechanism must exist to explain the observed mode interaction (Chapellier et al. 2012).

1.3 The *Kepler* mission

The *Kepler Space Telescope* has revolutionised our understanding of pulsating stars, including δ Sct and γ Dor stars (Uytterhoeven et al. 2011; Balona 2014). The *Kepler* spacecraft was launched in 2009 March into a 372.5-d Earth-trailing orbit with a primary goal to locate Earth-like exoplanets orbiting solar-like stars using the transit method (Borucki et al. 2010). A high photometric precision of order a few μmag, a high duty-cycle (Koch et al. 2010) and data spanning 1470.5 d (4 yr) for more than 150 000 stars, allow us to probe the structure of stars with a significantly higher precision than any ground-based telescope. Observations were made using a 29.5-min long cadence (LC) and 58.5-s short cadence (SC) (Gilliland et al. 2010).

Approximately 200 000 targets stars were observed by *Kepler*, many of which were characterized with values of T_{eff}, log g and [Fe/H] using *griz* and 2MASS *JHK* broad-band photometry prior to the launch of the telescope. These parameters were collated into the *Kepler* Input Catalogue (KIC; Brown et al. 2011) and allowed

stars to be placed on the HR diagram. Since the end of the nominal *Kepler* mission, Huber et al. (2014) revised the stellar parameters for the ∼200 000 *Kepler* targets and concluded that a colour-dependent offset exists compared to other sources of photometry (e.g. Sloan). This resulted in KIC temperatures for stars hotter than $T_{\text{eff}} > 6500$ K being, on average, 200 K lower than temperatures obtained from Sloan photometry or the infrared flux method (Pinsonneault et al. 2012). Also, log *g* values for hot stars were overestimated by up to 0.2 dex. Huber et al. (2014) stresses that the log *g* and [Fe/H] values and their respective uncertainties should not be used for a detailed analysis on a star-by-star basis, as they are only accurate in a statistical sense.

The 4-yr *Kepler* observations provide a Rayleigh resolution criterion in frequency of $1/\Delta T = 0.000\,68$ d^{-1} (8 nHz). Using signal-to-noise ratios of the most stable frequencies, an amplitude precision of 1 μmag is achievable with *Kepler* data (Kurtz et al. 2014). This unprecedented frequency and amplitude precision has been utilized to study frequency and amplitude modulation in δ Sct stars (e.g. Bowman & Kurtz 2014; Barceló Forteza et al. 2015; Bowman, Holdsworth & Kurtz 2015). In this paper, we extend the search for amplitude modulation to a large number of δ Sct stars observed by the *Kepler* mission, and use case studies to demonstrate how to distinguish among different physical causes.

In this paper we discuss the various causes of amplitude modulation in Section 2 and our method of identifying the δ Sct stars in our ensemble that exhibit amplitude modulation in Section 3. We present our catalogue of δ Sct stars and demonstrate the diversity in pulsational behaviour using case studies of individual stars in Section 4. We discuss beating models in Section 5 and coupling models in Section 6. Finally, we discuss statistics from the ensemble study in Section 7 and our conclusions in Section 8.

2 CAUSES OF AMPLITUDE MODULATION

The various causes of why δ Sct stars exhibit variable pulsation amplitudes (and/or frequencies) can be loosely grouped as intrinsic and extrinsic, i.e. those physical and interior to the star and those caused by external effects, respectively. In the following subsections, we discuss examples of the different mechanisms that can cause variable pulsation amplitudes and/or frequencies.

2.1 Intrinsic: beating

A study of seven well-known δ Sct stars by Breger & Bischof (2002) found that pairs of close-frequency pulsation modes, with spacings less than 0.01 d^{-1}, were not uncommon. Moreover, these pairs of close-frequency modes were found near the expected frequencies of radial modes in these stars (Breger & Bischof 2002). Such close-frequency pulsation modes are unlikely to be explained by rotational effects as most δ Sct stars are fast rotators. For example, even the slowly rotating δ Sct star 44 Tau (HD 26322) with $v \sin i = 3 \pm 2$ km s^{-1} (Zima et al. 2006) would produce a rotational splitting of approximately 0.02 d^{-1} (Breger, Lenz & Pamyatnykh 2009). The study by Breger & Bischof (2002), however, only included a small sample of δ Sct stars limited by the frequency precision obtained from intermittent ground-based data spanning a few decades.

Later, it was shown that pulsation mode frequencies in δ Sct stars are not distributed at random, and that many non-radial modes had frequencies near radial mode frequencies (Breger et al. 2009). These regularities in the amplitude spectra were explained by mode trapping in the stellar envelope (Dziembowski & Krolikowska 1990), which was clearly demonstrated as the cause of regularities in the

amplitude spectrum of the δ Sct star FG Vir (HD 106384) by Breger et al. (2009).

The variability of the δ Sct star 4 CVn (HD 107904) was first discovered by Jones & Haslam (1966), and the star has been extensively studied since, with 26 independent pulsation mode frequencies and many more combination frequencies discovered (Breger et al. 1990, 1999; Breger 2000b, 2009, 2016; Schmid et al. 2014). This makes it one of the longest- and best-studied δ Sct stars. Many of the pulsation mode frequencies show frequency and amplitude variations, some of which can be explained by a mode coupling mechanism (Breger 2000b) or the beating of two close frequencies (Breger 2009). The two pulsation mode frequencies, 6.1007 d^{-1} and 6.1170 d^{-1}, were highly variable in amplitude over the observations (Breger 2010). The changes in frequency and amplitude of these two pulsation mode frequencies were used to construct beating models, which were matched to the observations of amplitude modulation in 4 CVn (Breger 2010).

These investigations of δ Sct stars may not contain a large number of stars, but they do demonstrate the diverse pulsational behaviour. In our study, we use the definition from Breger & Bischof (2002) of close frequencies having a separation of less than 0.01 d^{-1}. We emphasize that it is only studying the *changes* in amplitude and frequency (i.e. phase at fixed frequency) of pulsation modes that allows one to construct beating models of close-frequency pulsation modes and pure amplitude modulation of a single pulsation mode (Breger & Bischof 2002). This cannot be achieved from simple inspection of the light curve or amplitude spectrum of a pulsating star, regardless of the data precision, because the convolved amplitude and frequency modulation signals cannot be disentangled.

The beating of a pair of close and resolved pulsation mode frequencies appears as periodic amplitude modulation, with a characteristic sharp change in phase at the epoch of minimum amplitude for each frequency in the pair (e.g. Breger & Pamyatnykh 2006). The simplest scenario is the example of two similar frequency cosinusoids with equal amplitude, each of the form

$$y = A \cos(2\pi\nu t + \phi), \tag{1}$$

where A is the amplitude, ν is the frequency and ϕ is the phase. Using the sum rule in trigonometry for two equal-amplitude cosinusoids with frequencies ν_1 and ν_2, each with a phase of 0.0 rad, a summation is given by

$$
\begin{aligned}
y_1 + y_2 &= A \cos 2\pi\nu_1 t + A \cos 2\pi\nu_2 t \\
&= 2A \cos 2\pi \frac{\nu_1 + \nu_2}{2} t \cos 2\pi \frac{\nu_1 - \nu_2}{2} t,
\end{aligned} \tag{2}
$$

from which, the beat frequency is defined by

$$\nu_{\text{beat}} = |\nu_1 - \nu_2|, \tag{3}$$

which is the absolute difference in frequency of the two cosinusoids.

The characteristic behaviour of beating is most easily recognized with two cosinusoids of equal amplitude. In such a case the visible (and assumed single) frequency will vary sinusoidally in amplitude with a period equal to the beat period, but also vary in phase: a half cycle (i.e. π rad) change in phase will occur at the epoch of minimum amplitude (Breger & Pamyatnykh 2006), and the amplitude will modulate between 2A and 0. If the cosinusoids have increasingly different amplitudes, the amplitude and phase changes get progressively smaller. However, the amplitude and phase must always vary synchronously with a phase lag (shift) close to π/2 rad, such that the epoch of minimum amplitude in the beat cycle occurs at the time of average and most rapid change in phase (Breger &

Pamyatnykh 2006). We construct beating models for δ Sct stars observed by *Kepler* in Section 5.

2.2 Intrinsic: non-linearity and mode coupling

There are different non-linear effects that can create combination frequencies in the amplitude spectrum of a pulsating star. Combination frequencies are mathematical sum and difference frequencies of pulsation mode frequencies, ν_i and ν_j, that have the form $n\nu_i \pm m\nu_j$, in which n and m are integers. Possible mechanisms to explain combination frequencies in variable DA and DB white dwarfs discussed by Brickhill (1992) were that the stellar medium does not respond linearly to the pulsation wave, or that the dependence of emergent flux variation is not a linear transformation from the temperature variation ($F = \sigma T^4$), which are often grouped into what is termed a non-linear distortion model (e.g. Degroote et al. 2009).

Combination frequencies are common in δ Sct stars, for example KIC 11754974 (Murphy et al. 2013b) and KIC 8054146 (Breger et al. 2012b; Breger & Montgomery 2014), but also in SPB, Be and γ Dor stars (Kurtz et al. 2015; Van Reeth et al. 2015). Identifying which peaks are combination frequencies and which are real pulsation mode frequencies is important, so that the amplitude spectra of pulsating stars can be greatly simplified (e.g. Pápics 2012; Kurtz et al. 2015); the real pulsation mode frequencies are the main parameters used for asteroseismic modelling. One method of identifying combination frequencies is by mathematically generating all the possible combination terms from a small number of parent frequencies, fitting them by least-squares and removing them by pre-whitening. Alternatively, iterative pre-whitening can be used to extract all statistically-significant frequencies and then exclude those that satisfy a combination frequency relation (e.g. Van Reeth et al. 2015). However, the physical mechanism that causes these frequencies is not immediately obvious.

At this juncture, it is important to note that there is a subtle difference between combination frequencies and coupled frequencies. Combination frequencies and harmonics occur due to the mathematical representation of the summation of sine and cosine terms when calculating the Fourier transform caused by pulsational non-linearity. This effect differs to families of pulsation mode frequencies that are resonantly excited due to the coupling of modes inside the star (e.g. Breger & Montgomery 2014). Mode coupling through the resonant interaction of pulsation modes has been discussed theoretically in detail by Dziembowski (1982) and Buchler, Goupil & Hansen (1997). This form of pulsational non-linearity gives rise to variable frequencies and amplitudes in pulsation modes over time (Buchler et al. 1997), which will appear as a cluster of unresolved peaks in the amplitude spectrum if the length of observations is shorter than the modulation cycle. From the unresolved behaviour, it is difficult to determine if a cluster of peaks represents a single pulsation mode with frequency and/or amplitude variability, or multiple independent close-frequency pulsation modes.

Theoretical models of δ Sct stars often predict much larger pulsation mode amplitudes than are observed, which suggests that an amplitude limitation mechanism or limit cycle is required (Breger 2000a). An example of how non-linearity can act as an amplitude limitation mechanism in δ Sct stars is the parametric resonance instability (Dziembowski 1982), which states that two linearly unstable low-frequency modes (i.e. parent modes) can damp a high-frequency unstable mode (i.e. child mode) once it reaches a critical amplitude. Resonant mode coupling has been suggested as the amplitude limitation mechanism operating in δ Sct stars but not in HADS stars, which explains the large difference in pulsa-

tion mode amplitudes between the two subgroups (Dziembowski & Krolikowska 1985).

Coupled frequencies are grouped into families of child and parent modes (e.g. Breger & Montgomery 2014), and this coupling can facilitate the exchange of energy between different members of the family (Dziembowski 1982; Buchler et al. 1997; Nowakowski 2005). Coupled child and parent modes must satisfy the resonance condition of

$$\nu_1 \simeq \nu_2 \pm \nu_3, \tag{4}$$

where ν_1 is the child mode, and ν_2 and ν_3 are the parent modes. The δ Sct star KIC 8054146 was found to exhibit several families of pulsation modes (Breger et al. 2012a), some of which were later suggested to be caused by resonant mode coupling (Breger & Montgomery 2014). The authors commented that it is difficult to distinguish physically coupled modes from combination frequencies, emphasizing the need to study the frequency, amplitude and phase of the members within each family.

However, the frequency resonance criterion given in equation (4) does not solely distinguish which frequency within a family is a combination or coupled mode frequency of the other two. To make this distinction, Breger & Montgomery (2014) modelled the amplitude of a child mode as a product of the two parent mode amplitudes using

$$A_1 = \mu_c(A_2 A_3), \tag{5}$$

and the linear combination of the parent phases

$$\phi_1 = \phi_2 \pm \phi_3, \tag{6}$$

where A_i and ϕ_i represent amplitude and phase of the child and parent modes, respectively, and μ_c is defined as the coupling factor. For combination frequencies arising from a non-linear distortion model, small values of μ_c are expected and thus the amplitude and/or phase variability in combination frequencies will simply mimic the parent modes that produce them (Brickhill 1992; Wu 2001; Breger & Lenz 2008). However, for resonant mode coupling, one expects the amplitudes of the three modes to be similar and values of μ_c to be larger because mode energy is physically being exchanged between the child and parent modes. In the case of KIC 8054146, μ_c was of the order 1000 for coupled modes for parent mode amplitudes of order 0.1 mmag (Breger & Montgomery 2014).

For the case of resonant mode coupling discussed by Dziembowski & Krolikowska (1985), the most likely outcome in δ Sct stars is two linearly damped g-mode parents coupling with an unstable p-mode child. The coupling of these modes would cause the growth and decay of the child p mode in anti-correlation with the parent modes, as energy is exchanged among the family members (Dziembowski & Krolikowska 1985). Furthermore, the parent g modes may not be excited to observable amplitudes at the surface of the star and are thus undetectable. This was suggested as a plausible mechanism for the observed amplitude modulation in the δ Sct star KIC 7106205 by Bowman & Kurtz (2014), who showed that a single p-mode frequency decreased significantly in amplitude over 4 yr with no change in amplitude or phase in any other visible pulsation mode. Further work by Bowman et al. (2015) extended this study back to 2007 using archive data from the Wide Angle Search for Planets (WASP; Pollacco et al. 2006). It is possible that the observed amplitude modulation in KIC 7106205 could be caused by an amplitude limitation mechanism, i.e. resonant mode coupling, transferring energy from the child p mode to undetectable parent g modes in the core of the star; otherwise, the p-mode pulsation energy was lost to an unknown damping region. It was concluded

for the case of KIC 7106205 that the visible pulsation energy was not conserved (Bowman & Kurtz 2014).

In their analysis of KIC 8054146, Breger et al. (2012b) stated that even if three frequencies within a family obey the frequency, amplitude and phase relations outlined in equations (4)–(6), it does not *prove* that they are combination frequencies, but merely behave like combination frequencies, thus variable modes can be interpreted as being caused by non-linearity from a non-linear distortion model or resonant mode coupling. The coupling coefficient μ_c in equation (5) represents the *strength* of non-linearity in a star and thus how much coupling exists among the different members within a family. Therefore, the testable prediction for resonant mode coupling between a child and two parent modes in δ Sct stars is large-scale amplitude modulation in three similar-amplitude modes with large values of μ_c (Breger & Montgomery 2014). Using a similar approach, we test the coupling hypothesis in Section 6 for the δ Sct star KIC 4733344, which contains families of pulsation modes satisfying equations (4)–(6).

2.3 Extrinsic: binarity and multiple systems

A spectroscopic study of 4 CVn by Schmid et al. (2014) revealed that it is in an eccentric binary with $P_{\rm orb} = 124.44 \pm 0.03$ d and $e = 0.311 \pm 0.003$. After removing the binary signature, further amplitude and phase variability on time-scales of the order 1 yr remained in pulsation modes. This variability could not be explained by the beating of two (or more) close-frequency modes, because the beating cycle was unresolved in the length of the observations (Schmid et al. 2014).

Binarity in a system can also be tested with photometric data using the Frequency Modulation technique (FM; Shibahashi & Kurtz 2012; Shibahashi, Kurtz & Murphy 2015) and the Phase Modulation technique (PM; Murphy et al. 2014; Murphy & Shibahashi 2015). The FM technique uses the fact that the motion of a pulsating star about the Barycentre of a binary (or multiple) system will perturb a pulsation mode frequency throughout the orbit and introduce a small frequency shift. If observations are longer than the orbital period, then the perturbation on a pulsation mode frequency is resolved and produces sidelobes on either side of the pulsation mode frequency in the amplitude spectrum (Shibahashi & Kurtz 2012). The orbital period, can be directly measured as the inverse of the separation in frequency between the central peak and the sidelobes of a multiplet in the amplitude spectrum.

Similarly, the PM technique uses the fact that there will be a difference in the light travel time across the orbit in a multiple system and thus the phases of pulsation modes will vary on the same time-scale as the orbit (Murphy et al. 2014). The amplitude of the observed phase modulation is a function of frequency when expressed as light travel time delays (see equation 3 from Murphy et al. 2014). If all the pulsation modes in a star vary in phase with the same period, this can be explained by the Doppler effect modulating the signal throughout the orbital period (Murphy et al. 2014). The significance of the FM and PM techniques is made evident as not only can the orbital period be determined, but also e, $a \sin i$, $f(m)$ and argument of periastron without obtaining radial velocity measurements. An excellent example of the PM technique used to study hybrid pulsators using *Kepler* data was that of Schmid et al. (2015) and Keen et al. (2015), who demonstrated that KIC 10080943 is an eccentric binary system containing two hybrid pulsators with masses $M_1 = 2.0 \pm 0.1$ M$_\odot$ and $M_2 = 1.9 \pm 0.1$ M$_\odot$. From the common phase modulation, Schmid et al. (2015) were able to identify which pulsa-

tion modes originated from each hybrid star and confirm the orbital period of $P_{\rm orb} = 15.3364 \pm 0.0003$ d for KIC 10080943.

3 METHOD

To study amplitude modulation using a statistical ensemble, the time series for all *Kepler* targets with effective temperatures between $6400 \leq T_{\rm eff} \leq 10\,000$ K in the KIC (Brown et al. 2011) were downloaded. We used the publicly available (msMAP) PDC data (Stumpe et al. 2012; Smith et al. 2012), which can be downloaded from the Mikulski Archive for Space Telescopes (MAST).[1] The extracted time series were stored locally in the format of reduced Barycentric Julian Date (BJD $- 2\,400\,000$) and magnitudes, which were normalized to be zero in the mean, for each quarter of LC and month of SC data. Amplitude spectra for each quarter of LC data were calculated using the methodology described by Deeming (1975), which produced a data catalogue for all of the $\sim$10 400 stars in this $T_{\rm eff}$ range.

3.1 Creating an amplitude modulation catalogue

To maximize the outputs from this study, the final ensemble of stars comprised the targets that met *all* of the following criteria.

(i) Characterized by $6400 \leq T_{\rm eff} \leq 10\,000$ K in the KIC;
(ii) Observed continuously in LC from Q0 (or Q1) to Q17;
(iii) Contain peaks in the amplitude spectrum in the sub-Nyquist p-mode frequency regime ($4 \leq \nu \leq 24$ d^{-1}) with amplitudes greater than 0.10 mmag;

which resulted in 983 δ Sct and hybrid stars. In the following paragraphs, we justify the motivation for each of these criteria.

We chose the lower $T_{\rm eff}$ limit of 6400 K for our search for amplitude modulation, because this is the observational red edge of the classical instability strip for δ Sct stars (Rodríguez & Breger 2001). The ZAMS red edge was calculated to be approximately 6900 K by Dupret et al. (2004), but cooler high-luminosity δ Sct stars are found below 6900 K and so we chose a lower limit of 6400 K to include these targets. Only about 10 δ Sct stars were found in the KIC effective temperature range of $6400 \leq T_{\rm eff} \leq 6500$, supporting the observational red edge defined by Rodríguez & Breger (2001). An upper limit of $T_{\rm eff} \leq 10\,000$ K was chosen to exclude pulsators that do not lie within the classical instability strip, such as SPB and β Cep stars (e.g. see Balona et al. 2011; McNamara, Jackiewicz & McKeever 2012).

We chose to use LC data as this gives the largest number of stars in our ensemble observed over the largest possible time span of 4 yr. Only a small fraction of intermediate (and high) mass stars were observed in SC and even fewer for many consecutive SC months. We do not include any δ Sct stars that lie on module 3 because of the lower duty-cycle. Module 3 of the *Kepler* CCD failed during the 4-yr mission, thus these stars have every fourth data quarter missing in their light curves and have complex window patterns in their amplitude spectra. This choice is motivated by previously studied δ Sct stars that have amplitude modulation of the order of years and decades (Breger et al. 1999; Breger 2000b, 2016), and so complete data coverage over the maximum of 4 yr is most useful.

We selected stars that contain pulsation mode frequencies within $4 \leq \nu \leq 24$ d^{-1}, because the LC Nyquist frequency is

[1] MAST website: http://archive.stsci.edu/kepler/

$\nu_{\rm Nyq} = 24.4$ d^{-1}. Even though δ Sct stars can pulsate at higher frequencies than $\nu_{\rm Nyq}$ (e.g. Holdsworth et al. 2014), we made this selection because alias peaks are subject to frequency (phase) variations and amplitude suppression (Murphy, Shibahashi & Kurtz 2013a). *Kepler* data were sampled at a regular cadence on board the spacecraft, but Barycentric time stamp corrections were made resulting in a non-constant cadence. Therefore, real and alias frequencies can be identified without the need to calculate an amplitude spectrum beyond the LC Nyquist frequency. Note that if a star pulsates with frequencies that lie above and below the LC Nyquist frequency, it was included in our sample as some of its extracted frequencies will not be super-Nyquist aliases. We chose an amplitude cut-off of 0.10 mmag, which is much higher than the typical noise level in *Kepler* data of order a few μmag. This choice is so that reasonable phase uncertainties are generated as they are dependent on the amplitude signal-to-noise ratio (Montgomery & O'Donoghue 1999).

3.2 Identifying pulsation modes with variable amplitudes

After identifying the ensemble of 983 δ Sct stars for this project, an automated tracking routine was used to determine amplitude and phase variations (at fixed frequency) for the 12 highest amplitude peaks in the amplitude spectrum using the 4-yr data set for each star. The choice of tracking specifically 12 peaks is somewhat arbitrary. The main motivation was to identify the dominant (changes in) pulsational behaviour in δ Sct stars. For a star that pulsates in only a few modes, extracting 12 peaks was more than sufficient. On the other hand, for a star that pulsates in dozens of modes and has hundreds of combination frequencies in its amplitude spectrum, 12 frequencies may not be enough to fully disentangle the star, but does provide vital information on the most dominant behaviour. Note that only peaks with amplitudes greater than 0.10 mmag were extracted in our analysis, so fewer than the maximum number of 12 frequencies can be extracted for a star.

After extracting the appropriate number of frequencies by sequentially pre-whitening a star's amplitude spectrum, the frequencies were optimized using a simultaneous multifrequency non-linear least-squares fit to the 4-yr data set, ensuring the highest possible frequency and amplitude precision were obtained. We then divided the data set into 30 time bins, each 100 d in length (except the last bin) with a 50-d overlap, and optimized amplitude and phase at fixed frequency using linear least-squares in each bin for each frequency. This approach has previously been used to study the amplitude and phase variability in the δ Sct star KIC 7106205 (Bowman & Kurtz 2014). The amplitudes and phases of each time bin for the frequencies were plotted against time in what we term tracking plots, which allowed us to investigate similar variability in different frequencies within each star.

3.3 Defining significant amplitude modulation

Classifying a significant change in amplitude for each frequency in each star by visual inspection is straightforward, but time consuming for a large sample. Therefore we automated this process using the following methodology. A mean amplitude was calculated from the time bins[2] for each frequency and any bins that were more than $\pm 5\sigma$ in amplitude away from this mean were flagged. An example of this is shown in Fig. 1 using a solid line as the mean value and dashed lines as the $\pm 5\sigma$ significance interval, for the three highest

---

[2] For clarity, the last time bin is often excluded from the tracking plots, as it contains fewer data points.
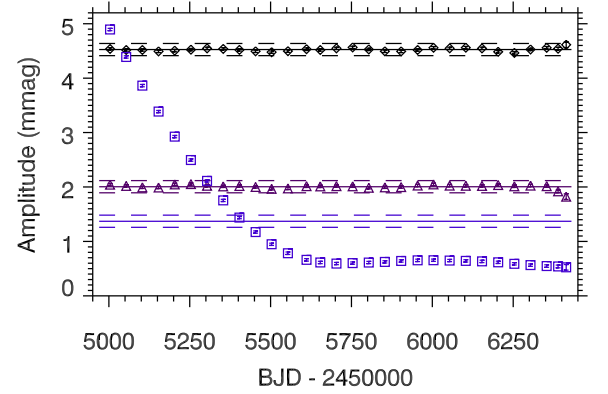

Figure 1. Amplitude tracking plot for KIC 7106205 showing pulsation mode frequencies $\nu_1 = 10.032\,366$ d^{-1}, $\nu_2 = 10.727\,317$ d^{-1} and $\nu_3 = 13.394\,175$ d^{-1} as diamonds, triangles and squares, respectively. The solid line for each frequency is the mean of 30 time bins and the dashed lines represent the $\pm 5\sigma$ amplitude significance interval from the mean. A frequency is flagged as exhibiting significant amplitude modulation if 15 (half) of its bins lie outside the $\pm 5\sigma$ amplitude from the mean.

amplitude pulsation modes in KIC 7106205. We chose to define a frequency as exhibiting *significant* amplitude modulation if at least 15 (i.e half) of its amplitude bins were more than $\pm 5\sigma$ from its mean value. For example, only $\nu_3 = 13.394\,175$ d^{-1} in KIC 7106205 satisfied the significant amplitude modulation criterion described, which is shown in Fig. 1. All other frequencies were flagged as having constant amplitudes.

This method was applied to each of the extracted frequencies and the number of amplitude-modulated peaks was noted for each star in our ensemble. We use the abbreviations of AMod (Amplitude Modulated) to describe the δ Sct stars that exhibit at least a single pulsation mode that is variable in amplitude over the 4-yr *Kepler* data set, and NoMod (No Modulation) for those that do not.

3.4 Phase adjustment

For the purpose of calculating phases in the tracking plots, a zero-point in time was chosen as the centre of the 4-yr *Kepler* data set, specifically $t_0 = 2455\,688.770$ BJD, in the cosinusoid function $y = A\cos(2\pi\nu(t - t_0) + \phi)$. Phase is defined in the interval $-\pi \leq \phi \leq \pi$ rad, and so can be adjusted by adding or subtracting integer values of 2π rad. If the difference between consecutive phase bins exceeded 5 rad in a tracking plot, then a 2π rad phase adjustment was made. As previously discussed in Section 2.1, the phase change for beating cannot exceed π rad so this phase adjustment did not remove any beating signals in pulsation mode frequencies.

3.5 Pulsation mode identification

For high-amplitude pulsators, the period ratios of pulsation modes can be used to identify modes. The period ratio of the first overtone to fundamental mode for δ Sct stars is between $P_1/P_0 = (0.756 - 0.787)$, and subsequent ratios of $P_2/P_0 = (0.611 - 0.632)$ and $P_3/P_0 = (0.500 - 0.525)$ for the second and third overtones, respectively (Stellingwerf 1979).

Pulsation modes can also be identified by calculating pulsation constants using

$$Q = P\sqrt{\frac{\bar{\rho}}{\bar{\rho}_\odot}}, \tag{7}$$

where Q is the pulsation constant in days, P is the pulsation period in days, and $\bar{\rho}$ is the mean stellar density. Equation (7) can be re-written as

$$\log Q = \log P + \frac{1}{2}\log g + \frac{1}{10}M_{\text{Bol}} + \log T_{\text{eff}} - 6.454, \qquad (8)$$

where $\log g$ is the surface gravity in cgs units, M_{Bol} is the Bolometric absolute magnitude and T_{eff} is the effective temperature in K. A value of M_{Bol} can be calculated using T_{eff} and $\log g$ values in comparison with the Pleiades main-sequence stars. Typical values of pulsation constants for the fundamental, first and second-overtone radial p modes in δ Sct stars lie between $0.022 \leq Q \leq 0.033$ d (Breger & Bregman 1975). The pulsation constant can be used to identify the order (overtone number, n) of radial modes (Stellingwerf 1979), but the calculation using equation (8) is dependent on the stellar parameters used, particularly $\log g$. For example, Breger (1990) quotes fractional uncertainties in Q values as high as 18 per cent, which could cause a first overtone radial mode to be confused for the fundamental or second overtone radial mode. Therefore, caution is advised when applying this method of mode identification.

4 CATALOGUE DISCUSSION

The analysis of 983 δ Sct stars have been collated into a single catalogue.[3] In the following subsections, individual stars are used as case studies to demonstrate the diversity of pulsational behaviour in δ Sct stars. For each star presented in this paper, Table 1 lists the stellar parameters from Huber et al. (2014), the number of AMod and NoMod frequencies, and the pulsator type as either δ Sct or hybrid based on its frequencies.

4.1 Super-Nyquist asteroseismology

To demonstrate the super-Nyquist asteroseismology (sNa) technique described by Murphy et al. (2013a), we have applied our amplitude and phase tracking method to a real frequency peak and its super-Nyquist alias in the HADS star KIC 5950759. This HADS star acts as a useful example because of the high S/N in its pulsation mode frequencies and because simultaneous LC and SC are available. The LC and SC amplitude spectra for KIC 5950759 are given in the left-hand panel of Fig. 2, which contain the fundamental radial mode at $\nu_1 = 14.221\,372$ d^{-1}, and its harmonic $2\nu_{1,\,r} = 28.442\,744$ d^{-1} labelled with 'r', which lies above the LC Nyquist frequency indicated by a vertical dashed line. The alias of the harmonic $\nu_{1,\,a} = 20.496203$ d^{-1} is labelled 'a'. The middle panel in Fig. 2 shows a zoom-in of the amplitude spectrum using LC data, showing the multiplet structure split by the *Kepler* satellite's orbital frequency of the alias peak in the top panel, compared to the real peak shown below for comparison.

The right-hand panel of Fig. 2 shows the results of the tracking method for the real and alias harmonics of the fundamental radial mode frequency. The alias peak experiences phase modulation with a peak-to-peak amplitude of approximately $\pi/2$ rad and a period equal to the *Kepler* satellite orbital period (372.5 d). The Barycentric correction to the data time stamps creates a variable Nyquist frequency. The reflection of a peak across the variable Nyquist frequency causes a variable alias peak with sidelobes split

by the *Kepler* orbital frequency and reduced central peak amplitude (Murphy et al. 2013a). The example of KIC 5950759 in Fig. 2 acts as a useful case study for other stars with sNa peaks that are extracted using the method described in Section 3. Aliases of real frequencies are easily identified from the 372.5-d periodic phase modulation (see also, fig. 2 from Murphy et al. 2014). Frequencies identified as super-Nyquist aliases are labelled as sNa in figure captions and in Table 1.

4.2 Constant amplitudes and phases: NoMod stars

There are 380 δ Sct stars that have been classified as NoMod stars within our ensemble, thus 38.7 per cent of stars exhibit little or no change in their pulsation mode amplitudes. This subset supports the view that δ Sct stars are coherent and periodic pulsators. Four examples of NoMod δ Sct stars that exhibit constant-amplitude and constant-phase pulsation modes are shown in Fig. 3.

The δ Sct star KIC 2304168 was studied by Balona & Dziembowski (2011), who used a subset of *Kepler* data and asteroseismic modelling to identify the two principal pulsation mode frequencies (which they term $f_1 = 8.1055$ d^{-1} and $f_2 = 10.4931$ d^{-1}) as the fundamental and first overtone radial modes, respectively. With a much longer data set available, we have re-analysed this star and calculated that the period ratio from 4 yr of *Kepler* data for $\nu_1 = 8.107\,739$ d^{-1} and $\nu_2 = 10.495495$ d^{-1} is 0.7725, which is typically associated with the ratio of the first overtone and fundamental radial modes. We calculate pulsation constants for ν_1 and ν_2 as 0.028 and 0.022, respectively, which are consistent with the mode identification by Balona & Dziembowski (2011) considering the typical uncertainties discussed by Breger (1990). The first harmonic of ν_1 is also present with significant amplitude, labelled as ν_6 in the second row of Fig. 3. KIC 2304168 is an excellent example of a NoMod δ Sct star, as its amplitude spectrum has low mode density and mode identification is possible, but most importantly, all pulsation mode frequencies in its amplitude spectrum are completely stable over 4 yr. This raises the question: for stars of similar T_{eff}, $\log g$ and [Fe/H], what mechanism is driving amplitude modulation and non-linearity in some δ Sct stars, yet is absent in others?

4.3 Amplitude and phase modulation due to beating of close-frequency modes

We find two δ Sct stars in our ensemble, KIC 4641555 and KIC 8246833, that are AMod from the beating of pulsation modes spaced closer than 0.001 d^{-1}. This emphasises the superiority of *Kepler* data purely because of the length: 4 yr is only just long enough to resolve these pulsation mode frequencies. The amplitude spectra and tracking plots for KIC 4641555 and KIC 8246833 are shown in the left and right columns of Fig. 4, respectively. We discuss how beating models of close-frequency pulsation modes can be used to distinguish between pure amplitude modulation and beating in Section 5.

4.4 Pure amplitude modulation with no phase variability

In this subsection, we present four examples of δ Sct stars that exhibit amplitude modulation with no change in phase in at least one pulsation mode. This pure form of amplitude modulation is unlikely to be caused by beating of unresolved pulsation modes or mode coupling because no phase modulation is observed, which is required by both mechanisms. This subgroup contains perhaps the most interesting δ Sct stars, with no obvious selection effect that

---

[3] The amplitude modulation catalogue containing the amplitude spectra and tracking plots of all 983 δ Sct stars can be obtained from http://uclandata.uclan.ac.uk/id/eprint/42 as a PDF.

Table 1. Stellar parameters for the δ Sct stars discussed in this paper, as listed in Huber et al. (2014). For each star, the number of constant-amplitude and variable-amplitude pulsation mode frequencies, N_ν, above our amplitude cut-off of 0.10 mmag are listed under the columns NoMod and AMod, respectively. Super-Nyquist alias peaks are identified using sNa. Orbital periods obtained using the PM technique (Murphy et al. 2014) are consistent with the phase modulation in the four example stars identified as binary systems. Each star is labelled as either a δ Sct or a hybrid in the pulsator type column based on its frequencies. A version of this table for all 983 stars is given as online-only material as a PDF, with a machine-readable version available through CDS.

| KIC ID	$T_{\rm eff}$ (K)	log g (cgs)	[Fe/H] (dex)	Kp (mag)	Pulsator type	N_ν NoMod	AMod	Comments
NoMod (constant amplitude) stars:								
1718594	7800 ± 270	3.97 ± 0.22	0.07 ± 0.30	10.37	δ Sct	8	0	ν_4 is sNa
2304168	7220 ± 270	3.67 ± 0.19	-0.06 ± 0.30	12.41	δ Sct	11	0	Balona & Dziembowski (2011)
6613627	7310 ± 280	4.14 ± 0.24	-0.02 ± 0.31	12.55	δ Sct	5	0	
9353572	7420 ± 280	3.95 ± 0.21	-0.40 ± 0.31	10.62	δ Sct	5	0	
AMod explainable by the beating of close-frequency pulsation modes:								
4641555	7170 ± 250	4.22 ± 0.25	-0.12 ± 0.32	12.61	δ Sct	8	1	$P_{\rm beat} = 1166 \pm 1$ d
8246833	7330 ± 270	3.96 ± 0.22	-0.32 ± 0.30	11.87	δ Sct	9	3	$P_{\rm beat} = 1002 \pm 1$ d
AMod explainable by non-linearity:								
4733344	7210 ± 260	3.50 ± 0.23	-0.12 ± 0.28	10.08	hybrid	3	9	
Stars with pure AMod:								
2303365	7520 ± 270	3.64 ± 0.18	0.00 ± 0.28	11.14	δ Sct	10	2	ν_{10} has a ~250-d beat signal
5476273	7430 ± 280	4.17 ± 0.23	-0.22 ± 0.35	13.62	δ Sct	11	1	ν_9 is sNa
7685307	7690 ± 280	3.80 ± 0.20	-0.20 ± 0.31	12.14	δ Sct	5	2	
8453431	7180 ± 270	3.63 ± 0.19	-0.06 ± 0.29	12.53	δ Sct	2	1	
Stars with phase modulation explainable by binarity and confirmed using the PM technique:								
3650057	7320 ± 280	4.06 ± 0.22	-0.10 ± 0.32	13.92	δ Sct	9	3	$P_{\rm orb} = 804.6 \pm 2.0$ d
4456107	7250 ± 280	4.08 ± 0.24	0.06 ± 0.28	13.83	δ Sct	11	1	$P_{\rm orb} = 335.5 \pm 0.5$ d
5647514	7410 ± 280	4.13 ± 0.23	-0.04 ± 0.32	12.43	δ Sct	10	2	$P_{\rm orb} = 1123 \pm 6$ d
9651065	7010 ± 150	3.83 ± 0.13	-0.10 ± 0.15	11.07	hybrid	12	0	$P_{\rm orb} = 272.7 \pm 0.8$ d
HADS stars:								
5950759	8040 ± 270	4.05 ± 0.22	-0.10 ± 0.33	13.96	HADS	2	10	$\nu_{4, 6, 9, 10, 12}$ are sNa
9408694	6810 ± 140	3.78 ± 0.11	-0.08 ± 0.15	11.46	HADS	7	5	Balona et al. (2012)
Other special cases:								
7106205	6900 ± 140	3.70 ± 0.13	0.32 ± 0.13	11.46	δ Sct	8	1	Bowman & Kurtz (2014)
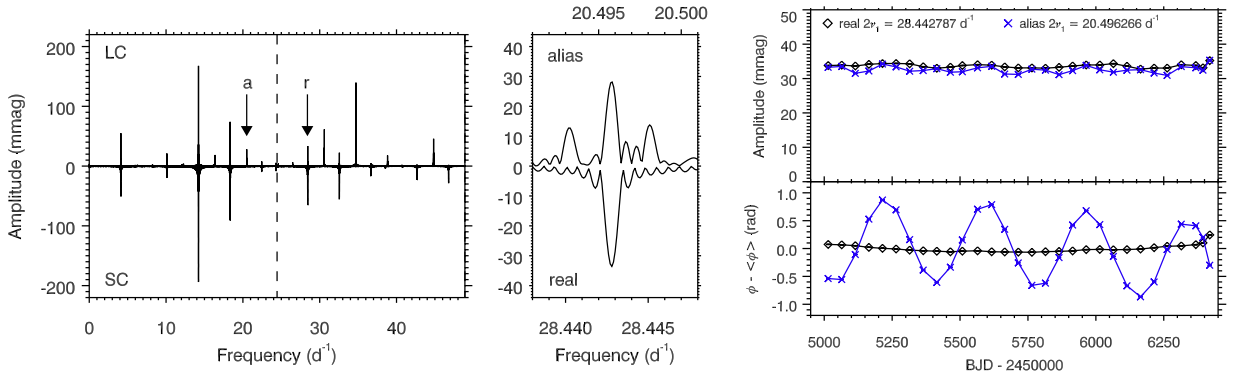
Figure 2. Demonstration of super-Nyquist asteroseismology with the HADS star KIC 5950759. Real and alias peaks associated with the harmonic of the fundamental radial mode are marked by 'r' and 'a', respectively, in the LC amplitude spectrum given in the left-hand panel. The LC Nyquist frequency is indicated by the vertical dashed line and the SC amplitude spectrum is shown below for comparison. The middle panel contains inserts of the LC amplitude spectrum showing the real peak below and the alias peak above. The alias peak is easily identified as its multiplet structure is split by the *Kepler* orbital frequency. The right-hand panel shows the amplitude and phase tracking plot revealing the periodic phase modulation of the alias peak created from the Barycentric time-stamp corrections made to *Kepler* data, whereas the real peak has approximately constant phase. Some peaks that exist in the SC amplitude spectrum do not appear in the LC amplitude spectrum as they lie close to the LC sampling frequency and are heavily suppressed in amplitude.

determines why some stars do this and others do not. At this stage, we conjecture that pure amplitude modulation could be caused by variable driving and/or damping within a star. Therefore, it remains an unsolved problem why this occurs. Four examples of pure AMod δ Sct stars are shown in Fig. 5.

A good example of a pure AMod star is KIC 8453431, which is shown in the bottom row of Fig. 5, as it only contains three pulsation mode frequencies with amplitudes greater than 0.01 mmag, specifically $\nu_1 = 13.859\,080$ d^{-1}, $\nu_2 = 22.154\,964$ d^{-1} and $\nu_3 = 10.380\,567$ d^{-1}. The period ratio of ν_2 and ν_1 gives 0.6256 and the
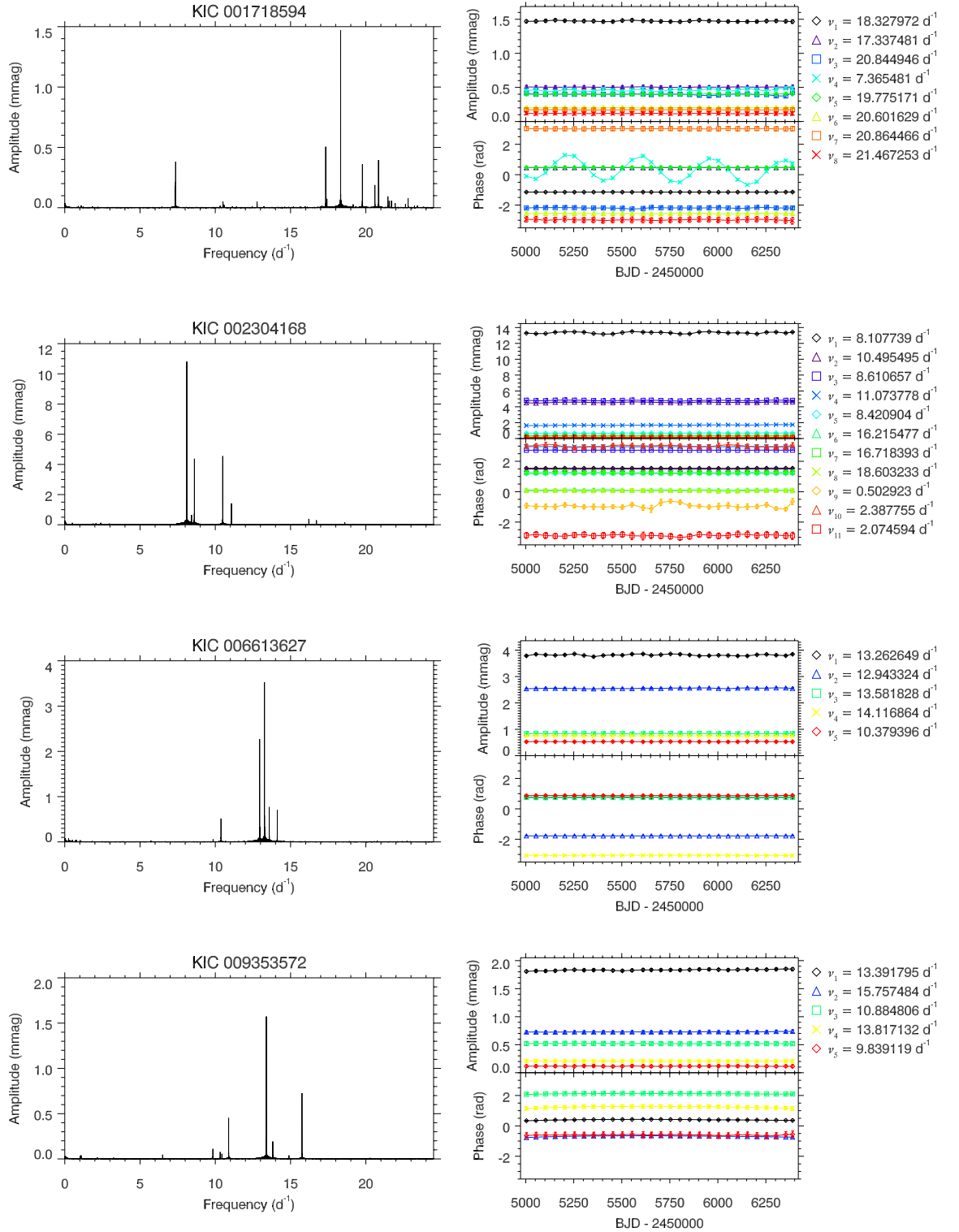
Figure 3. Four examples of NoMod δ Sct stars in the KIC range $6400 \leq T_{\mathrm{eff}} \leq 10\,000$ K that show constant amplitudes and phases over the 4-yr *Kepler* data set. From top to bottom: KIC 1718594 (ν_4 is a super-Nyquist alias), KIC 2304168, KIC 6613627 and KIC 9353572. The left-hand panels are the 4-yr amplitude spectra calculated out to the LC Nyquist frequency. The right-hand panels show the amplitude and phase tracking plots which demonstrate the lack of variability in pulsation amplitudes and phases over 4 yr in each of these four NoMod stars.
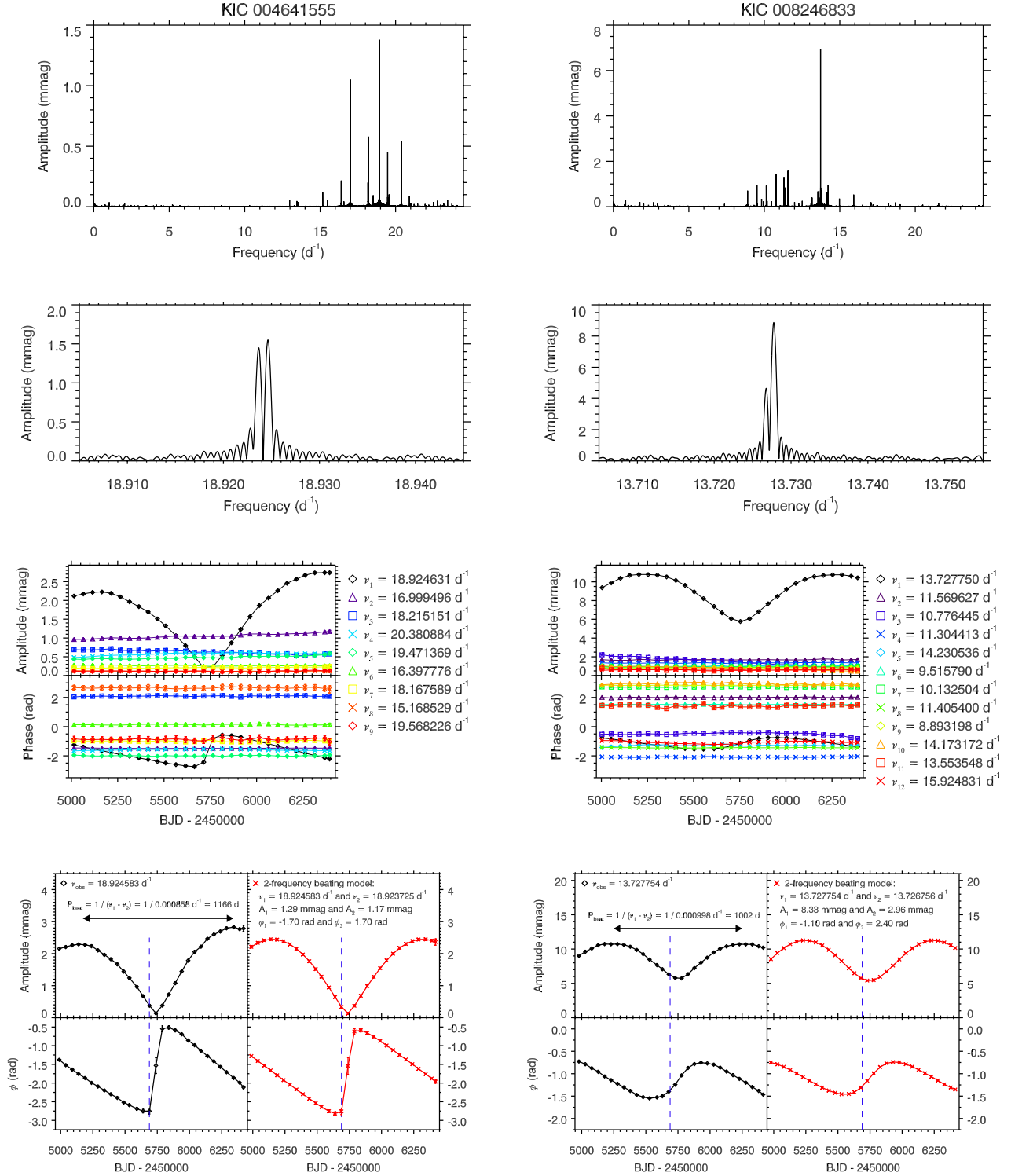
Figure 4. Two examples of AMod δ Sct stars in the KIC range $6400 \leq T_{\mathrm{eff}} \leq 10\,000$ K that show variable pulsation amplitudes and phases over the 4-yr *Kepler* data set from beating of extremely close-frequency modes. The left and right columns are KIC 4641555 and KIC 8246833, respectively. From top to bottom are the 4-yr amplitude spectrum calculated out to the LC Nyquist frequency; a zoom-in of the pair of close-frequency modes in the amplitude spectrum; the amplitude and phase tracking plots; and the accurate beating model (shown as crosses) matching the observed amplitude modulation (shown as diamonds). The dashed vertical line indicates the centre of the *Kepler* data set that has been chosen as the zero-point in time, specifically $t_0 = 2455\,688.770$ BJD. In each of these two example stars, KIC 4641555 (left column) and KIC 8246833 (right column), a pair of high-amplitude pulsation mode frequencies lie closer than 0.001 d^{-1} in frequency, resulting in beat periods of 1166 ± 1 d and 1002 ± 1 d, respectively.
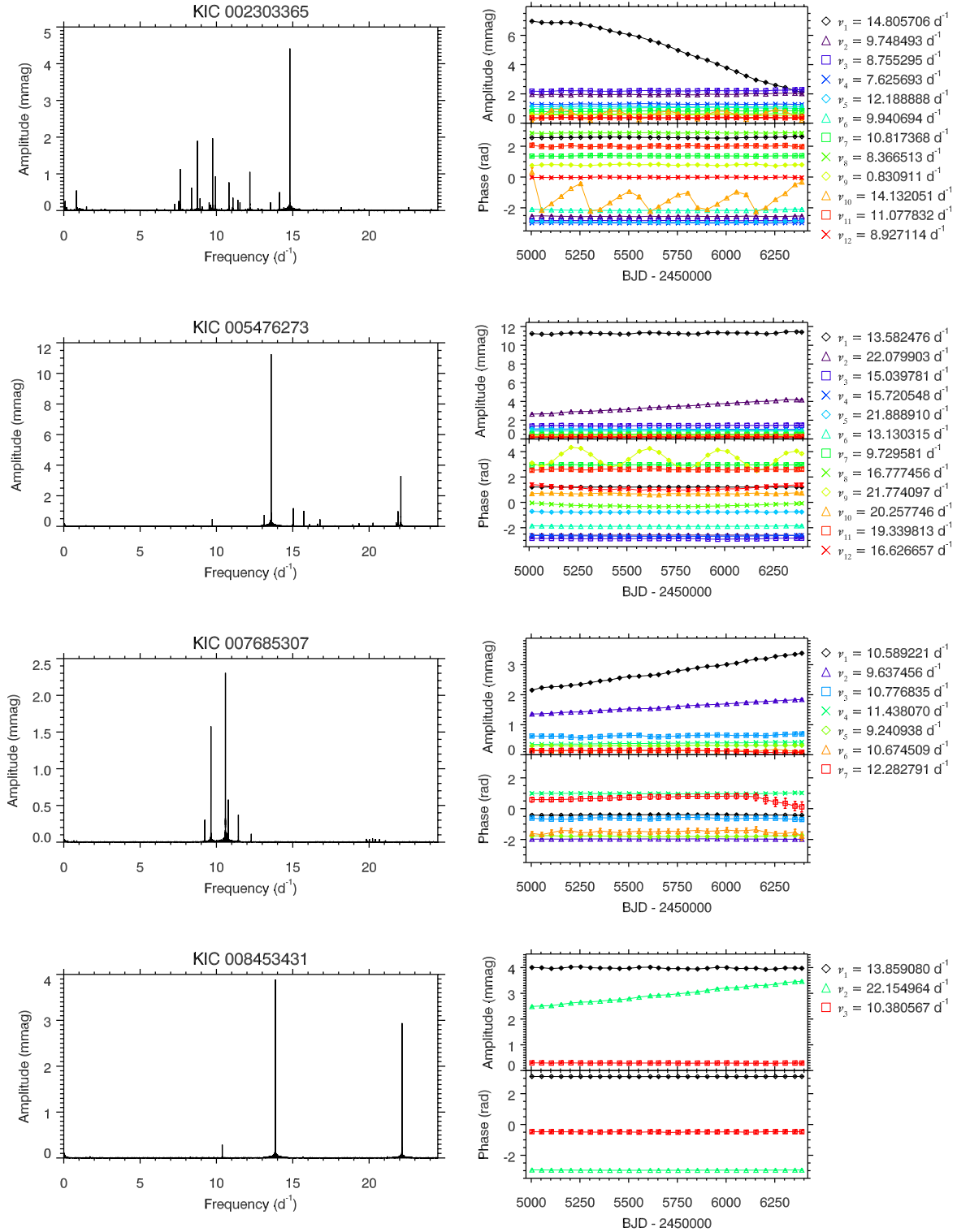
Figure 5. Four examples of pure AMod δ Sct stars in the KIC range $6400 \leq T_{\text{eff}} \leq 10\,000$ K that show variable pulsation amplitudes with constant phases over the 4-yr *Kepler* data set. From top to bottom: KIC 23093365 (ν_1 is pure AMod and ν_{10} contains a ∼250-d beat signal), KIC 5476273 (ν_2 is pure AMod and ν_9 is a super-Nyquist alias), KIC 7685307 (ν_1 and ν_2 are pure AMod) and KIC 8453431 (ν_2 is a pure AMod frequency). The left-hand panels are the 4-yr amplitude spectra calculated out to the LC Nyquist frequency. The right-hand panels show the amplitude and phase tracking plots which demonstrate the modulation in pulsation amplitudes but constant phases over 4 yr.

period ratio of ν_3 and ν_1 gives 0.7490, but calculation of pulsation constants using equation (8) suggest that neither ν_3 or ν_1 is the fundamental radial mode. Therefore, we conclude that these three mode frequencies are likely low-overtone radial modes considering the typical uncertainties associated with calculating Q values (Breger 1990). Regardless of the method for mode identification, only a single pulsation mode frequency, ν_2, slowly increases in amplitude whilst staying at constant phase.

4.5 Phase modulation due to binarity

Binarity within a stellar system causes all the pulsation modes to be phase modulated with the same period, i.e. the orbital period of the star. A previously confirmed binary δ Sct star included in our study is KIC 9651065, which was analysed using the PM technique by Murphy et al. (2014), who calculated an orbital period of $P_{\rm orb} = 272.7 \pm 0.8$ d. Later, Shibahashi et al. (2015) used the FM technique to study KIC 9651065 and found pulsation mode frequencies with first, second and third FM sidelobes in the amplitude spectrum, meaning that the star is highly eccentric. An eccentricity of $e = 0.569 \pm 0.030$ was calculated from the amplitude ratio of the FM sidelobes (Shibahashi et al. 2015).

Four examples of stars identified as binary systems from this study are shown in Fig. 6. These stars are also AMod stars which appears unrelated to the phase modulation caused by the presence of a companion object. The bottom row of Fig. 6 shows the amplitude spectrum (left-hand panel) and the tracking plot (right-hand panel) of the well-studied star KIC 9651065 in which the period of the phase modulation is the orbital period of $P_{\rm orb} = 272.7 \pm 0.8$ d calculated by Murphy et al. (2014). The search for binarity among the δ Sct stars observed by *Kepler* is not the goal of this study so we do not discuss it any further.

4.6 HADS stars

There are few stars in our ensemble that meet the HADS definition from McNamara (2000) of peak-to-peak light amplitude variations greater than 0.3 mag. Some stars were only observed for limited subsets of LC data, and consequently have not been included in our ensemble as we only chose stars for which 4 yr of continuous *Kepler* observations were available. We did not, however, preferentially exclude HADS stars from our sample. Since there are several thousand A and F stars in the *Kepler* data set, the classical instability strip is well-sampled near the TAMS – for example see Niemczura et al. (2015), thus the implication from our study is that HADS stars are rare in *Kepler* data. We find only two HADS stars within our ensemble, KIC 5950759 and KIC 9408694, which are shown in the top and bottom rows of Fig. 7, respectively.

For KIC 5950759, the period ratio of $\nu_1 = 14.221\,394$ d^{-1} and $\nu_2 = 18.337\,294$ d^{-1} gives 0.7755, which identifies these frequencies as the fundamental and first overtone radial modes, respectively. For KIC 9408694, the period ratio of $\nu_1 = 5.661\,057$ d^{-1} and $\nu_3 = 7.148\,953$ d^{-1} gives 0.7919, which is outside the expected range for the fundamental and first overtone radial modes. KIC 9408694 was studied by Balona et al. (2012) who concluded that the fast rotation of KIC 9408694, which is unusual for a HADS star, perturbs the observed pulsation mode frequencies. A model including fast rotation successfully identified ν_1 and ν_3 as the fundamental and first overtone radial modes, respectively (Balona et al. 2012). We find that both HADS stars in our ensemble exhibit fractional amplitude variability of order a few per cent with a period equal to the *Kepler* orbital period – each has several AMod frequencies using our $\pm 5\sigma$

significance criterion. If this instrumental amplitude modulation is removed, both HADS stars have little or no variability in the amplitudes of their radial modes. This was also concluded by Balona et al. (2012) for KIC 9408694.

The same amplitude limitation mechanism predicted for the low-amplitude δ Sct stars (Breger 2000a) does not seem to be at work within HADS stars, which pulsate at much higher amplitudes and yet do not continue to grow exponentially. It is interesting to note that high amplitude pulsations are typically associated with non-linearity in the form of harmonics and combination frequencies, which are found in KIC 5950759 and KIC 9408694, but not normally associated with variable mode amplitudes. This implies that HADS stars are more similar to Cepheid variables[4] than their low-amplitude δ Sct star counterparts (McNamara 2000).

4.7 Pure phase modulation

Pulsation mode frequencies change with evolution of stellar structure, and the concomitant changes in the pulsation cavities of individual modes. Are these changes observable over the 4-yr *Kepler* data set? In our study of 983 δ Sct stars, we searched for pure phase modulation with no associated amplitude modulation of independent pulsation modes, and found no obvious cases. This, of course, excluded those stars which have phase modulation driven by an extrinsic cause, such as binarity, or because the frequencies are super-Nyquist aliases. However, there are cases of non-sinusoidal light variations that changed in shape over 4 yr, observed as phase modulation of harmonics of pulsation mode frequencies. For example, slight phase modulation is observed in the harmonic of the fundamental radial mode frequency, $2\nu_1 = 28.442\,787$ d^{-1}, in the HADS star KIC 5950759, which is shown in the tracking plot in the right-hand panel of Fig. 2.

4.8 Special case study stars

4.8.1 KIC 4733344

Frequency analysis of the δ Sct star KIC 4733344 revealed that its pulsation mode frequencies $\nu_2 = 7.226\,764$ d^{-1} and $\nu_3 = 9.412\,445$ d^{-1} have a period ratio of 0.7678, which is typically associated with the fundamental and first overtone radial modes. Calculating pulsation constants using equation (8) for ν_2 and ν_3 indicated they are likely the fundamental and the first overtone radial modes, respectively, considering the typical uncertainties associated with calculating Q values (Breger 1990). The highest amplitude pulsation mode frequency, $\nu_1 = 8.462\,183$ d^{-1}, is not easily identifiable as it lies between ν_2 and ν_3, thus suggesting it is likely a non-radial mode. This is not surprising as non-radial modes can have higher amplitudes than radial modes (see fig. 1.5 from Aerts et al. 2010). Our tracking routine revealed that these three pulsation modes are variable in amplitude and phase, and so KIC 4733344 pulsates with two variable low-overtone radial modes, ν_2 and ν_3. KIC 4733344 has a log g value of 3.50 ± 0.23 (Huber et al. 2014), suggesting that it is likely in a post-main-sequence state of evolution.

Previously, in Section 4.2 we discussed the example of the NoMod δ Sct star KIC 2304168, which has similar $T_{\rm eff}$, log g and [Fe/H] values to the AMod δ Sct star KIC 4733344. Both of these δ Sct stars have been shown to pulsate in low-overtone radial modes,

---

[4] For example, Eggen (1976) referred to δ Sct stars as ultrashort-period Cepheids (USPC). They have also been called dwarf Cepheids.

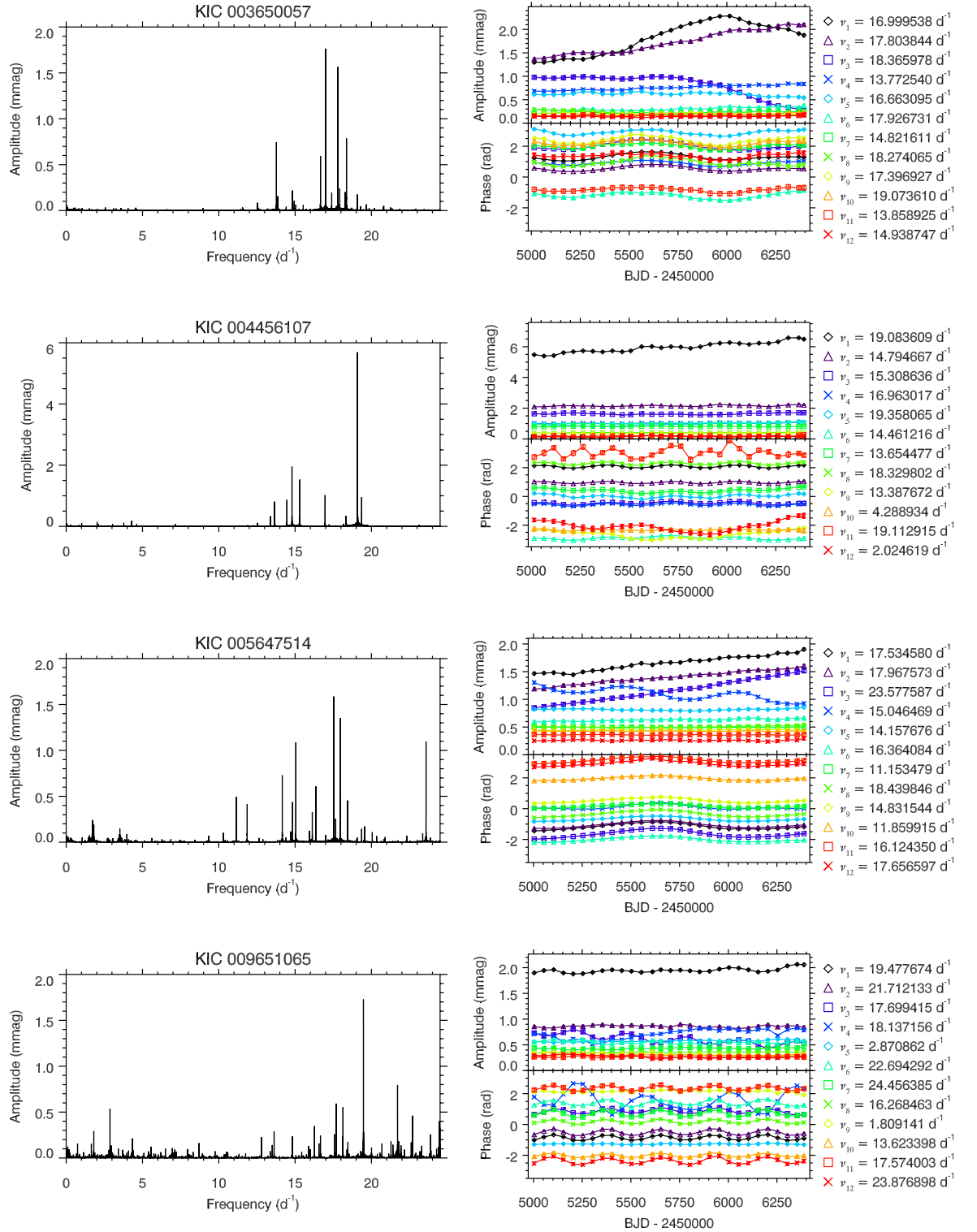**Figure 6.** Four examples of δ Sct stars in the KIC range 6400 ≤ T_{eff} ≤ 10 000 K that show phase modulation over the 4-yr *Kepler* data set because of binarity, but are also AMod stars. From top to bottom: KIC 3650057, KIC 4456107, KIC 5647514 and KIC 9651065 (ν_4 is a super-Nyquist alias). The left-hand panels are the 4-yr amplitude spectra calculated out to the LC Nyquist frequency. The right-hand panels show the amplitude and phase tracking plots which demonstrate the modulation in pulsation amplitudes and phases over 4 yr. The orbital period is calculated from the period of the phase modulation in the tracking plot, and is consistent with the result from the PM technique given in Table 1 for each star.
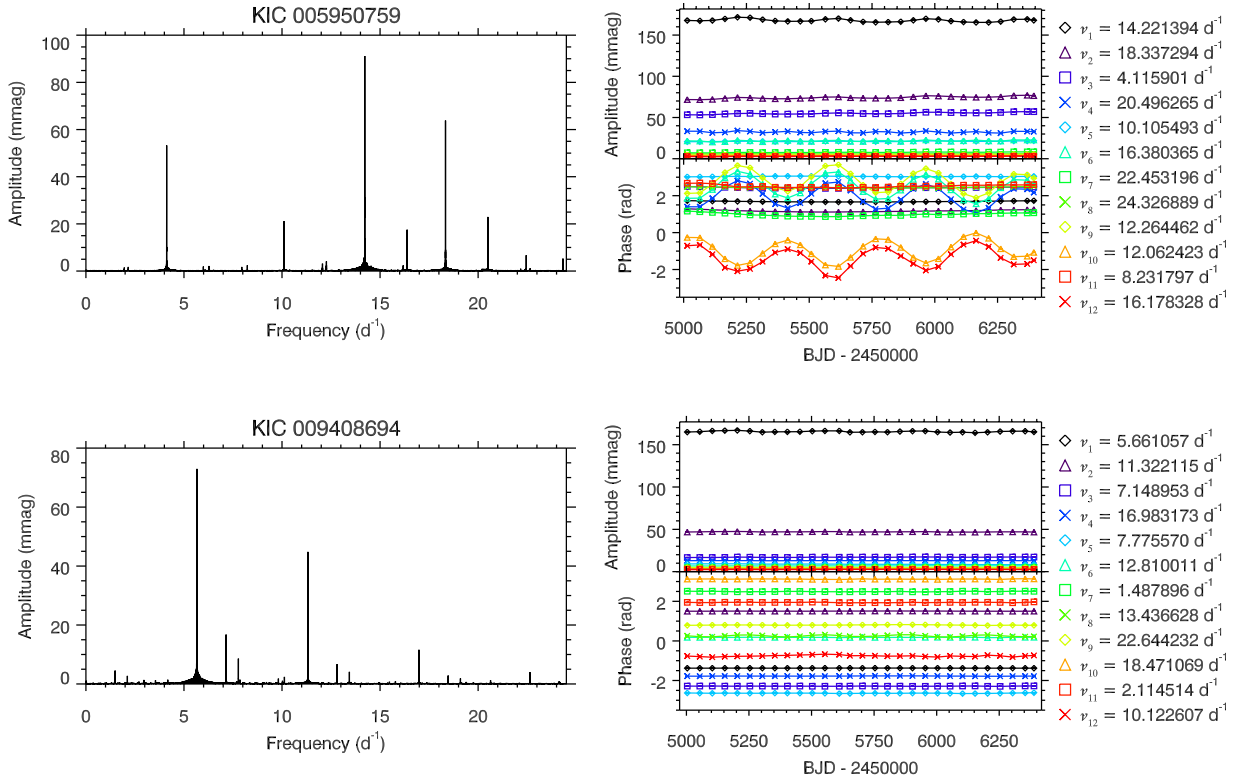
Figure 7. Two HADS stars in the KIC range $6400 \leq T_{\mathrm{eff}} \leq 10\,000$ K that show little or no variability in their high-amplitude radial pulsation modes over the 4-yr *Kepler* data set. The top row is KIC 5950759 (ν_4, ν_6, ν_9, ν_{10} and ν_{12} are super-Nyquist aliases) and the bottom row is KIC 9408694. The left-hand panels are the 4-yr amplitude spectra calculated out to the LC Nyquist frequency. The right-hand panels show the amplitude and phase tracking plots for these two HADS stars over 4 yr. There is little or no variability in the amplitudes and phases of the radial pulsation modes, if instrumental modulation caused by the *Kepler* satellite is removed.

in particular the fundamental and first overtone radial modes. This makes us ponder the possible differences in the driving and damping mechanisms at work within these two δ Sct stars. In Section 6, we discuss coupling models for families of pulsation mode frequencies in KIC 4733344.

4.8.2 KIC 7106205

The δ Sct star KIC 7106205 was investigated by Bowman & Kurtz (2014) and found to contain only a single pulsation mode with variable amplitude whilst all other pulsation modes remained constant in amplitude and phase between 2009 and 2013. Further work by Bowman et al. (2015) extended this study back to 2007 using archive data from the WASP project. The amplitude spectrum and tracking plot for the nine pulsation mode frequencies that have amplitudes higher than 0.10 mmag are shown in Fig. 8. Since no other pulsation modes were observed to vary in amplitude or phase, it was concluded that the visible pulsation mode energy was not conserved in this star (Bowman & Kurtz 2014).

5 MODELLING BEATING

Pure amplitude modulation of a single pulsation mode may appear as a group of close-frequency peaks in the amplitude spectrum (Buchler et al. 1997), and thus the presence of multiple peaks does not *prove* the existence of multiple independent pulsation modes.

Pure amplitude modulation of a single pulsation mode excludes phase variability (Breger & Pamyatnykh 2006), thus it is only by studying the amplitude *and* frequency (i.e. phase at fixed frequency) variations of peaks in the amplitude spectrum that it can be determined if the variability is caused by the pure amplitude modulation of a single mode, or the beating pattern of multiple close-frequency pulsation modes.

We tested this concept using synthetic data, specifically 4-yr of *Kepler* time stamps with calculated magnitudes using

$$y = A e^{-t/\tau} \cos(2\pi\nu(t - t_0) + \phi), \tag{9}$$

where τ is an exponential decay time of 300 d, A is an amplitude of 5.0 mmag, ν is a frequency of 10.0 d^{-1} and ϕ is a phase of 0.0 rad relative to the centre of the data set (i.e. $t_0 = 2455\,688.770$ BJD). Calculating the amplitude spectrum of an exponentially decaying signal produces a Lorentzian profile peak in the Fourier domain, which is shown in the top panel of Fig. 9. We then applied our amplitude and phase tracking method to this input frequency with the results shown in the bottom panel of Fig. 9. The cosinusoidal signal calculated using equation (9) has a constant frequency and phase but a decaying amplitude,[5] which is made clear by the pure amplitude modulation and no phase variation shown in the bottom panel of Fig. 9.

---

[5] A similar result is obtained if a $\tanh(-t/\tau)$ factor is used instead of $e^{-t/\tau}$ as an amplitude modulation factor.
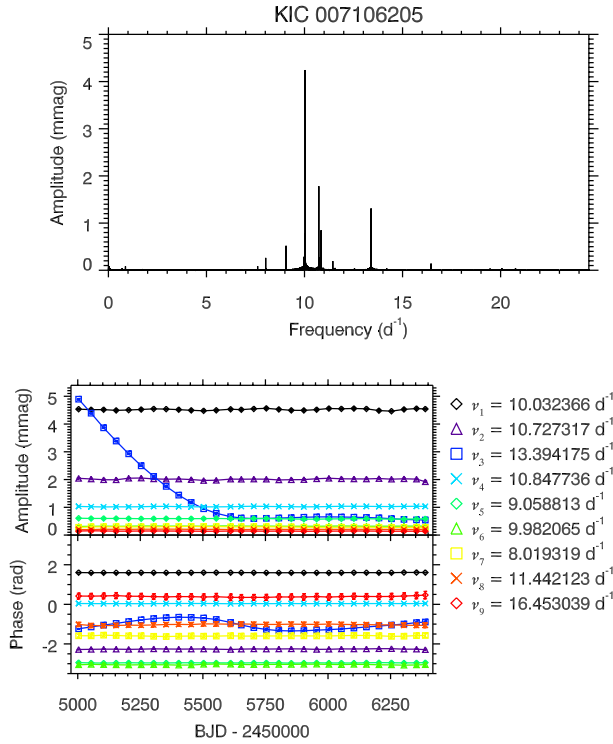
Figure 8. KIC 7106205: the 4-yr amplitude spectrum calculated out to the LC Nyquist frequency is shown in the top panel, and the amplitude and phase tracking plot showing variability in pulsation mode amplitudes and phases over time is shown in the bottom panel.

As previously discussed in Section 2.1, the relative amplitudes and separations in close-frequency pulsation modes governs the amplitude and phase modulation of the beating signal. In observations of δ Sct stars, close-frequency pulsation modes are not uncommon (Breger & Bischof 2002) and unlikely to be explained by rotation. Also, one cannot attribute a pair of resolved close-frequency pulsation modes to being caused by the pure amplitude modulation of a single pulsation mode, as this leads to a more complex structure in the amplitude spectrum, and not two resolved peaks. From previous studies of δ Sct stars, for which mode identification was possible, non-radial modes were commonly found to cluster around radial modes because of mode trapping (Breger et al. 2009).

We constructed beating models of the two pairs of close-frequency pulsation modes in KIC 4641555 and KIC 8246833 using synthetic data, specifically using 4-yr of *Kepler* time stamps and magnitudes calculated containing only white noise and the two resolved frequency cosinusoids causing the beating pattern. The frequencies, amplitudes and phases of the two pulsation modes can be calculated because the peaks are resolved using 4 yr of *Kepler* data. These models were successfully matched to observations of amplitude modulation in KIC 4641555 and KIC 8246833, yielding beat periods of 1166 ± 1 d and 1002 ± 1 d, respectively. The observed amplitude modulation of the highest amplitude pulsation mode frequency is shown as diamonds and the beating model is shown as crosses in the bottom panels of Fig. 4 for each star. This demonstrates that it is possible for a δ Sct star to pulsate with low-degree p-mode frequencies that lie very close to the Rayleigh resolution criterion in frequency for the 4-yr *Kepler* data set and yet maintain their independent identities.
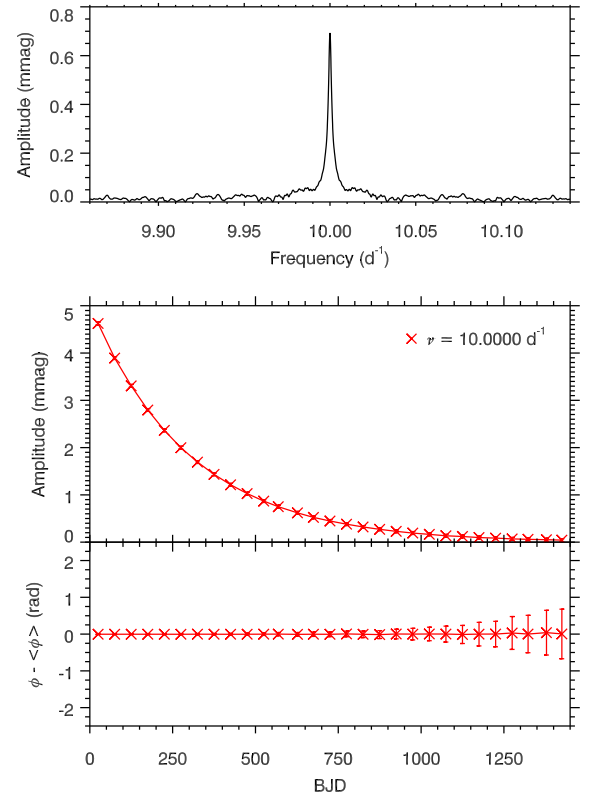
Figure 9. Pure amplitude modulation for an exponentially decaying amplitude and fixed frequency and phase cosinusoid using synthetic *Kepler* data. The top panel shows the Lorentzian profile peak produced in the amplitude spectrum and the bottom panel is the amplitude and phase tracking plot for pure amplitude modulation with no associated phase variation.

It is plausible that many more AMod δ Sct stars can be explained by the beating of unresolved close-frequency pulsation modes. In a similar way, beating models of multiple unresolved frequencies could be constructed to explain amplitude modulation in many δ Sct stars, but this requires the number of frequencies to be known a priori. Theoretically, it is possible for many non-radial pulsation mode frequencies to exist in a frequency range of less than 0.000 68 d^{-1} and maintain their independent identity over several years (Saio, *priv. comm.*). If this is the case for many of the AMod δ Sct stars in this study, it would explain the non-sinusoidal modulation cycles because of the complicated beating pattern of multiple unresolved close-frequency pulsation modes.

6 MODELLING NON-LINEARITY

In the mode coupling hypothesis, it is required that all three members of a family are variable in amplitude so that the child mode can be identified and a model predicting its behaviour can be constructed as a function of the product of the amplitudes of the parent modes. In Section 2.2, it was discussed how families of frequencies must satisfy the frequency criterion given in equation (4) and the phase criterion given in equation (6), but also how equation (5) can be used to distinguish among possible causes of non-linearity in a star. By trying different values of the coupling coefficient μ$_c$, the *strength* of coupling and non-linearity among pulsation mode frequencies can be estimated. In this way, families of frequencies that satisfy equation (4) can be distinguished as coupling between a child
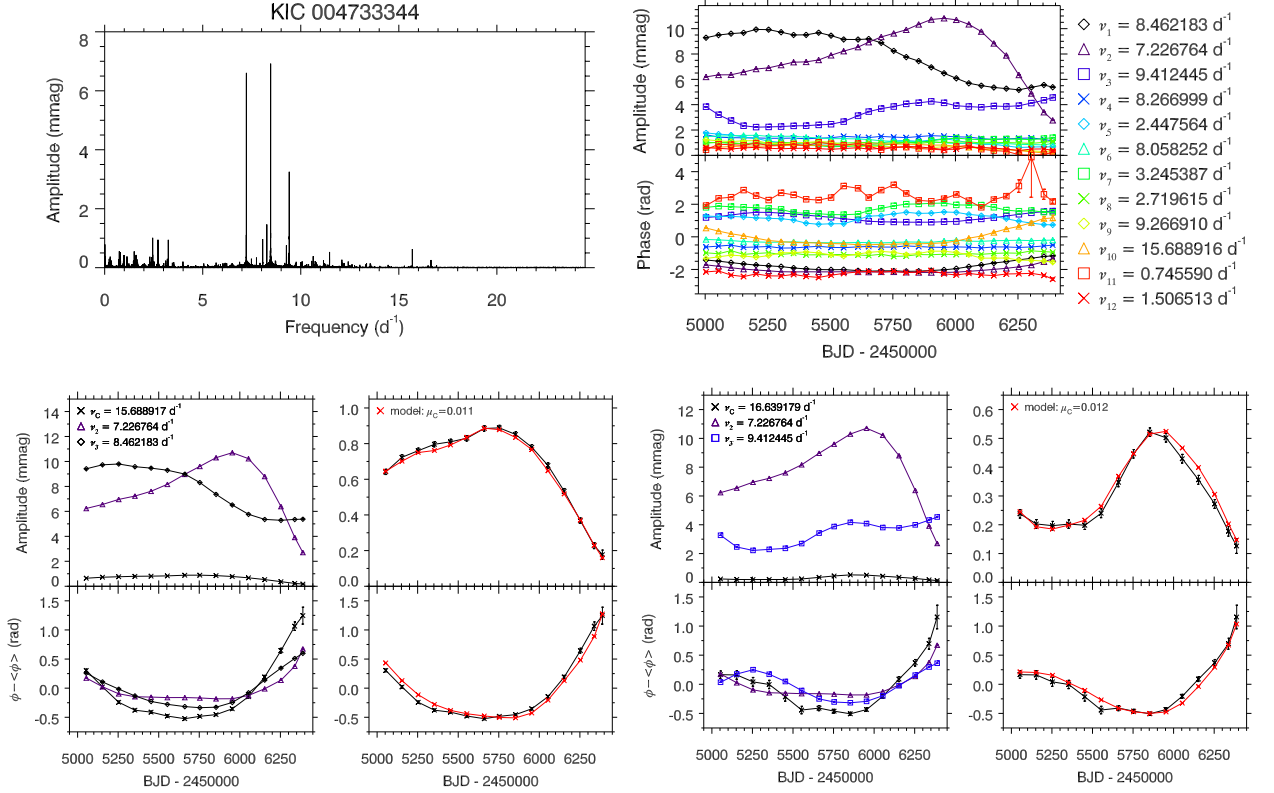
Figure 10. The AMod δ Sct (hybrid) star KIC 4733344 has variable pulsation amplitudes and phases over the 4-yr *Kepler* data set, which can be explained by non-linearity. The top-left panel is the 4-yr amplitude spectrum calculated out to the LC Nyquist frequency and the top-right panel shows the amplitude and phase tracking plot which demonstrates the variability in pulsation amplitudes and phases over 4 yr. The bottom panels show the coupling models as crosses, which are consistent with observations of the child mode variability for two families of frequencies taken from the tracking plot, specifically $\nu_1 + \nu_2$ (left) and $\nu_2 + \nu_3$ (right).

and two parent modes or combination frequencies. Small values of μ_c imply weak-coupling and favour the non-linear distortion model producing combination frequencies, whereas large values of μ_c imply strong coupling and favour resonant mode coupling (Breger & Montgomery 2014).

Note that a large value of μ_c is defined by the amplitudes of the parent modes and thus is specific to each family. For example, using equation (5), if $A_2 = A_3 = 2$ mmag, then to achieve a similar child mode amplitude of $A_1 \simeq 2$ mmag, a value of $\mu_c \simeq 0.25$ is required. Using the same parent mode amplitudes, a small value of $\mu_c \simeq 0.01$ would produce a child mode amplitude of $A_1 \simeq 0.04$ mmag. Therefore, in this hypothetical example, $\mu_c \geq 0.1$ is considered strong coupling and $\mu_c \leq 0.01$ is considered weak coupling.

Coupling models for two families of frequencies in KIC 4733344 are shown in Fig. 10. These two families have similar small values of the coupling coefficient $\mu_c \simeq 0.01$, which imply non-linearity in the form of combination frequencies from the non-linear distortion model. For example, since the parent modes have amplitudes of $A_2 \simeq 6$ mmag and $A_3 \simeq 9$ mmag at the start of the data set (see the bottom-left panel of Fig. 10), a coupling coefficient of $\mu_c \simeq 0.1$ would produce a child mode amplitude of $A_1 \simeq 5$ mmag, which is an order of magnitude larger than the observed amplitude of the child mode, $A_1 \simeq 0.6$ mmag. Therefore, we conclude that resonant mode coupling is unlikely the cause of non-linearity and amplitude modulation in KIC 4733344.

7 ENSEMBLE STUDY STATISTICS

Our ensemble comprised 983 δ Sct stars that lie in the KIC effective temperature range of $6400 \leq T_{\text{eff}} \leq 10\,000$ K, pulsate in p-mode frequencies between $4 \leq \nu \leq 24$ d^{-1} and were observed continuously by the *Kepler Space Telescope* for 4 yr. As previously described in Section 3, we flagged the number of peaks that have amplitudes greater than 0.10 mmag (up to a maximum number of 12) in each star that exhibit significant amplitude modulation, with each star labelled as either NoMod or AMod. The criterion of significant amplitude modulation was chosen as at least half of a frequency's time bins being greater than $\pm 5\sigma$ in amplitude from the mean, which is shown graphically in Fig. 1. It is important to note that our method for studying amplitude modulation in δ Sct stars does not automatically determine if an extracted frequency is a combination frequency, or the cause of the observed amplitude modulation, such as beating or non-linearity.

We found that 380 stars (38.7 per cent) were classed as NoMod and 603 stars (61.3 per cent) had at least a single AMod peak. The histogram for the distribution of the number of stars against the number of AMod frequencies in a star is shown in the top-left panel of Fig. 11. A significant conclusion from this study is that the majority of δ Sct stars have at least a single AMod frequency. More interestingly, 201 stars (20.4 per cent) have only a single AMod frequency, with all other frequencies remaining constant in amplitude. This has previously been demonstrated for KIC 7106205, but the
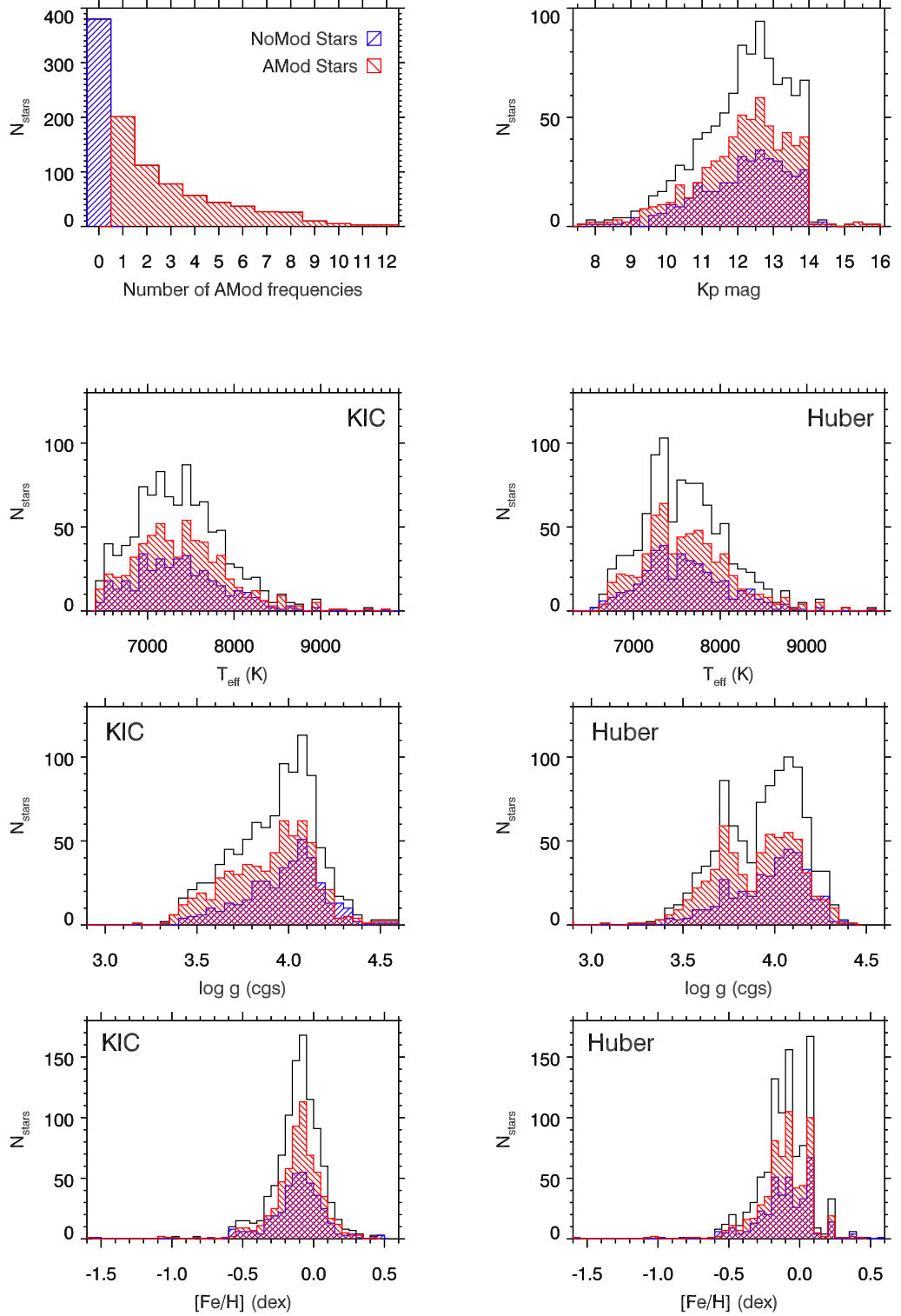
Figure 11. The histogram of the distribution of the number of stars against the number of AMod peaks in our ensemble is shown in the top-left panel. Histograms for the number stars against T_{eff}, log g, [Fe/H] and Kp mag, in which black represents all 983 stars in our ensemble, the blue hatched region represents the 380 NoMod stars and red hatched region represents the 603 AMod stars. Histograms for T_{eff}, log g and [Fe/H] using the original KIC values are shown in the left-hand panels, and the revised values from Huber et al. (2014) are shown in the right-hand panels.

discovery that this behaviour is common among δ Sct stars has not been demonstrated before; it is a new result from this work.

We created histograms of various stellar parameters for all stars, which are shown in Fig. 11, for both the original KIC values (Brown et al. 2011) and the revised values given in Huber et al. (2014). In these histograms, the unhatched region represents all stars and the hatched regions show the NoMod and AMod stars in the various panels. The distributions of T_{eff}, log g, [Fe/H] and Kp magnitude for the NoMod and AMod stars are similar, demonstrating that amplitude modulation is common across the classical instability strip. Therefore, we conclude that the physics that determines which modes have variable amplitudes does not simply depend on the fundamental stellar parameters. Our histograms also show the 200 K systematic offset in T_{eff} that Huber et al. (2014) found in hot *Kepler* stars. This is most clear when comparing the KIC and Huber et al. (2014) T_{eff} histograms in Fig. 11.

One might expect the more evolved δ Sct stars (i.e. stars with lower log g values) to have variable pulsation mode amplitudes, because they likely contain mixed modes or because the structure of the star is changing in a relatively small period of time. Even whilst on the main sequence the convective core can increase or decrease in mass depending on the initial mass (see fig. 3.6 from Aerts et al. 2010). However, the NoMod and AMod log g distributions in Fig. 11 are centred on approximately the same value. There is, however, a bimodality in the Huber et al. (2014) log g values for the AMod stars compared to the NoMod stars. This supports the above argument that evolved δ Sct stars are more likely to be AMod, but since this bimodality is not seen in the KIC log g values, it is likely an artefact of the Huber et al. (2014) method.

We also constructed $T_{eff} - $ log g diagrams using the original and revised KIC values, which are shown in Fig. 12, for the NoMod and AMod stars. Observational blue and red edges of the instability strip, taken from Rodríguez & Breger (2001), are also plotted in Fig. 12. There is no obvious correlation between the physical mechanisms that cause amplitude modulation and stellar parameters such as T_{eff} or log g in our ensemble. An inference from this study is that amplitude modulation is not directly dependent on the fundamental stellar parameters of a star, but intrinsically related to the pulsation excitation mechanism itself. Further investigation and theoretical work is needed to address this question.

8 CONCLUSIONS

In this paper, we have presented the results from a search for amplitude modulation in 983 δ Sct stars that were continuously observed by the *Kepler Space Telescope* for 4 yr. The *Kepler* data set provides extremely high frequency and amplitude precision, which we used to track amplitude and phase at fixed frequency in 100-d bins with a 50-d overlap, for a maximum number of 12 peaks with amplitudes greater that 0.10 mmag in each star. We collated our results into an amplitude modulation catalogue and have presented a selection of case study stars to demonstrate the diversity in pulsational behaviour. A total of 603 δ Sct stars (61.3 per cent) exhibit at least one pulsation mode that varies significantly in amplitude over 4 yr, and so amplitude modulation is common among δ Sct stars.

The 380 NoMod δ Sct stars comprise 38.7 per cent of our ensemble and represent the stars for which the highest precision measurements of amplitude and frequency are possible. This is extremely important in the search for planets orbiting these stars when using the FM method (Shibahashi & Kurtz 2012). The upcoming TESS mission (Ricker et al. 2015) will provide short time-scale observations of a large area of the sky, and continuous observations near the
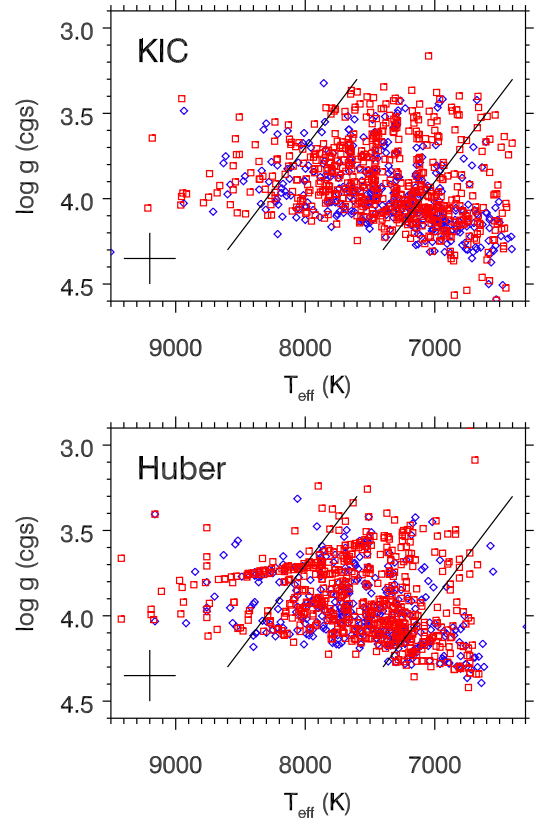

Figure 12. $T_{eff} - $ log g diagrams for the stellar parameters listed in the KIC (top panel) and the revised values given by Huber et al. (2014) (bottom panel). The diamonds represent the 380 NoMod stars and the squares represent the 603 AMod stars. The solid lines are the observational blue and red edges of the classical instability strip from Rodríguez & Breger (2001), and the cross represents the typical uncertainty for each point.

polar regions. These NoMod stars are the ideal targets for determining precise frequencies and amplitudes for asteroseismic modelling. They also represent a subset of *ideal* δ Sct stars that can be compared to observations of δ Sct stars in the continuous viewing zones with the TESS mission data.

The causes of variable pulsation amplitudes in δ Sct stars, which we termed AMod stars, can be categorised into those that are caused by extrinsic or intrinsic causes. The extrinsic causes of phase variability include binarity (or multiplicity) in the stellar system which acts as a perturbation to the pulsation mode frequencies observed (Shibahashi & Kurtz 2012). A pulsating star can also be easily recognized as being part of a multiple system as its pulsation modes will all be phase modulated by the orbital period (Murphy et al. 2014). Similarly, super-Nyquist aliases are easily identifiable because they are periodically phase modulated by a variable Nyquist frequency. This was demonstrated graphically for KIC 5950759 in Fig. 2.

The sub-group of stars that exhibit amplitude modulation with no phase change is particularly interesting. In these stars, the amplitude change is non-periodic and is often monotonically variable over many years. Approximately the same number of stars with linearly increasing and decreasing amplitudes are seen, but also non-linearly increasing and decreasing amplitudes in this sub-group. We are possibly observing these stars undergoing slow changes in the relative depths of pulsation cavities driven by stellar evolution. For example, stellar evolution was suggested as the cause of the observed

amplitude modulation in the ρ Pup star KIC 3429637 (Murphy et al. 2012). On the other hand, pure amplitude modulation in δ Sct stars may be observations of changes in driving and/or damping within a star. These stars remain a challenge to understand and so we can only speculate.

Beating effects from pairs (or groups) of close-frequency pulsation modes are not uncommon in δ Sct stars (Breger & Bischof 2002; Breger & Pamyatnykh 2006). A resolved beating pattern is most recognisable from the periodic amplitude modulation, but most importantly, from a phase change occurring at the epoch of minimum amplitude. This phase change is π rad for two equal-amplitude cosinusoids, and tends to zero as the amplitudes get significantly different from each other. We successfully constructed beating models for two pairs of close-frequency modes separated by less than 0.001 d^{-1} in KIC 4641555 and KIC 8246833, shown in Fig. 4, resulting in beating periods of 1166 $\pm$ 1 d and 1002 $\pm$ 1 d, respectively.

Stars that exhibit non-linearity are evident from the non-sinusoidal shape of the light curve and the presence of harmonics and combination frequencies in the amplitude spectrum. The frequency, amplitude and phase of a coupled mode or combination frequency are a function of the two parent modes, and so we used a coupling coefficient, μ_c, to distinguish between these two forms of non-linearity within a star. Small values of μ_c imply combination frequencies from a non-linear distortion model that mimic any variability in the parent modes (Brickhill 1992; Wu 2001; Breger & Lenz 2008), whereas large values of μ_c imply resonant mode coupling with mode energy being exchanged among similar-amplitude family members (Breger & Montgomery 2014). We have modelled mode coupling in the δ Sct star KIC 4733344 and studied the possible energy exchange among pulsation modes. For two families of frequencies in KIC 4733344, we found $\mu_c \simeq 0.01$ implying combination frequencies caused by the non-linear distortion model (i.e. non-linearities in the pulsation waves of the parent modes), and not strongly coupled modes. For many δ Sct stars, the visible pulsation mode energy is not conserved in 4 yr of *Kepler* observations. For example, the δ Sct star KIC 7106205 has only a single variable pulsation mode, which is shown in Fig. 8. This may be caused by mode coupling to invisible high-degree modes (Dziembowski & Krolikowska 1985). Using *Kepler* photometry means we are not sensitive to high-degree modes from geometric cancellation (Dziembowski 1977), and so it is difficult to determine if the amplitude modulation in a low-degree child p-mode is caused by high-degree parent modes.

Recent work by Fuller et al. (2015) and Stello et al. (2016) has shown that many red giant stars have suppressed dipolar modes ($\ell = 1$), which can be explained by the scattering of mode energy into high-degree modes as they interact with a magnetic field in a star's core. This effect, termed the Magnetic Greenhouse Effect (Fuller et al. 2015), essentially traps the mode energy in the magnetised core of a red giant star resulting in low surface amplitudes for the dipole modes. Stello et al. (2016) demonstrated that not all red giant stars exhibit suppressed dipole modes and that it is a strong function of stellar mass. Among other pulsating stars, Cantiello, Fuller & Bildsten (2016) modelled a 1.6 M$_\odot$ main-sequence γ Dor star and suggested that it is possible for a dynamo-generated magnetic field to be induced near the core in such as star. This could alter the pulsational behaviour of a star and redistribute mode energy into higher degrees, hence dramatically reduce their visible amplitudes (Cantiello et al. 2016). We speculate that a similar mechanism could be the cause for some of the AMod δ Sct stars in our ensemble. The A and F stars have small convective cores and if a magnetic field is sustained throughout the transition from post-main sequence to

the red giant branch, it is reasonable to assume that the progenitors of red giant stars with suppressed dipole modes also had magnetic fields near their cores on the main sequence. The progenitors of such suppressed dipole mode red giant stars could be within our ensemble of δ Sct stars.

There are various theoretical and observational synergies between pulsating A and B stars, such that β Cep stars can be considered analogues of δ Sct stars, from the similar pulsation mode frequencies observed. The κ-mechanism operating in the metal bump (or 'Z bump') in opacity, causes low-order p modes to become unstable (Dziembowski & Pamiatnykh 1993). Hybrid B stars pulsating in both g- and p-mode frequencies have also been observed (Degroote et al. 2012). Further similarity between β Cep and δ Sct stars exists, as Degroote et al. (2009) found evidence for non-linear resonant mode coupling in the β Cep star HD 180642. It would be interesting to investigate the synergy in mode coupling within hybrid stars, between A and B stars.

Our catalogue of 983 δ Sct stars utilizing 4 yr of *Kepler* data demonstrates that observations spanning years (and longer) are often needed to study and resolve pulsational behaviour in these stars. Our catalogue will be useful for comparison purposes when studying observations of δ Sct stars from K2 (Howell et al. 2014) and TESS (Ricker et al. 2015). Eventually, these missions will observe a large area of the sky, but for only a short length of time. Therefore, *Kepler* may represent the best data set for studying δ Sct stars as its 4-yr length of continuous observations will not be surpassed for some time.

REFERENCES

Aerts C., Christensen-Dalsgaard J., Kurtz D. W., 2010, Asteroseismology. Springer-Verlag, Berlin
Bailey S. I., 1902, Ann. Harv. Coll. Obs., 38, 1
Balona L. A., 2011, MNRAS, 415, 1691
Balona L. A., 2014, MNRAS, 437, 1476
Balona L. A., Dziembowski W. A., 2011, MNRAS, 417, 591
Balona L. A., Krisciunas K., Cousins A. W. J., 1994, MNRAS, 270, 905
Balona L. A. et al., 2011, MNRAS, 413, 2403
Balona L. A. et al., 2012, MNRAS, 419, 3028
Barceló Forteza S., Michel E., Roca Cortés T., García R. A., 2015, A&A, 579, A133
Borucki W. J. et al., 2010, Science, 327, 977
Bowman D. M., Kurtz D. W., 2014, MNRAS, 444, 1909
Bowman D. M., Holdsworth D. L., Kurtz D. W., 2015, MNRAS, 449, 1004
Breger M., 1990, Delta Scuti Star Newsl., 2, 13

Breger M., 2000a, in Breger M., Montgomery M., eds, ASP Conf. Ser. Vol. 210, Delta Scuti and Related Stars. Astron. Soc. Pac., San Francisco, p. 3

Breger M., 2000b, MNRAS, 313, 129

Breger M., 2009, in Guzik J. A., Bradley P. A., eds, AIP Conf. Ser. Vol. 1170, Stellar Pulsation: Challenges for theory and observation. Astron. Soc. Pac., San Francisco, p. 410

Breger M., 2010, in Sterken C., Samus N., Szabados L., eds, Variable Stars, the Galactic halo and Galaxy Formation. Sternberg Astronomical Institute of Moscow Univ., Russia, p. 95

Breger M., 2016, preprint (arXiv:1605.01649)

Breger M., Bischof K. M., 2002, A&A, 385, 537

Breger M., Bregman J. N., 1975, ApJ, 200, 343

Breger M., Lenz P., 2008, A&A, 488, 643

Breger M., Montgomery M. H., 2014, ApJ, 783, 89

Breger M., Pamyatnykh A. A., 2006, MNRAS, 368, 571

Breger M., McNamara B. J., Kerschbaum F., Huang L., Jiang S.-J., Guo S.-Z.-H., Poretti E., 1990, A&A, 231, 56

Breger M. et al., 1999, A&A, 349, 225

Breger M., Lenz P., Pamyatnykh A. A., 2009, MNRAS, 396, 291

Breger M. et al., 2012a, Astron. Nachr., 333, 131

Breger M. et al., 2012b, ApJ, 759, 62

Brickhill A. J., 1992, MNRAS, 259, 519

Brown T. M., Latham D. W., Everett M. E., Esquerdo G. A., 2011, AJ, 142, 112

Buchler J. R., Goupil M.-J., Hansen C. J., 1997, A&A, 321, 159

Cantiello M., Fuller J., Bildsten L., 2016, preprint (arXiv:1602.03056)

Chapellier E., Mathias P., Weiss W. W., Le Contel D., Debosscher J., 2012, A&A, 540, A117

Chevalier C., 1971, A&A, 14, 24

Christensen-Dalsgaard J., 2000, in Breger M., Montgomery M., eds, ASP Conf. Ser. Vol. 210, Delta Scuti and Related Stars. Astron. Soc. Pac., San Francisco, p. 187

Cox J. P., 1963, ApJ, 138, 487

Deeming T. J., 1975, Ap&SS, 36, 137

Degroote P. et al., 2009, A&A, 506, 111

Degroote P. et al., 2012, A&A, 542, A88

Dupret M. A., Grigahcène A., Garrido R., Gabriel M., Scuflaire R., 2004, A&A, 414, L17

Dupret M. A., Grigahcène A., Garrido R., Gabriel M., Scuflaire R., 2005, A&A, 435, 927

Dziembowski W., 1977, Acta Astron., 27, 203

Dziembowski W., 1982, Acta Astron., 32, 147

Dziembowski W., Krolikowska M., 1985, Acta Astron., 35, 5

Dziembowski W., Krolikowska M., 1990, Acta Astron., 40, 19

Dziembowski W. A., Pamiatnykh A. A., 1993, MNRAS, 262, 204

Eddington A. S., 1917, The Observatory, 40, 290

Eddington A. S., 1926, The Internal Constitution of the Stars. Cambridge Univ. Press, Cambridge

Eggen O. J., 1976, PASP, 88, 402

Fuller J., Cantiello M., Stello D., Garcia R. A., Bildsten L., 2015, Science, 350, 423

Gilliland R. L. et al., 2010, PASP, 122, 131

Grigahcène A. et al., 2010, ApJ, 713, L192

Guzik J. A., Kaye A. B., Bradley P. A., Cox A. N., Neuforge C., 2000, ApJ, 542, L57

Holdsworth D. L. et al., 2014, MNRAS, 439, 2078

Houdek G., 2000, in Breger M., Montgomery M., eds, ASP Conf. Ser. Vol. 210, Delta Scuti and Related Stars. Astron. Soc. Pac., San Francisco, p. 454

Howell S. B. et al., 2014, PASP, 126, 398

Huber D. et al., 2014, ApJS, 211, 2

Jones D. H. P., Haslam C. M., 1966, The Observatory, 86, 34

Kaye A. B., Handler G., Krisciunas K., Poretti E., Zerbi F. M., 2000, in Szabados L., Kurtz D., eds, ASP Conf. Ser. Vol. 203, IAU Colloq. 176: The Impact of Large-Scale Surveys on Pulsating Star Research. Astron. Soc. Pac., San Francisco, p. 426

Keen M. A., Bedding T. R., Murphy S. J., Schmid V. S., Aerts C., Tkachenko A., Ouazzani R.-M., Kurtz D. W., 2015, MNRAS, 454, 1792

Koch D. G. et al., 2010, ApJ, 713, L79

Kraft R. P., 1967, ApJ, 150, 551

Kurtz D. W., Saio H., Takata M., Shibahashi H., Murphy S. J., Sekii T., 2014, MNRAS, 444, 102

Kurtz D. W., Shibahashi H., Murphy S. J., Bedding T. R., Bowman D. M., 2015, MNRAS, 450, 3015

Lenz P., Pamyatnykh A. A., Zdravkov T., Breger M., 2010, A&A, 509, A90

McNamara D. H., 2000, in Breger M., Montgomery M., eds, ASP Conf. Ser. Vol. 210, Delta Scuti and Related Stars. Astron. Soc. Pac., San Francisco, p. 373

McNamara B. J., Jackiewicz J., McKeever J., 2012, AJ, 143, 101

Montgomery M. H., O'Donoghue D., 1999, Delta Scuti Star Newsl., 13, 28

Murphy S. J., 2014, PhD thesis, Jeremiah Horrocks Institute, University of Central Lancashire

Murphy S. J., Shibahashi H., 2015, MNRAS, 450, 4475

Murphy S. J., Grigahcène A., Niemczura E., Kurtz D. W., Uytterhoeven K., 2012, MNRAS, 427, 1418

Murphy S. J., Shibahashi H., Kurtz D. W., 2013a, MNRAS, 430, 2986

Murphy S. J. et al., 2013b, MNRAS, 432, 2284

Murphy S. J., Bedding T. R., Shibahashi H., Kurtz D. W., Kjeldsen H., 2014, MNRAS, 441, 2515

Murphy S. J., Fossati L., Bedding T. R., Saio H., Kurtz D. W., Grassitelli L., Wang E. S., 2016, MNRAS, 459, 1201

Niemczura E. et al., 2015, MNRAS, 450, 2764

Nowakowski R. M., 2005, Acta Astron., 55, 1

Osaki J., 1975, PASJ, 27, 237

Pamyatnykh A. A., 2003, Ap&SS, 284, 97

Pápics P. I., 2012, Astron. Nachr., 333, 1053

Pinsonneault M. H., An D., Molenda-Żakowicz J., Chaplin W. J., Metcalfe T. S., Bruntt H., 2012, ApJS, 199, 30

Pollacco D. L. et al., 2006, PASP, 118, 1407

Ricker G. R. et al., 2015, J. Astron. Telesc. Instrum. Syst., 1, 014003

Rodríguez E., Breger M., 2001, A&A, 366, 178

Saio H., Kurtz D. W., Takata M., Shibahashi H., Murphy S. J., Sekii T., Bedding T. R., 2015, MNRAS, 447, 3264

Schmid V. S. et al., 2014, A&A, 570, A33

Schmid V. S. et al., 2015, A&A, 584, A35

Shibahashi H., Kurtz D. W., 2012, MNRAS, 422, 738

Shibahashi H., Kurtz D. W., Murphy S. J., 2015, MNRAS, 450, 3999

Smith J. C. et al., 2012, PASP, 124, 1000

Stellingwerf R. F., 1979, ApJ, 227, 935

Stello D., Cantiello M., Fuller J., Huber D., García R. A., Bedding T. R., Bildsten L., Aguirre V. S., 2016, Nature, 529, 364

Stumpe M. C. et al., 2012, PASP, 124, 985

Triana S. A., Moravveji E., Pápics P. I., Aerts C., Kawaler S. D., Christensen-Dalsgaard J., 2015, ApJ, 810, 16

Uytterhoeven K. et al., 2011, A&A, 534, A125

Van Reeth T. et al., 2015, ApJS, 218, 27

Wu Y., 2001, MNRAS, 323, 248

Zima W. et al., 2006, A&A, 455, 235

Zorec J., Royer F., 2012, A&A, 537, A120

SUPPORTING INFORMATION

Additional Supporting Information may be found in the online version of this article:

Table 1. Stellar parameters as listed in Huber et al. (2014), and the number of AMod and NoMod frequencies for all 983 delta Scuti stars (http://www.mnras.oxfordjournals.org/lookup/suppl/doi:10.1093/mnras/stw1153/-/DC1).

Please note: Oxford University Press are not responsible for the content or functionality of any supporting materials supplied by the authors. Any queries (other than missing material) should be directed to the corresponding author for the article.

This paper has been typeset from a TEX/LATEX file prepared by the author.

5.3 Amplitude modulation catalogue extract

In this section, my amplitude modulation catalogue for all 983 δ Sct stars is presented[1]. Using a similar approach to the *Kepler* data catalogues discussed in chapter 2, each page of my amplitude modulation catalogue contains a star's unique KIC number and the stellar parameters listed in the KIC at the top of the page. However, in the amplitude modulation catalogue there is only a single page per star as the entire 4 yr *Kepler* data set was used to calculate the amplitude spectrum and tracking plot for each star.

The following page is an extract from the automated amplitude modulation catalogue for the δ Sct star KIC 7106205. The top panel is the amplitude spectrum using 4 yr of LC *Kepler* data calculated out to the LC Nyquist frequency. The amplitude and phase tracking plot is shown in the bottom panel, in which nine peaks (out of a maximum of 12) that have amplitudes greater than 0.1 mmag are tracked in 100-d bins with a 50-d overlap. This amplitude modulation catalogue, and especially the example of KIC 7106205, clearly demonstrates how δ Sct stars can be aperiodic and can have dramatic variability in pulsation mode amplitudes. This catalogue will remain of great use to myself and the research community for years to come as the length of the 4-yr *Kepler* data set will not be surpassed for some time.

A commonly used criterion for whether a peak in an amplitude spectrum is statistically significant is if it has a signal-to-noise ratio in amplitude of $S/N \geq 4$ (Breger et al. 1993). However, in my catalogue a maximum number of twelve frequencies were extracted up to a chosen amplitude cut-off off $A \geq 0.1$ mmag, for the reasons specified by Bowman et al. (2016). As previously mentioned, the δ Sct star KIC 7106205 has a low mode density in its amplitude spectrum, which is why only nine frequencies are extracted.

---

[1]My complete amplitude modulation catalogue for all 983 δ Sct stars can be obtained in PDF format from http://uclandata.uclan.ac.uk/42/

kic007106205

Teff= 6967
log(g)= 4.052
Radius= 1.775 $R_\odot$

$[Fe/H]$= -0.012
Contam= 0.005
Kep Mag= 11.455

v_1 = 10.032366 d^{-1}
v_2 = 10.727317 d^{-1}
v_3 = 13.394175 d^{-1}
v_4 = 10.847736 d^{-1}
v_5 = 9.058813 d^{-1}
v_6 = 9.982065 d^{-1}
v_7 = 8.019319 d^{-1}
v_8 = 11.442123 d^{-1}
v_9 = 16.453039 d^{-1}
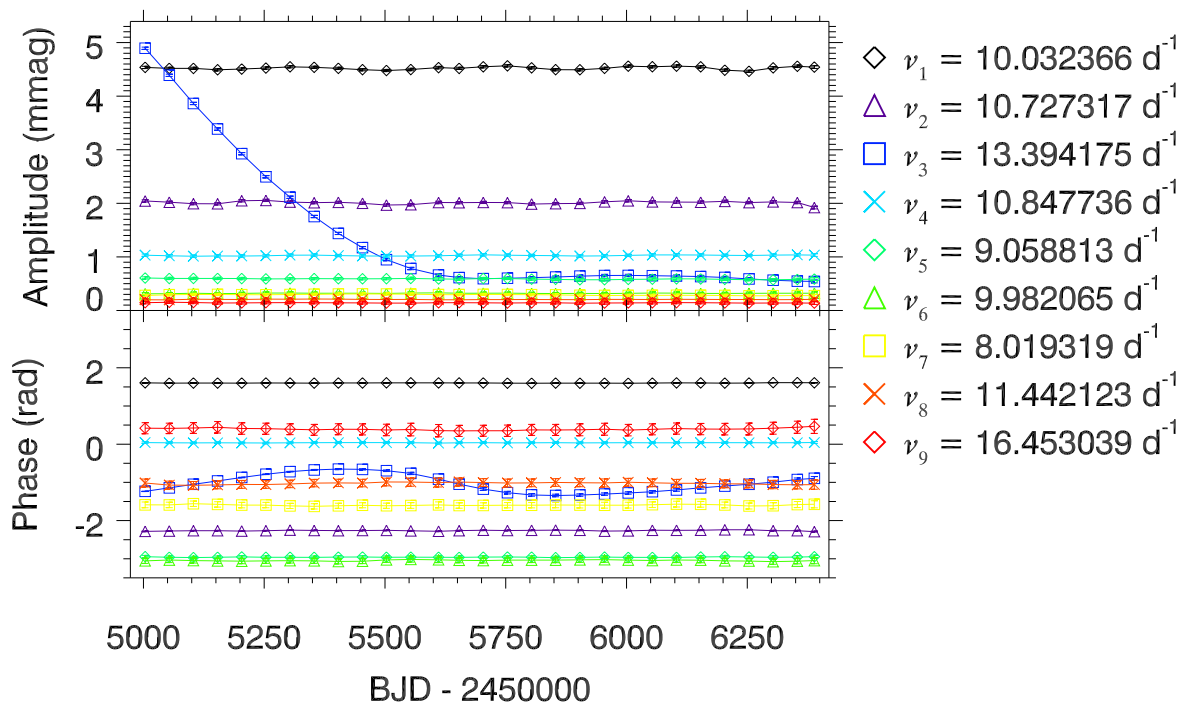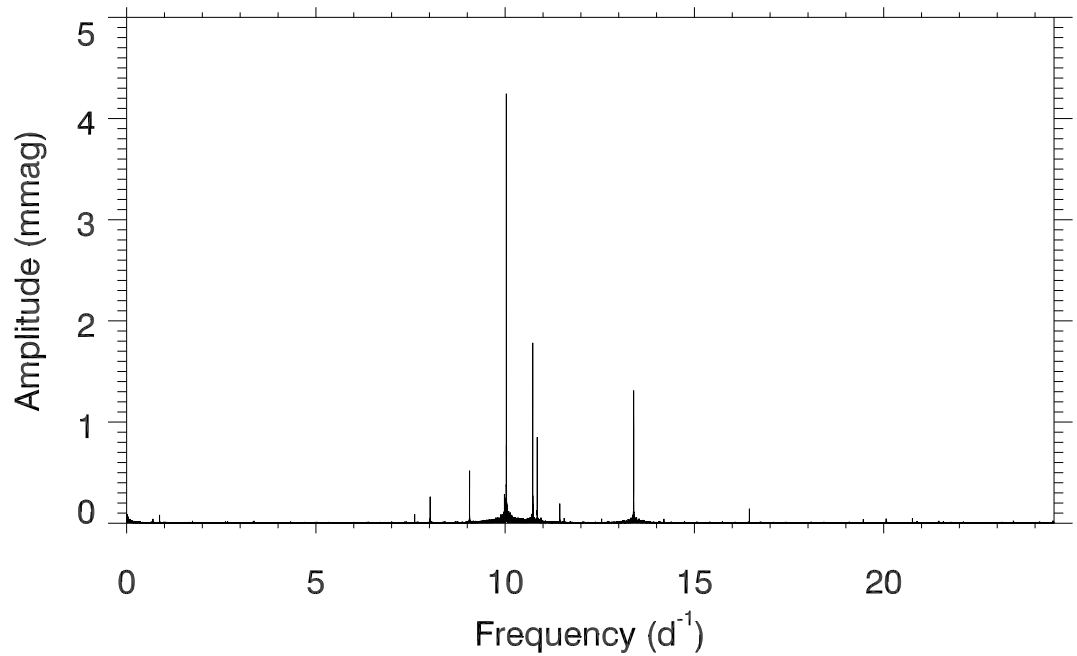
5.4 Ruling out rotation as the cause of AMod

There is no obvious correlation between a star being classified as AMod and the rotational velocity of a star. This is investigated using the subsample of δ Sct stars studied by Niemczura et al. (2015), for which accurate values of $v \sin i$ determined from high-resolution spectroscopy are available. The relationship between the frequency of the highest amplitude pulsation mode against $v \sin i$ from Fig. 4.14 has been regenerated in Fig. 5.1, but with each star denoted as a blue diamond or a red square to represent if it is NoMod or AMod, respectively. AMod and NoMod stars are found amongst the slow and fast rotators in the subsample of δ Sct stars studied by Niemczura et al. (2015), so it is unlikely to be related to the amplitude modulation in δ Sct stars.

5.5 Investigating the unresolved close-frequency mode hypothesis

It is certainly plausible that many AMod δ Sct stars can be explained by the beating of unresolved close-frequency pulsation modes. Using a similar method to that discussed by Bowman et al. (2016) for resolved pulsation mode frequencies, beating models of multiple unresolved frequencies could be constructed to explain amplitude modulation in many δ Sct stars, but this requires the number of frequencies to be known *a priori*. Theoretically, it is possible for many non-radial pulsation mode frequencies to exist closer than the 4-yr *Kepler* resolution limit of 0.00068 d^{-1}, and maintain their independent identity over several years (H. Saio, *private communication*). If this is the case for many of the AMod δ Sct stars in this study, it would explain the non-sinusoidal modulation cycles because of the complicated beating pattern of multiple unresolved close-frequency pulsation modes (Bowman et al. 2016).

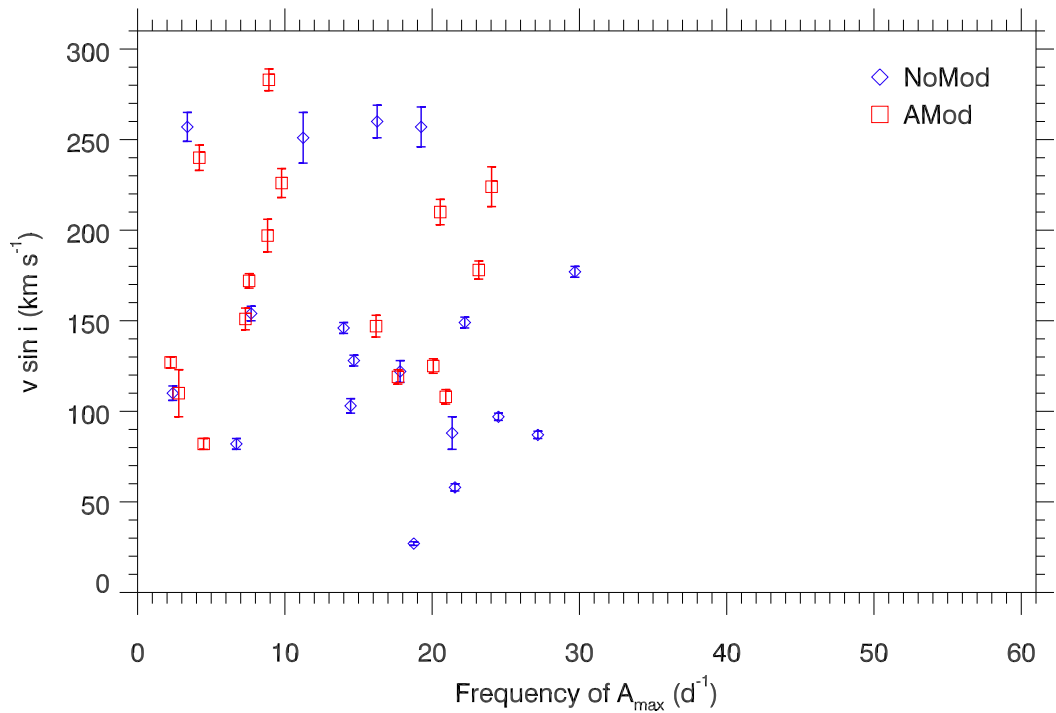Figure 5.1: Relationship between rotation, pulsation and amplitude modulation. The same subsample of δ Sct stars studied by Niemczura et al. (2015) as shown in Fig. 4.14 are given here, but each star is now denoted as a blue diamond or red square if it is NoMod or AMod, respectively. For the few stars in this figure, there is no obvious correlation between rotational velocity and amplitude modulation.

CHAPTER 5

Table 5.1: Parameters of three hypothetical pulsation modes used to demonstrate amplitude and phase modulation caused by the beating of unresolved frequencies in a synthetic *Kepler* data set.

	Frequency (d^{-1})	Amplitude (mmag)	Phase (rad)
ν_1	13.393837	5.00	-3.00
ν_2	13.394177	10.00	-1.00
ν_3	13.394517	5.00	2.00

To test this hypothesis, synthetic *Kepler* data with appropriate white noise and three hypothetical unresolved pulsation modes are generated using 4 yr of *Kepler* time stamps and the frequencies, amplitudes and phases given in Table 5.1. The properties of these three hypothetical pulsation modes are chosen to emulate the observed amplitude modulation in the δ Sct star KIC 7106205, which was discussed in chapter 3. The resultant light curve and a zoom-in of the unresolved peak in the amplitude spectrum are shown in the top and middle panels of Fig. 5.2, respectively.

The amplitude and phase tracking routine discussed by Bowman et al. (2016) is applied to the synthetic data set, such that frequency, amplitude and phase values are extracted and optimised using a non-linear least-squares fit. Subsequently, amplitude and phase are tracked in 100-d bins with a 50-d overlap at fixed frequency using linear least-squares throughout the 1500-d synthetic data set. Note that only a single frequency is extracted from the amplitude spectrum because the other two lie within the 4-yr *Kepler* resolution limit and are not resolved. The amplitude and phase tracking plot for the extracted frequency, $\nu = 13.393998$ d^{-1}, is shown in the bottom panel of Fig. 5.2.

The amplitude and phase modulation for this synthetic data set is qualitatively similar to the observed amplitude and phase modulation in KIC 7106205 studied by Bowman & Kurtz (2014) and discussed in chapter 3. For example, the extracted peak at $\nu = 13.393998$ d^{-1} experiences an approximately linear decrease in
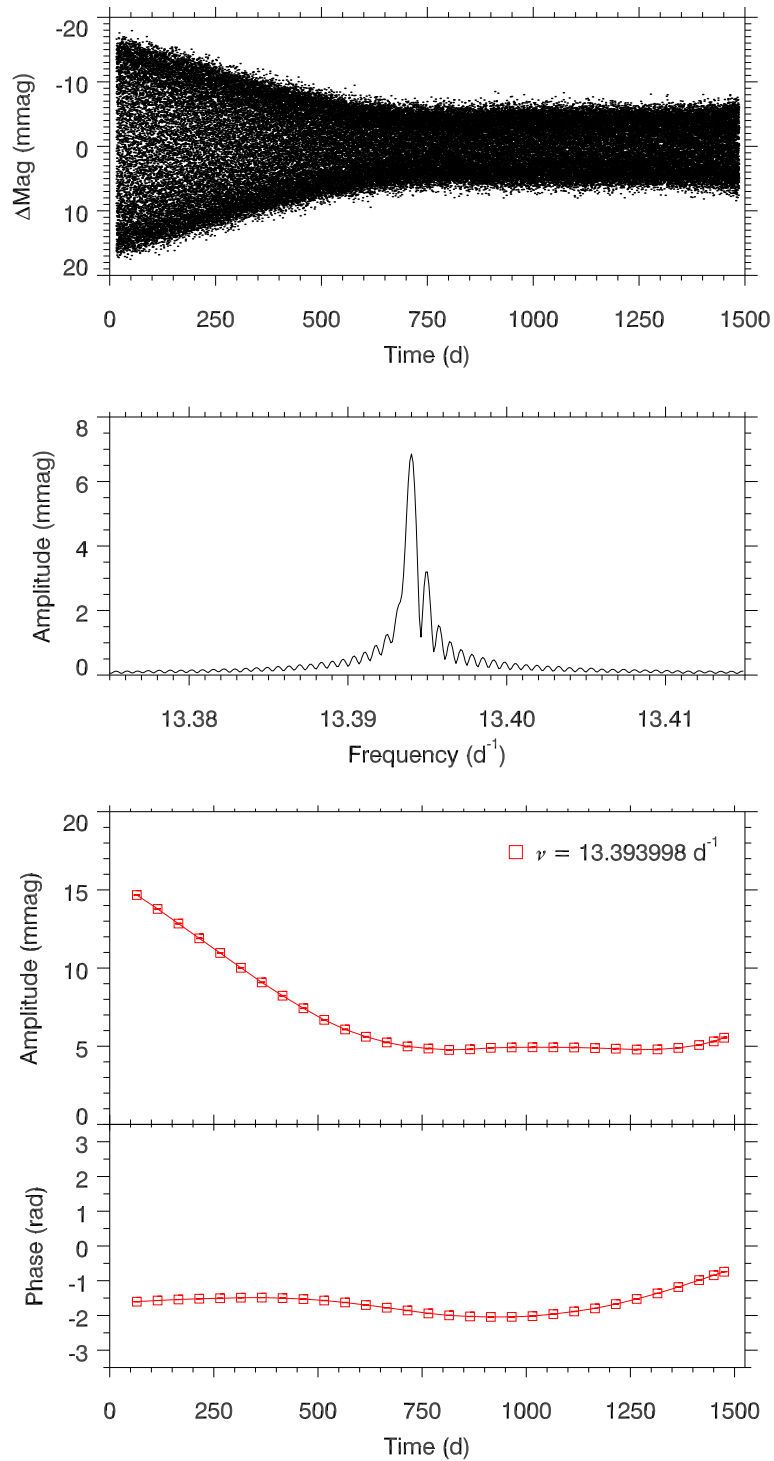
Figure 5.2: Analysis of synthetic *Kepler* data with three hypothetical unresolved pulsation modes. The top panel is the 1500-d light curve. The middle panel is a zoom-in of the unresolved peaks in the amplitude spectrum. The bottom panel is the resultant amplitude and phase tracking plot for the extracted frequency of $\nu = 13.393998$ d^{-1}.

amplitude and then stays approximately constant in amplitude over 4 yr, whilst a quasi-sinusoidal phase modulation is observed. The cause of the amplitude modulation in KIC 7106205 was not definitively established by Bowman & Kurtz (2014), who were unable to conclude if beating, mode coupling to invisible pulsation modes or variable driving/damping in the star was the cause. The similar characteristic amplitude modulation observed using this hypothetical case study demonstrates that beating of unresolved close-frequency pulsation modes is a viable solution, not only for the observed amplitude modulation in KIC 7106205 but in other δ Sct stars as well.

The characteristic behaviour of beating is most easily recognised with two cosinusoids of equal amplitude, which was demonstrated for the δ Sct stars KIC 4641555 and KIC 8246833 by Bowman et al. (2016). In this scenario, the visible (and assumed single frequency) peak varies sinusoidally in amplitude with a period equal to the beat period, but also varies in phase: a half cycle (i.e., π rad) change in phase occurs at the epoch of minimum amplitude (Breger & Pamyatnykh 2006), and the amplitude modulates between 2A and 0. If the cosinusoids have increasingly different amplitudes, the amplitude and phase changes get progressively smaller. However, the amplitude and phase must always vary synchronously with a phase lag (shift) close to $\pi/2$ rad, such that the epoch of minimum amplitude in the beat cycle occurs at the time of average and most rapid change in phase (Breger & Pamyatnykh 2006; Bowman et al. 2016).

For beating from multiple unresolved close-frequency pulsation modes, the number of unresolved pulsation modes and their frequencies, amplitudes and phase determine the observed amplitude modulation. It was concluded by Bowman et al. (2016) that the functional form of the curves in an amplitude and phase tracking plot can be used to estimate the number of input modes needed, but a reliable method is needed to determine the frequencies, amplitudes and phases of these modes. One

such method is discussed next in section 5.5.1.

5.5.1 MCMC simulations

In this section, a discussion of the feasibility of using a Bayesian Markov-chain Monte-Carlo (MCMC) simulation for investigating if amplitude modulation is caused by the beating of close-frequency pulsation modes is provided. This method is computationally expensive compared to frequency extraction by iterative pre-whitening and optimisation by least-squares, but may offer a solution to extracting unresolved pulsation mode frequencies. The EMCEE software used to carry out this simulation was first implemented by Foreman-Mackey et al. (2013) and has been extensively discussed by Hambleton (2016). In the following paragraphs, a brief outline of how the MCMC simulation works is provided; we refer the reader to Hambleton (2016) for full details.

A Monte Carlo simulation is the random sampling of variables to obtain a distribution of possible results. A Markov chain is a stochastic chain of events that changes state in discrete steps, which has the special property that the transition between steps only depends on the current state and not on a previous state (Hambleton 2016). These two principles were first combined by Metropolis et al. (1953) who proposed using a series of chains to perform a random walk using the following prescription. The walkers are given a range of inputs for each variable (i.e., priors), which are used to perform a computation and calculate a probability. The result of the next step is compared to the result of the previous step and only results that improve the value of the probability are accepted.

After many iterations each chain will have sampled the parameter space where the probability density is highest and converged to the best-fitting solution. The initial period is called the burn-in period, which is when the chains are still converging to the optimum solution, from which the posterior distributions of the amplitude,

frequency and phase parameters can be determined. The mean and standard deviation of these parameters are determined by fitting a Gaussian to each distribution.

Implementation for a single pulsation mode

As a preliminary test, a single pulsation mode with frequency $\nu = 10.0$ d^{-1}, amplitude $A = 10.0$ mmag and phase $\phi = 0.0$ rad is used as an input signal in a synthetic time series and an MCMC simulation is performed using uniform priors to search for the optimum cosinusoid solution. Specifically, the priors for each parameter are $9.5 \leq \nu \leq 10.5$ d^{-1}, $0.1 \leq A \leq 50$ mmag and $-\pi \leq \phi \leq \pi$ rad, respectively, which are chosen to be consistent with observations of δ Sct stars.

The results from the search for a pulsation mode using a MCMC simulation are shown in Fig. 5.3, which contains the 1D histograms and 2D contour plots showing the minimum in the log-likelihood probability, thus indicating convergence to the correct solution. The frequency, amplitude and phase solutions and their 1σ uncertainties are given above each column in Fig. 5.3, with the values and uncertainties calculated from the centroids and standard deviations, respectively, of the Gaussian fits to the 1D histogram in each column.

The successful implementation of a Bayesian MCMC simulation to find a single pulsation mode using synthetic *Kepler* data is a proof of concept exercise. It has been demonstrated that this method is able to converge to the correct multi-parameter solution using this hypothetical scenario. In the following section, a MCMC simulation is used to find three unresolved pulsation modes that lie closer together than the 4-yr *Kepler* frequency resolution.

Implementation for three unresolved pulsation modes

Using a similar method to that discussed in the previous section for a single pulsation mode, a MCMC simulation is used to search for three pulsation modes in the
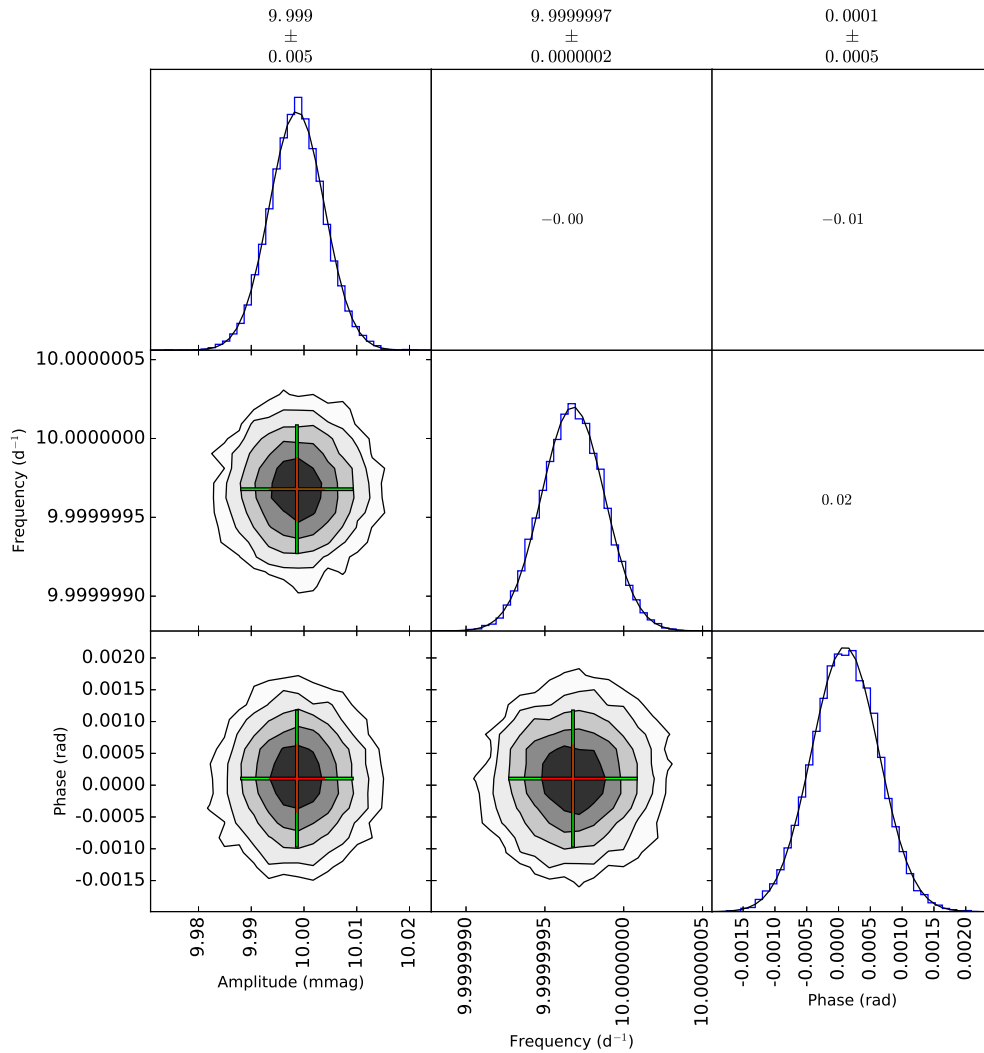
Figure 5.3: Results from a successful MCMC simulation to find the parameters of a single pulsation mode using synthetic *Kepler* data. The contour plots in the lower-left sub-plots show cross-sections of the posterior probability distribution functions for the amplitude, frequency and phase, with the red and green crosses showing the 1σ and 2σ uncertainties, respectively. The sub-plots on the diagonal from top-left to bottom-right show histograms of the probability distribution for each parameter, with a mean value and its 1σ uncertainty obtained from a Gaussian fit given above each column of the plot. The numbers in the top-right sub-plots give the correlation between two parameters with 1 indicating direct correlation and -1 indicating direct anti-correlation.

synthetic data set created using the parameters given in Table 5.1. The priors in amplitude, frequency and phase used are $13.0 \leq \nu \leq 13.8$ d^{-1}, $0.1 \leq A \leq 50$ mmag and $-\pi \leq \phi \leq \pi$ rad, respectively. The results from the search for these three pulsation modes using a MCMC simulation are shown in Fig. 5.4, which has a similar layout to Fig. 5.3 but has a grid of nine rows and columns for the three pulsation modes and their respective frequencies, amplitudes and phases. Similarly to the previous example, this MCMC simulation has successfully converged to the correct solution, with the parameters and their respective errors given above plot in Fig. 5.4, which are within 1σ of the input parameters given in Table 5.1.

This MCMC simulation is also another useful proof of concept exercise that demonstrates that it is possible to determine the parameters of unresolved pulsation modes in a δ Sct star in the *Kepler* data set. It should be noted that the synthetic data used in this and the previous example do not contain any other pulsation modes, thus these simulations should be considered idealistic scenarios. Most importantly, the *number* of pulsation modes is known in these hypothetical scenarios, which is certainly not true when applying this technique to real observations of δ Sct stars in the *Kepler* data set.

In a similar way, a multifrequency solution could be found that accurately describes the observed amplitude modulation in at least a few of the AMod δ Sct stars discussed by Bowman et al. (2016). However, such a simulation is computationally expensive to run, and is therefore inefficient for frequency extraction compared to, for example, Fourier analysis and iterative pre-whitening techniques. In the next section, the implementation of MCMC simulations is discussed for the δ Sct star KIC 7106205 studied by Bowman & Kurtz (2014) and discussed in chapter 3.
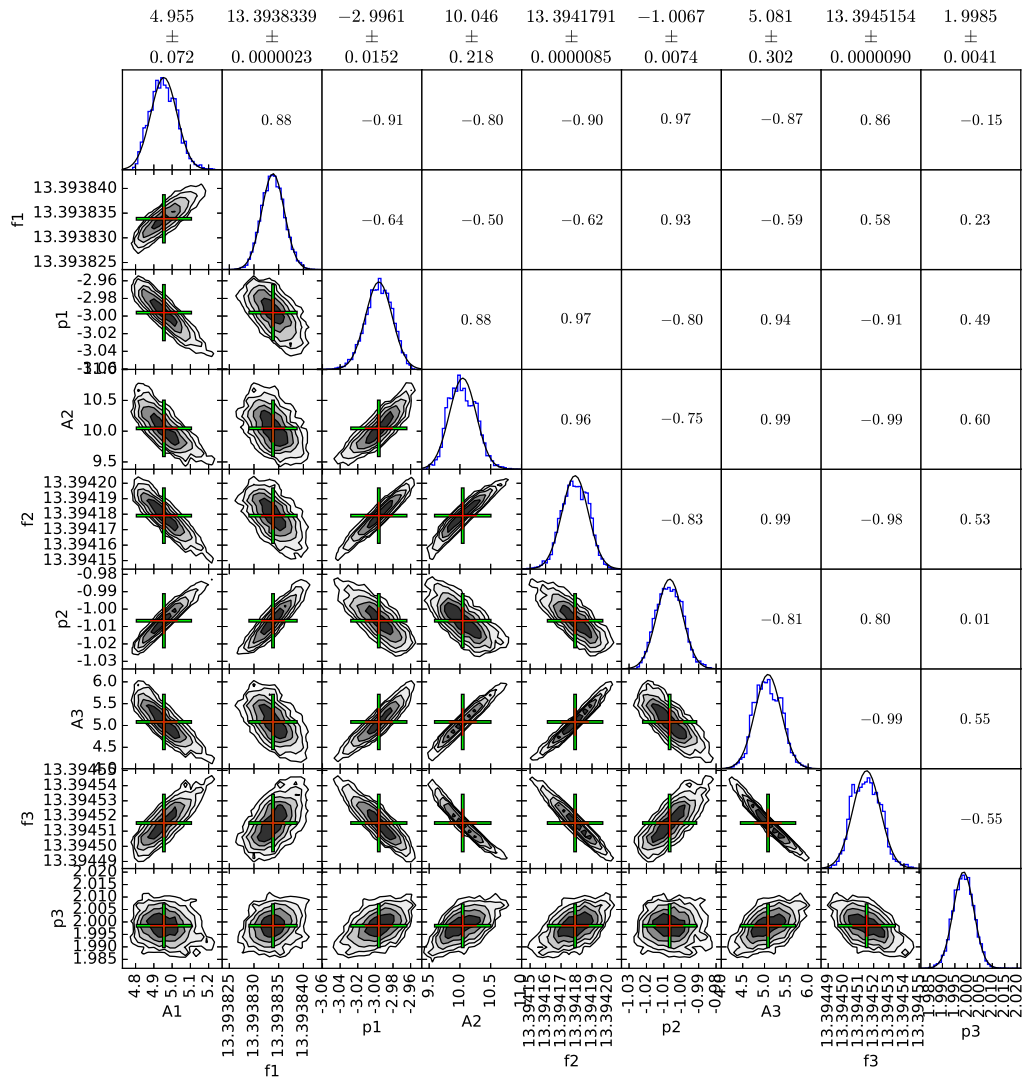
Figure 5.4: Results from a successful MCMC simulation to find the parameters of three pulsation modes that lie closer than the 4-yr *Kepler* frequency resolution using synthetic data. The layout of this figure is similar to that of Fig. 5.3, but has three frequencies, amplitudes and phases instead.

CHAPTER 5

Application to KIC 7106205

It is shown by Bowman et al. (2016) that the beating of two cosinusoid signals produces periodic amplitude modulation and a phase change at the epoch of minimum amplitude. The observed amplitude modulation in KIC 7106205 is not periodic over the 4-yr *Kepler* data set, indicating that if beating of unresolved close-frequency pulsation modes is responsible, a minimum of three pulsation modes would be needed. MCMC simulations using two, three and four pulsation modes were implemented for the *Kepler* data set for the δ Sct star KIC 7106205, but these simulations do not converge to a reasonable solution, thus do not produce meaningful posterior probability distributions.

Since in the previous section it is demonstrated that an MCMC simulation is able to converge to the correct solution and extract the parameters of three unresolved pulsation modes using synthetic *Kepler* data, it can be inferred that the beating of two, three of four pulsation modes is not responsible for the observed amplitude modulation in KIC 7106205. It is unlikely that five or more independent pulsation modes can lie closer together than the 4-yr *Kepler* frequency resolution of $0.00068 \, \mathrm{d}^{-1}$ (8 nHz) in a star with a low mode density such as KIC 7106205. Therefore, the amplitude modulation in the δ Sct star KIC 7106205 remains an unsolved problem.

5.6 Discussion

In this chapter, the results of a thorough search for amplitude modulation in 983 δ Sct stars that were continuously observed by the *Kepler* Space Telescope for 4 yr have been presented. The *Kepler* data set provides extremely high frequency resolution and amplitude precision, which were used to track amplitude and phase at fixed frequency in 100-d bins with a 50-d overlap for a maximum number of 12 peaks with amplitudes greater that 0.10 mmag for each star in the ensemble of 983 δ Sct

stars, with the results collated into an amplitude modulation catalogue published by Bowman et al. (2016). Various case studies of stars were used by Bowman et al. (2016) to demonstrate the diversity in pulsational behaviour of δ Sct stars including binarity, beating and non-linearity, which was discussed in section 5.2. An extract of the amplitude modulation catalogue[2] from Bowman et al. (2016) was presented in section 5.3.

The main conclusion from this study is that 603 of the 983 δ Sct stars in the ensemble (61.3 per cent) exhibit at least one pulsation mode that varies significantly in amplitude over 4 yr, and so amplitude modulation is common among δ Sct stars (Bowman et al. 2016). The causes of variable pulsation amplitudes in δ Sct stars, which were termed AMod stars by Bowman et al. (2016), can be categorised into those that are caused by extrinsic or intrinsic causes. The extrinsic causes of phase variability include binarity (or multiplicity) in the stellar system which acts as a perturbation to the pulsation mode frequencies observed (Shibahashi & Kurtz 2012; Shibahashi et al. 2015). A pulsating star can also be easily recognised as being part of a multiple system as all its pulsation modes will be phase modulated by the orbital period of the stellar system (Murphy et al. 2014). Similarly, super-Nyquist aliases are easily identifiable because they are periodically phase modulated by a variable Nyquist frequency with the orbital period of the *Kepler* Space Telescope (Murphy et al. 2013b; Bowman et al. 2016).

Intrinsic causes of amplitude modulation include beating and non-linearity, the latter of which is discussed in more detail in chapter 6. It has been demonstrated by different studies how pulsational non-linearity is likely the cause of amplitude modulation in δ Sct stars (e.g., Breger & Montgomery 2014; Barceló Forteza et al. 2015). Clearly, further work is needed to identify more δ Sct stars with mode coupling and

---

[2]My complete amplitude modulation catalogue for all 983 δ Sct stars can be obtained in PDF format from http://uclandata.uclan.ac.uk/42/

study them in greater detail. The subgroup of stars that exhibit amplitude modulation with no phase change is particularly interesting. In these stars, the amplitude change is non-periodic and often is monotonically variable over the 4-yr *Kepler* data set. Approximately the same number of stars with linearly increasing and decreasing amplitudes, but also non-linearly increasing and decreasing amplitudes were noted in this subgroup by Bowman et al. (2016). These pure AMod stars remain a challenge to understand, so one can only speculate until further investigation is carried out.

Beating of unresolved close-frequency pulsation modes is a plausible explanation for the amplitude modulation observed in many δ Sct stars, but it is yet to be established how and why this could occur in stars with such low mode densities in their amplitude spectra (e.g., KIC 7106205). To test this hypothesis, a Bayesian MCMC simulation was successfully able to extract pulsation mode parameters from a synthetic data set containing three unresolved pulsation modes. This technique may be computationally expensive and time-consuming compared to frequency extraction by iterative pre-whitening, but it was a useful proof of concept exercise. However, the implementation of this technique for the δ Sct star KIC 7106205 yielded inconclusive results. Thus, the observed amplitude modulation remains unexplained in this δ Sct star.

The 380 δ Sct stars classified as NoMod (No Modulation) by Bowman et al. (2016) comprise 38.7 per cent of the ensemble of 983 δ Sct stars and represent the stars for which the highest precision measurements of amplitude and frequency are possible. This is important in the search for planets orbiting these stars when using the FM method (Shibahashi & Kurtz 2012; Shibahashi et al. 2015). These NoMod stars are excellent targets for determining precise frequencies and amplitudes for asteroseismic modelling (Bowman et al. 2016), and warrant further study.

CHAPTER 5

Note that from an observational point of view, the cause of the amplitude modulation in δ Sct stars is interesting, but not necessarily important. What is important to realise is that short term observations of the order a few years provide an *average* amplitude of a pulsation mode, if it is varying on time-scales of the order a few decades or longer. Naturally, it is interesting to determine the mechanism that causes amplitude modulation, as it has implications for our understanding of non-linearity, driving and damping processes in these stars, which is discussed in further detail chapter 6.

The catalogue of 983 δ Sct stars published by Bowman et al. (2016), which used 4 yr of *Kepler* data demonstrates that observations spanning years (and longer) are often needed to study and resolve pulsational behaviour in these stars. My catalogue will be useful for comparison purposes when studying δ Sct stars observed by K2 (Howell et al. 2014) and TESS (Ricker et al. 2015). Eventually, these missions will observe a large area of the sky, but for only a short length of time. Therefore, *Kepler* may represent the best data set for studying δ Sct stars as its 4-yr length of continuous observations will not be surpassed for some time.

Chapter 6

Characterising pulsational non-linearity

Some of the discussions in this chapter, specifically sections 6.2.2 and 6.2.3, were published by Bowman et al. (2016) in August 2016, and are therefore also included in chapter 5.

6.1   Introductory remarks

It has been known for some time that non-linear stellar models are needed to accurately reproduce observations of δ Sct stars (Cox 1980; Stellingwerf 1980; Saio & Cox 1980), with linear models providing no predictive power of pulsation mode amplitudes. The observed temporal variability in pulsation mode frequencies, amplitudes and phases demonstrated for the majority of δ Sct stars in chapter 5 is beyond the linear theory of non-radial stellar pulsation given by Unno et al. (1989). Furthermore, non-linear theoretical models of δ Sct stars often predict much larger pulsation mode amplitudes than are observed, which suggests that an amplitude limitation mechanism or limit cycle is required to stop the exponential growth of pulsation mode amplitudes (Breger 2000a; Aerts et al. 2010).

In this chapter, the non-linearity of pulsations in δ Sct and γ Dor stars is investigated. It is only recently that high-quality observations, such as those provided by the *Kepler* Space Telescope, have allowed theoretical predictions of non-linearity to be investigated in δ Sct stars. Using models of mode coupling discussed by Breger & Montgomery (2014) and Bowman et al. (2016), the strength of non-linearity can be investigated in pulsating stars. In section 6.2, the distinction between combination frequencies and mode coupling of pulsation modes is discussed, with the application of the mode coupling hypothesis for δ Sct and γ Dor stars presented in sections 6.3 and 6.4, respectively. In section 6.5 the pulsational energy budget is discussed in the context of amplitude modulation in δ Sct stars.

6.2   Coupling versus combination frequencies?

Although Fourier analysis is the preferred method for analysing pulsating stars, with a stellar time series being represented as a series of sinusoids or cosinusoids, harmonics and combination frequencies are mathematically required to describe non-linearity in the frequency domain. This is analogous to a non-sinusoidal light curve describing non-linearity of pulsations in the time domain. One form of non-linearity is quicker rise times than fall times over the pulsation cycle in the light curves of high amplitude pulsators, which is commonly observed in type I Cepheids and RRab stars (see section 1.4.4). These stars have asymmetric light curves that are often characterised as 'upwards' light curves, but it has also been shown that non-linearity can be responsible for the 'downwards' asymmetry seen in the light curves of γ Dor and SPB stars (Kurtz et al. 2015).

Therefore, one of the important tasks when studying a pulsating star is to identify which peaks in the amplitude spectrum are pulsation mode frequencies and which peaks are combination frequencies and harmonics. Not only can this greatly simplify an amplitude spectrum, but the pulsation mode frequencies are the main parameters

used for asteroseismic modelling. This task can be difficult for stars with high pulsation mode densities in their amplitude spectra — for example, see Pápics (2012), Breger & Montgomery (2014) and Kurtz et al. (2015).

It is discussed in chapter 5 how there is a subtle difference between combination frequencies and coupled pulsation mode frequencies from an observational perspective. Combination frequencies and harmonics occur due to the mathematical representation of the summation of cosine terms for a non-linear signal when calculating the Fourier transform. Physically, this effect differs to a family of pulsation modes, which contain parent modes that are able to interact and resonantly excite a child mode in a star (e.g., Breger & Montgomery 2014). Therefore, it is important to be able to distinguish these two effects and extract the real pulsation mode frequencies of a star.

The study of non-linearity in pulsating stars is complicated because it was shown mathematically and observationally by Kurtz et al. (2015) that combination frequencies can have higher amplitudes than the parent pulsation modes that create them. In this section, a method for identifying combination frequencies and the strength of non-linearity in a star is discussed, with a specific case study example of the δ Sct star KIC 8054146 studied by Breger & Montgomery (2014) presented in section 6.2.4.

6.2.1 Combination frequencies

Combination frequencies and harmonics are common in many types of pulsating stars across the HR diagram, which include δ Sct stars (see e.g., Breger et al. 2012; Murphy et al. 2013a; Breger & Montgomery 2014), and also SPB and γ Dor stars (see e.g., Kurtz et al. 2015; Van Reeth et al. 2015b) and pulsating white dwarf stars (see e.g., Wu & Goldreich 2001; Wu 2001). Combination frequencies are mathematical sum and difference frequencies of pulsation mode frequencies, ν_i and ν_j, that have the form $n\nu_i \pm m\nu_j$, in which n and m are integers. Combination frequencies have

been extensively studied in pulsating DA and DB white dwarf stars, and therefore a significant fraction of the literature on combination frequencies is based on g mode pulsators with thin convective envelopes (Brickhill 1983, 1990, 1991a,b, 1992b,a; Brassard et al. 1993; Wu & Goldreich 2001; Wu 2001; Montgomery 2005).

Possible mechanisms to explain combination frequencies in variable DA and DB white dwarfs are that the stellar medium does not respond linearly to the pulsation wave, or that the dependence of emergent flux variation is not a linear transformation from the temperature variation ($F = \sigma T^4$). These are often grouped into what is termed a non-linear distortion model (e.g., Degroote et al. 2009). The assumptions and predictions made from these studies of variable white dwarfs may not apply to all types of pulsator, but act as a useful starting point for an investigation of non-linearity in main sequence stars.

In the case of the β Cep star HD 180642, Degroote et al. (2009) found that the sum and difference combination frequencies had similar amplitudes, but that there were more sum combination frequencies in the star's amplitude spectrum. The comparable amplitudes of three peaks, which were related in frequency and phase and formed a family of modes, did not distinguish between non-linearity in the form of a non-linear distortion model and non-linearity in the form of resonant mode coupling (Degroote et al. 2009).

The simplest and lowest order non-linear combination signal, $y_{\mathrm{c}}(t)$, that can be produced from the mixing of

$$y_1(t) = A_1 \cos\left(2\pi\nu_1 t + \phi_1\right)$$

and

$$y_2(t) = A_2 \cos\left(2\pi\nu_2 t + \phi_2\right)$$

is given by

$$y_c(t) \propto y_1 \, y_2$$

$$\propto A_1 \cos\left(2\pi\nu_1 t + \phi_1\right) A_2 \cos\left(2\pi\nu_2 t + \phi_2\right)$$

$$\equiv A_c \cos\left(2\pi\nu_{c+} t + \phi_{c+}\right) + A_c \cos\left(2\pi\nu_{c-} t + \phi_{c-}\right) \, ,$$

where

$$A_c = \frac{1}{2}A_1 A_2$$

$$\nu_{c\pm} = \nu_1 \pm \nu_2$$

$$\phi_{c\pm} = \phi_1 \pm \phi_2 \, .$$

This was discussed in detail by (Brickhill 1992b) and Wu (2001), who stated that since combination frequencies are not intrinsic pulsation mode frequencies and are caused by non-linearities within a star, then their amplitudes and phases must mimic the parent frequencies, $y_1(t)$ and $y_2(t)$, that create them. However, it was shown by Kurtz et al. (2015) that it is possible for combination frequencies to have larger observed amplitudes than the parent modes. This demonstrates that our understanding of combination frequencies, specifically how they are formed, is far from complete.

One method of identifying combination frequencies is to mathematically generate all the possible combination terms from a small number of parent frequencies, fit them by least-squares and remove them by pre-whitening (e.g., Kurtz et al. 2015). Alternatively, iterative pre-whitening can be used to extract all statistically-significant frequencies and then exclude those that satisfy a combination frequency relation (e.g., Van Reeth et al. 2015b). However, the physical mechanism that causes combination frequencies is not immediately obvious.
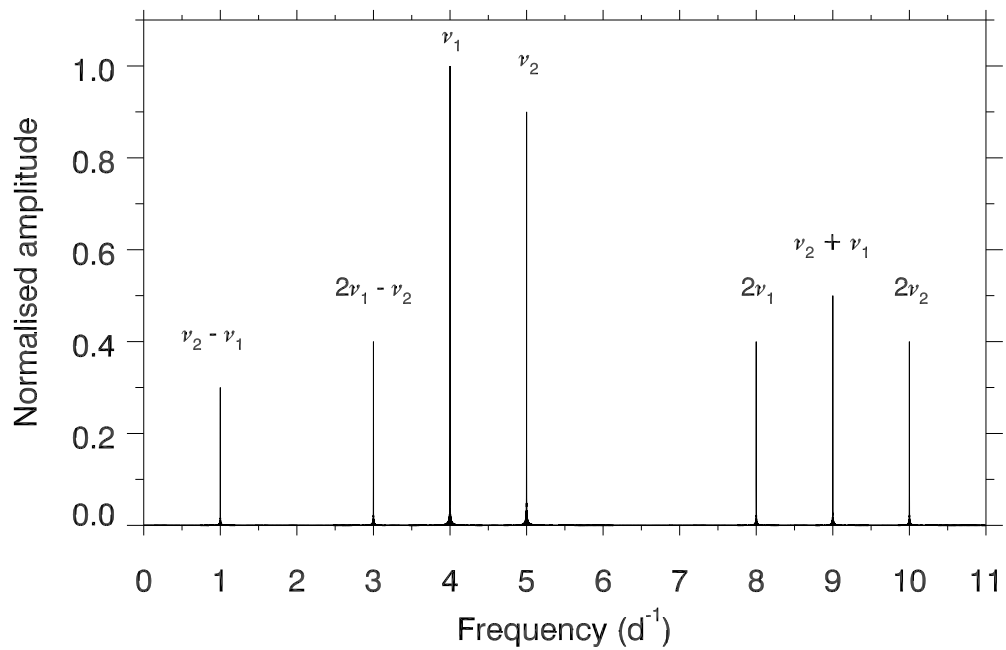
Figure 6.1: Schematic demonstrating how two non-linear pulsation frequencies, ν_1 and ν_2, can create combination frequency triplets, for example, $2\nu_1$, $\nu_2 + \nu_1$ and $2\nu_2$, and apparent regularities in an amplitude spectrum. Figure inspired by Breger & Kolenberg (2006), their figure 1.

In Fig. 6.1, synthetic data are used to demonstrate how triplets of exactly equally-split frequencies can be made from two intrinsic pulsation modes, ν_1 and ν_2. The two pulsation mode frequencies, the harmonics of ν_1 and ν_2, the combination frequencies $\nu_1 + \nu_2$, $\nu_2 - \nu_1$ and $2\nu_1 - \nu_2$ are labelled in Fig. 6.1, showing how regularities in the amplitude spectrum of a pulsating star can be created from only two pulsation mode frequencies. It is important to note that the combination frequency, $2\nu_1 - \nu_2$, and the second pulsation mode frequency, ν_2, could be misinterpreted as part of an equally split triplet around ν_1, which was demonstrated by Breger & Kolenberg (2006). Mathematically, combination frequencies produce exactly equally-split multiplets, whereas the second-order effects of rotation perturb the symmetry of frequencies in a rotationally split multiplet (Goupil et al. 2000; Pamyatnykh 2003; Aerts et al. 2010). This is especially true for stars that are moderate and fast rotators, such as the δ Sct star KIC 8054146 (Breger et al. 2013; Breger & Montgomery 2014) discussed in section 6.2.4.

6.2.2   The role of resonances in pulsating stars

The role of non-linearity and resonances within pulsators driven by the heat engine driving mechanism is clearly non-trivial, and has been extensively studied in the literature (Dziembowski 1982; Buchler & Goupil 1984; Dziembowski & Krolikowska 1985; Moskalik 1985; Dziembowski et al. 1988; Dziembowski & Krolikowska 1990; Dziembowski & Goode 1992; Goupil & Buchler 1994; Van Hoolst 1994; Buchler et al. 1995, 1997; Goupil et al. 1998; Wu & Goldreich 2001; Wu 2001; Nowakowski 2005). In this section, an overview of the main forms of resonances in pulsating stars is given.

CHAPTER 6

Direct resonances: parents and children

An example of how non-linearity can act as an amplitude limitation mechanism in δ Sct stars is resonant mode coupling between a child mode and two parent modes (Dziembowski 1982). This form of pulsational non-linearity gives rise to variable frequencies and amplitudes in pulsation modes over time, which appear as a cluster of unresolved peaks in the amplitude spectrum. Resonant mode coupling has been suggested as the amplitude limitation mechanism operating in δ Sct stars but not in HADS stars, which explains the large difference in pulsation mode amplitudes between the two subgroups (Dziembowski & Krolikowska 1985). This form of resonance is commonly referred to as a direct resonance (Dziembowski 1982) or parent-child mode coupling (Breger & Montgomery 2014), and is discussed further in section 6.2.3.

Rotationally induced resonance

For a slowly rotating star, a non-radial pulsation mode will be split into its $2\ell + 1$ components. Taking a particular case of a dipole mode, a nearly equally split triplet of frequencies will be formed with a central frequency, ν_0, that corresponds to the $m = 0$ component and frequencies ν_- and ν_+ that correspond to the $m = -1$ and $m = +1$ components, respectively. It was first discussed by Buchler et al. (1995, 1997) and later by Goupil et al. (1998) how a resonance condition that satisfies $2\nu_0 \simeq \nu_+ + \nu_-$ exists, and causes variable pulsation mode amplitudes. This form of resonant mode coupling can be separated into three regimes.

First is the case of non-linear frequency locking. In this regime the triplet of frequency is exactly equally split, which produces constant amplitudes and thus no amplitude modulation. The second, so-called intermediate regime is when the frequency splitting of the triplet is no longer symmetric, which causes periodic amplitude modulation amongst the components of the triplet on the time-scale of

$P_{\mathrm{mod}} \sim \frac{1}{\delta\nu}$, where $\delta\nu$ is the asymmetry of the triplet (Goupil et al. 1998). When the frequency splitting is significantly asymmetric, for example in the presence of rapid rotation, the resonance condition is no longer satisfied because the non-linear frequency perturbations are very small, such that the observed frequencies are closer to the linear values (Buchler et al. 1995, 1997; Goupil et al. 1998).

This form of resonant mode coupling has also been studied in pulsating white dwarf stars (Vauclair 2013; Zong et al. 2016b) and pulsating sdB stars (Zong et al. 2016a). For example, the DBV star KIC 8626021 was studied by Østensen et al. (2011) and later by Zong et al. (2016b), who used approximately 684 d of SC *Kepler* data to discover several rotationally-split dipole modes that exhibit amplitude modulation. From the asymmetry of the frequency splitting in the triplets and the variable pulsation mode amplitudes, Zong et al. (2016b) were able to study the hyperfine structure of the component frequencies in the various triplets and conclude that non-linearity in the form of resonant mode coupling was responsible for the observed amplitude modulation.

Parametric resonance instability

The parametric resonance instability, which is also called a decay instability, was discussed by Dziembowski (1982) who demonstrated that two linearly damped low-frequency modes are able to damp a linearly driven high frequency pulsation mode when it has reached a critical amplitude. In his study, Dziembowski (1982) concluded that the most likely scenario is two linearly damped g modes coupling with an unstable p mode, which would cause the growth and decay of the p and g modes in anti-correlation as energy is exchanged among them (Dziembowski 1982; Dziembowski & Krolikowska 1985). Furthermore, the g modes may not have observable surface amplitudes – in this case, the modes are referred to as internal g modes

(Dziembowski & Krolikowska 1985) – making the testing of this theoretical prediction difficult (see e.g., Bowman & Kurtz 2014). To first order, the modulation time-scale is the inverse of the growth rate of the child mode involved in the resonance, which can produce modulation time-scales between days and several decades (Nowakowski 2005).

6.2.3 Mode coupling

In this section, the direct resonance scenario and the coupling of pulsation modes are discussed. Coupled pulsation modes are grouped into families of child and parent modes (e.g., Breger & Montgomery 2014), and this coupling can facilitate the exchange of energy between different members of the family (Dziembowski 1982; Buchler et al. 1997; Nowakowski 2005). In a direct resonance, a child mode must have a frequency very close to the sum, or difference, of the frequencies of two linearly-driven (unstable) parent modes, thus satisfy

$$\nu_1 \simeq \nu_2 \pm \nu_3 \ , \tag{6.1}$$

where ν_1 is the frequency of the child mode, and ν_2 and ν_3 are the frequencies of the parent modes. However, the frequency resonance criterion given in Eqn 6.1 does not solely distinguish which frequency within a family is a combination or coupled mode frequency of the other two, as demonstrated by Fig. 6.1.

To make this distinction, the amplitude of a child mode can be modelled as a product of the two parent mode amplitudes using

$$A_1 = \mu_{\mathrm{c}}(A_2 A_3) \ , \tag{6.2}$$

and the linear combination of the parent phases

$$\phi_1 = \phi_2 \pm \phi_3 \; , \tag{6.3}$$

where A_i and ϕ_i represent amplitude and phase of the child and parent modes, respectively, and μ_{c} is defined as the coupling factor. For combination frequencies arising from a non-linear distortion model, small values of μ_{c} are expected and thus the amplitude and/or phase variability in combination frequencies will mimic the parent modes that produce them (Brickhill 1992b; Wu 2001; Breger & Lenz 2008b). However, for resonant mode coupling, one expects the amplitudes of the three modes to be comparable with larger values of μ_{c} because mode energy is physically being exchanged between the child and parent modes.

In the steady state solution described by Dziembowski (1982), the coupling coefficient, μ_{c}, in Eqn 6.2 is a measure of the damping rate, γ_1, and mode inertia, I_1 of the child mode in the form

$$\mu_{\mathrm{c}} = \frac{H}{2\sigma_1 \gamma_1 I_1} \tag{6.4}$$

where H is a coefficient that determines the strength of the coupling between the child mode ν_1 and the parent modes ν_2 and ν_3, and σ_1 is the dimensionless frequency of the child mode. The coupling coefficient μ_{c} was introduced by Breger & Montgomery (2014) because the quantities σ_1, γ_1 and I_1 cannot be determined observationally from an amplitude spectrum, such that by using Eqn 6.2 the authors were able to measure the *strength* of coupling between pulsation modes in the δ Sct star KIC 8054146. This is discussed further in section 6.2.4.

The method described here to is similar to the approach devised by van Kerkwijk et al. (2000a) to study non-linearity in pulsating sdB stars. They defined the parameter, R, as

$$R = \frac{A_1}{A_2 A_3} \tag{6.5}$$

where A_1, A_2 and A_3 are the amplitudes of pulsation modes with corresponding frequencies ν_1, ν_2 and ν_3 involved in a resonance. The value of the parameter R was found to be less than 10 for combination frequencies from a non-linear distortion model (van Kerkwijk et al. 2000a), whereas for families of frequencies that have R values greater than 10, the amplitude of a coupled (child) mode is being strengthened by being in resonance with the parent pulsation modes.

6.2.4 Resonant mode coupling in the delta Scuti star KIC 8054146

The fast rotating ($v \sin i \simeq 300 \ \mathrm{km\,s^{-1}}$) δ Sct star KIC 8054146 contains interactions between low- and high-frequency families of pulsation modes which create regularities in its amplitude spectrum (Breger et al. 2012). KIC 8054146 contains 349 statistically significant frequencies between $0 < \nu \leq 200 \ \mathrm{d^{-1}}$ including two high-amplitude triplets, with its amplitude spectrum shown in Fig. 6.2. This star acts as a useful example of how the g- and p-mode frequency regimes are not independent of one another in a δ Sct star. For example, Breger et al. (2013) found that peaks in the high frequency regime contained p modes and high-degree g modes, specifically high-degree prograde sectoral modes.

KIC 8054146 was later analysed by Breger & Montgomery (2014), who investigated the incidence of resonant mode coupling between two parent modes and a single child mode, as predicted by the direct resonance criterion (Dziembowski 1982). The 928-d SC data set (spanning Q5 – Q14) was divided into 45-d bins as a compromise between temporal and frequency resolution, and the amplitudes and phases of different peaks were tracked over time. The observed amplitude modulation in ten dominant pulsation modes is shown in Fig. 6.3. Breger & Montgomery (2014) found three separate families of frequencies whose amplitude variations of the low-frequency members correlated with the high-frequency ones.
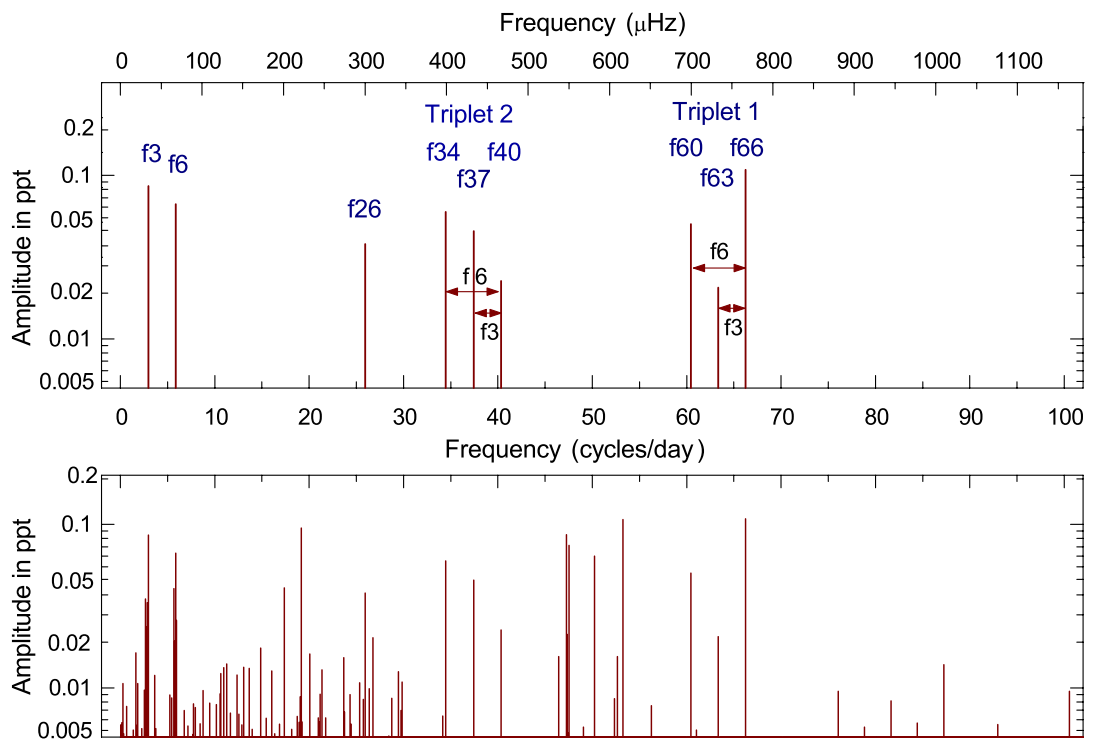
Figure 6.2: The amplitude spectrum for the δ Sct star KIC 8054146. The top panel shows only the nine dominant peaks, labelled as the "T family" by Breger & Montgomery (2014), which contain two triplets, T1 and T2. The bottom panel shows all the peaks in the amplitude spectrum of KIC 8054146 below $\nu \leq 100$ d^{-1}. Figure from Breger & Montgomery (2014), their figure 1. © AAS; reproduced with permission from author and AAS.

CHAPTER 6

A coupled mode is predicted to follow the product of the amplitude variability of the two parent modes, as given by Eqn 6.2, so the child and parent modes in a family can be identified. In the case of KIC 8054146, the value of the coupling coefficient, μ_c, in Eqn 6.2 is of the order 1000 for coupled modes in families with parent mode amplitudes of order 0.1 mmag (Breger & Montgomery 2014). It is concluded that the amplitudes of coupled modes are larger than expected because they are strengthened by resonant mode coupling (Breger & Montgomery 2014).

The observed phase variability of an individual frequency family is given in the $O - C$ diagram in Fig. 6.4, which contains the high-frequency component of triplets T1 and T2, and $\nu = 25.9509$ d^{-1} (labelled as f 26). Breger & Montgomery (2014) use a mode coupling mode in Eqn 6.3 to predict the phase variability for the coupled mode in T2, which accurately matches the observations. Thus, the visible energy associated with the observed amplitude modulation is conserved in KIC 8054146 (Breger & Montgomery 2014).

In their analysis of KIC 8054146, Breger et al. (2012) stated that even if three frequencies within a family obey the frequency, amplitude and phase relations, which are given in Eqns 6.1, 6.2 and 6.3, respectively, it does not *prove* that they are combination frequencies, but merely behave like combination frequencies, thus variable pulsation mode amplitudes can be interpreted as being caused by either non-linearity from a non-linear distortion model or resonant mode coupling.

Therefore, the testable prediction for resonant mode coupling between a child and two parent modes in δ Sct stars is significant amplitude modulation in three similar amplitude modes with large values of μ_c (Breger & Montgomery 2014; Bowman et al. 2016). From the study of pulsation mode variability discussed in chapter 5, it is clear that it is not a simple task to distinguish physically coupled modes from combination frequencies, emphasising the need to study the frequency, amplitude and phase variability of each of the members within each family.
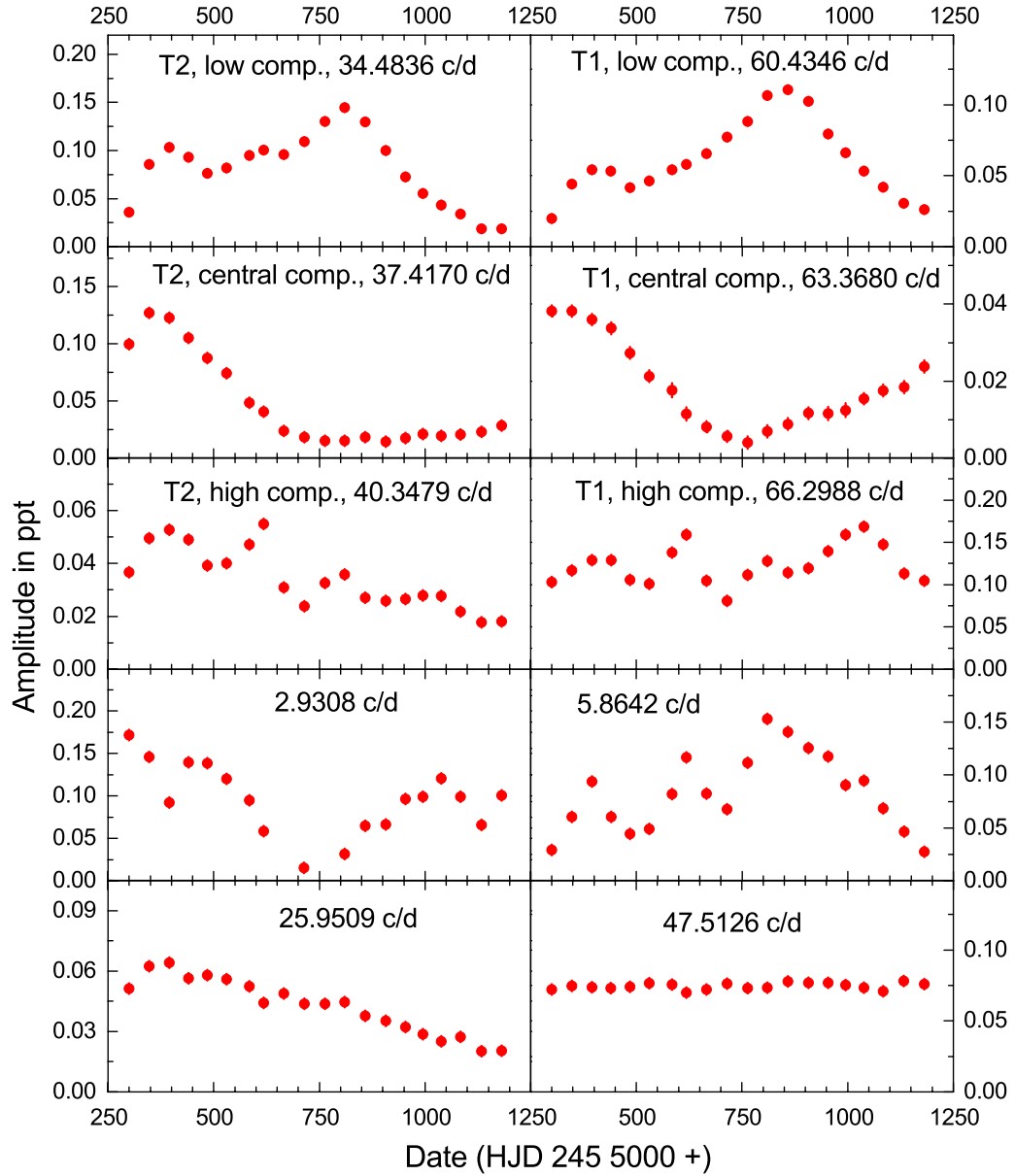
Figure 6.3: Amplitude modulation caused by mode coupling for various pulsation modes in the δ Sct star KIC 8054146. The observed amplitude modulation in each component frequency in each triplet, T1 and T2, is correlated, which can be seen by comparing the left and right columns for each row. Figure from Breger & Montgomery (2014), their figure 2. © AAS; reproduced with permission from author and AAS.
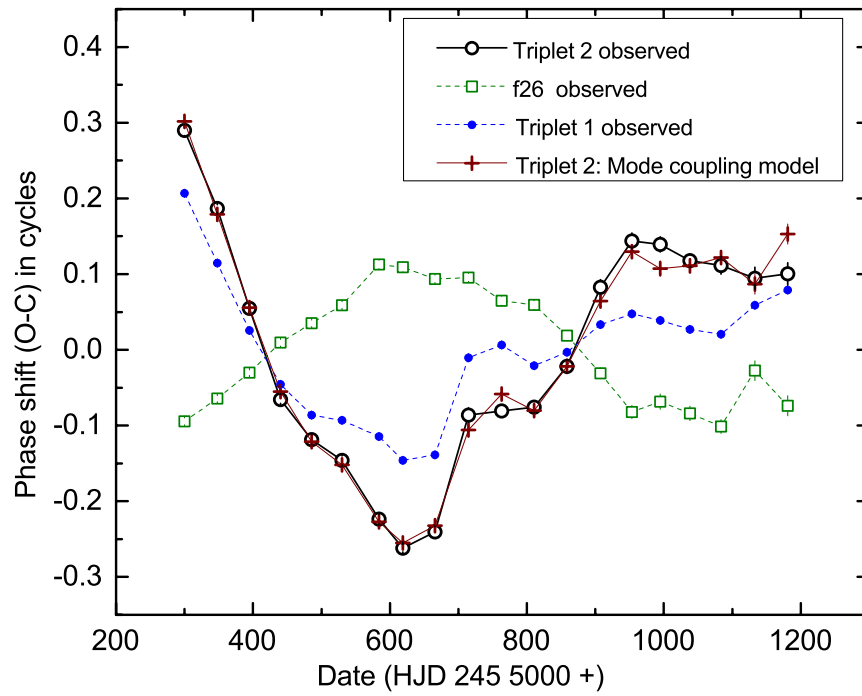
Figure 6.4: An O-C diagram for the observed phase variability in the high-frequency component of T1 and T2, of $\nu = 25.9509$ d^{-1} (labelled as f 26), and the predicted phase variability of T2 by a mode coupling model. The agreement between the predicted and observed phase variability indicates mode coupling between parent pulsation modes, f 26 and T1, and the coupled mode in T2. Figure from Breger & Montgomery (2014), their figure 5. © AAS; reproduced with permission from author and AAS.

6.3 Non-linearity in delta Scuti stars

In chapter 5, it was discussed how Bowman et al. (2016) studied amplitude modulation caused by non-linearity in the δ Sct star KIC 4733344. By trying different values of the coupling coefficient μ_c, the strength of coupling and non-linearity among pulsation mode frequencies can be estimated in a star, with small values of μ_c implying weak coupling that favours the non-linear distortion model producing combination frequencies, whereas large values of μ_c imply strong coupling and favour resonant mode coupling (Breger & Montgomery 2014; Bowman et al. 2016). This method was used by Bowman et al. (2016) to study KIC 4733344, and it was concluded that the small values of the coupling coefficient μ_c indicate non-linearity in the form combination frequencies from a non-linear distortion model in this star.

Note that a large value of μ_c is defined by the amplitudes of the parent modes and thus is specific to each family. For example, using Eqn 6.2, if $A_2 = A_3 = 2$ mmag, then to achieve a similar child mode amplitude of $A_1 \simeq 2$ mmag, a value of $\mu_c \simeq 0.25$ is required. Using the same parent mode amplitudes, a small value of $\mu_c \simeq 0.01$ would produce a child mode amplitude of $A_1 \simeq 0.04$ mmag. Therefore, in this hypothetical example, $\mu_c \gtrsim 0.1$ is considered strong coupling and $\mu_c \lesssim 0.01$ is considered weak coupling.

It is also important to emphasise that when studying the possible energy exchange between pulsation modes in this thesis, the peak in the amplitude spectrum which potentially represents a coupled mode, ν_c, is extracted from an amplitude spectrum and optimised using a non-linear least-squares fit to the data set. The difference in the observed frequency, ν_c, from the expected combination frequency value from the two parent modes does not necessarily prove or disprove that ν_c is a combination frequency or a coupled mode, because the difference is smaller than the frequency resolution of the 4-yr *Kepler* data set (0.00068 d^{-1}).

In the following sections, the methodology for studying amplitude modulation

Table 6.1: Stellar parameters of the δ Sct star KIC 5857714 from the KIC (Brown et al. 2011) and the revised values from Huber et al. (2014).

	T_{eff} (K)	$\log g$ (cgs)	[Fe/H] (dex)
KIC	6710 ± 200	3.80 ± 0.20	-0.23 ± 0.20
Huber et al. (2014)	7050 ± 220	3.81 ± 0.22	0.24 ± 0.30

and non-linearity employed by Bowman et al. (2016) is extended to another δ Sct star, KIC 5857714, and two γ Dor stars observed by the *Kepler* Space Telescope. Furthermore, energy conservation of the visible pulsation modes is also studied in these stars.

6.3.1   KIC 5857714

In this section, the study of non-linearity of pulsation modes in the δ Sct KIC 5857714 is presented. Note that this star, however, is not a member of the ensemble of 983 stars discussed in chapters 4 and 5 because it is a module 3 star. It acts as a useful example here because it has high amplitude pulsations with significant amplitude modulation, and because it has a low mode density in its amplitude spectrum. The stellar parameters of KIC 5857714 from the KIC and Huber et al. (2014) are given in Table 6.1, which characterise it as an evolved early-F star.

The light curve of KIC 5857714 is shown in the top-left panel of Fig. 6.5, in which the gaps caused by the failure of module 3 of the *Kepler* CCD can clearly be seen. The amplitude spectrum of KIC 5857714 is shown in the bottom-left panel of Fig. 6.5, in which the two highest amplitude pulsation mode frequencies, $\nu_1 = 12.227331$ d^{-1} and $\nu_2 = 10.273765$ d^{-1}, and their first-order sum and difference frequencies are labelled. A zoom-in of ν_1 in the amplitude spectrum is given in the right panel of Fig. 6.5, in which a more-complicated spectral window pattern can be seen because KIC 5857714 is a module 3 star. KIC 5857714 pulsates with two
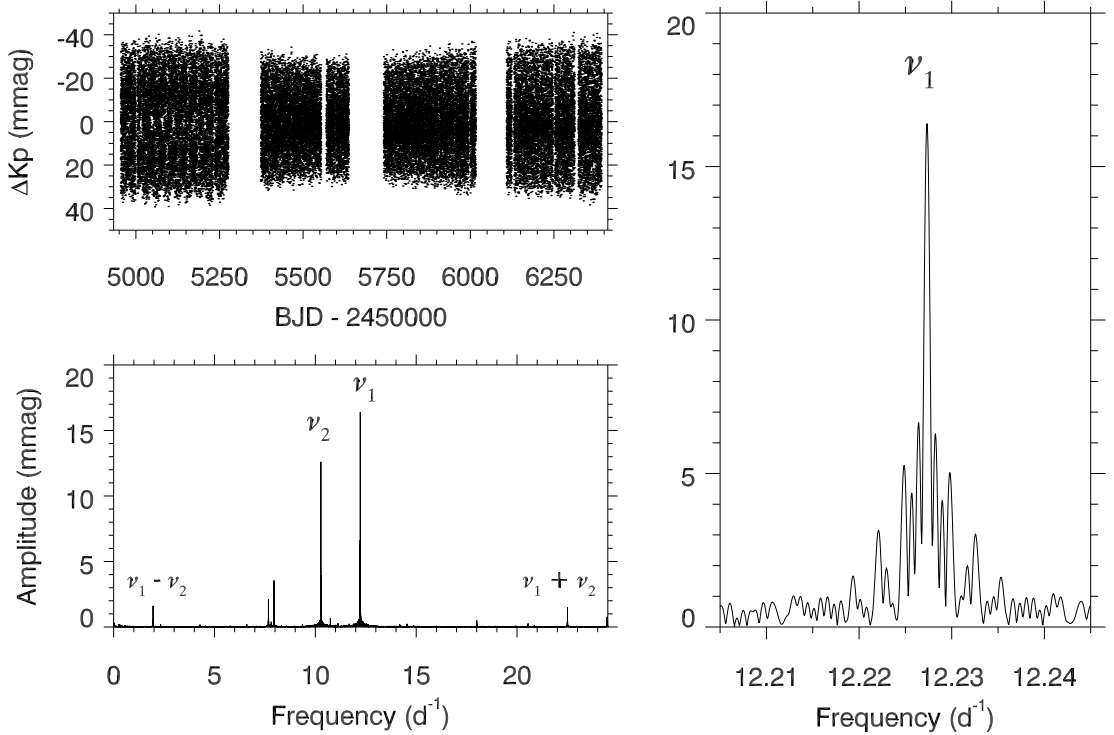
Figure 6.5: The top-left panel is the 4-yr LC light curve for the δ Sct star KIC 5857714, which falls on module 3 of the *Kepler* CCD array resulting in the large gaps. The bottom-left panel is the amplitude spectrum for the δ Sct star KIC 5857714 calculated out to the LC *Kepler* Nyquist frequency. The two parent p-mode frequencies, labelled as $\nu_1 = 12.227331$ d^{-1} and $\nu_2 = 10.273765$ d^{-1}, non-linearly interact to form frequencies at $\nu_1 + \nu_2 = 22.501101$ d^{-1} and $\nu_1 - \nu_2 = 1.953569$ d^{-1}, respectively. The right panel is a zoom-in of the highest amplitude parent mode, ν_1, which has a complicated window pattern from the gaps in the data set.

high-amplitude parent p modes, ν_1 and ν_2, which are non-linearly interacting to form frequencies at $\nu_1 + \nu_2 = 22.501101$ d^{-1} and $\nu_1 - \nu_2 = 1.953569$ d^{-1}, and other higher order combination frequencies and harmonics.

Using the method employed by Bowman et al. (2016), the strength of the non-linearity in these sum and difference combination frequencies is tested by constructing mode coupling models and determining the optimum value of the coupling coefficient, μ_c, with the results shown in Fig. 6.6. The two parent modes vary considerably in amplitude over the 4-yr *Kepler* data set, and the peaks at $\nu_1 + \nu_2$ and $\nu_2 - \nu_1$ mimic
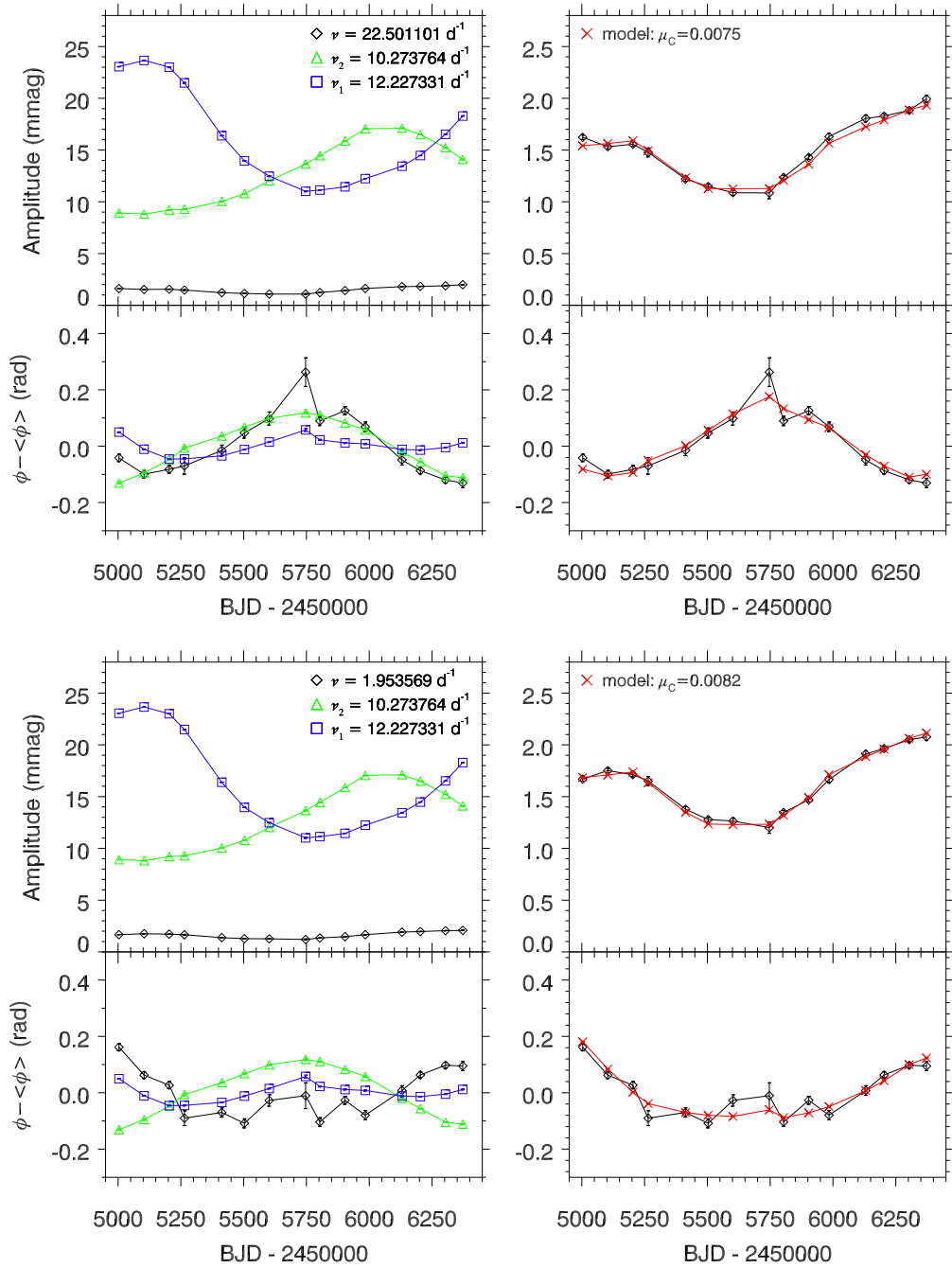
Figure 6.6: Coupling models for two families of frequencies in KIC 5857714. In both panels, the amplitude and phase changes of the two parent frequencies $\nu_1 = 12.227331$ d^{-1} and $\nu_2 = 10.273765$ d^{-1} are shown in blue and green, with the corresponding frequencies, $\nu_1 + \nu_2$ (top panel) and $\nu_1 - \nu_2$ (bottom panel) are shown in black. The coupling model is plotted in red on the right hand side for both amplitude and phase variability for each chosen value of the coupling coefficient μ_c. The amplitude ordinate scale has been kept the same in each column for comparison.

the behaviour of the amplitude modulation in the parent modes. The small value of $\mu_c \simeq 0.008$ in KIC 5857714 indicates that the sum and difference frequencies are combination frequencies from a non-linear distortion model and not coupled modes involved in a direct resonance.

Similarly to KIC 4733344 discussed in chapter 5, the observed amplitude modulation in KIC 5857714 raises the question: where does the energy associated with these parent pulsation modes go to and come from if not to the other visible pulsation modes? The conservation of visible pulsation mode energy is explored further in section 6.5. Many δ Sct stars exhibit similar significant amplitude modulation to KIC 5857714 and KIC 4733344, and do not conserve their visible pulsation energy budget over 4 yr of *Kepler* observations (Bowman et al. 2016).

6.4   Non-linearity in gamma Doradus stars

Non-linearity is certainly important in γ Dor stars in addition to the δ Sct stars. This was demonstrated by Kurtz et al. (2015), who found that the asymmetry of SPB and γ Dor light curves can be explained by the phases of combination frequencies relative to the parent pulsation modes. It was also shown that the 'frequency groups' in these stars were a result of non-linearity in the form of high-order combination frequencies — once identified and removed, the amplitude spectra are greatly simplified (Kurtz et al. 2015). Non-linearity is often associated with high-amplitude pulsations with the high-order combinations in some γ Dor and SPB stars indicating extremely high amplitude g-mode pulsations in the cores of these stars (Kurtz et al. 2015).

Although rarer and more difficult to study because of the high mode densities in the amplitude spectra of γ Dor stars, amplitude modulation is also found among these stars. In the following subsections, two unique examples of γ Dor stars are presented. The first is KIC 4731916, in which the combination frequencies do not mimic the variability of the parent g mode frequencies — this is unexpected and is

as yet unexplained. The second is KIC 4358571, in which there are no peaks in the amplitude spectrum, neither combination frequencies nor coupled pulsation modes, that can explain the amplitude modulation observed in the parent g modes.

6.4.1   KIC 4731916

In section 6.2.1 and in Fig. 6.1, it is demonstrated how multiplets of equally-spaced frequencies can be present from the non-linear interaction of parent frequencies that produce combination frequencies. In this scenario, a multiplet is made from sum and difference combination frequencies, so the splitting of the multiplet must be exact. It is therefore appropriate to generate possible combination terms using a small number of parent frequencies, and fit the frequencies to the light curve using least-squares to find the respective amplitudes and phases.

The 4-yr *Kepler* light curve and amplitude spectrum of the pure γ Dor star KIC 4731916 are shown in the top-left and bottom panels of Fig. 6.7, respectively. The stellar parameters listed in the KIC and the revised values from Huber et al. (2014) for KIC 4731916 are given in Table 6.2, which characterise it as an early-F star and place it inside the γ Dor instability region. Note that KIC 4731916 is closer to the TAMS than the ZAMS star from its log g value, which is not uncommon considering the quoted uncertainties and that typically log $g \simeq 4$ for γ Dor stars observed by *Kepler* (Tkachenko et al. 2013; Van Reeth et al. 2015b). Its current state of evolution may shed light on the unusual pulsational behaviour in KIC 4731916, which is discussed in later sections.

Light curve asymmetry

Upon first inspection of the 4-yr light curve, shown in the top-left panel of Fig. 6.7, two forms of variability that modulate the intrinsic pulsations are evident. The first is a regular beat period of approximately 105 d resulting from two closely-spaced

Table 6.2: Stellar parameters of the γ Dor star KIC 4731916 from the KIC (Brown et al. 2011) and the revised values from Huber et al. (2014).

	T_{eff} (K)	$\log g$ (cgs)	[Fe/H] (dex)
KIC	6640 ± 200	3.85 ± 0.20	-0.14 ± 0.20
Huber et al. (2014)	6910 ± 240	3.87 ± 0.23	-0.14 ± 0.29

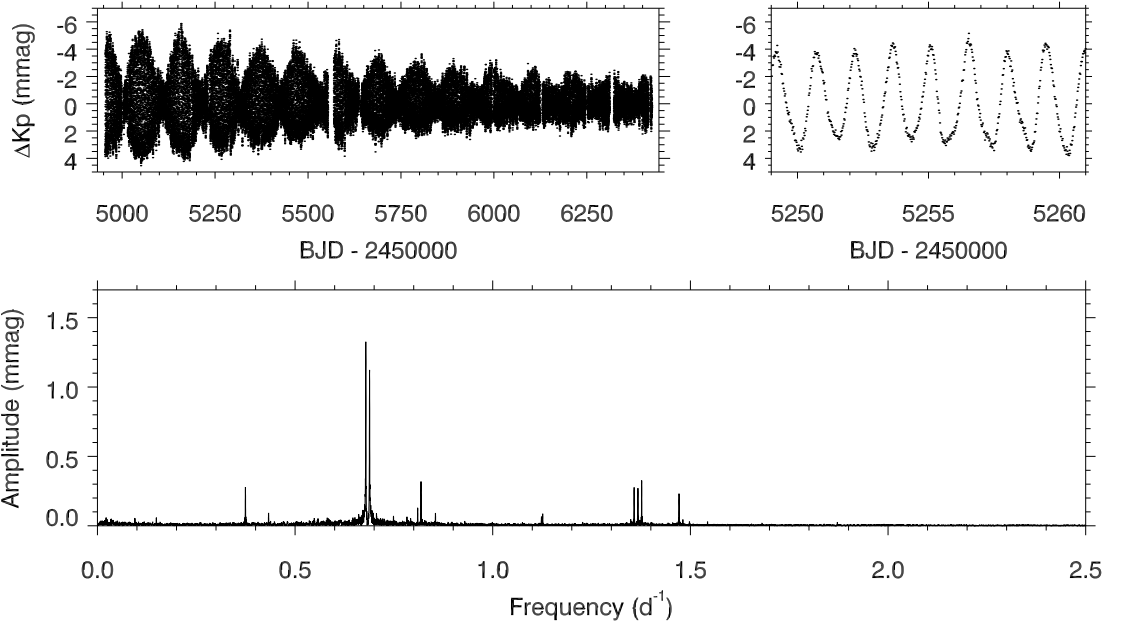Figure 6.7: The 4-yr LC *Kepler* light curve, in which a $\sim$105-d beat period and amplitude modulation envelope can be seen, is shown in the top-left panel and a 12-d insert of the LC light curve is shown in the top-right panel. The bottom panel is the LC amplitude spectrum between $0 \le \nu \le 2.5$ d^{-1}. KIC 4731916 is a pure γ Dor star with only g mode and combination frequencies.

frequencies. The second form of variability is an envelope of decreasing amplitude which modulates the light curve excursions.

The light curve is asymmetric with larger upward than downward excursions about the mean, which has been set to zero. This can also be seen in the 12-d insert of the light curve shown in the top-right panel of Fig. 6.7. The phases of combination frequencies relative to the parent frequencies govern the asymmetry of a light curve (Kurtz et al. 2015). Combination frequencies with relative phases near 0 (or 2π) to the parent phases produce an upwards light curve, whereas combination frequencies with relative phases near π to the parent phases produce a downwards light curve (Kurtz et al. 2015). This effect is not very strong in KIC 4731916, resulting in only a slightly upwards light curve.

Frequency analysis

In the amplitude spectrum of KIC 4731916, two relatively high amplitude peaks at $\nu_1 = 0.6788739 \, \mathrm{d}^{-1}$ and $\nu_2 = 0.6883655 \, \mathrm{d}^{-1}$ can be seen. A zoom-in of the amplitude spectrum for ν_1 and ν_2 is shown in the left panel of Fig. 6.8. These peaks lie within the typical frequency range for a γ Dor star ($0.3 < \nu < 3 \, \mathrm{d}^{-1}$), and are likely g-mode pulsation frequencies. There are no p mode frequencies ($4 < \nu < 100 \, \mathrm{d}^{-1}$) associated with δ Sct pulsations, but there are other low-amplitude g-mode pulsation frequencies in the expected g-mode frequency range. A triplet of equally-spaced frequencies is also present, a zoom-in of which is shown in the right panel of Fig. 6.8.

To find combination frequencies present within KIC 4731916, a non-linear least-squares fit using the cosine function, $\Delta m = A \cos(2\pi\nu(t - t_0) + \phi)$, of the two parent frequencies is used. All possible combination frequencies up to order 3ν with amplitudes greater than 0.012 mmag (i.e., 3σ of the error in amplitude) produces 12 combination terms, which are given in Table 6.3. Higher order terms may exist in the amplitude spectrum, but only those with amplitudes greater than the amplitude
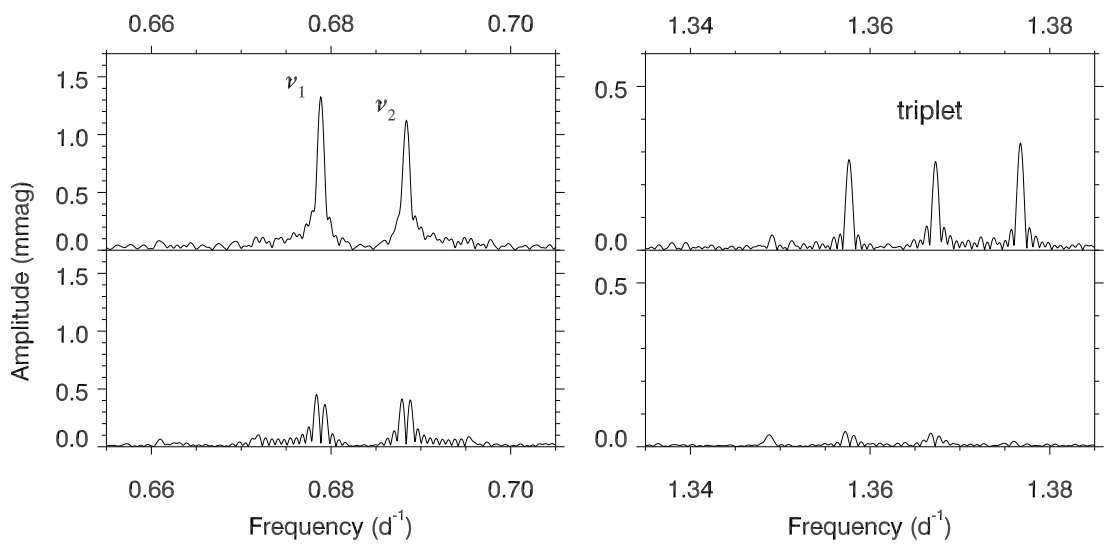
Figure 6.8: An zoom-in of the LC amplitude spectrum of the γ Dor star KIC 4731916, for the two parent g modes (left panel) and the combination frequency triplet (right panel). Note the difference in ordinate scales between the two panels. The amplitude spectrum is shown before and after pre-whitening the data using a non-linear multifrequency least-squares fit as top and bottom, respectively. The combination triplet is removed but the two parent g modes are not because of their intrinsic amplitude modulation.

Table 6.3: A non-linear least-squares fit of the two parent pulsation mode frequencies of KIC 4731916, plus a linear least-squares fit of 12 additional combination frequencies up to order 3ν with amplitudes greater than 0.012 mmag. The zero point of the time-scale is BJD $2\,455\,688.770$.

Label	Frequency (d^{-1})	Amplitude (mmag) ± 0.004	Phase (rad)
ν_1	0.6788739 ± 0.0000013	1.337	-0.287 ± 0.003
ν_2	0.6883655 ± 0.0000015	1.142	-0.193 ± 0.004
$-\nu_1 + \nu_2$	0.0094916	0.015	-1.607 ± 0.273
$-2\nu_1 + 2\nu_2$	0.0189832	0.046	1.866 ± 0.088
$-3\nu_1 + 3\nu_2$	0.0284748	0.019	0.163 ± 0.216
$2\nu_1 - \nu_2$	0.6693823	0.069	0.913 ± 0.059
$-\nu_1 + 2\nu_2$	0.6978571	0.072	2.176 ± 0.057
$-2\nu_1 + 3\nu_2$	0.7073487	0.017	-1.029 ± 0.242
$3\nu_1 - \nu_2$	1.3482562	0.014	1.042 ± 0.299
$2\nu_1$	1.3577478	0.278	2.995 ± 0.015
$\nu_1 + \nu_2$	1.3672394	0.273	2.052 ± 0.015
$2\nu_2$	1.3767310	0.325	-2.345 ± 0.013
$-\nu_1 + 3\nu_2$	1.3862226	0.016	0.185 ± 0.264
$3\nu_1 + \nu_2$	2.7249872	0.025	2.821 ± 0.163

cut-off are included in Table 6.3, along with their respective amplitudes and phases.

Subsequently, a multi-frequency fit of these 14 frequencies using linear least-squares is performed and the data set are pre-whitened to find any remaining variance. The amplitude spectrum of the residuals is re-calculated and the triplet of frequencies is almost completely removed, with before and after pre-whitening shown in the top and bottom panels of Fig. 6.8, respectively. This clearly demonstrates that the triplet is comprised of harmonics and a combination frequency of the two parent frequencies, specifically $2\nu_1 = 1.3577478$ d^{-1}, $\nu_1 + \nu_2 = 1.3672394$ d^{-1} and $2\nu_2 = 1.3767309$ d^{-1}. It is important to emphasise that the combination frequency hypothesis requires a multiplet in an amplitude spectrum to be *exactly* equally-split, since harmonics and combination terms are a mathematical representation of the non-linearity and non-sinusoidal shape of the light curve. This is the case for the

triplet found in KIC 4731916.

There are other peaks in the amplitude spectrum (e.g., a peak lies to the left of the triplet in the right panel of Fig. 6.8), which are not removed after pre-whitening the multi-frequency fit demonstrating that these peaks are not combination frequencies of the two parent g-modes. The triplet contains the only combination frequencies with relatively high amplitudes in the amplitude spectrum of KIC 4731916.

Discounting a spot model

Inhomogeneities or spots on the surface of a star do not produce combination frequencies in an amplitude spectrum of a pulsating star (Kurtz et al. 2015). The presence of the $\nu_1 + \nu_2$ combination frequency cannot be explained in a spot model. Furthermore, there are many peaks over a large frequency range shown in Fig. 6.7, which are likely other g-mode pulsation frequencies. A spot model would have to conjecture differential rotation greater than a factor of three in rotation frequency to explain *all* frequencies observed in KIC 4731916, when no star has ever been observed or modelled to have such behaviour.

No regular period spacing pattern is detected in the amplitude spectrum of KIC 4731916, which is also true for many γ Dor stars. However, the period spacing between ν_1 and ν_2 of 0.0203 d ($\simeq$ 1754 s) is consistent with consecutive dipole modes of the same azimuthal order, supporting the inference that these frequencies are g modes and not rotational modulation caused by spots. It has been shown that a cool γ Dor star with essentially no rotation can have period spacings of $\simeq$ 0.0203 d — see figure 8 of Kurtz et al. (2014) to see how the period spacings change with age for stars in the $1.6 - 2.2$ $M_\odot$ mass range; 0.0203 d is not surprising. This, coupled with the impossibility of explaining the combination frequency with spots, completely rules out any spot model for KIC 4731916.
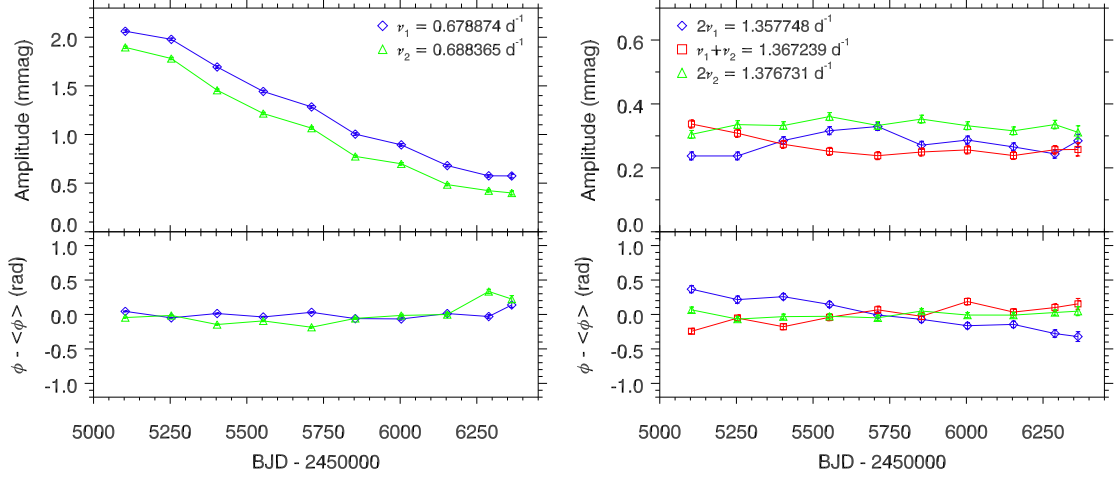
Figure 6.9: Tracking plots for the two parent g modes and combination frequency triplet in the γ Dor star KIC 4731916. Amplitude and phase are calculated at a fixed frequency using least-squares in a series of 300-d bins with 150-d overlap. The left panel shows the two parent g-mode frequencies $\nu_1 = 0.678874$ d^{-1} and $\nu_2 = 0.688365$ d^{-1} as blue diamonds and green triangles, respectively. The right panel shows the harmonics $2\nu_1 = 1.357748$ d^{-1}, $2\nu_2 = 1.376731$ d^{-1} as blue diamonds and green triangles, respectively, and the combination term $\nu_1 + \nu_2 = 1.367239$ d^{-1} as red squares, which together form an equally split frequency triplet. Note the difference in ordinate scale between the two panels.

Variable pulsation mode amplitudes

To study the variability in amplitude and phase of ν_1, ν_2 and the combination frequency triplet, the 4-yr *Kepler* data set for KIC 4731916 is divided into 300-d bins using a 150-d overlap for consecutive bins, and values of amplitude and phase are optimised at fixed frequency in each bin using linear least-squares. The difference in the two parent frequencies, $\nu_2 - \nu_1 = 0.0094916$ d^{-1}, results in a beat period of $P_{\text{beat}} = 105.36 \pm 0.02$ d. Therefore a bin size of 300 d with 150-d overlap is large enough to resolve the beating of this pair of close frequencies. Using a 150-d overlap smoothes variation in amplitude and phase between bins. This method is a similar amplitude and phase tracking method used by Bowman et al. (2016).

The resulting tracking plots are shown in Fig. 6.9, in which the phases of all frequencies have been normalised to be zero in the mean so that any relative phase

variability is clear. Note that a constant amplitude, frequency and phase cosinusoid would appear as a perfectly flat horizontal line in both amplitude and phase panels. The two parent frequencies steadily decrease in amplitude over the 4-yr *Kepler* observations. Specifically, ν_1 decreases from 2.06 ± 0.01 to 0.57 ± 0.02 mmag, and ν_2 decreases from 1.90 ± 0.01 to 0.40 ± 0.02 mmag, with neither frequency exhibiting any significant change in phase. The lack of significant phase changes suggests that the amplitudes of ν_1 and ν_2 are intrinsically variable rather than exhibit amplitude modulation because of mode coupling or beating from close-frequency pulsation modes (see figure 9 and associated discussion from Bowman et al. 2016). The amplitude variability can also be seen in the zoom-in of the parent frequencies in the amplitude spectrum in Fig. 6.8. Neither peak is a sinc function, thus the behaviour is unresolved. The mode energy associated with this decrease in amplitude is not transferred to any new or existing mode frequency visible in the amplitude spectrum.

The most remarkable result from the variability analysis of KIC 4731916 is that the members of the combination frequency triplet do not mirror the two parent frequencies that create it. This is unexpected. Since harmonics and combination frequencies describe the non-linearity and non-sinusoidal shape of the light curve, any changes in the amplitude or phase of the parent frequencies should cause similar changes in the combination terms. The amplitudes and phases of combination frequencies in white dwarf stars are a function of the parent frequencies (Brickhill 1992b; Wu 2001), and combination frequencies are observed to mirror variability in the parent frequencies in δ Sct stars (Breger & Lenz 2008b; Bowman et al. 2016). This is not the case for the γ Dor star KIC 4731916, which is evident by comparing the two panels in Fig. 6.9.

As discussed by Kurtz et al. (2015), the strong non-linear interactions of g modes visible at the surface of a γ Dor star imply high mode amplitudes in the cores of these stars. In the case of KIC 4731916 and its decreasing parent mode amplitudes,

Table 6.4: Stellar parameters of the γ Dor star KIC 4358571 from the KIC (Brown et al. 2011) and the revised values from Huber et al. (2014).

	T_{eff} (K)	$\log g$ (cgs)	[Fe/H] (dex)
KIC	6870 ± 200	4.01 ± 0.20	-0.17 ± 0.02
Huber et al. (2014)	7150 ± 230	3.99 ± 0.23	-0.16 ± 0.31

at some point the non-linearity should change, because it may disappear at low amplitudes. Since the combination frequency is observed to remain at a constant amplitude whilst the parent modes decrease shows that the non-linearity is *increasing* with decreasing amplitude. This is even more unexpected.

6.4.2 KIC 4358571

In this section, another unique example of amplitude modulation in a γ Dor star is presented, specifically KIC 4358571. The stellar parameters of this star from the KIC and from Huber et al. (2014) are given in Table 6.4, which characterise it as an early-F star inside the γ Dor instability region. The 4-yr *Kepler* light curve and amplitude spectrum of KIC 4358571 are shown in the top- and bottom-left panels of Fig. 6.10, respectively. An zoom-in of the amplitude spectrum is shown in the right panel of Fig. 6.10, in which the three highest amplitude peaks are labelled and are likely g modes.

The same amplitude and phase tracking method was used to study amplitude modulation of the three principal frequencies, specifically $\nu_1 = 1.307952$ d^{-1}, $\nu_2 = 1.497101$ d^{-1}, and $\nu_3 = 1.662438$ d^{-1}, with the results shown in Fig. 6.11. Similarly to KIC 4731916, the parent g modes in KIC 4358571 shown in Fig. 6.11 are variable in amplitude over the 4 yr *Kepler* data set. Higher frequency peaks are present in the amplitude spectrum, but no combination frequencies with significant amplitude of the three parent g-modes could be identified. Therefore, the mode energy associated
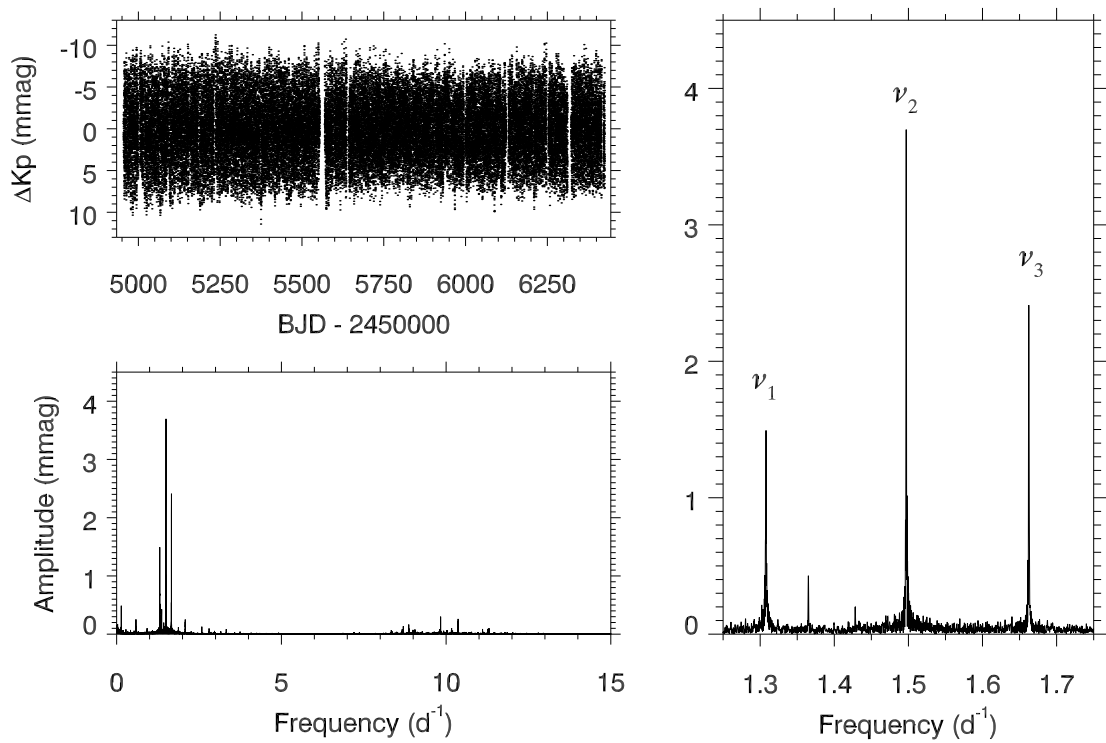
Figure 6.10: The top-left panel shows the 4 yr light curve using LC data for KIC 4358571. The amplitude spectrum calculated out to the LC Nyquist frequency is given in the bottom-left panel and a zoom-in of the three parent g-mode frequencies is shown in the right panel.
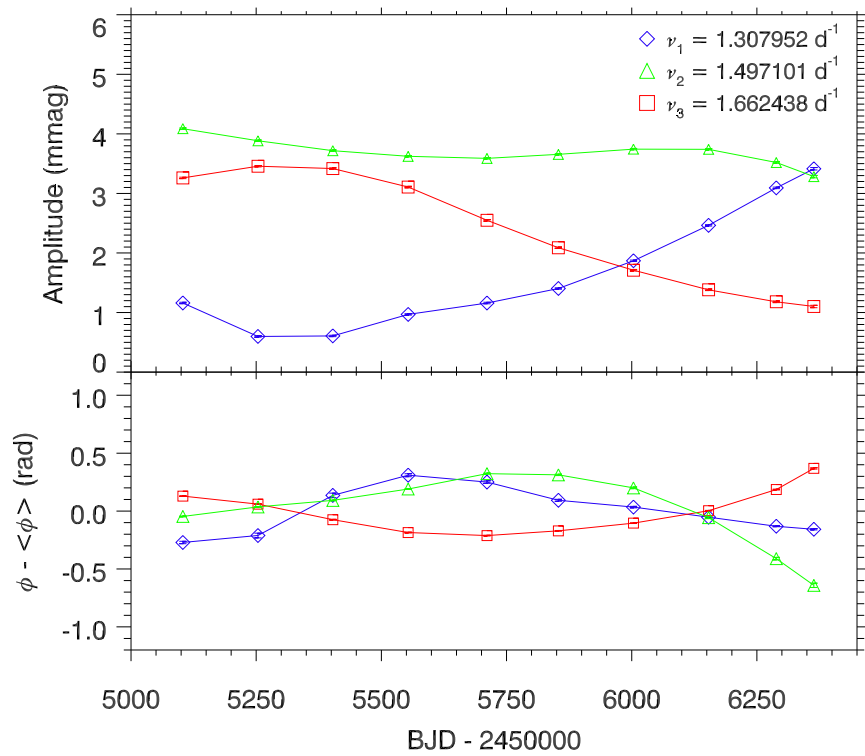
Figure 6.11: Tracking plots showing amplitude and phase variation at fixed frequency in KIC 4358571 of the three high-amplitude parent g mode frequencies, using 300 d bins with 150-d overlap. There are no significant combination frequencies of the three parent frequencies.

with the variable parent g modes is not transferred to any of the other visible pulsation modes in this star.

In the current and previous sections, two γ Dor stars have been presented, KIC 4731916 and KIC 4358571, which demonstrate that amplitude modulation is also found among g-mode pulsators. Mode coupling models using Eqn 6.2 could not be used to study KIC 4731916 because the combination frequencies did not mimic the variability in the parent g modes, whereas no combination frequencies could be found in KIC 4358571. Therefore, it is possible for γ Dor stars to not conserve their visible pulsation budget over 4 yr.

6.5 Energy conservation of pulsation modes

The Sun is the only star for which the total pulsational energy budget can be measured, because pulsation modes over many radial orders covering a large range in angular degree are observable. The pulsation mode energy in the Sun and stars with solar-like oscillations is determined by the physics of the convective envelope, with the connection between convection and pulsation in the Sun having been studied extensively in the literature (Goldreich & Keeley 1977a,b; Libbrecht & Woodard 1991; Goldreich et al. 1994).

An observational measurement of the energy contained within the radial modes of the Sun was achieved by Chaplin et al. (1998) using data from the Birmingham Solar-Oscillations Network (BiSON)[1]. It was found that the solar mode energy peaks at a frequency of approximately 3200 μHz with a value of $E \sim 10^{28}$ erg (Chaplin et al. 1998). Independently, Komm et al. (2000) used data from the Global Oscillation Network Group (GONG)[2] to measure the total energy for modes with angular degrees of $9 \leq \ell \leq 150$, and found a consistent value of the energy per mode as

---

[1]BiSON website: http://bison.ph.bham.ac.uk
[2]GONG website: http://www.gong.noao.edu

$E \simeq 2.2 \times 10^{28}$ erg. The mode energy is a function of frequency and if extrapolated to cover the frequency range between $0.4 \leq \nu \leq 5.0$ mHz (i.e., $\ell \lesssim 1000$), then the total energy contained in the Sun's acoustic waves was calculated to be $E_{\mathrm{Tot}} \simeq 4.2 \times 10^{34}$ erg (Komm et al. 2000).

Although it is not directly responsible for the pulsations, convection is undoubtedly important in intermediate-mass γ Dor and δ Sct stars – see Houdek & Dupret (2015) for a recent thorough review – since it may be responsible for the non-linearity that creates harmonics and combination frequencies. For early-A stars that are near the blue edge of the classical instability strip, models have indicated that granulation produces of order 10 ppm μHz^{-1}, which is non-negligible (Kallinger & Matthews 2010). The interaction between convection and pulsation is also important, especially near the red edge of the classical instability strip at which the δ Sct pulsation modes are returned to stability (Houdek et al. 1999b; Houdek 2000; Xiong & Deng 2001; Dupret et al. 2005; Grigahcène et al. 2005).

Using *Kepler* observations, one is unable to measure the total pulsational energy budget of a star, but proxies such as pulsation mode amplitudes can be used instead to test variable driving/damping over time. Nowakowski (2005) defines a general formula for mode energy, E, as

$$E = \frac{1}{2} I \left| \nu^2 A^2 \right| \, ,$$ (6.6)

where I is the mode inertia, ν is the frequency, and A is the amplitude. If this is normalised using units of $\frac{1}{2} I_0 \nu_0^2$ (see equation 19 of Nowakowski 2005), then the energy of a pulsation mode can be simplified to

$$E = \left| A^2 \right| \, .$$ (6.7)

In the next section, Eqn 6.7 is used to study energy conservation of pulsation

modes in δ Sct stars that exhibit amplitude modulation.

6.5.1 Application to case studies of delta Scuti stars

In this section, an observable called "energy" using Eqn 6.7 is introduced to study energy conservation of pulsation modes over time in δ Sct and γ Dor stars. The amplitude tracking routine is adapted to plot the total visible pulsation energy in a star, E_T, as a function of time using

$$E_T(t) = \sum_i^N A_i^2(t) \ , \tag{6.8}$$

where N is the number of pulsation mode amplitudes, A_i, at a given time step.

The total visible pulsation energy for the δ Sct and γ Dor stars discussed in this chapter, specifically KIC 5857714, KIC 4731916 and KIC 4358571 along with KIC 7106205, is plotted in Fig. 6.12. Clearly, these stars do not conserve their visible pulsation energy budget over time, such that the decay in amplitude of one pulsation mode does not coincide with a comparable increase in amplitude of another, or vice versa. This is best demonstrated using the δ Sct star KIC 7106205, discussed in chapter 3, in which a single pulsation mode was responsible for the observed amplitude modulation whilst all other pulsation modes remained constant in amplitude over the 4-yr *Kepler* data set. Many other δ Sct stars observed by the *Kepler* Space Telescope also do not conserve their visible energy budget — simply put, where does the mode energy go or come from if not the other pulsation modes?

There are several astrophysical possibilities that may explain the unconserved pulsation mode energy in these stars. First, resonant mode coupling to high-degree pulsation modes or internal g modes, which are invisible in broad-band photometric observations (Dziembowski 1977a), can explain observations of amplitude modulation (Dziembowski 1982; Dziembowski & Krolikowska 1985; Nowakowski 2005). For
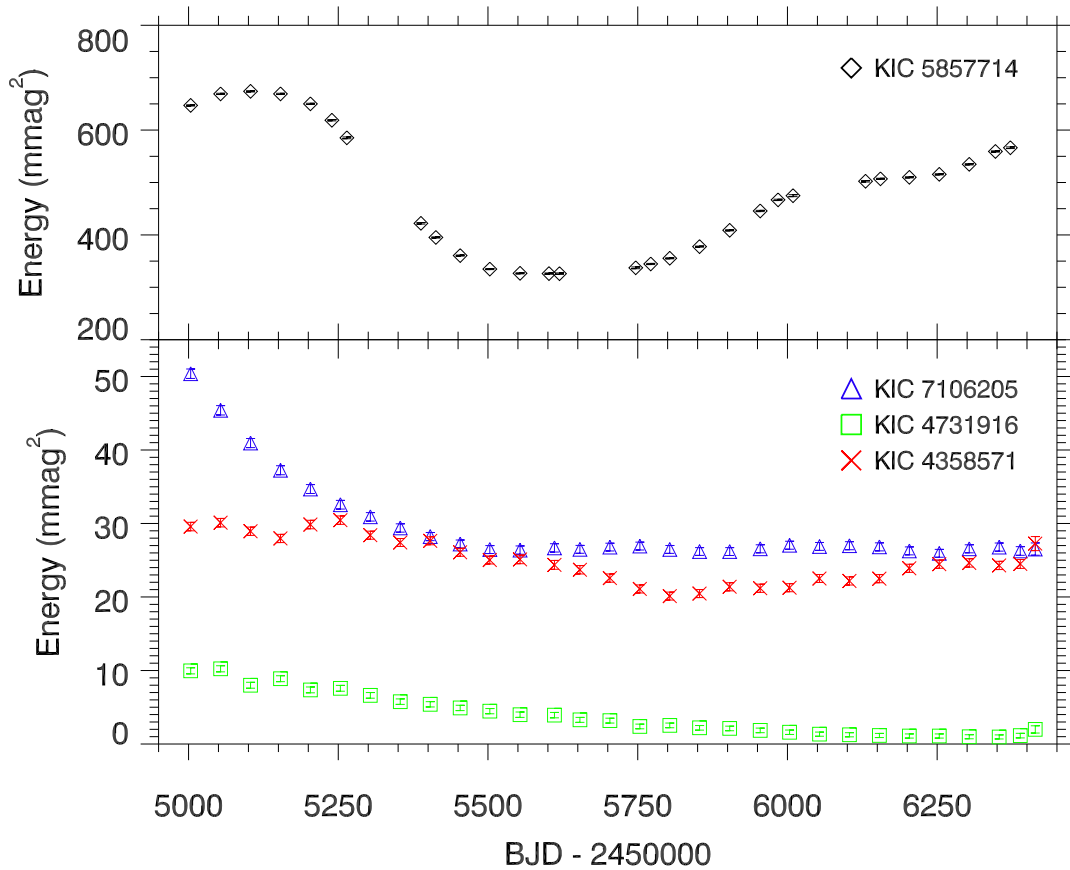
Figure 6.12: The observable "energy" $(= A^2)$ is used to study energy conservation of visible pulsation modes in a selection of case study δ Sct and γ Dor stars discussed in this chapter. The top panel shows the high amplitude (module 3) δ Sct star KIC 5857714 as black diamonds. The bottom panel shows the δ Sct star KIC 7106205 and the γ Dor stars KIC 4731916 and KIC 4358571 as blue triangles, green squares and red crosses, respectively.

the δ Sct stars this is a convincing and realistic possibility but is difficult to test. One must also explain why this is not observed in all δ Sct stars, since the analysis of 983 δ Sct stars in this thesis demonstrates that approximately 40 per cent of δ Sct stars do not show variable pulsation mode amplitudes (Bowman et al. 2016). Therefore, if mode coupling is the solution, why is it not ubiquitous?

A second solution is that the interplay between pulsation and convection facilitates the exchange of mode energy with the stellar medium on time-scales of order a few years. Models of δ Sct stars near the red edge of the instability strip show that, for example, turbulent pressure is important in returning a star to stability (Houdek 2008), but also that turbulent pressure is able to excite high-frequency pulsation modes in δ Sct stars in the centre of the classical instability strip (Antoci et al. 2014). Further work on modelling individual δ Sct stars is clearly needed to explain the diverse range of pulsation behaviour observed in all δ Sct stars.

6.6   Discussion

Stars that exhibit non-linearity are evident from the non-sinusoidal shape of the light curve and the presence of harmonics and combination frequencies in their amplitude spectra. The frequency, amplitude and phase of a coupled or combination frequency are a function of the two parent modes, and so a coupling coefficient, μ_c, can be used to distinguish between these two forms of non-linearity within a star. Small values of μ_c imply combination frequencies from a non-linear distortion model that mimic any variability in the parent modes (Brickhill 1992b; Wu 2001; Breger & Lenz 2008b), whereas large values of μ_c imply resonant mode coupling with mode energy being exchanged among similar amplitude family members (van Kerkwijk et al. 2000a; Breger & Montgomery 2014).

In chapter 5, the mode coupling model given in Eqn 6.2 was applied to the δ Sct star KIC 4733344 by Bowman et al. (2016), who studied the possible energy

exchange among pulsation modes. For two families of frequencies in KIC 4733344, values of $\mu_c \lesssim 0.01$ were found, which indicated the sum and difference frequencies were combination frequencies caused by the non-linear distortion model and were not strongly-coupled modes (Bowman et al. 2016). In this chapter, the same mode coupling model has also been applied to another δ Sct star KIC 5857714, which yielded similar results. Many δ Sct stars contain combination frequencies but the physical cause of this form of non-linearity in δ Sct stars is as yet understood (see e.g., Breger & Lenz 2008a; Pápics 2012; Balona 2012, 2016a).

For many δ Sct stars, the total visible pulsation mode energy is not conserved in 4 yr of *Kepler* observations (Bowman et al. 2016). This was demonstrated in Fig. 6.12 using the δ Sct star KIC 5857714, the γ Dor stars KIC 4731916 and KIC 4358571, and the δ Sct star KIC 7106205, which was discussed in chapter 3. The unconserved mode energy in many δ Sct stars may be caused by mode coupling to invisible high-degree modes, or internal g modes (Dziembowski 1982; Dziembowski & Krolikowska 1985), or intrinsic variability in driving and/or damping rates within a star. Photometry from the *Kepler* Space Telescope is insensitive to high-degree modes from geometric cancellation (Dziembowski 1977a), and so it is difficult to determine if the amplitude modulation in a low-degree child p-mode is caused by high-degree parent modes, or internal g modes.

The intermediate-mass stars have thin surface convective envelopes, which in γ Dor stars are responsible for exciting g modes (Guzik et al. 2000; Dupret et al. 2005). Similarly, the turbulent pressure in the surface convection zone has also been shown to excite high overtone p modes in δ Sct stars (Antoci et al. 2014). The convective envelopes of these stars could also mix the eigenmode signals, distort the light curve and produce combination frequencies and harmonics in δ Sct stars, which has been extensively discussed for variable white dwarf stars (Brickhill 1992b; Brassard et al. 1993; Wu & Goldreich 2001; Wu 2001; Montgomery 2005).

CHAPTER 6

In this chapter, the unique γ Dor star KIC 4731916 has been presented. The only significant harmonics and combination frequencies in this star comprise an equally-split triplet, whose amplitudes and phases do *not* mirror the variability of the two parent pulsation modes. There is little chance that these peaks are not combination frequencies, because of the *exact* values of the frequency splitting. This is a significant advantage of generating the frequency cross-terms mathematically (see e.g., Kurtz et al. 2015), as the likelihood of finding false combination terms is greatly reduced compared to frequency extraction by iterative pre-whitening. The lack of expected variability in combination frequencies created from intrinsically variable parent frequencies has implications for future work on γ Dor stars, both observationally and theoretically. Physically, how can combination frequencies act independently? The γ Dor star KIC 4731916 is an important example for expanding our understanding of intrinsically variable pulsation modes and how combination frequencies are generated in pulsating stars, especially in γ Dor stars.

It is clear that non-linearity is at work within many, if not all, δ Sct stars, and also in a few γ Dor stars, which can appear as amplitude modulation caused by resonant mode coupling and/or combination frequencies and harmonics from a non-linear distortion model. Modelling studies of individual δ Sct stars using the stellar evolutionary code `MESA` (Paxton et al. 2011, 2013, 2015) and the stellar oscillation code `GYRE` (Townsend & Teitler 2013) are needed to test the hypothesis that variable driving and/or damping could be cause of the observed amplitude modulation on time-scales of order years, and the nature of the mechanism that causes combination frequencies and harmonics in γ Dor and δ Sct stars.

Chapter 7

Investigating the HADS stars with *Kepler* data

Some of the discussion in this chapter, specifically in section 7.4, was published by Bowman et al. (2016) in August 2016, and is therefore also included in chapter 5.

7.1 Introductory remarks

The high-amplitude δ Sct (HADS) stars are a subgroup of δ Sct stars that are typically slow rotators and predominantly pulsate in the fundamental and/or first overtone radial mode (Petersen & Christensen-Dalsgaard 1996; Breger 2000a; McNamara 2000; Rodríguez et al. 2000). As discussed in section 1.2.6, the HADS stars were originally defined by McNamara (2000) as δ Sct stars with peak-to-peak light amplitudes exceeding 0.3 mag with pulsation periods between 1 and 6 hr. These stars are rare, making up less than one per cent of pulsating stars within the classical instability strip (Lee et al. 2008), and exhibit similarities to evolved pulsators such as Cepheids in the classical instability strip (Soszyński et al. 2008; Poleski et al. 2010).

There have been several detailed studies of HADS stars in the literature, which

aimed to determine if these stars are distinct from δ Sct stars. For example, Petersen & Christensen-Dalsgaard (1996) claimed that HADS stars are able to pulsate at significantly higher amplitudes because they are in a post-main sequence stage of evolution. On the other hand, Breger (2000a) conjectured that the slow rotation in these stars, which is typically $v \sin i \lesssim 40 \, \mathrm{km \, s^{-1}}$ (McNamara 2000; Rodríguez et al. 2000), facilitates the high amplitude pulsations. If HADS stars are in a post-main sequence stage of evolution, then these stars represent a subsample of δ Sct stars to investigate possible period changes in radial pulsation modes caused by stellar evolution.

In this chapter, a review of studying stellar evolution from observations of changes in pulsation periods is given in section 7.2 for δ Sct stars and SX Phe stars. In section 7.3, a case study from the literature of possible stellar evolution in the ρ Pup star KIC 3429637 is revisited using 4 yr of *Kepler* observations. In section 7.4, the only two HADS stars observed by the *Kepler* Space Telescope are analysed for possible period changes caused by stellar evolution.

7.2 Pulsation period changes caused by stellar evolution

One of the goals of astrophysics is to improve the models of stellar evolution by using observations, which as a consequence has wide implications — for example, the study of the Milky Way Galaxy using galactic archaeology (see e.g., Miglio et al. 2013; Casagrande et al. 2014, 2016). The evolutionary path of an intermediate-mass star ($M \simeq 2 \, \mathrm{M_\odot}$) from the main sequence to the red giant branch was extensively discussed by Iben (1966, 1967a,b,c, 2013a,b), with the main-sequence lifetime lasting approximately 1 Gyr. Stellar evolution theory predicts that when the hydrogen in the core of a 2 $\mathrm{M_\odot}$ star has been exhausted at the TAMS, the star ignites hydrogen

shell burning around the degenerate helium core to prevent collapse and maintain hydrostatic equilibrium. The star's core contracts, raising its temperature as the hydrogen shell moves outwards and more helium is added to the inert core, which causes the star's radius and luminosity to increase and its surface temperature to decrease.

The consequence of stellar evolution on the structure of a star is that an increase in stellar radius causes the period of the fundamental radial mode to increase (Breger & Pamyatnykh 1998). Clearly, the main sequence lifetime of a star is extremely long when compared to even the longest observations available, but a higher chance of observing evolutionary changes exists for stars in a post-main sequence state of evolution because the subgiant expansion phase of a 2 $M_\odot$ is approximately between $20 - 50$ Myr (Breger & Pamyatnykh 1998).

One of the traditional methods for inferring changes to the structure of a pulsating star is to measure the change in period of its oscillations. However, Percy et al. (1980) caution *"the study of period changes has had a long and sometimes dubious history"* and *"in most cases is a source of confusion and frustration"*. Since the time of Percy et al. (1980), some authors have had success in observing changes in pulsation periods, yet it is not clear if the observed changes are caused by stellar evolution; for example, in chapter 6 it was discussed how non-linearity causes pulsation modes to change in period over time and so it can be difficult to disentangle these signals.

Based on the work of Percy et al. (1980) and later developed by Breger & Pamyatnykh (1998), period changes in pulsation modes can be determined from

$$(O - C) = \frac{1}{2} \left(\frac{1}{P} \frac{dP}{dt} \right) t^2 \, , \tag{7.1}$$

where $(O-C)$ is the difference between the observed and calculated times of maxima in units of days, t is the length of the observations in days, and P is the period of

the signal in d such that a factor of 365.25 is needed to convert the fractional period change, $\left(\frac{1}{P}\frac{dP}{dt}\right)$, into the conventional units of yr^{-1}. Thus, according to Eqn 7.1 a quadratic change in phase or $O - C$, is expected for a uniformly changing period. For a star on the main sequence, stellar evolution predicts an increasing period, which would produce a concave upwards parabola with a local minima (Percy et al. 1980; Breger & Pamyatnykh 1998).

The technique of studying period changes has been employed in a variety of pulsators with differing levels of success — for example, δ Sct stars (Breger 1990a; Rodríguez et al. 1995; Breger & Pamyatnykh 1998; Walraven et al. 1992), β Cep stars (Neilson & Ignace 2015), sdBV stars (Kilkenny 2010) and variable white dwarf stars (Fontaine & Brassard 2008; Hermes et al. 2013). In the following sections, a review of studying period changes in δ Sct and SX Phe stars is given.

7.2.1   Period changes in delta Scuti stars

Contrary to stellar evolution theory, many evolved δ Sct stars have been observed to exhibit decreasing periods (e.g., Breger 1990a and Guzik & Cox 1991). Breger & Pamyatnykh (1998) found that approximately an equal number of Population I δ Sct stars had increasing periods as decreasing periods in radial modes, with typical period changes of $\left|\frac{1}{P}\frac{dP}{dt}\right| \simeq 10^{-7}$ yr^{-1}, which are an order of magnitude larger than those predicted by evolutionary models. For radial pulsation modes, stellar models predict a decreasing period throughout the pre-main sequence and contraction phase just before the TAMS, and an increasing period throughout the main sequence and post-main sequence, with the rate of the period change governed by the rate of stellar evolution (Breger & Pamyatnykh 1998; Walraven et al. 1992).

An important case study of amplitude modulation and period changes in the HADS star AI Velorum is given by Walraven et al. (1992). The authors discovered that this HADS star pulsates in the fundamental and first-overtone radial modes

and possibly also a non-radial mode (Walraven et al. 1992). The discovery of the period increase of the first overtone radial mode was unlikely to be caused by an evolutionary change in radius as no concomitant period change was observed in the fundamental radial mode (Walraven et al. 1992). The studies of δ Sct stars, including AI Velorum, have revealed that observed period changes often cannot be attributed to stellar evolution, because the magnitudes of the observed period changes were significantly larger than those predicted by evolutionary models (Walraven et al. 1992; Rodríguez et al. 1995; Breger & Pamyatnykh 1998). Furthermore, it is difficult to extract reliable period changes in δ Sct stars because many of these stars exhibit amplitude and phase modulation caused by non-linearity or beating from close-frequency pulsation modes (Bowman et al. 2016).

7.2.2 Period changes in SX Phe stars

The history of studying period changes in Population II SX Phe stars is somewhat different to that of δ Sct stars. Similarly to the δ Sct stars, stellar evolution theory cannot explain the decreasing periods of radial modes observed in many SX Phe stars (Rodríguez et al. 1995). However, the SX Phe stars present another layer of complexity because sudden jumps in the observed periods are common between observations, rather than smooth variation over time (see Rodríguez et al. 1995 and references therein). An example of such an SX Phe star is SX Phe itself, with sudden jumps in pulsation period noted by Coates et al. (1982) and Thompson & Coates (1991). Without a gradual change in the pulsation period over time, it is difficult to draw any significant conclusions from these stars.

Table 7.1: Stellar parameters of the ρ Pup star KIC 3429637 from the KIC, the revised values from Huber et al. (2014), and from spectroscopic observations from Catanzaro et al. (2011) and Murphy et al. (2012).

	T_{eff} (K)	$\log g$ (cgs)	$v \sin i$ (km s^{-1})
KIC	6960 ± 150	3.42 ± 0.20	
Huber et al. (2014)	7210 ± 150	3.99 ± 0.15	
Catanzaro et al. (2011)	7100 ± 150	3.0 ± 0.2	50 ± 5
Murphy et al. (2012)	7300 ± 100	3.0 ± 0.1	51 ± 1

7.3 The ρ Pup star KIC 3429637

In this section, the ρ Pup star KIC 3429637 (HD 178875) is discussed in the context of detecting changes in pulsation modes caused by stellar evolution. KIC 3429637 was studied by Murphy et al. (2012) using 2 yr of *Kepler* data and was found to exhibit amplitude and phase modulation, which was conjectured to be caused by stellar evolution. The ρ Pup stars are evolved Am stars (Gray & Garrison 1989), many of which pulsate and are also δ Sct stars (Kurtz 1976). Pulsating Am stars observed by *Kepler* were discussed by Balona et al. (2011c) and those observed from the ground using the WASP project were discussed by Smalley et al. (2011), who found that approximately 14 per cent of Am stars have δ Sct pulsations.

As part of a spectroscopic survey of bright stars within the classical instability strip by Catanzaro et al. (2011), KIC 3429637 was classified with the spectral type F0 III m, which is consistent with the original classification of KIC 3429637 being an Am star by Abt (1984). High-resolution spectroscopy of KIC 3429637 obtained by Murphy et al. (2012) allowed accurate T_{eff}, $\log g$ and metallicity to be determined and classify the star as a ρ Pup star. A comparison of the stellar parameters obtained by Catanzaro et al. (2011) and Murphy et al. (2012) is given in Table 7.1, as well as the stellar parameters from the KIC and from Huber et al. (2014).
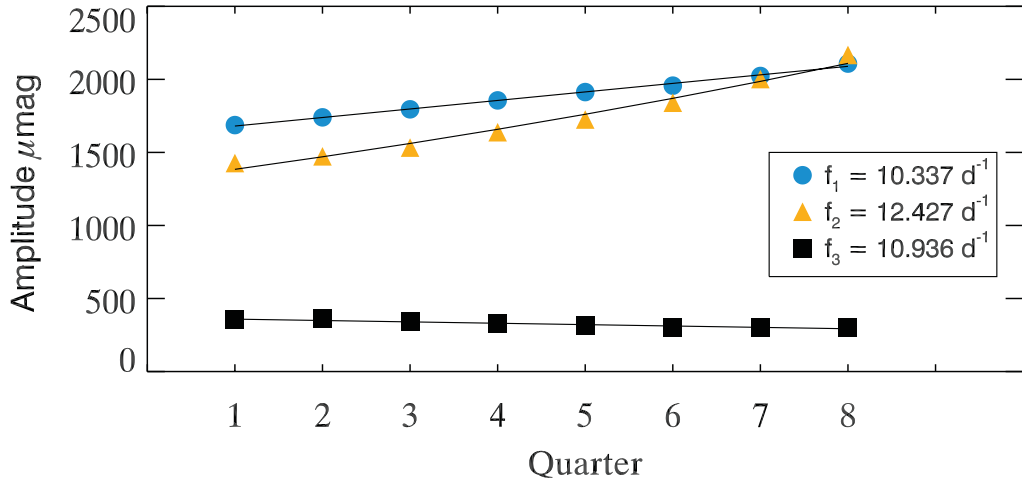
Figure 7.1: Amplitude modulation of the three highest-amplitude pulsation modes using approximately 670 d (Q1 – Q8) of LC *Kepler* data. Figure from Murphy et al. (2012), their figure 3.

7.3.1 Asteroseismic analysis of KIC 3429637

The ρ Pup star KIC 3429637 was observed by the *Kepler* Space Telescope between Q1 – Q17 in LC and Q7 – Q10 in SC, and is the ninth brightest star among all the δ Sct stars observed with a magnitude of Kp = 7.71 in the *Kepler* passband. Using 670-d (Q1 – Q8) of LC data, Murphy et al. (2012) discovered that KIC 3429637 exhibits amplitude modulation with a linear increase in the amplitude of the two dominant pulsation modes and a linear decrease in a third pulsation mode occurring throughout the initial 2 yr of the *Kepler* mission. Each pulsation mode required different functional forms to fit the amplitude variability, which demonstrated that this was not an instrumental effect, as all modes would decrease or increase with the same functional form if the modulation was instrumental (Murphy et al. 2012). The amplitude modulation observed by Murphy et al. (2012) in the three highest-amplitude pulsation modes, denoted $f_1 = 10.337$ d^{-1}, $f_2 = 12.427$ d^{-1} and $f_3 = 10.936$ d^{-1}, is shown in Fig. 7.1.

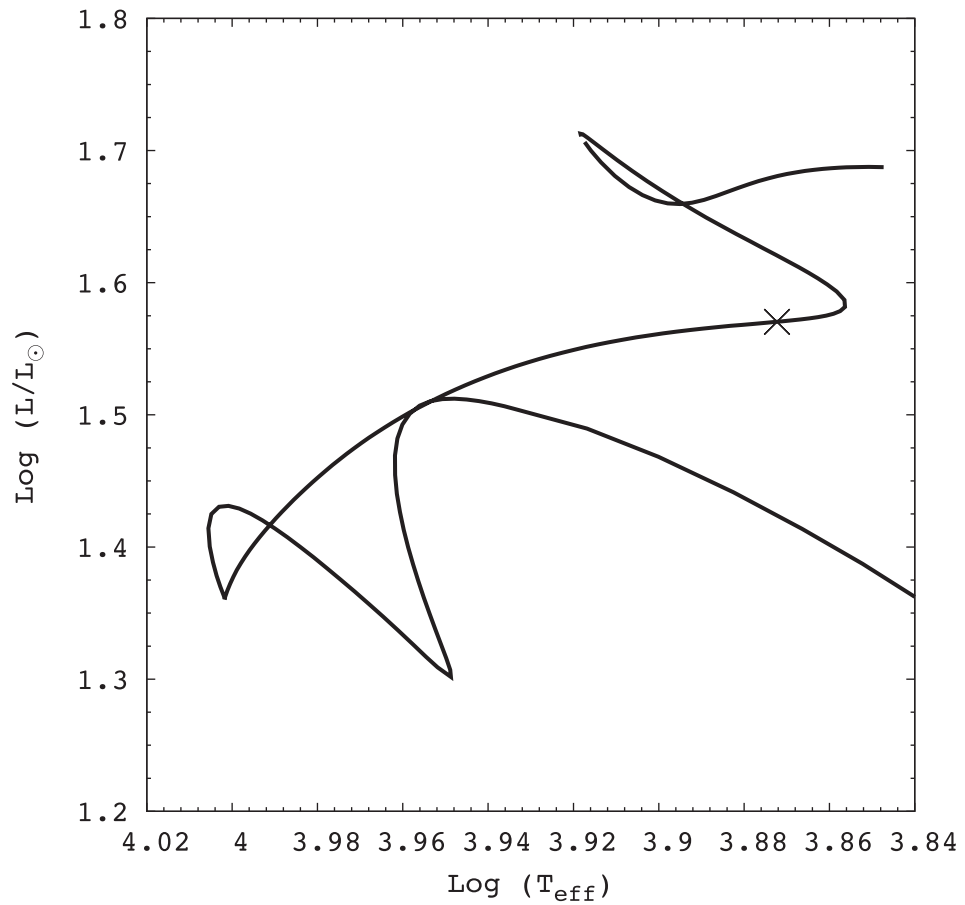From asteroseismic modelling using the Code Liégeois d'Évolution Stellaire (CLES;

Figure 7.2: The location of the ρ Pup star KIC 3429637 in the HR diagram is shown by the cross, which places it near the TAMS. The solid line represents the best-fitting evolutionary model to the spectroscopic stellar parameters. Figure from Murphy et al. (2012), their figure 6.

Scuflaire et al. 2008), the mode frequencies f_1 and f_2 were identified as the third and fourth radial overtone modes (Murphy et al. 2012). The location of KIC 3429637 in the HR diagram is shown in Fig. 7.2, which contains the best-fitting evolutionary model with $M = 2.178$ M$_\odot$, $T_{\text{eff}} = 7452$ K, $\log L = 1.570$ L$_\odot$, $\log g = 3.648$, $R = 3.666$ R$_\odot$, and an age of 898.2 Myr (Murphy et al. 2012).

The discovery that KIC 3429637 is located near the TAMS inspired Murphy et al. (2012) to speculate that the amplitude modulation may be caused by stellar evolution. As the star evolves, the structural changes in the relative depths of different pulsation cavities, particularly the location of the He II ionisation zone, could be modulating the observed pulsation amplitudes and causing the observed amplitude modulation (Murphy et al. 2012).

7.3.2 Revisiting the analysis of KIC 3429637

Since the study of KIC 3429637 by Murphy et al. (2012), an additional 2 yr of *Kepler* observations have become available. If the entire 4-yr data set of KIC 3429637 is analysed using the amplitude and phase tracking routine discussed in chapter 5, the same functions to describe the observed amplitude modulation used by Murphy et al. (2012) are no longer valid. Specifically, the linear increase in the mode amplitude for $\nu_2 = 12.471494$ d^{-1} is not maintained over 4 yr, which is shown in the bottom panel of Fig. 7.3. Specifically, after $t \simeq 5800$ (BJD $- 2\,450\,000$), the amplitude reaches a maximum and turns over, with a significant change in phase occurring at the epoch of minimum amplitude. The non-linear amplitude modulation in this mode suggests beating or a mode coupling mechanism is at work in this star.

If stellar evolution is the cause of the observed amplitude modulation in the ρ Pup star KIC 3429637, then phase modulation of its pulsation modes following the quadratic function given in Eqn 7.1 is also expected. However, this is not the case as can be seen in Fig. 7.3. Although the discussion of structural changes driven
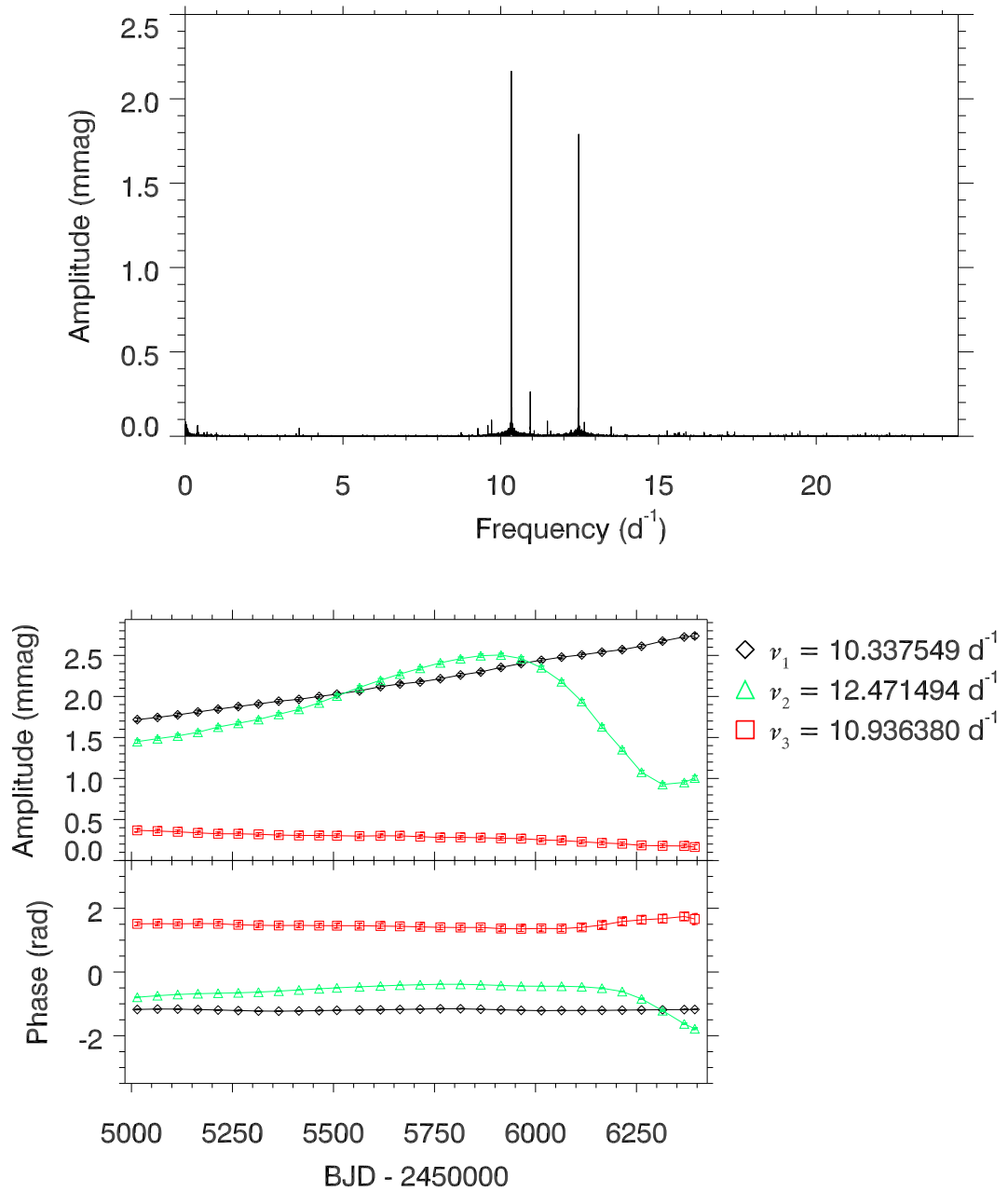
Figure 7.3: Amplitude modulation in KIC 3429637. The top panel is the amplitude spectrum using 4 yr of *Kepler* data. The bottom panel is the tracking plot, showing the changes in the amplitudes and phases between the first and second halves of the *Kepler* mission.

Table 7.2: Stellar parameters of the two HADS stars observed by *Kepler*, KIC 5950579 and KIC 9408694, from the KIC (Brown et al. 2011) and the revised values from Huber et al. (2014). The results of a spectroscopic analysis of KIC 9408694 by Balona et al. (2012) are also included.

	$T_{\rm eff}$ (K)	$\log g$ (cgs)	[Fe/H] (dex)	
KIC 5950759	7840 ± 300	4.03 ± 0.25	-0.07 ± 0.25	KIC
	8040 ± 270	4.05 ± 0.22	-0.10 ± 0.33	Huber et al. (2014)
KIC 9408694	7480 ± 200	3.62 ± 0.20	-0.43 ± 0.20	KIC
	6810 ± 140	3.78 ± 0.11	-0.08 ± 0.15	Huber et al. (2014)
	7300 ± 150	3.5 ± 0.1		Balona et al. (2012)

by stellar evolution from Murphy et al. (2012) is still valid because KIC 3429637 is near the TAMS, this star is clearly yet another example of a δ Sct star with amplitude modulation. KIC 3429637 was classified as an AMod star by Bowman et al. (2016) and is one of the 603 δ Sct stars with significant amplitude modulation in the *Kepler* data set discussed in chapter 5.

7.4 The *Kepler* HADS stars

In this section, *Kepler* data are used to investigate observations of non-linearity and possible structural changes caused by stellar evolution in HADS stars. Using the definition of a HADS star as a δ Sct star with a peak-to-peak light amplitude variation greater than 0.3 mag (McNamara 2000), only two HADS were observed by *Kepler*, specifically KIC 5950759 and KIC 9408694 (Bowman et al. 2016). Some δ Sct stars were only observed for limited subsets of LC data and consequently were not included in the ensemble of 983 stars by Bowman et al. (2016). Fortuitously, the two HADS stars were observed by *Kepler* continuously for 4 yr and were included in the ensemble (Bowman et al. 2016). The stellar parameters of KIC 5950759 and KIC 9408694 are given in Table 7.2.

CHAPTER 7

The HADS stars observed by *Kepler* have also been studied by Balona (2016a), who did not restrict his sample to only stars that were observed continuously for 4 yr. Balona (2016a) concurs that only two *conventional* HADS stars using the definition from McNamara (2000) exist in the *Kepler* data set. If, however, the definition is relaxed to light excursions exceeding 0.1 mag, three more δ Sct stars are included as (possible) HADS stars (Balona 2016a).

Although the criterion of 0.3 mag is somewhat arbitrary, it is non-trivial as it clearly demonstrates the rarity of high-amplitude pulsators on or near the main sequence in the classical instability strip. There are several thousand A and F stars in the *Kepler* data set, resulting in the classical instability strip being well-sampled near the TAMS (see e.g., Niemczura et al. 2015), which is the expected location of the HADS stars (McNamara 2000). Therefore, the implication from finding few HADS stars in a large and complete data set such as *Kepler*, is that HADS stars are rare (Lee et al. 2008; Bowman et al. 2016).

In his study of HADS stars observed by *Kepler*, Balona (2016a) compared the location of his five (possible) HADS stars in the HR diagram to the largest known catalogues of δ Sct stars by Rodríguez et al. (2000) and Poleski et al. (2010), which contain approximately 600 and 1200 stars, respectively. However, five stars were not enough to infer any significant conclusions. Balona (2016a) found that the number and relative amplitudes of harmonics and combination frequencies was not a viable criterion to distinguish δ Sct and HADS stars because non-linearity is also common among δ Sct stars — a result that has been previously demonstrated in chapters 5 and 6 of this thesis.

The prospect of determining a significant physical distinction between HADS stars and their low-amplitude δ Sct counterparts remains to be established and warrants further study. In particular, it has not be definitively established why the HADS stars are so rare, or whether these stars are in a post-main sequence stage of

evolution as conjectured by Petersen & Christensen-Dalsgaard (1996). The nature of non-linearity in the high amplitude pulsations of these stars, and if this is related to their slow rotational velocities of $v \sin i \lesssim 40 \text{ km s}^{-1}$, has also not been established (Breger 2000a; McNamara 2000; Rodríguez et al. 2000).

7.4.1   KIC 5950759

The first of the two HADS stars is KIC 5950759, which pulsates with mode frequencies $\nu_1 = 14.221394 \text{ d}^{-1}$ and $\nu_2 = 18.337294 \text{ d}^{-1}$, with a period ratio of 0.7755, thus identifying them as fundamental and first overtone radial modes, respectively (Bowman et al. 2016). The amplitude spectrum and tracking plot from Bowman et al. (2016) are shown in the top and bottom panels of Fig. 7.4. The HADS star KIC 5950759 shows significant amplitude modulation using the criterion of half the bins lying more than $\pm 5\sigma$ from the mean value (Bowman et al. 2016). This can be seen in the top and bottom panels of Fig. 7.5 for the fundamental and first overtone radial modes, which are labelled as ν_1 and ν_2, respectively. However, the observed quasi-periodic amplitude modulation in Fig. 7.5 is instrumental in origin and is caused by the changing pixel mask as the *Kepler* Space Telescope rotated 90 degrees every ~ 93 d. If the $P_{\text{Kep}} \simeq 372.5$-d amplitude modulation is removed, then only a slight linear decrease in the fundamental radial mode, and increase in the first overtone radial mode are observed.

The observed phase modulation in Fig. 7.5, however, is not instrumental — could this be evidence of stellar evolution altering the structure of the star? As discussed by Percy et al. (1980) and Breger & Pamyatnykh (1998), and given in Eqn 7.1, a quadratic change in phase is expected for a uniformly changing pulsation period. Note that a linear change in phase means that an incorrect frequency has been used to calculate phase. The shape of the observed phase modulation in the fundamental and first overtone radial modes in KIC 5950759 shown in the top and
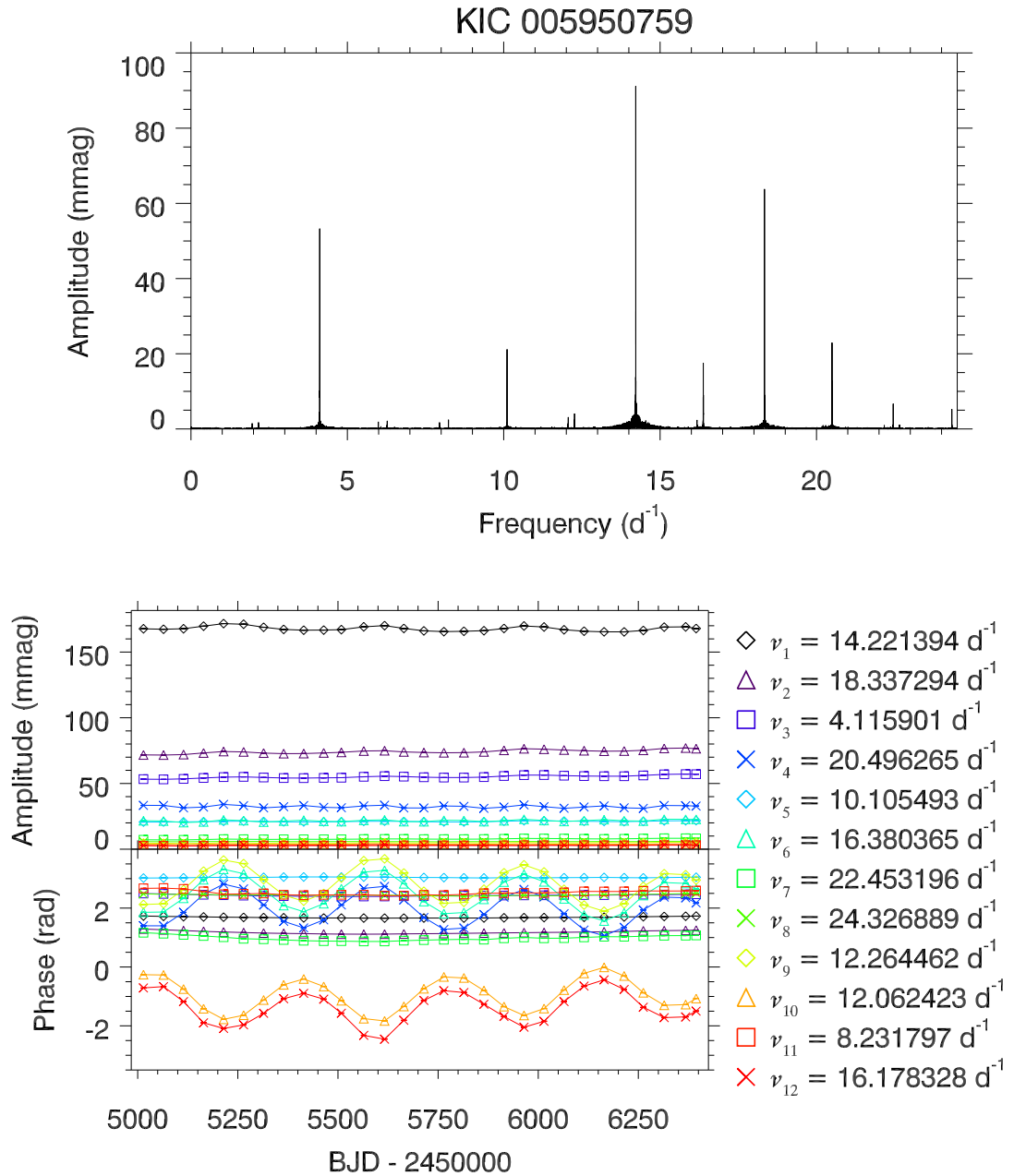
Figure 7.4: The top panel is the 4-yr amplitude spectrum calculated out to the LC Nyquist frequency for the HADS star KIC 5950759 (ν_4, ν_6, ν_9, ν_{10} and ν_{12} are super-Nyquist aliases). The bottom panel shows the amplitude and phase tracking plot, in which there is little or no variability in the amplitudes and phases of the radial pulsation mode frequencies, if instrumental modulation caused by the *Kepler* satellite is removed. Figure adapted from Bowman et al. (2016), their figure 7.
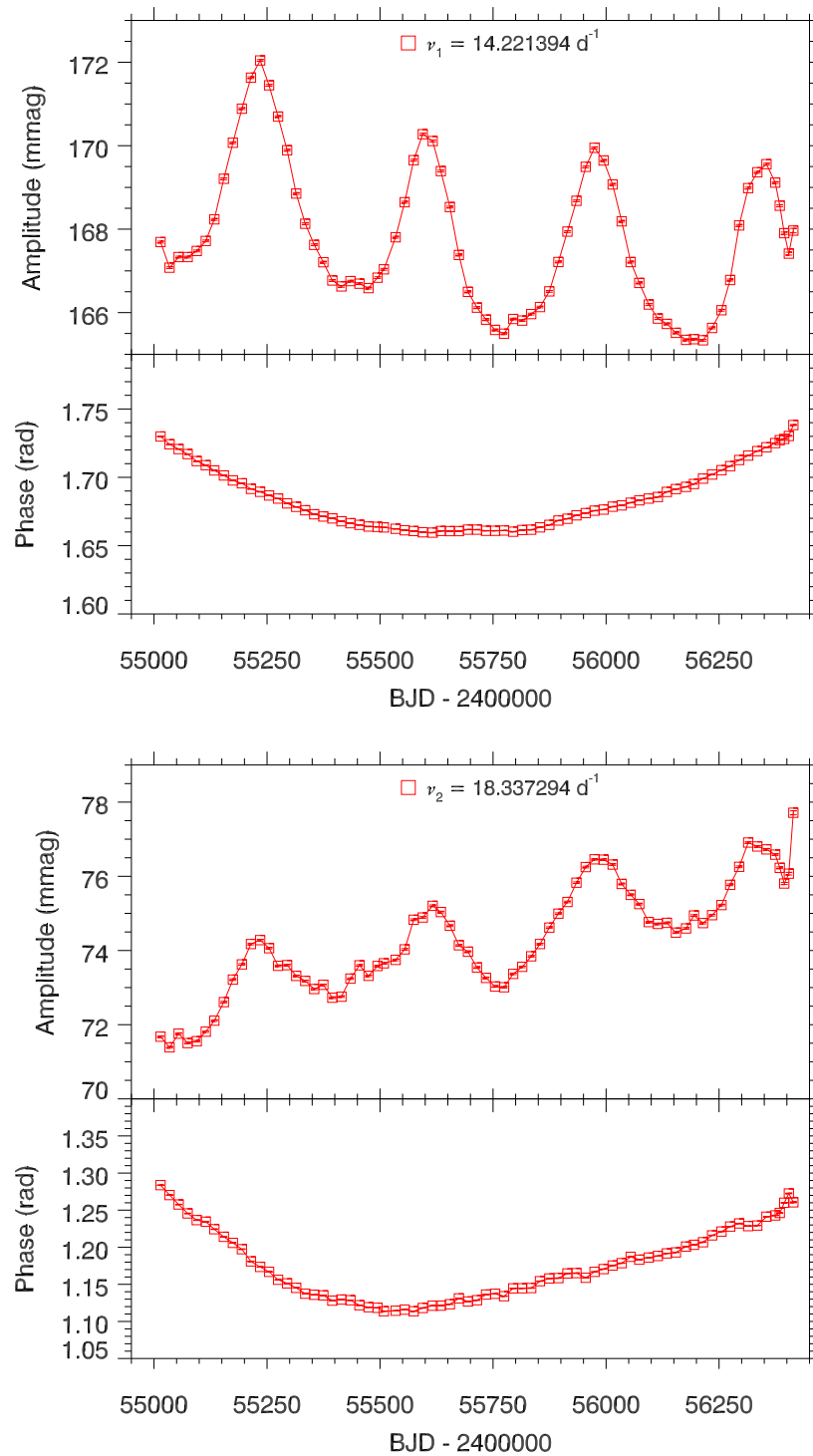
Figure 7.5: Amplitude and phase modulation in the HADS star KIC 5950759. Top and bottom panels are the amplitude and phase tracking plots for the fundamental and first overtone radial modes, respectively, using 100-d bins and 80-d overlaps. Note the difference in ordinate scales when comparing the two panels.

bottom panels of Fig. 7.5, respectively, is not only parabolic, but is also indicative of an increasing period. The periods of radial modes are predicted to increase throughout the majority of a δ Sct star's main sequence lifetime (Percy et al. 1980; Breger 1990a; Rodríguez et al. 1995; Breger & Pamyatnykh 1998). This raises an interesting question: can a time-scale as short as 4 yr be considered significant in terms of the structural evolution of a star?

The phase modulation of the fundamental and first overtone radial modes in KIC 5950759 shown in the top and bottom panels of Fig. 7.5, respectively, was converted into time delays $(O - C)$ using

$$O - C = \frac{\phi(t)}{2\pi\nu} \; , \tag{7.2}$$

where $\phi(t)$ is the phase of a pulsation mode at a given time in units of rad, which has a known and assumed fixed frequency of ν in units of d^{-1}. The $O - C$ values were normalised to a reference time BJD $2\,455\,688.770$ and were plotted for the fundamental and first overtone radial modes in the top and bottom panels of Fig. 7.6, respectively. The quadratic change in the $O - C$ diagram was fitted using Eqn 7.1 with the term $\left(\frac{1}{P}\frac{dP}{dt}\right)$ as a free parameter, m. The optimum parabolic fit is shown as the solid black lines in Fig. 7.6, with the parameter m representing the fractional rate of change in period in units of d^{-1} since t and $O - C$ are in units of d. Thus, m was converted into $\left(\frac{1}{P}\frac{dP}{dt}\right)$ in units of yr^{-1} by being multiplied by 365.25, which resulted in 1.18×10^{-6} yr^{-1} and 1.82×10^{-6} yr^{-1} for the fundamental and first overtone radial modes, respectively.

Stellar evolution theory predicts positive values of $\left(\frac{1}{P}\frac{dP}{dt}\right) \sim 1 \times 10^{-8}$ yr^{-1} for radial pulsation modes in δ Sct stars (Percy et al. 1980; Breger 1990a; Rodríguez et al. 1995; Breger & Pamyatnykh 1998). The observed values of $\left(\frac{1}{P}\frac{dP}{dt}\right)$ for KIC 5950759 are the correct sign for an increasing period, but are much larger than those predicted by stellar evolution theory. It is not clear if the observed phase modulation
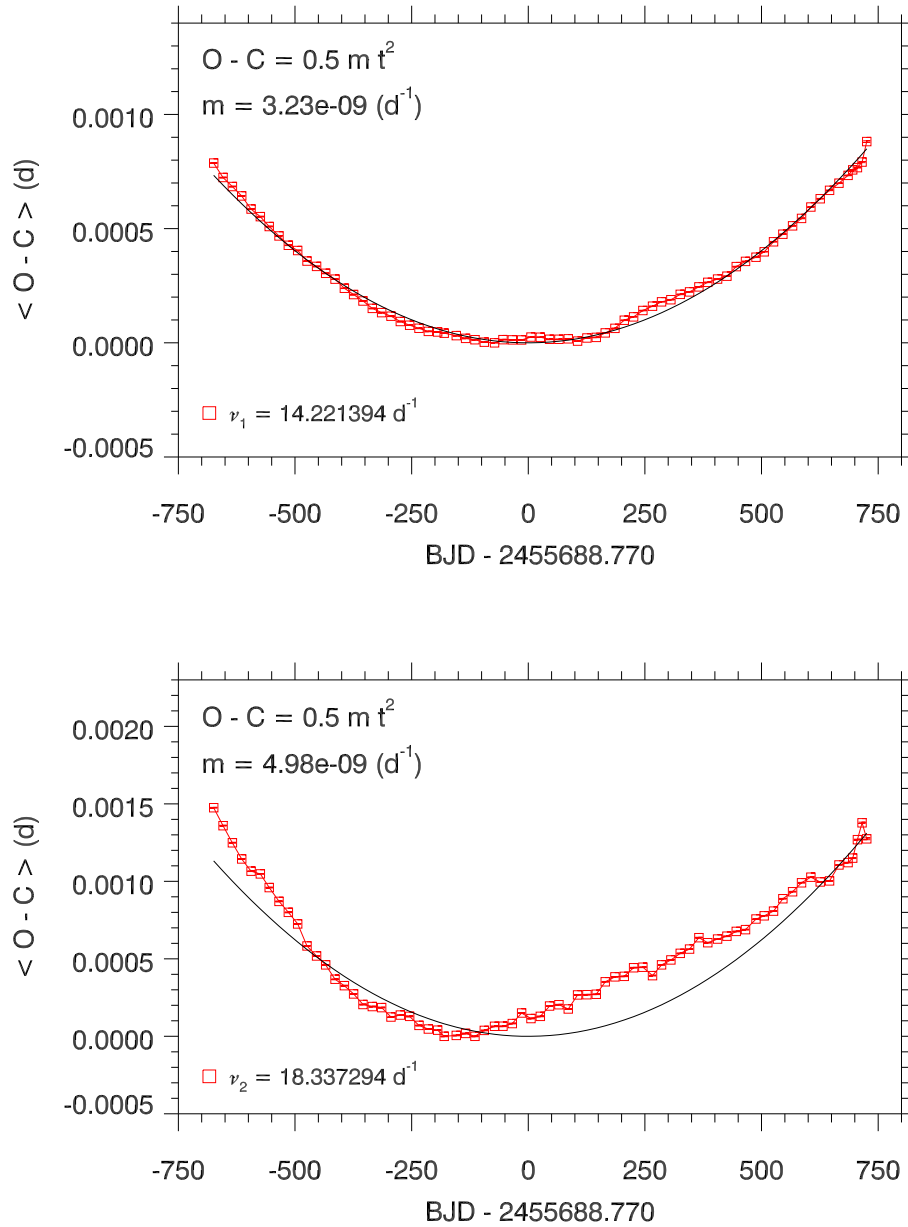
Figure 7.6: $O - C$ diagram for the HADS star KIC 5950759. Top and bottom panels are the observed period changes for the fundamental and first overtone radial modes, respectively. The solid black line represents the parabolic fit to the observations with m as a free parameter, which represents the fractional rate of change in the period of the pulsation mode.

in KIC 5950759 is caused by stellar evolution driving structural changes in this HADS stars, as the period changes may not be uniform during the main sequence — for example, larger period changes may be expected for a star near or beyond the TAMS compared to the ZAMS. Historically, observations covering decades have been needed to infer evolutionary changes to the pulsation modes in HADS stars and δ Sct stars (Percy et al. 1980; Breger 1990a; Rodríguez et al. 1995; Breger & Pamyatnykh 1998).

On the other hand, it could be concluded that the observed phase modulation in KIC 5950759 is evolutionary, since the period of the fundamental and first overtone radial modes are increasing over time. In β Cep stars studied by Neilson & Ignace (2015), period changes of order $\sim 10^{-5}$ yr^{-1} were observed in several stars, including β Cep itself. Perhaps stellar evolutionary models underestimate the rate of period change for δ Sct stars near the TAMS, and that values of $\left(\frac{1}{P}\frac{dP}{dt}\right)$ could be significantly larger than $\sim 1 \times 10^{-8}$ yr^{-1}. The analysis of KIC 5950759 clearly shows that the pulsation periods of the fundamental and first overtone radial modes are increasing over the 4-yr data set. Further work, including modelling the period changes in this HADS star, is needed to understand these observations.

7.4.2   KIC 9408694

The second HADS star is KIC 9408694 and pulsates with mode frequencies $\nu_1 = 5.661057$ d^{-1} and $\nu_3 = 7.148953$ d^{-1} with a period ratio of 0.7919, which is outside the expected range for the fundamental and first overtone radial modes (Stellingwerf 1979). The amplitude spectrum and tracking plot from Bowman et al. (2016) are shown in the top and bottom panels of Fig. 7.7, respectively. KIC 9408694 was analysed spectroscopically by Balona et al. (2012) who determined an effective temperature and surface gravity for KIC 9408694, which are included in Table 7.2 for comparison. From the spectroscopic analysis, Balona et al. (2012) discovered

that KIC 9408694 had a rotational velocity of $v \sin i = 100 \pm 10 \text{ km s}^{-1}$, which is unusually high for HADS stars, which have typical rotational velocities of $v \sin i \lesssim 40 \text{ km s}^{-1}$ (Breger 2000a; McNamara 2000; Rodríguez et al. 2000). The high rotation rate of KIC 9408694 perturbed the observed pulsation mode frequencies and was found to be responsible for the atypical period ratio in this star, with a model including fast rotation successfully identifying ν_1 and ν_3 as the fundamental and first overtone radial modes, respectively (Balona et al. 2012).

Similarly to KIC 5950759, the HADS star KIC 9408694 also exhibits instrumental periodic amplitude modulation in its fundamental radial mode, which can be seen in the top panel of Fig. 7.8. However, unlike KIC 5950759, only a small fractional change in phase is observed in the fundamental radial mode of KIC 9408694. This was also noted by Balona et al. (2012), who stated that the observed modulation in the fundamental radial mode of KIC 9408694 was likely an instrumental effect. As can be seen in Fig. 7.8, there is no quadratic change in phase for either the fundamental or first overtone radial modes in KIC 9408694. Thus, a calculation of the observed period changes in this star cannot be performed.

This raises the question: can these two HADS stars be considered at similar stages of stellar evolution, since their stellar parameters given in Table 7.2 are significantly different? Moreover, the analysis of the amplitude and phase modulation in their fundamental and first overtone radial pulsation modes yielded significantly different results, with only KIC 5950759 exhibiting increasing pulsation periods over time as predicted by stellar evolutionary models. Since there are only two HADS to study in the *Kepler* data set, it is difficult to draw any meaningful conclusions about the general properties of the HADS stars, but the analysis of stars presented in this chapter provides motivation for further investigation.

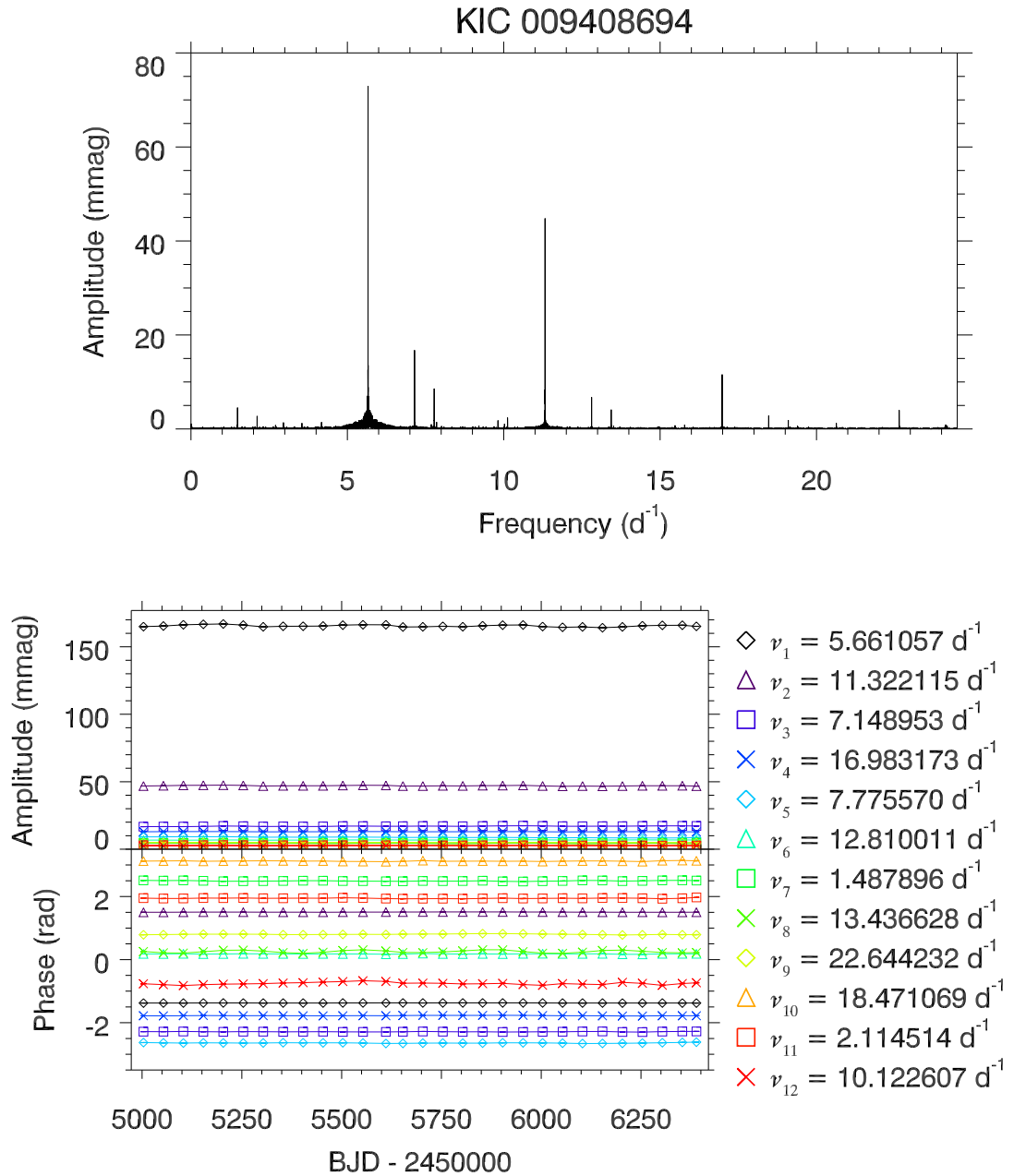Figure 7.7: The top panel is the 4-yr amplitude spectrum calculated out to the LC Nyquist frequency for the HADS star KIC 9408694. The bottom panel shows the amplitude and phase tracking plot, in which there is little or no variability in the amplitudes and phases of the radial pulsation mode frequencies, if instrumental modulation caused by the *Kepler* satellite is removed. Figure adapted from Bowman et al. (2016), their figure 7.
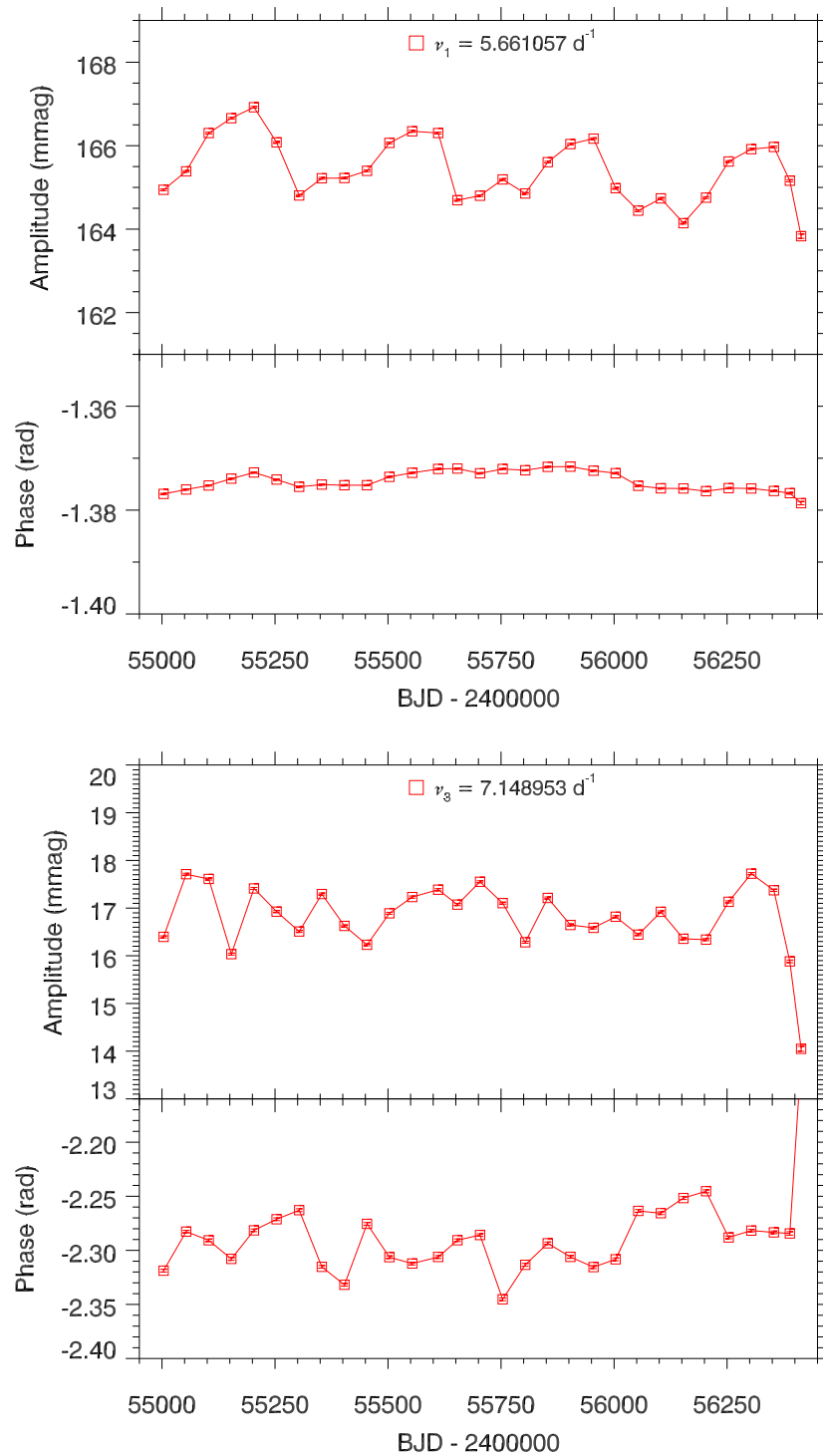
Figure 7.8: Amplitude and phase modulation in the HADS star KIC 9408694. Top and bottom panels are the amplitude and phase tracking plots for the fundamental and first overtone radial modes, respectively, using 100-d bins with 50-d overlaps. Note the difference in ordinate scales when comparing the two panels.

7.5   Discussion

Many studies over the last few decades have attempted to measure the period changes in pulsation modes caused by evolutionary changes in stellar structure of δ Sct stars (Percy et al. 1980; Breger 1990a; Rodríguez et al. 1995; Breger & Pamyatnykh 1998). All stars are evolving with time, but the question remains whether the observable parameters of a star, specifically pulsation mode frequencies, amplitudes and phases, are influenced on time-scales as short as the 4-yr *Kepler* data set. Although it remains small, the likelihood of observing evolutionary changes in a star is increased for a star near the TAMS or in a post-main sequence stage of evolution, as the structure of the star is changing on much shorter time-scales relative to its main sequence lifetime. For example, for A and F stars, the second contraction phase lasts approximately between $20 - 50$ Myr and the post-main sequence expansion phase lasts approximately between $50 - 100$ Myr (Breger & Pamyatnykh 1998), but this is still several orders of magnitude larger than the longest-studied δ Sct stars (e.g., 4 CVn Breger et al. 1990; Breger 2000b, 2016).

The ρ Pup star KIC 3429637 remains a useful case study of amplitude modulation, because a study using high-resolution spectroscopy, *Kepler* photometry and accurate asteroseismic modelling was performed by Murphy et al. (2012). This star was determined to be near the TAMS and its amplitude modulation was conjectured to be caused by structural changes driven by stellar evolution (Murphy et al. 2012). Few δ Sct stars have been observed using high-resolution spectroscopy and even fewer have been modelled asteroseismically. However, it was shown in section 7.3, that KIC 3429637 exhibits amplitude and phase modulation that is typical of δ Sct stars in the 4-yr *Kepler* data set (Bowman et al. 2016). Further work is needed to perform similar analyses of other AMod stars, which were discussed in chapters 5 and 6, to determine if the observed amplitude and phase modulation is related to stellar evolution.

CHAPTER 7

The HADS stars offer the opportunity to study non-linearity and possible structural changes caused by stellar evolution in a subgroup of high-amplitude, slowly-rotating δ Sct stars (Petersen & Christensen-Dalsgaard 1996; Breger 2000a; McNamara 2000; Rodríguez et al. 2000). Only two HADS stars were observed by *Kepler*, KIC 5950759 and KIC 9408694, which exhibit fractional amplitude variability of order 1 per cent with a period equal to the *Kepler* orbital period — each has several AMod frequencies using the $\pm 5\sigma$ significance criterion of Bowman et al. (2016). From only two HADS stars no significant conclusions can be made about the location of HADS stars in the HR diagram (see e.g., Balona 2016a).

The same amplitude limitation mechanism predicted for the low-amplitude δ Sct stars does not seem to be at work within HADS stars, which pulsate at much higher amplitudes (Breger 2000a). It is interesting to note that high amplitude pulsations are typically associated with non-linearity in the form of harmonics and combination terms, which are found in KIC 5950759 and KIC 9408694, but the lack of significant amplitude modulation in these HADS stars suggests that non-linearity in the form of resonant mode coupling is not at work (Bowman et al. 2016). This result is interesting since it has been suggested that resonant mode coupling is the amplitude limitation mechanism that operates in δ Sct stars but not in HADS stars, thus explaining the large difference in pulsation mode amplitudes between the two subgroups (Dziembowski & Krolikowska 1985).

Furthermore, HADS stars have similarities to Cepheid variables (Eggen 1976; Breger 2000a; McNamara 2000; Soszyński et al. 2008; Poleski et al. 2010). It was suggested by Dziembowski (1977b) that radiative damping is stronger in more massive stars, leading to fewer non-radial pulsation modes, which may explain why the so-called transitionary δ Sct stars, i.e., the HADS and ρ Pup stars, pulsate in mainly radial pulsation modes and evolved stars such as Cepheids pulsate exclusively in radial modes.

CHAPTER 7

On the other hand, HADS stars also share similarities to δ Sct stars. For example, HADS stars have been confirmed to contain low-amplitude non-radial modes in addition to high-amplitude radial modes (Mathias et al. 1997; Poretti 2003; Balona et al. 2012). Although significant amplitude modulation was not found in KIC 5950759 and KIC 9408694, Poretti et al. (2011) discovered quasi-periodic amplitude modulation – similar to the Blazhko effect in RR Lyr stars – in the fundamental radial mode in the CoRoT HADS star ID 101155310. Also, amplitude modulation in the second overtone radial mode in the triple-mode HADS star GSC 03144-595 was recently discovered by Mow et al. (2016), whilst the fundamental and first overtone radial modes had constant amplitudes. These studies support the view that HADS stars are transitionary objects within the classical instability strip, and are in a post-main sequence stage of stellar evolution (Poretti et al. 2011; Mow et al. 2016).

In section 7.4.1 it was discussed how one of the two HADS stars, KIC 5950759, showed parabolic phase modulation in its fundamental and first overtone radial modes, whereas KIC 9408694 showed approximately constant phases. The parabolic phase modulation observed in KIC 5950759 was fitted using Eqn 7.1 and yielded fractional period changes, $\left(\frac{1}{P}\frac{dP}{dt}\right)$, of 1.18×10^{-6} yr^{-1} and 1.82×10^{-6} yr^{-1} for the fundamental and first overtone radial modes, respectively, which is two orders of magnitude larger than predicted by stellar evolutionary models (Percy et al. 1980; Breger 1990a; Rodríguez et al. 1995; Breger & Pamyatnykh 1998). Therefore, assuming that the period changes predicted by stellar evolutionary models are correct, the observed period changes in KIC 5950759 are too large to be caused by stellar evolution and represent shorter time-scale changes to the pulsation cavities of KIC 5950759. On the other hand, the evolutionary models may be incorrect, or may not be accurate for stars near the TAMS that possibly evolve at a different rate compared to at the ZAMS, so further work is needed to address this, as clearly the periods of the radial modes in KIC 5950759 are increasing in time.

CHAPTER 7

Note that in chapter 5, it was demonstrated that the majority of δ Sct stars have variable pulsation amplitudes, many also with associated phase modulation over the 4-yr *Kepler* data set. It was also demonstrated in chapters 5 and 6 that frequency and amplitude modulation of pulsation modes can be caused by beating or non-linearity, with either of these mechanisms causing a larger magnitude of phase variability than is expected from stellar evolution. Thus, it becomes difficult to disentangle modulation caused by non-linearity and possible phase modulation caused by stellar evolution.

The HADS stars are certainly interesting stars to study, with each one being unique for a different reason. Large-number studies of δ Sct stars in the LMC (Poleski et al. 2010) and the Milky Way galaxy (Lee et al. 2008) have established that HADS stars are rare, making up fewer than 1 per cent of pulsating main sequence stars inside the classical instability strip. There are two possible inferences to consider when studying HADS stars, which are not necessarily mutually exclusive: the HADS stars are transitionary δ Sct stars in a post-main sequence stage of evolution (Petersen & Christensen-Dalsgaard 1996); or, slow rotation is a prerequisite for large pulsation amplitudes (Breger 2000a; Rodríguez et al. 2000). The small number of HADS stars observed by *Kepler* means one must be cautious when defining the characteristics of a group of stars (e.g., Balona 2016a). In the future, it will be interesting to create large catalogue of HADS stars and build on the methods developed in this thesis to study non-linearity, and the effects of slow rotation and stellar evolution in these stars.

Chapter 8

Conclusions and future work

8.1 Conclusions

The δ Sct stars represent a diverse group of pulsating stars, in which many aspects of physics, such as rotation, binarity, magnetism and chemical peculiarities, play important roles. In this thesis, an ensemble of 983 δ Sct stars that were observed continuously by *Kepler* over 4 yr was created and used to study the pulsational properties of these stars, and primarily the incidence of amplitude modulation of their pulsation modes.

It was discussed in chapter 2, how the *Kepler* Space Telescope provided continuous observations of approximately 150 000 stars for 4 yr with a photometric precision of order a few μmag (Borucki et al. 2010; Koch et al. 2010; Gilliland et al. 2010). The advent of space telescopes created a photometry revolution and has allowed different aspects of physics to be probed in detail for the first time in a large number of δ Sct stars, which could not be achieved from ground-based observations. In chapter 2, it was demonstrated how the amplitude visibility function when using LC data causes amplitude suppression for, on average, high-frequency signals, which biases observations of pulsating stars to low frequency pulsation modes. However, few δ Sct stars were observed for long periods of time with SC, so LC observations

represent a more complete data set with increased frequency resolution for studying these stars.

The δ Sct star KIC 7106205 studied by Bowman & Kurtz (2014) and discussed in chapter 3 is an archetypal example of amplitude modulation in δ Sct stars, as it contains few pulsation modes in its amplitude spectrum with only a single p mode that changed significantly in amplitude over 4 yr. A further study of KIC 7106205 by Bowman et al. (2015) using ground-based photometry from the Wide Angle Search for Planets (WASP; Pollacco et al. 2006) project was also discussed in chapter 3, in which WASP data were used to extend the study of amplitude modulation in KIC 7106205 2 yr prior to the launch of the *Kepler* Space Telescope. It was shown that a single pulsation mode decreased in amplitude from 11.70 ± 0.05 mmag in 2007, to 5.87 ± 0.03 mmag in 2009, and to 0.58 ± 0.06 mmag in 2013 (Bowman et al. 2015). Time spans of years and decades are clearly important in δ Sct stars, with the study of KIC 7106205 demonstrating that different pulsation mode amplitudes would be obtained if only short and intermittent observations of this star were used. The analysis of the KIC 7106205 provided clear and strong evidence that a physical mechanism within the star is causing the observed amplitude modulation. Furthermore, the visible pulsation energy budget in this star was not conserved over 6 yr of combined WASP and *Kepler* observations (Bowman & Kurtz 2014; Bowman et al. 2015). Spectroscopic observations of KIC 7106205 revealed that this star is not a classical Am star, but does have some relatively strong metal lines for its Ca K line strength and can be considered a marginal Am star. However, the metallic line strengths are unrelated to the observed amplitude modulation.

From the study of radial pulsation modes in δ Sct stars from the ground, it was established that hotter δ Sct stars typically have higher pulsation mode frequencies (Breger & Bregman 1975; Breger 2000a). Hotter δ Sct stars have the He II ionisation zone located closer to the stellar surface, which facilitates higher

overtone and therefore higher frequency modes to be excited (Pamyatnykh 1999, 2000; Christensen-Dalsgaard 2000; Dupret et al. 2004, 2005). In chapter 4, an ensemble of 983 δ Sct stars that were observed continuously by *Kepler* for 4 yr was presented, and the statistical properties of these stars were investigated, including relationships between stellar parameters and the frequency of the dominant pulsation mode, defined as the frequency of the highest amplitude pulsation mode. It was found that the hotter δ Sct stars typically have higher pulsation mode frequencies, as shown by Fig. 4.7 and the $T_{\text{eff}} - \log g$ diagrams in Figs 4.12 and 4.13. However, the bias towards low frequency pulsation modes caused by the LC amplitude visibility function resulted in few hot δ Sct stars to be included in the ensemble. Consequently, the correlation found between the frequency of the highest amplitude pulsation mode and effective temperature is a lower bound of the true correlation as there are few δ Sct stars included in the ensemble of 983 stars with frequencies above $\nu \gtrsim 40$ d^{-1}. Another outcome from the statistical study of δ Sct stars discussed in section 4.7 was that a small yet significant fraction of δ Sct and γ Dor stars are found outside of their respective instability regions, such that the observational edges of the classical instability strip need to be updated.

A statistical study of amplitude modulation in all 983 δ Sct stars by Bowman et al. (2016) was presented in chapter 5. The results of this study provide strong evidence that variable pulsation amplitudes are common in δ Sct stars, with 61.3 per cent of the 983 δ Sct stars exhibiting significant amplitude modulation in at least one pulsation mode over the 4-yr *Kepler* data set. Similarly to KIC 7106205, the most remarkable result from this analysis is that many δ Sct stars to do not conserve their visible pulsation energy budget over 4 yr (Bowman et al. 2016). Moreover, the 38.7 per cent of NoMod δ Sct stars that exhibit constant pulsation amplitudes and phases, were found across the classical instability strip in the HR diagram, thus the mechanisms that cause variable pulsation amplitudes are not restricted to a

small region in the HR diagram (Bowman et al. 2016). My amplitude modulation catalogue of 983 δ Sct stars utilising 4 yr of continuous *Kepler* observations will be a valuable resource for comparison to observations of similar stars with K2 (Howell et al. 2014) and TESS (Ricker et al. 2015). Eventually, these missions will observe a large area of the sky, but for only a short length of time. Therefore, the *Kepler* data set will remain the best data set for studying δ Sct stars as its 4-yr length of continuous observations will not be surpassed for some time.

It was demonstrated by Bowman et al. (2016) how a pair of close-frequency pulsation modes produce amplitude modulation, with a characteristic beat period as the inverse of the difference in pulsation mode frequencies. Amplitude modulation caused by beating is most easily recognised because a phase change occurs at the epoch of minimum amplitude, which is equal to π rad for two equal-amplitude cosinusoids. For increasingly different amplitudes, this phase change gets progressively smaller. It was shown in chapter 5 that some of the stars classified as AMod by Bowman et al. (2016) are the result of beating from close-frequency pulsation modes. Specifically, two pairs of close-frequency modes separated by less than 0.001 d^{-1} in the δ Sct stars KIC 4641555 and KIC 8246833, were used to construct beating models that accurately reproduced observations. These stars demonstrate that it is possible for δ Sct stars to contain pulsation mode frequencies that are barely resolved using the 4-yr *Kepler* data set (Bowman et al. 2016).

Therefore, it is possible that other AMod δ Sct stars are the result of beating from unresolved close-frequency pulsation modes. In chapter 5, a Bayesian MCMC simulation was used to extract the parameters of three hypothetical pulsation modes using a synthetic *Kepler* data set. The simulation was able to accurately extract the frequencies, amplitudes and phases of these modes, which were chosen to emulate the observed amplitude modulation in the δ Sct star KIC 7106205. However, the implementation of two-, three- and four-mode MCMC simulations to the *Kepler*

observations of KIC 7106205 did not converge to a solution. This supports the conclusions from Bowman & Kurtz (2014) that the observed amplitude modulation in KIC 7106205 is caused by a mode coupling mechanism to high-degree p modes or internal g modes; or energy lost to an unknown damping/driving region; and is not caused by beating.

The observation of concomitant amplitude and phase modulation can be used to distinguish between cases of intrinsic amplitude modulation of a single pulsation mode or beating from unresolved close-frequency pulsation modes (Breger & Pamyatnykh 2006; Bowman et al. 2016). A subgroup of pure AMod stars was defined by Bowman et al. (2016), which contained stars with at least a single variable amplitude pulsation mode but not in phase. This pure form of amplitude modulation cannot be explained by beating or a mode coupling mechanism. These pure AMod stars are arguably the most interesting of all the AMod stars, since they were an unexpected discovery and are as yet unexplained. It was conjectured by Bowman et al. (2016) that pure AMod δ Sct stars are caused by slow changes in the relative driving and damping in these stars, but further work is needed to address this.

In chapters 5 and 6, the mathematical relationships in frequency, amplitude and phase between two parent modes and a child mode were discussed. Models of mode coupling were also used to distinguish between different forms of non-linearity in δ Sct stars, particularly combination frequencies arising from a non-linear distortion model or coupled modes from resonant mode coupling. If a child mode is resonantly excited from a mode coupling mechanism, it will have a larger amplitude than a combination frequency from a non-linear distortion model (van Kerkwijk et al. 2000b; Breger & Montgomery 2014; Bowman et al. 2016). Moreover, the observed amplitude modulation in the parent modes allowed the strength of non-linearity between a child and parent modes to be quantified. The coupling strength was tested for a selection of δ Sct stars with amplitude modulation, specifically KIC 4733344

in chapter 5 and KIC 5857714 in chapter 6, which distinguished whether a child mode is excited by resonant mode coupling or is a combination frequency from a non-linear distortion model (Bowman et al. 2016).

Non-linearity in the form of harmonics and combination frequencies are ubiquitous in all types of pulsators driven by the κ mechanism. The frequencies and phases of combination frequencies are predicted to be locked to the parent pulsation modes, with any variability in the parent pulsation modes being mirrored by the combination frequencies (Brickhill 1992b; Wu & Goldreich 2001; Wu 2001), which is commonly found for different types of pulsator including δ Sct stars (see e.g., KIC 4733344 and KIC 5857714, or Breger & Lenz 2008b). However, in chapter 6 it was shown that this was not the case for the γ Dor star KIC 4731916. The amplitude variability of a triplet of combination frequencies ($2\nu_1$, $\nu_1 + \nu_2$ and $2\nu_2$) did not mirror the amplitude variability of the two parent g modes, ν_1 and ν_2. This is an unexpected result and the γ Dor star KIC 4731916 demonstrates that we lack a complete physical description of combination frequencies, and how they are generated. Clearly, non-linearity is at work in this star, but the interplay between the mechanism that generates the combination frequencies and the mechanism that causes the amplitude modulation requires further investigation.

In chapter 7, the concept of measuring period changes in pulsation modes was investigated for the ρ Pup star KIC 3429637 and the HADS stars KIC 5790759 and KIC 9408694. The ρ Pup and HADS stars are considered evolved stars (Petersen & Christensen-Dalsgaard 1996; Breger 2000a; Murphy et al. 2012), so there is a greater likelihood of observing real-time stellar evolutionary changes in their observed pulsation modes. However, from ground-based observations, an even distribution of increasing and decreasing pulsation periods was seen in δ Sct stars (Breger 1990a; Guzik & Cox 1991; Rodríguez & Breger 2001). This cannot be explained by stellar evolution since pulsation periods should predominantly increase throughout the

main sequence and post-main sequence (Percy et al. 1980; Breger 1990a; Rodríguez et al. 1995; Breger & Pamyatnykh 1998).

Most importantly, it was demonstrated in chapters 5, 6 and 7 that the observed phase modulation in δ Sct stars is often much larger than the quadratic change in phase predicted by stellar evolution models, with fractional changes in pulsation periods of $\left(\frac{1}{P}\frac{dP}{dt}\right) \sim 10^{-8}$ yr^{-1} predicted by stellar evolutionary models (Percy et al. 1980; Breger 1990a; Rodríguez et al. 1995; Breger & Pamyatnykh 1998). The parabolic phase modulation observed in the HADS star KIC 5950759 yielded fractional period changes, $\left(\frac{1}{P}\frac{dP}{dt}\right)$, of 1.18×10^{-6} yr^{-1} and 1.82×10^{-6} yr^{-1} for the fundamental and first overtone radial modes, respectively. Thus, it was concluded that 4 yr is sufficient to observe period changes in a δ Sct star, but these may not necessarily be caused by stellar evolution, because modulation signals from non-linearity typically dominate observations on this time-scale. On the other hand, it was clearly demonstrated that the pulsation periods are increasing in KIC 5950759, and evolutionary models may underestimate period changes for stars near the TAMS.

HADS stars also offer the opportunity to study non-linearity in the form of harmonics and combination frequencies from a non-linear distortion model, typically in the absence of amplitude modulation and non-linearity in the form of resonant mode coupling. It remains to be established if HADS stars are demonstrably separate from their low-amplitude δ Sct counterparts. With so few HADS stars available to study with high-quality observations, further observations and theoretical work on modelling non-linearity in the HADS stars and their low-amplitude δ Sct counterparts is needed.

8.2   Future work

Much of the work presented in this thesis has demonstrated that the δ Sct stars commonly exhibit amplitude modulation on time-scales of order years and longer, but

that there is also a large range in the diversity of the temporal behaviour observed. In sections 1.4.3 and 1.4.4 it was discussed how pulsating main sequence B stars and evolved stars, such as RR Lyr, sdBV and variable white dwarfs, all show amplitude modulation of their respective pulsation modes if the length of observations is long enough to resolve the behaviour. A question resulting from this work is: are the δ Sct stars similar to other pulsating stars driven by the κ mechanism in terms of the mechanism(s) that causes non-linearity in the form of amplitude modulation and combination frequencies? This is an interesting question as most types of stars do show some form of amplitude modulation.

There are various theoretical and observational synergies between pulsating A and B stars, such that β Cep stars can be considered analogues of δ Sct stars, from the similar pulsation mode frequencies observed. The κ mechanism operating in the Z bump in opacity causes low-order p modes to become unstable (Dziembowski & Pamyatnykh 1993a). Hybrid B stars pulsating in both g- and p-mode frequencies have also been observed (Handler 2009; Degroote et al. 2012), which can be explained by increasing opacity in the Z bump (Pamyatnykh et al. 2004). Further similarity exists, as Degroote et al. (2009) found evidence for resonant mode coupling in the β Cephei star HD 180642 using CoRoT photometry. The authors found that the sum and difference combination frequencies had similar amplitudes, but a greater number of sum combination frequencies (Degroote et al. 2009). It would be interesting to investigate the synergy in mode coupling within hybrid stars, between A and B stars, both observationally and theoretically.

To achieve this, modelling of individual stars using stellar evolution codes such as `MESA` (Paxton et al. 2011, 2013, 2015) and pulsation codes such as `GYRE` (Townsend & Teitler 2013), is needed to fully understand the observed behaviour. The following questions need to be tested: why do only some and not all of the δ Sct stars, and by extension different pulsators driven by the κ mechanism, show variable pulsation

mode amplitudes over time-scales of years and longer? Is this behaviour governed by stellar evolution, or the pulsation excitation mechanism or both? A starting point for such a project is to study stars for which there is low mode-density and mode identification is relatively simple; for example, the HADS stars. The HADS stars have large pulsation amplitudes and exhibit non-linearity in the form of harmonics and combination frequencies, but non-linearity in the form of amplitude modulation and resonant mode coupling is absent in these stars (Bowman et al. 2016). Resonant mode coupling has been suggested as the amplitude limitation mechanism operating in δ Sct stars to explain the large difference in pulsation mode amplitudes between HADS stars and their low-amplitude δ Sct counterparts (Dziembowski & Krolikowska 1985). Further work is needed to establish why the HADS stars are rare and the possible physical differences between them and the δ Sct stars, especially if they are transitionary objects in a post-main sequence stage of stellar evolution.

Recent work by Fuller et al. (2015) and Stello et al. (2016) has shown that many red giant stars have suppressed dipole modes, which can be explained by the scattering of mode energy into high-degree modes as the modes interact with a magnetic field in a star's core. This effect, termed the Magnetic Greenhouse Effect (Fuller et al. 2015), essentially traps the mode energy in the magnetised core of a red giant star resulting in low surface amplitudes for the dipole modes. Stello et al. (2016) demonstrated that not all red giant stars exhibit suppressed dipole modes and that it is a strong function of stellar mass.

Among other pulsating stars, Cantiello et al. (2016) modelled a 1.6-$M_\odot$ main sequence γ Dor star and suggested that it is possible for a dynamo-generated magnetic field to be induced near the core in such a star. This could alter the pulsational behaviour of a star and redistribute mode energy into higher degrees, hence dramatically reduce their visible amplitudes (Cantiello et al. 2016). Could a similar mechanism be the cause for a number of the AMod δ Sct stars in the ensemble of

δ Sct star presented in this thesis? The A and F stars have convective cores on the main sequence and if a magnetic field is sustained throughout the transition from post-main sequence to the red giant branch, it is reasonable to assume that the progenitors of red giant stars with suppressed dipole modes also had magnetic fields near their cores on the main sequence. The evolutionary progenitors of the suppressed dipole mode red giant stars from Fuller et al. (2015) and Stello et al. (2016) are within my ensemble of δ Sct stars.

8.2.1   Spectroscopic follow-up of delta Scuti stars

As previously discussed in section 3.4, spectroscopic follow-up observations of 23 δ Sct stars were made with the Intermediate dispersion Spectrograph and Imaging System (ISIS) on the William Herschel Telescope (WHT). Details of these stars, including their positions and apparent visual magnitudes, were given in Table 3.1. All of these stars were observed spectroscopically because they are relatively bright targets for *Kepler* stars, with a mixture of δ Sct stars that exhibit amplitude modulation and others that do not.

It was shown in section 3.4, that the spectrum of the δ Sct star KIC 7106205 indicated that this star has signatures of being a marginal Am star. In the future, it is intended to supplement this study with the analysis of the other stars, to determine if amplitude modulation is more commonly found in chemically normal or peculiar stars, fast or slowly-rotating stars, or a combination of these parameters. Ultimately, the aim is to understand if chemical peculiarity is related to amplitude modulation in δ Sct stars.

8.2.2   Future missions

The future of asteroseismology is bright with ongoing projects such as WASP, K2 and BRITE continuing to produce many interesting and exciting results. In the

near future, the NASA TESS mission (Ricker et al. 2015) and the ESA PLATO 2.0 mission (Rauer et al. 2014) will be launched in 2017 and 2022, respectively, which will vastly increase the number of stars studied in the Milky Way galaxy.

The TESS mission

The Transiting Exoplanet Survey Satellite (TESS; Ricker et al. 2015) will be launched in 2017, with a primary goal of finding exoplanets around late-type stars. To achieve this, it will have a passband of 600 to 1000 nm, which is redder than the passband of 420 to 900 nm of the *Kepler* Space Telescope (Koch et al. 2010). For an early-F star with $T_{\text{eff}} = 7000$ K star, pulsation mode amplitudes will be approximately 47 per cent that of *Kepler* from the difference in passband, which is shown graphically in the top panel of Fig. 8.1. For an early-A star with $T_{\text{eff}} = 10\,000$ K star, this value is reduced with pulsation mode amplitudes that will be approximately 39 per cent that of *Kepler* from the difference in passband, which is shown graphically in the bottom panel of Fig. 8.1.

Eventually, TESS will observe a large fraction of the sky, with observing runs that last from 27 d up to 1 yr in the continuous viewing zones near the ecliptic polar regions (Ricker et al. 2015). After data downlinks, TESS will start re-observing at a random phase, which will create a variable Nyquist frequency and successfully allow the sNa technique to be implemented for pulsation mode frequencies that lie above the TESS Nyquist frequency (Murphy 2015). Although TESS is optimised to study cool stars, asteroseismology of many different types of stars will be possible.

The GAIA mission

GAIA will change everything. Results from the GAIA mission (Perryman et al. 2001) will soon be available to the scientific community, which will allow almost all *Kepler* targets to be accurately placed in the HR diagram — see Lindegren et al.
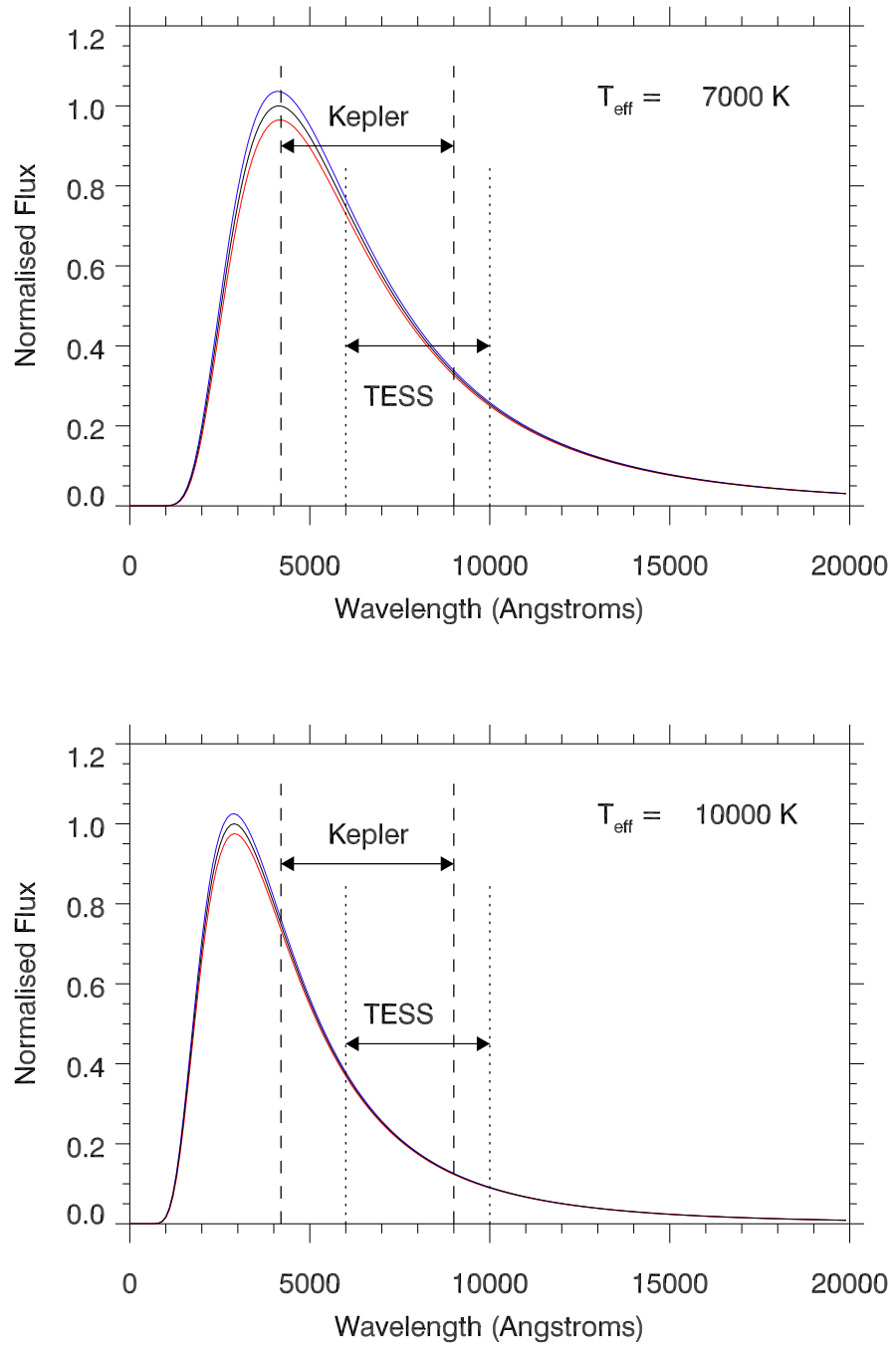
Figure 8.1: The Planck blackbody functions for a $T_{\rm eff} = 7000$ K and a $T_{\rm eff} = 10\,000$ K star are shown in the top and bottom panels, respectively, as black solid curves. The red and blue curves show the change in the planck function for ± 50 K change in temperature in each star. Approximate *Kepler* and TESS passbands are plotted as dashed and dotted lines, respectively.

(2008, 2012) for more details. GAIA is currently measuring parallaxes for many stars in the Milky Way and will provide distances for more than 150 000 stars that are accurate to 0.1 per cent, and distances for more than a million stars that are accurate to 1 per cent. This will be a phenomenal improvement to current estimates of luminosity for practically all previously observed stars in the Milky Way and will constrain future observations and in turn models of stellar structure and evolution.

8.3   Final remarks

It has been a privilege and a pleasure to work within the *Kepler* Asteroseismic Science Consortium (KASC) on the analysis of δ Sct stars. I trust that this thesis and the publications contained within it are of use to others. We are currently in a golden age of astronomy, a Space Photometry Revolution, and I hope that the success of asteroseismology will continue to grow exponentially, and improve our understanding of stellar structure and evolution for intermediate-mass stars.

Bibliography

Abt, H. A. 1961, ApJS, 6, 37

Abt, H. A. 1967, in Magnetic and Related Stars, ed. R. C. Cameron, 173

Abt, H. A. 1984, ApJ, 285, 247

Abt, H. A. 2009, AJ, 138, 28

Abt, H. A. & Levy, S. G. 1985, ApJS, 59, 229

Abt, H. A. & Morrell, N. I. 1995, ApJS, 99, 135

Abt, H. A. & Snowden, M. S. 1973, ApJS, 25, 137

Aerts, C. 2015, Astronomische Nachrichten, 336, 477

Aerts, C., Christensen-Dalsgaard, J., & Kurtz, D. W. 2010, Asteroseismology (Springer)

Aerts, C., De Cat, P., Peeters, E., et al. 1999, A&A, 343, 872

Aerts, C. & Rogers, T. M. 2015, ApJL, 806, L33

Antoci, V., Cunha, M., Houdek, G., et al. 2014, ApJ, 796, 118

Antoci, V., Handler, G., Campante, T. L., et al. 2011, Nature, 477, 570

Antoci, V., Handler, G., Grundahl, F., et al. 2013, MNRAS, 435, 1563

Aurière, M., Silvester, J., Wade, G. A., et al. 2004, in IAU Symposium, Vol. 224, The A-Star Puzzle, ed. J. Zverko, J. Ziznovsky, S. J. Adelman, & W. W. Weiss, 633–636

Auvergne, M., Bodin, P., Boisnard, L., et al. 2009, A&A, 506, 411

Babcock, H. W. 1960, ApJ, 132, 521

Baglin, A., Breger, M., Chevalier, C., et al. 1973, A&A, 23, 221

Bailey, S. I. 1902, Annals of Harvard College Observatory, 38, 1

Balmforth, N. J. 1992, MNRAS, 255, 603

Balmforth, N. J. & Gough, D. O. 1990, Solar Physics, 128, 161

Balona, L. A. 2011, MNRAS, 415, 1691

Balona, L. A. 2012, MNRAS, 422, 1092

Balona, L. A. 2013, MNRAS, 431, 2240

Balona, L. A. 2014, MNRAS, 437, 1476

Balona, L. A. 2016a, MNRAS, 459, 1097

Balona, L. A. 2016b, MNRAS, 457, 3724

Balona, L. A., Baran, A. S., Daszyńska-Daszkiewicz, J., & De Cat, P. 2015a, MNRAS, 451, 1445

Balona, L. A., Daszyńska-Daszkiewicz, J., & Pamyatnykh, A. A. 2015b, MNRAS, 452, 3073

Balona, L. A. & Dziembowski, W. A. 1999, MNRAS, 309, 221

Balona, L. A. & Dziembowski, W. A. 2011, MNRAS, 417, 591

Balona, L. A., Guzik, J. A., Uytterhoeven, K., et al. 2011a, MNRAS, 415, 3531

Balona, L. A., Krisciunas, K., & Cousins, A. W. J. 1994, MNRAS, 270, 905

Balona, L. A., Lenz, P., Antoci, V., et al. 2012, MNRAS, 419, 3028

Balona, L. A. & Nemec, J. M. 2012, MNRAS, 426, 2413

Balona, L. A., Pigulski, A., Cat, P. D., et al. 2011b, MNRAS, 413, 2403

Balona, L. A., Ripepi, V., Catanzaro, G., et al. 2011c, MNRAS, 414, 792

Barceló Forteza, S., Michel, E., Roca Cortés, T., & García, R. A. 2015, A&A, 579, A133

Barlow, B. N., Dunlap, B. H., Rosen, R., & Clemens, J. C. 2008, ApJL, 688, L95

Beck, P. G., Montalban, J., Kallinger, T., et al. 2012, Nature, 481, 55

Bessell, M. S. 1979, PASP, 91, 589

Bessell, M. S. 2005, ARA&A, 43, 293

Bigot, L. & Dziembowski, W. A. 2002, A&A, 391, 235

Bigot, L. & Kurtz, D. W. 2011, A&A, 536, A73

Blažko, S. 1907, Astronomische Nachrichten, 175, 325

Blomme, R., Mahy, L., Catala, C., et al. 2011, A&A, 533, A4

Bono, G., Caputo, F., & Santolamazza, P. 1997, A&A, 317, 171

Borucki, W. J., Koch, D., Basri, G., et al. 2010, Science, 327, 977

Borucki, W. J., Koch, D. G., Basri, G., et al. 2011, ApJ, 728, 117

Bouabid, M.-P., Dupret, M.-A., Salmon, S., et al. 2013, MNRAS, 429, 2500

Bouabid, M.-P., Montalbán, J., Miglio, A., et al. 2011, A&A, 531, A145

Bowman, D. M., Holdsworth, D. L., & Kurtz, D. W. 2015, MNRAS, 449, 1004

Bowman, D. M. & Kurtz, D. W. 2014, MNRAS, 444, 1909

Bowman, D. M. & Kurtz, D. W. 2015, in European Physical Journal Web of Conferences, Vol. 101, European Physical Journal Web of Conferences, 6013

Bowman, D. M., Kurtz, D. W., Breger, M., Murphy, S. J., & Holdsworth, D. L. 2016, MNRAS, 460, 1970

Brassard, P., Fontaine, G., Wesemael, F., & Talon, A. 1993, in NATO Advanced Science Institutes (ASI) Series C, Vol. 403, NATO Advanced Science Institutes (ASI) Series C, ed. M. A. Barstow, 485

Breger, M. 1970, ApJ, 162, 597

Breger, M. 1979, PASP, 91, 5

Breger, M. 1981, ApJ, 249, 666

Breger, M. 1990a, in Astronomical Society of the Pacific Conference Series, Vol. 11, Confrontation Between Stellar Pulsation and Evolution, ed. C. Cacciari & G. Clementini, 263–273

Breger, M. 1990b, Delta Scuti Star Newsletter, 2, 13

Breger, M. 2000a, in Astronomical Society of the Pacific Conference Series, Vol. 210, Delta Scuti and Related Stars, ed. M. Breger & M. Montgomery, 3

Breger, M. 2000b, MNRAS, 313, 129

Breger, M. 2009, in American Institute of Physics Conference Series, Vol. 1170, Stellar Pulsation: Challenges for theory and observation, ed. J. A. Guzik & P. A. Bradley (American Institute of Physics Conference Series), 410–414

Breger, M. 2016, A&A, 592, A97

Breger, M. & Bischof, K. M. 2002, A&A, 385, 537

Breger, M. & Bregman, J. N. 1975, ApJ, 200, 343

Breger, M., Fossati, L., Balona, L., et al. 2012, ApJ, 759, 62

Breger, M., Handler, G., Garrido, R., et al. 1999, A&A, 349, 225

Breger, M. & Kolenberg, K. 2006, A&A, 460, 167

Breger, M. & Lenz, P. 2008a, Communications in Asteroseismology, 157, 292

Breger, M. & Lenz, P. 2008b, A&A, 488, 643

Breger, M., Lenz, P., & Pamyatnykh, A. A. 2009, MNRAS, 396, 291

Breger, M., Lenz, P., & Pamyatnykh, A. A. 2013, ApJ, 773, 56

Breger, M., McNamara, B. J., Kerschbaum, F., et al. 1990, A&A, 231, 56

Breger, M. & Montgomery, M. H. 2014, ApJ, 783, 89

Breger, M. & Pamyatnykh, A. A. 1998, A&A, 332, 958

Breger, M. & Pamyatnykh, A. A. 2006, MNRAS, 368, 571

Breger, M., Stich, J., Garrido, R., et al. 1993, A&A, 271, 482

Brickhill, A. J. 1983, MNRAS, 204, 537

Brickhill, A. J. 1990, MNRAS, 246, 510

Brickhill, A. J. 1991a, MNRAS, 251, 673

Brickhill, A. J. 1991b, MNRAS, 252, 334

Brickhill, A. J. 1992a, MNRAS, 259, 529

Brickhill, A. J. 1992b, MNRAS, 259, 519

Brown, T. M., Latham, D. W., Everett, M. E., & Esquerdo, G. A. 2011, AJ, 142, 112

Buchler, J. R. & Goupil, M.-J. 1984, ApJ, 279, 394

Buchler, J. R., Goupil, M.-J., & Hansen, C. J. 1997, A&A, 321, 159

Buchler, J. R., Goupil, M. J., & Serre, T. 1995, A&A, 296, 405

Buysschaert, B., Aerts, C., Bloemen, S., et al. 2015, MNRAS, 453, 89

Campbell, W. W. & Wright, W. H. 1900, ApJ, 12, 254

Cantiello, M., Fuller, J., & Bildsten, L. 2016, ApJ, 824, 14

Casagrande, L., Silva Aguirre, V., Schlesinger, K. J., et al. 2016, MNRAS, 455, 987

Casagrande, L., Silva Aguirre, V., Stello, D., et al. 2014, ApJ, 787, 110

Catanzaro, G., Ripepi, V., Bernabei, S., et al. 2011, MNRAS, 411, 1167

Chapellier, E., Mathias, P., Weiss, W. W., Le Contel, D., & Debosscher, J. 2012, A&A, 540, A117

Chaplin, W. J., Basu, S., Huber, D., et al. 2014, ApJS, 210, 1

Chaplin, W. J., Bedding, T. R., Bonanno, A., et al. 2011a, ApJL, 732, L5

Chaplin, W. J., Elsworth, Y., Isaak, G. R., et al. 1998, MNRAS, 298, L7

Chaplin, W. J., Elsworth, Y., Isaak, G. R., Miller, B. A., & New, R. 2000, MNRAS, 313, 32

Chaplin, W. J., Elsworth, Y., Miller, B. A., Verner, G. A., & New, R. 2007, ApJ, 659, 1749

Chaplin, W. J., Kjeldsen, H., Christensen-Dalsgaard, J., et al. 2011b, Science, 332, 213

Chaplin, W. J. & Miglio, A. 2013, ARA&A, 51, 353

Chevalier, C. 1971, A&A, 14, 24

Christensen-Dalsgaard, J. 2000, in Astronomical Society of the Pacific Conference Series, Vol. 210, Delta Scuti and Related Stars, ed. M. Breger & M. Montgomery, 187

Christensen-Dalsgaard, J., Dappen, W., Ajukov, S. V., et al. 1996, Science, 272, 1286

Christensen-Dalsgaard, J., Gough, D. O., & Thompson, M. J. 1991, ApJ, 378, 413

Coates, D. W., Halprin, L., & Thompson, K. 1982, MNRAS, 199, 135

Colacevich, A. 1935, Lick Observatory Bulletin, 17, 171

Conti, P. S. 1970, PASP, 82, 781

Cowley, A., Cowley, C., Jaschek, M., & Jaschek, C. 1969, AJ, 74, 375

Cox, J. P. 1963, ApJ, 138, 487

Cox, J. P. 1980, Theory of stellar pulsation (Princeton Series in Astrophysics)

Cox, J. P., King, D. S., & Stellingwerf, R. F. 1972, ApJ, 171, 93

Cunha, M. S. 2002, MNRAS, 333, 47

Cunha, M. S., Aerts, C., Christensen-Dalsgaard, J., et al. 2007, Astronomy & Astrophysics Reviews, 14, 217

Cunha, M. S., Alentiev, D., Brandão, I. M., & Perraut, K. 2013, MNRAS, 436, 1639

De Cat, P. & Aerts, C. 2002, A&A, 393, 965

Deeming, T. J. 1975, Ap&SS, 36, 137

Degroote, P., Aerts, C., Michel, E., et al. 2012, A&A, 542, A88

Degroote, P., Briquet, M., Catala, C., et al. 2009, A&A, 506, 111

Deheuvels, S., Ballot, J., Beck, P. G., et al. 2015, A&A, 580, A96

Deheuvels, S., Doğan, G., Goupil, M. J., et al. 2014, A&A, 564, A27

Deheuvels, S., García, R. A., Chaplin, W. J., et al. 2012, ApJ, 756, 19

Duchêne, G. & Kraus, A. 2013, ARA&A, 51, 269

Dufour, P., Fontaine, G., Liebert, J., Schmidt, G. D., & Behara, N. 2008, ApJ, 683, 978

Dufour, P., Green, E. M., Fontaine, G., et al. 2009, ApJ, 703, 240

Dufour, P., Liebert, J., Fontaine, G., & Behara, N. 2007, Nature, 450, 522

Dupret, M. A., Grigahcène, A., Garrido, R., Gabriel, M., & Scuflaire, R. 2004, A&A, 414, L17

Dupret, M. A., Grigahcène, A., Garrido, R., Gabriel, M., & Scuflaire, R. 2005, A&A, 435, 927

Dziembowski, W. 1977a, Acta Astronomica, 27, 203

Dziembowski, W. 1977b, Acta Astronomica, 27, 95

Dziembowski, W. 1982, Acta Astronomica, 32, 147

Dziembowski, W. & Krolikowska, M. 1985, Acta Astronomica, 35, 5

Dziembowski, W. & Krolikowska, M. 1990, Acta Astronomica, 40, 19

Dziembowski, W., Krolikowska, M., & Kosovichev, A. 1988, Acta Astronomica, 38, 61

Dziembowski, W. A. & Goode, P. R. 1992, ApJ, 394, 670

Dziembowski, W. A., Goode, P. R., Pamyatnykh, A. A., & Sienkiewicz, R. 1995, in Astronomical Society of the Pacific Conference Series, Vol. 76, GONG 1994. Helio- and Astro-Seismology from the Earth and Space, ed. R. K. Ulrich, E. J. Rhodes, Jr., & W. Dappen, 124

Dziembowski, W. A., Moskalik, P., & Pamyatnykh, A. A. 1993, MNRAS, 265, 588

Dziembowski, W. A. & Pamyatnykh, A. A. 1993a, in Astronomical Society of the Pacific Conference Series, Vol. 40, IAU Colloq. 137: Inside the Stars, ed. W. W. Weiss & A. Baglin, 721

Dziembowski, W. A. & Pamyatnykh, A. A. 1993b, MNRAS, 262, 204

Eddington, A. S. 1917, The Observatory, 40, 290

Eddington, A. S. 1926, The Internal Constitution of the Stars (Cambridge University Press)

Eggen, O. J. 1956, PASP, 68, 238

Eggen, O. J. 1976, PASP, 88, 402

Eggen, O. J. & Iben, Jr., I. 1989, AJ, 97, 431

Fath, E. A. 1935, Lick Observatory Bulletin, 17, 175

Fitzgerald, M. P. 1970, A&A, 4, 234

Fontaine, G. & Brassard, P. 2008, PASP, 120, 1043

Fontaine, G., Brassard, P., Charpinet, S., et al. 2003, ApJ, 597, 518

Fontaine, G., Brassard, P., & Dufour, P. 2008, A&A, 483, L1

Foreman-Mackey, D., Hogg, D. W., Lang, D., & Goodman, J. 2013, PASP, 125, 306

Frolov, M. S. & Irkaev, B. N. 1984, Information Bulletin on Variable Stars, 2462

Fuller, J., Cantiello, M., Stello, D., Garcia, R. A., & Bildsten, L. 2015, Science, 350, 423

Gilliland, R. L., Brown, T. M., Christensen-Dalsgaard, J., et al. 2010, PASP, 122, 131

Goldreich, P. & Keeley, D. A. 1977a, ApJ, 211, 934

Goldreich, P. & Keeley, D. A. 1977b, ApJ, 212, 243

Goldreich, P., Murray, N., & Kumar, P. 1994, ApJ, 424, 466

Gough, D. & Toomre, J. 1991, ARA&A, 29, 627

Gough, D. O. 1977, ApJ, 214, 196

Gough, D. O. 1986, in Hydrodynamic and Magnetodynamic Problems in the Sun and Stars, ed. Y. Osaki, 117

Goupil, M.-J. & Buchler, J. R. 1994, A&A, 291, 481

Goupil, M. J., Dziembowski, W. A., & Fontaine, G. 1998, Baltic Astronomy, 7, 21

Goupil, M.-J., Dziembowski, W. A., Pamyatnykh, A. A., & Talon, S. 2000, in Astronomical Society of the Pacific Conference Series, Vol. 210, Delta Scuti and Related Stars, ed. M. Breger & M. Montgomery, 267

Gray, D. F. 2005, The Observation and Analysis of Stellar Photospheres, 3rd edn. (Cambridge University Press)

Gray, R. O. & Corbally, J., C. 2009, Stellar Spectral Classification (Princeton Series in Astrophysics)

Gray, R. O. & Garrison, R. F. 1989, ApJS, 69, 301

Grigahcène, A., Antoci, V., Balona, L., et al. 2010a, ApJL, 713, L192

Grigahcène, A., Dupret, M.-A., Gabriel, M., Garrido, R., & Scuflaire, R. 2005, A&A, 434, 1055

Grigahcène, A., Uytterhoeven, K., Antoci, V., et al. 2010b, Astronomische Nachrichten, 331, 989

Guzik, J. A. & Cox, A. N. 1991, Delta Scuti Star Newsletter, 3, 6

Guzik, J. A., Kaye, A. B., Bradley, P. A., Cox, A. N., & Neuforge, C. 2000, ApJL, 542, L57

Hambleton, K. M. 2016, PhD thesis, Jeremiah Horrocks Institute, University of Central Lancashire, UK

Hambleton, K. M., Kurtz, D. W., Prša, A., et al. 2013, MNRAS, 434, 925

Handler, G. 1999, MNRAS, 309, L19

Handler, G. 2009, MNRAS, 398, 1339

Handler, G., Balona, L. A., Shobbrook, R. R., et al. 2002, MNRAS, 333, 262

Handler, G. & Shobbrook, R. R. 2002a, in Astronomical Society of the Pacific Conference Series, Vol. 256, Observational Aspects of Pulsating B- and A Stars, ed. C. Sterken & D. W. Kurtz, 117

Handler, G. & Shobbrook, R. R. 2002b, MNRAS, 333, 251

Handler, G., Shobbrook, R. R., Jerzykiewicz, M., et al. 2004, MNRAS, 347, 454

Hermes, J. J., Montgomery, M. H., Mullally, F., Winget, D. E., & Bischoff-Kim, A. 2013, ApJ, 766, 42

Holdsworth, D. L., Smalley, B., Gillon, M., et al. 2014a, MNRAS, 439, 2078

Holdsworth, D. L., Smalley, B., Kurtz, D. W., et al. 2014b, MNRAS, 443, 2049

Houdek, G. 2000, in Astronomical Society of the Pacific Conference Series, Vol. 210, Delta Scuti and Related Stars, ed. M. Breger & M. Montgomery, 454

Houdek, G. 2008, Communications in Asteroseismology, 157, 137

Houdek, G., Balmforth, N. J., Christensen-Dalsgaard, J., & Gough, D. O. 1999a, A&A, 351, 582

Houdek, G., Balmforth, N. J., Christensen-Dalsgaard, J., & Gough, D. O. 1999b, in Astronomical Society of the Pacific Conference Series, Vol. 173, Stellar Structure: Theory and Test of Connective Energy Transport, ed. A. Gimenez, E. F. Guinan, & B. Montesinos, 317

Houdek, G. & Dupret, M.-A. 2015, Living Reviews in Solar Physics, 12

Howell, S. B., Sobeck, C., Haas, M., et al. 2014, PASP, 126, 398

Huber, D., Bedding, T. R., Stello, D., et al. 2011, ApJ, 743, 143

Huber, D., Silva Aguirre, V., Matthews, J. M., et al. 2014, ApJS, 211, 2

Iben, Jr., I. 1966, ApJ, 143, 483

Iben, Jr., I. 1967a, ApJ, 147, 650

Iben, Jr., I. 1967b, ARA&A, 5, 571

Iben, Jr., I. 1967c, ApJ, 147, 624

Iben, Jr., I. 2013a, Stellar Evolution Physics, Volume 1: Physical Processes in Stellar Interiors (Cambridge University Press)

Iben, Jr., I. 2013b, Stellar Evolution Physics, Volume 2: Advanced Evolution of Single Stars (Cambridge University Press)

Iglesias, C. A. & Rogers, F. J. 1996, ApJ, 464, 943

Jeffery, C. S. & Saio, H. 2006a, MNRAS, 371, 659

Jeffery, C. S. & Saio, H. 2006b, MNRAS, 372, L48

Jeffery, C. S. & Saio, H. 2016, MNRAS, 458, 1352

Jenkins, J. M., Caldwell, D. A., Chandrasekaran, H., et al. 2010, ApJL, 713, L87

Johnson, H. L. & Morgan, W. W. 1953, ApJ, 117, 313

Jones, D. H. P. & Haslam, C. M. 1966, The Observatory, 86, 34

Kallinger, T. & Matthews, J. M. 2010, ApJL, 711, L35

Kaye, A. B., Handler, G., Krisciunas, K., Poretti, E., & Zerbi, F. M. 1999, PASP,
    111, 840

Keen, M. A., Bedding, T. R., Murphy, S. J., et al. 2015, MNRAS, 454, 1792

Kennelly, E. J., Brown, T. M., Kotak, R., et al. 1998, ApJ, 495, 440

Kilkenny, D. 2007, Communications in Asteroseismology, 150, 234

Kilkenny, D. 2010, Ap&SS, 329, 175

Kilkenny, D., Copley, C., Zietsman, E., & Worters, H. 2007, MNRAS, 375, 1325

Kilkenny, D., Koen, C., O'Donoghue, D., & Stobie, R. S. 1997, MNRAS, 285, 640

Kilkenny, D., O'Donoghue, D., Koen, C., Lynas-Gray, A. E., & van Wyk, F. 1998,
    MNRAS, 296, 329

Kjeldsen, H. & Bedding, T. R. 1995, A&A, 293, 87

Koch, D. G., Borucki, W. J., Basri, G., et al. 2010, ApJL, 713, L79

Kochukhov, O. 2011, in IAU Symposium, Vol. 273, Physics of Sun and Star Spots,
    ed. D. Prasad Choudhary & K. G. Strassmeier, 249–255

Kolenberg, K., Fossati, L., Shulyak, D., et al. 2010a, A&A, 519, A64

Kolenberg, K., Szabó, R., Kurtz, D. W., et al. 2010b, ApJL, 713, L198

Kolláth, Z., Molnár, L., & Szabó, R. 2011, MNRAS, 414, 1111

Komm, R. W., Howe, R., & Hill, F. 2000, ApJ, 543, 472

Korzennik, S. G. & Eff-Darwich, A. 2011, Journal of Physics Conference Series, 271,
    012067

Kraft, R. P. 1967, ApJ, 150, 551

Kumar, P., Ao, C. O., & Quataert, E. J. 1995, ApJ, 449, 294

Kurtz, D. W. 1976, ApJS, 32, 651

Kurtz, D. W. 1978, ApJ, 221, 869

Kurtz, D. W. 1982, MNRAS, 200, 807

Kurtz, D. W. 1985, MNRAS, 213, 773

Kurtz, D. W. 1989, MNRAS, 238, 1077

Kurtz, D. W. 1990, ARA&A, 28, 607

Kurtz, D. W. 2000, in Astronomical Society of the Pacific Conference Series, Vol. 210, Delta Scuti and Related Stars, ed. M. Breger & M. Montgomery, 287

Kurtz, D. W., Bowman, D. M., Ebo, S. J., et al. 2016, MNRAS, 455, 1237

Kurtz, D. W., Saio, H., Takata, M., et al. 2014, MNRAS, 444, 102

Kurtz, D. W., Shibahashi, H., Murphy, S. J., Bedding, T. R., & Bowman, D. M. 2015, MNRAS, 450, 3015

Ledoux, P. 1951, ApJ, 114, 373

Lee, Y.-H., Kim, S. S., Shin, J., Lee, J., & Jin, H. 2008, PASJ, 60, 551

Lenz, P. & Breger, M. 2005, Communications in Asteroseismology, 146, 53

Lenz, P., Pamyatnykh, A. A., Zdravkov, T., & Breger, M. 2010, A&A, 509, A90

Libbrecht, K. G. & Woodard, M. F. 1991, Science, 253, 152

Lindegren, L., Babusiaux, C., Bailer-Jones, C., et al. 2008, in IAU Symposium, Vol. 248, A Giant Step: from Milli- to Micro-arcsecond Astrometry, ed. W. J. Jin, I. Platais, & M. A. C. Perryman, 217–223

Lindegren, L., Lammers, U., Hobbs, D., et al. 2012, A&A, 538, A78

Maeder, A. & Meynet, G. 2000, ARA&A, 38, 143

Mathias, P., Gillet, D., Aerts, C., & Breitfellner, M. G. 1997, A&A, 327, 1077

Mathys, G. 2015, in Astronomical Society of the Pacific Conference Series, Vol. 494, Physics and Evolution of Magnetic and Related Stars, ed. Y. Y. Balega, I. I. Romanyuk, & D. O. Kudryavtsev, 3

McNamara, B. J., Jackiewicz, J., & McKeever, J. 2012, AJ, 143, 101

McNamara, D. H. 2000, in Astronomical Society of the Pacific Conference Series, Vol. 210, Delta Scuti and Related Stars, ed. M. Breger & M. Montgomery, 373

Metropolis, N., Rosenbluth, A. W., Rosenbluth, M. N., Teller, A. H., & Teller, E. 1953, Journal of Chemical Physics, 21, 1087

Miglio, A., Chiappini, C., Morel, T., et al. 2013, MNRAS, 429, 423

Miglio, A., Montalbán, J., & Dupret, M.-A. 2007, MNRAS, 375, L21

Miglio, A., Montalbán, J., Noels, A., & Eggenberger, P. 2008, MNRAS, 386, 1487

Moe, M. & Di Stefano, R. 2016, ArXiv e-prints

Montgomery, M. H. 2005, ApJ, 633, 1142

Montgomery, M. H., Williams, K. A., Winget, D. E., et al. 2008, ApJL, 678, L51

Moskalik, P. 1985, Acta Astronomica, 35, 229

Moskalik, P. & Buchler, J. R. 1990, ApJ, 355, 590

Moskalik, P. & Kołaczkowski, Z. 2009, MNRAS, 394, 1649

Moskalik, P., Kołaczkowski, Z., & Mizerski, T. 2006, Memorie della Societ Astronomia Italiana, 77, 563

Mosser, B., Goupil, M. J., Belkacem, K., et al. 2012, A&A, 548, A10

Mow, B., Reinhart, E., Nhim, S., & Watkins, R. 2016, AJ, 152, 17

Murphy, S. J. 2014, PhD thesis, Jeremiah Horrocks Institute, University of Central Lancashire, UK

Murphy, S. J. 2015, MNRAS, 453, 2569

Murphy, S. J., Bedding, T. R., Niemczura, E., Kurtz, D. W., & Smalley, B. 2015a, MNRAS, 447, 3948

Murphy, S. J., Bedding, T. R., Shibahashi, H., Kurtz, D. W., & Kjeldsen, H. 2014, MNRAS, 441, 2515

Murphy, S. J., Corbally, C. J., Gray, R. O., et al. 2015b, PASA, 32, e036

Murphy, S. J., Fossati, L., Bedding, T. R., et al. 2016, MNRAS, 459, 1201

Murphy, S. J., Grigahcène, A., Niemczura, E., Kurtz, D. W., & Uytterhoeven, K. 2012, MNRAS, 427, 1418

Murphy, S. J., Pigulski, A., Kurtz, D. W., et al. 2013a, MNRAS, 432, 2284

Murphy, S. J., Shibahashi, H., & Kurtz, D. W. 2013b, MNRAS, 430, 2986

Neilson, H. R. & Ignace, R. 2015, A&A, 584, A58

Nemec, J. & Mateo, M. 1990, in Astronomical Society of the Pacific Conference Series, Vol. 11, Confrontation Between Stellar Pulsation and Evolution, ed. C. Cacciari & G. Clementini, 64–84

Niemczura, E., Murphy, S. J., Smalley, B., et al. 2015, MNRAS, 450, 2764

Nowakowski, R. M. 2005, Acta Astronomica, 55, 1

Olech, A., Dziembowski, W. A., Pamyatnykh, A. A., et al. 2005, MNRAS, 363, 40

Osaki, J. 1975, PASJ, 27, 237

Østensen, R. H., Bloemen, S., Vučković, M., et al. 2011, ApJL, 736, L39

Pamyatnykh, A. A. 1999, Acta Astronomica, 49, 119

Pamyatnykh, A. A. 2000, in Astronomical Society of the Pacific Conference Series, Vol. 210, Delta Scuti and Related Stars, ed. M. Breger & M. Montgomery, 215

Pamyatnykh, A. A. 2003, Ap&SS, 284, 97

Pamyatnykh, A. A., Handler, G., & Dziembowski, W. A. 2004, MNRAS, 350, 1022

Pápics, P. I. 2012, Astronomische Nachrichten, 333, 1053

Paunzen, E., Handler, G., Weiss, W. W., et al. 2002a, A&A, 392, 515

Paunzen, E., Iliev, I. K., Kamp, I., & Barzova, I. S. 2002b, MNRAS, 336, 1030

Paxton, B., Bildsten, L., Dotter, A., et al. 2011, ApJS, 192, 3

Paxton, B., Cantiello, M., Arras, P., et al. 2013, ApJS, 208, 4

Paxton, B., Marchant, P., Schwab, J., et al. 2015, ApJS, 220, 15

Percy, J. R., Matthews, J. M., & Wade, J. D. 1980, A&A, 82, 172

Perryman, M. A. C., de Boer, K. S., Gilmore, G., et al. 2001, A&A, 369, 339

Petersen, J. O. 1973, A&A, 27, 89

Petersen, J. O. & Christensen-Dalsgaard, J. 1996, A&A, 312, 463

Pinsonneault, M. H., An, D., Molenda-Żakowicz, J., et al. 2012, ApJS, 199, 30

Poleski, R., Soszyński, I., Udalski, A., et al. 2010, Acta Astronomica, 60, 1

Pollacco, D. L., Skillen, I., Collier Cameron, A., et al. 2006, PASP, 118, 1407

Poretti, E. 2003, A&A, 409, 1031

Poretti, E., Rainer, M., Weiss, W. W., et al. 2011, A&A, 528, A147

Preston, G. W. 1959, ApJ, 130, 507

Prša, A., Batalha, N., Slawson, R. W., et al. 2011, AJ, 141, 83

Rauer, H., Catala, C., Aerts, C., et al. 2014, Experimental Astronomy, 38, 249

Régulo, C., García, R. A., & Ballot, J. 2016, A&A, 589, A103

Richer, J., Michaud, G., & Turcotte, S. 2000, ApJ, 529, 338

Ricker, G. R., Winn, J. N., Vanderspek, R., et al. 2015, Journal of Astronomical Telescopes, Instruments, and Systems, 1, 014003

Rodríguez, E. & Breger, M. 2001, A&A, 366, 178

Rodríguez, E., López de Coca, P., Costa, V., & Martín, S. 1995, A&A, 299, 108

Rodríguez, E., López-González, M. J., & López de Coca, P. 2000, A&AS, 144, 469

Rogers, T. M. 2015, ApJL, 815, L30

Rogers, T. M., Lin, D. N. C., McElwaine, J. N., & Lau, H. H. B. 2013, ApJ, 772, 21

Royer, F., Zorec, J., & Gómez, A. E. 2007, A&A, 463, 671

Saio, H. 1981, ApJ, 244, 299

Saio, H. 2005, MNRAS, 360, 1022

Saio, H. & Cox, J. P. 1980, ApJ, 236, 549

Saio, H., Kurtz, D. W., Takata, M., et al. 2015, MNRAS, 447, 3264

Samadi, R., Goupil, M.-J., & Houdek, G. 2002, A&A, 395, 563

Schmid, V. S. & Aerts, C. 2016, A&A, 592, A116

Schmid, V. S., Themessl, N., Breger, M., et al. 2012, Astronomische Nachrichten, 333, 1080

Schmid, V. S., Themeßl, N., Breger, M., et al. 2014, A&A, 570, A33

Schöller, M., Correia, S., Hubrig, S., & Kurtz, D. W. 2012, A&A, 545, A38

Schou, J., Antia, H. M., Basu, S., et al. 1998, ApJ, 505, 390

Scuflaire, R., Théado, S., Montalbán, J., et al. 2008, Ap&SS, 316, 83

Seaton, M. J., Yan, Y., Mihalas, D., & Pradhan, A. K. 1994, MNRAS, 266, 805

Shibahashi, H. & Kurtz, D. W. 2012, MNRAS, 422, 738

Shibahashi, H., Kurtz, D. W., & Murphy, S. J. 2015, MNRAS, 450, 3999

Slettebak, A. 1954, ApJ, 119, 146

Slettebak, A. 1955, ApJ, 121, 653

Smalley, B., Kurtz, D. W., Smith, A. M. S., et al. 2011, A&A, 535, A3

Smalley, B., Niemczura, E., Murphy, S. J., et al. 2015, MNRAS, 452, 3334

Smalley, B., Southworth, J., Pintado, O. I., et al. 2014, A&A, 564, A69

Smith, J. C., Stumpe, M. C., Van Cleve, J. E., et al. 2012, PASP, 124, 1000

Smith, M. A. 1971a, A&A, 11, 325

Smith, M. A. 1971b, AJ, 76, 896

Smith, M. A. 1973, ApJS, 25, 277

Soszyński, I., Poleski, R., Udalski, A., et al. 2008, Acta Astronomica, 58, 163

Soszyński, I., Udalski, A., Szymański, M. K., et al. 2014, Acta Astronomica, 64, 177

Spiegel, E. A. & Zahn, J.-P. 1992, A&A, 265, 106

Stankov, A. & Handler, G. 2005, ApJS, 158, 193

Stępień, K. 2000, A&A, 353, 227

Stellingwerf, R. F. 1975a, ApJ, 195, 441

Stellingwerf, R. F. 1975b, ApJ, 199, 705

Stellingwerf, R. F. 1979, ApJ, 227, 935

Stellingwerf, R. F. 1980, in Lecture Notes in Physics, Berlin Springer Verlag, Vol. 125, Nonradial and Nonlinear Stellar Pulsation, ed. H. A. Hill & W. A. Dziembowski, 50–54

Stello, D., Cantiello, M., Fuller, J., et al. 2016, Nature, 529, 364

Stello, D., Chaplin, W. J., Basu, S., Elsworth, Y., & Bedding, T. R. 2009, MNRAS, 400, L80

Stibbs, D. W. N. 1950, MNRAS, 110, 395

Stumpe, M. C., Smith, J. C., Van Cleve, J. E., et al. 2012, PASP, 124, 985

Szabó, R., Benkő, J. M., Paparó, M., et al. 2014, A&A, 570, A100

Szabó, R., Kolláth, Z., Molnár, L., et al. 2010, MNRAS, 409, 1244

Talon, S., Zahn, J.-P., Maeder, A., & Meynet, G. 1997, A&A, 322, 209

Tassoul, M. 1980, ApJS, 43, 469

Théado, S., Vauclair, S., Alecian, G., & LeBlanc, F. 2009, ApJ, 704, 1262

Thompson, K. & Coates, D. W. 1991, Proceedings of the Astronomical Society of Australia, 9, 281

Thompson, S. E., Everett, M., Mullally, F., et al. 2012, ApJ, 753, 86

Titus, J. & Morgan, W. W. 1940, ApJ, 92, 256

Tkachenko, A., Aerts, C., Yakushechkin, A., et al. 2013, A&A, 556, A52

Townsend, R. H. D. 2005, MNRAS, 360, 465

Townsend, R. H. D. & Teitler, S. A. 2013, MNRAS, 435, 3406

Triana, S. A., Moravveji, E., Pápics, P. I., et al. 2015, ApJ, 810, 16

TSesevich, V. P. 1953, Trudy Gosudarstvennogo Astronomicheskogo Instituta, 23, 62

Turcotte, S., Richer, J., Michaud, G., & Christensen-Dalsgaard, J. 2000, A&A, 360, 603

Unno, W., Osaki, Y., Ando, H., Saio, H., & Shibahashi, H. 1989, Nonradial oscillations of stars, Tokyo: University of Tokyo Press, 2nd ed. (University of Tokyo Press)

Uytterhoeven, K., Moya, A., Grigahcène, A., et al. 2011, A&A, 534, A125

Van Hoolst, T. 1994, A&A, 292, 471

van Kerkwijk, M. H., Clemens, J. C., & Wu, Y. 2000a, MNRAS, 314, 209

van Kerkwijk, M. H., Kaspi, V. M., Klemola, A. R., et al. 2000b, ApJ, 529, 428

Van Reeth, T., Tkachenko, A., & Aerts, C. 2016, A&A, 593, A120

Van Reeth, T., Tkachenko, A., Aerts, C., et al. 2015a, A&A, 574, A17

Van Reeth, T., Tkachenko, A., Aerts, C., et al. 2015b, ApJS, 218, 27

Vanderburg, A., Latham, D. W., Buchhave, L. A., et al. 2016, ApJS, 222, 14

Vauclair, G. 2013, in Astronomical Society of the Pacific Conference Series, Vol. 479, Progress in Physics of the Sun and Stars: A New Era in Helio- and Asteroseismology, ed. H. Shibahashi & A. E. Lynas-Gray, 223

Waelkens, C. 1991, A&A, 246, 453

Walker, G., Matthews, J., Kuschnig, R., et al. 2003, PASP, 115, 1023

Wallerstein, G. 2002, PASP, 114, 689

Walraven, T., Walraven, J., & Balona, L. A. 1992, MNRAS, 254, 59

Winget, D. E. & Kepler, S. O. 2008, ARA&A, 46, 157

Wolff, S. C. 1968, PASP, 80, 281

Wu, Y. 2001, MNRAS, 323, 248

Wu, Y. & Goldreich, P. 2001, ApJ, 546, 469

Xiong, D. R. & Deng, L. 2001, MNRAS, 324, 243

Zahn, J.-P. 1992, A&A, 265, 115

Zima, W., Wright, D., Bentley, J., et al. 2006, A&A, 455, 235

Zong, W., Charpinet, S., & Vauclair, G. 2016a, A&A, 594, A46

Zong, W., Charpinet, S., Vauclair, G., Giammichele, N., & Van Grootel, V. 2016b,
    A&A, 585, A22

Zorec, J. & Royer, F. 2012, A&A, 537, A120